

AD-A218 476

DTIC

UNCLASSIFIED
SECURITY CLASSIFICATION OF THIS PAGE

(2)

REPORT DOCUMENTATION PAGE

1a. REPORT SECURITY CLASSIFICATION UNCLASSIFIED			1b. RESTRICTIVE MARKINGS		
2a. SECURITY CLASSIFICATION AUTHORITY DTIC ELECTE FEB 26 1990			3. DISTRIBUTION / AVAILABILITY OF REPORT Approved for public release, distribution unlimited		
2b. DECLASSIFICATION / DOWNGRADING SCHEDULE			5. MONITORING ORGANIZATION REPORT NUMBER AFOSR-TR-90-0200		
4. PERFORMING ORGANIZATION REPORT NUMBER(S) TSI-89-12-12-WB			7a. NAME OF MONITORING ORGANIZATION Air Force Office of Scientific Research		
6a. NAME OF PERFORMING ORGANIZATION Techno-Sciences, Inc.		6b. OFFICE SYMBOL (If applicable)		7b. ADDRESS (City, State, and ZIP Code) AFOSR/NA Bolling AFB, DC 20332-6448	
6c. ADDRESS (City, State, and ZIP Code) 7833 Walker Drive, Suite 620 Greenbelt, MD 20770		7c. ADDRESS (City, State, and ZIP Code) Bldg 410 Bolling AFB, DC 20332-6448			
8a. NAME OF FUNDING / SPONSORING ORGANIZATION AFOSR/NA Bolling AFB DC 20332-6448		8b. OFFICE SYMBOL (If applicable) NA		9. PROCUREMENT INSTRUMENT IDENTIFICATION NUMBER F49620-87-C-0103	
8c. ADDRESS (City, State, and ZIP Code) Bldg 410 Bolling AFB, DC 20332-6448		10. SOURCE OF FUNDING NUMBERS		PROGRAM ELEMENT NO PROJECT NO TASK NO WORK UNIT ACCESSION NO	
11. TITLE (Include Security Classification) Nonlinear Dynamics and Control of Flexible Structures (u)		12. PERSONAL AUTHOR(S) W. H. Bennett, H. G. Kwatny, G. L. Blankenship, O. Akhrif			
13a. TYPE OF REPORT ANNUAL		13b. TIME COVERED FROM 88/9 TO 89/8		14. DATE OF REPORT (Year, Month, Day) 89-12-12	
15. PAGE COUNT 127		16. SUPPLEMENTARY NOTATION			
17. COSATI CODES		18. SUBJECT TERMS (Continue on reverse if necessary and identify by block number)			
FIELD	GROUP	SUB-GROUP			
		Multibody dynamics, Nonlinear, Feedback/Control			
19. ABSTRACT Basic performance requirements for space-based directed energy weapons involve unprecedented requirements for integrated control of rapid retargeting and precision pointing of space structures. Multibody interactions excite nonlinear couplings which complicate the dynamic response. Attempts to reduce flexure response for such weapon platforms by passive techniques alone may be inadequate due to stringent pointing requirements. The principal objective of the research program is the validation and testing of high precision, nonlinear control of multibody systems with significant structural flexure where interactions arise due to rapid slewing. Dominant nonlinear couplings effecting LOS response have been identified based on a comprehensive model of the nonlinear multibody dynamics of a generic space weapon. The innovative approach to LOS slewing/pointing developed in this study is based on implementation of decoupling (by feedback control) of the principal nonlinear dynamics and structural flexure response. In this study we have focused on the implementation of partial feedback linearization and decoupling and have identified practical conditions for its implementation. A principal contribution of the study is the reconciliation of design of discontinuous control via sliding mode control with partial feedback linearization for rapid slewing of system effective LOS. The report includes extensive simulation and tradeoff studies of nonlinear control implementation of rapid slewing and precision pointing of a generic model of a space-based laser beam expander.					
20. DISTRIBUTION / AVAILABILITY OF ABSTRACT <input checked="" type="checkbox"/> UNCLASSIFIED/UNLIMITED <input checked="" type="checkbox"/> SAME AS RPT <input type="checkbox"/> DTIC USERS			21. ABSTRACT SECURITY CLASSIFICATION UNCLASSIFIED		
22a. NAME OF RESPONSIBLE INDIVIDUAL George K. Haritos			22b. TELEPHONE (Include Area Code) (202) 767-0463		22c. OFFICE SYMBOL NA

TSI-89-12-12-WB

Nonlinear Dynamics and Control of Flexible Structures

Annual Report

Sept. 1, 1988 - Aug. 31, 1989
for AFOSR Contract F49620-87-C-0103

W.H. Bennett, H.G. Kwatny, G.L. Blankenship,
O. Akhrif, C. LaVigna

SYSTEMS ENGINEERING, INC.
a Division of
TECHNO-SCIENCES, INC.
Greenbelt, MD 20770

Submitted to
Air Force Office of Scientific Research
Directorate of Mathematical and Information Sciences
Bolling Air Force Base, DC 20332-6448
Attn: Lt. Col. James M. Crowley

Date: Dec. 12, 1989

Approved for public release;
distribution unlimited.

AIR FORCE OFFICE OF SCIENTIFIC RESEARCH
NOTICE OF TRANSMITTAL TO DDC
This document has been reviewed and is
approved for public release IAW AFR 190-12.
DISSEMINATION IS UNLIMITED.
MATTHEW J. KEEFER
Chief, Technical Information Division

The views and conclusions contained in this document are those of the authors and should not be interpreted as necessarily representing the official policies or endorsements, either expressed or implied, of the Air Force Office of Scientific Research or the U.S. Government.

Foreword

This report describes results obtained in the second year of a three year research study on nonlinear modeling and control of flexible space structures with application to rapid slewing and precision pointing of space-based, directed energy weapons. The project is funded by SDIO/IST and managed by AFOSR/SDIO (AFSC). Results reported herein are for the period 1 Sept. 1988 - 31 Aug. 1989.

The project is managed by Lt. Colonel J. Crowley and Dr. A. Amos. We wish to thank both of these individuals for their insight and direction on this project.



Accession For	
NTIS GRA&I	<input checked="checked" type="checkbox"/>
DTIC TAB	<input type="checkbox"/>
Unannounced	<input type="checkbox"/>
Justification	
By _____	
Distribution/	
Availability Codes	
Dist	Avail and/or Special
A-1	

CONTENTS

ii

Contents

1 Research Objectives and Project Summary	1
2 Feedback Linearization and Stabilization of Nonlinear Systems	5
2.1 Computation of Partial Linearizing Feedback Compensation	7
2.2 Nonlinear System Transmission Zeros	9
2.3 PLF Computations for Nonlinear MIMO Systems	10
2.4 Partial Linearization and Variable Structure Control Systems	13
2.5 Robust Stabilization of Nonlinear Systems	16
2.6 Partial Linearization for Lagrangian Systems	19
3 Reduced Order Modeling of Multibody Systems and Nonlinear Control Design	22
3.1 PFL with Reduced Order Models	24
3.1.1 Quasi-Rigid Model	26
3.1.2 The reduced flexible model	28
3.1.3 Feedback linearization and decoupling of the quasi-rigid model	29
3.1.4 Partial feedback linearization of the Reduced Flexible Model	32
3.2 Conclusions and Directions	32
4 Some Design Approaches for Combined Rapid Slewing and Precision Pointing	34
4.1 Practical Implementation of Time-optimal Slewing for an Inertial Load . . .	37
4.2 Implementation of Rapid Slewing with Coordinated Modes of Actuation . .	41
4.3 Coordinating Control for System Slewing and Multibody Alignment	46
5 Simulation Tradeoff Studies for Multiaxis Slewing of SBL System Model	49
5.1 Multibody System Model for Multiaxis Slewing and Precision Alignment . .	49
5.1.1 FEM: Collocation by Splines	51
5.1.2 Reduction of the Kinetic Energy Function	51
5.1.3 Reduction of the Potential Energy and Dissipation Functions	52
5.1.4 Lagrange's Equations	54
5.2 Computer Simulation Model for Nonlinear Control Law Tradeoff Studies . .	54
5.2.1 Simulation model geometry assumptions and parameters	55
5.3 Simulation Results for PLF Control with Rapid Slewing and Precision Pointing	56
6 Conclusions and Directions	61
A Advantages of Gibbs vector description of nonlinear kinematics.	65
B Supporting Computations for area moment of inertia and B-spline model for 3-axis slewing with tripod shaped appendage	67
C Simulated Time Responses for Multiaxis Slewing	73

List of Figures

2.1	Nonlinear Control Concept Using Dynamical System Inverse	7
2.2	Partial Linearizing Feedback via Nonlinear Inverse Model	11
2.3	Partial Feedback Linearization and Zero Dynamics	11
4.1	Implementation of Time-Optimal Servo	41
4.2	Root Locus for Linear Mode Sensitivity of Saturation Mode Slewing	41
4.3	Coordinated Rapid Slewing Control Implementation	46
5.1	Simulation model.	55
2.1	Cross-section of tripod metering truss.	67

List of Tables

5.1	Standard Notation for Lagrangian Mechanics	50
5.2	Matrix of Simulation Models Considered	57
5.3	Matrix of PLF/Slewing Control Implementations	57
5.4	Slewing Times for Standard 3-axis Maneuver	58
5.5	Relative Peak Torque Increase with PLF Compensation DOF	59

1 Research Objectives and Project Summary

The objectives of the research project are to develop nonlinear control design techniques based on the idea of feedback linearization for application to control of flexible space structures. The first year effort focused on the development of a generic model of the dynamics of a multi-body system with elastic interactions undergoing large angle slewing motions. The model was specialized and scaled to represent available data on the SBL prototype system and a computer simulation was developed. The significance of partial feedback linearizing compensation where principal nonlinear couplings are dynamically compensated for by nonlinear feedback control was demonstrated for the problem of rapid and precision large angle slewing of a central rigid body with elastic structure. To achieve large angle slewing decoupling control was used in concert with nonlinear, time-optimal switching control for the rapid slew. Results were presented at the 27th IEEE CDC in Austin, Texas.

At the request of Dr. A. Amos, second year project activities included the development of a detailed simulation model including multiaxis attitude dynamics and structural flexure. The model is described in detail in Section 5.1 along with parameters chosen for simulation tradeoff studies. The system model parameters were chosen from available data to approximately model the dynamics of the test article under construction at the ASTREX facility at Air Force Astronautics Laboratory.

Implementation Alternatives for Feedback Linearizing Control. In the second year we have focused on several practical aspects of the implementation of such decoupling control laws. Reduced order modeling of the flexible structure elastic dynamics was considered for implementation of nonlinear feedback compensation. A time scale analysis was performed and simulation studies were performed to illustrate tradeoffs in LOS slewing and pointing precision vs. peak torque requirements. A relatively soft structural stiffness model was used to illustrate the tradeoffs. The time scale analysis based on singular perturbations identified several alternatives for enhanced precision of decoupling control implementation without model order increase. The use of structural actuators for deformation shaping in concert with slewing control was considered and additional simulation studies are being performed. Considerations for robust implementation of slewing control has focused on precision of the decoupling compensation and stability robustness with parasitic dynamics arising from elastic structure response. This question directs attention to the sensitivity of the control to structural damping and will provide direction for experiments to be designed in the last quarter of this years effort.

A critical observation in our studies of control architectures for SBL systems is the integration of a variety of actuators for spacecraft attitude control (e.g. thruster jets, momentum wheels, CMG's, etc.), multibody articulation, optical system components (e.g. steering and deformable focusing mirrors), and structural vibration control (e.g. proof mass devices, embedded piezoelectrics, etc.) to achieve principal system performance objectives. In this report we describe alternative implementations for coordinating control activity between actuators of different types.

Tradeoff Studies in Implementation of Nonlinear Decoupling Control Performed.

The idea behind feedback linearizing compensation is to compensate for nonlinear couplings by cancelation of critical nonlinear terms effecting system dynamics. Implementation involves the introduction of additional control authority and may suggest the use of special actuator configurations. Coordinating control activity between various types of actuators is an important feature of such control laws. As part of the second year effort detailed simulation studies were performed to delineate tradeoffs in implementation of feedback linearizing control of a SBL system model undergoing multiaxis slewing.

An important alternative implementation is possible based on the use of fast, switching control laws. The implementation of feedback linearization by smooth control involves *explicit* compensation for critical nonlinear dynamic couplings. In the current study we have shown that feedback linearization can be achieved by *implicit* compensation based on the notion of variable structure or sliding mode control (see Section 2.4). In this case the control law is discontinuous with respect to a switching or sliding surface in the model (slow time scale) state space. An important advantage is that the control law can be implemented based only on measurements of primary body attitude parameters. Given sufficient control authority to maintain sliding robust performance can be maintained independent of variations in flexible multibody dynamics.

New Results Obtained. A potentially important feature of feedback linearization is the extent to which the idea can be integrated with other standard design methods for multivariable control systems. We have described several alternatives which indicate advantages of the approach for control of flexible structures. In particular, the integration of relatively weak structural actuation for vibration suppression can be incorporated with the approach. The idea of deformation shaping control has been developed by Dr. T.A.W. Dwyer is reported in several papers prepared as part of this project. An alternative approach which is briefly described in this report is to study the tradeoff between implementation costs for feedback linearizing control with passive structural damping vs. active structural damping. An approach to the required feedforward compensation is developed based on computations of Partial Linearizing Feedback compensation in terms of the normal form equations of Byrnes and Isidori.

Robust stabilization and control performance of nonlinear systems is an important issue in applications. Several techniques for robust stabilization have been developed by Spong and Vidyassagor, Slotine and Sastry, Corless, Gutman, and others. These methods all rely on special structure matching conditions for the model uncertainty in developing robust control design methods. In this research we have developed a new approach which utilizes the framework of adaptive control to provide robust stabilization of nonlinear systems. The approach does not rely on structure matching conditions and represents a significant improvement over available methods.

Professional Personnel The principal investigator for this project is Dr. William H. Bennett and co-principal investigators are Drs. Harry G. Kwatny and Gilmer L. Blankenship from TSI. Dr. Thomas A. W. Dwyer was consultant on the project. We would also like to

acknowledge the parttime support from Dr. Oussima Akhrif who graduated in July 1989 with Ph. D. from Electrical Engineering Department of the University of Maryland. Dr. Akhrif's dissertation developed aspects of feedback linearization for the multibody SBL models developed in this study and some important results are summarized in this report.

Technical Reports/Presentations. As part of the research program we have organized two invited technical sessions, presented several technical papers, and submitted several additional papers for publication as follows.

1. *Nonlinear Dynamics and Control of Aerospace Systems*, invited session at 27th IEEE Cntrl. Dec. Conf., Austin, TX, Dec. 1989.
2. *Robust Control of Uncertain Nonlinear Systems*, invited session at 1989 Amer. Cntrl. Conf., Pittsburgh, PA, June 1989.

Publications/Presentations

1. H.G. Kwatny and W.H. Bennett, "Nonlinear Dynamics and Control Issues for Flexible Space Platforms," *Proc. IEEE Cntrl. Dec. Conf.*, Austin, TX, Dec. 1988.
2. T.A.W. Dwyer, III, "Slew-Induced Deformation Shaping", *Proc. IEEE Cntrl. Dec. Conf.*, Austin, TX, Dec. 1988.
3. O. Akhrif, G. L. Blankenship, and W.H. Bennett, "Robust Control for Rapid Reorientation of Flexible Structures," *Proc. 1989 Amer. Cntrl. Conf.*, Pittsburgh, PA, June 1989.
4. H.G. Kwatny and H. Kim, "Variable Structure Control of Partially Linearizable Dynamics," *Proc. 1989 Amer. Cntrl. Conf.*, Pittsburgh, PA, June 1989.
5. W.H. Bennett, "Frequency Response Modeling and Control of Flexible Structures: Computational Methods," *3rd Annual Conf. on Aerospace Computational Control*, Oxnard, CA, Aug.
6. T.A.W. Dwyer, III and F.K. Kim, "Nonlinear robust Variable Structure Control of Pointing and Tracking with Operator Spline Estimation", *Proc. IEEE International Symposium on Circuits and Systems*, Covallis, Oregon, May 9-11, 1989, Paper No. SSP15-5.
7. T.A.W. Dwyer, III and F.K. Kim, "Bilinear Modeling and Estimation of Slew-Induced Deformations," *J. Astro. Sci.* submitted.
8. T.A.W. Dwyer, III, "Slew-Induced Deformation Shaping on Slow Integral Manifolds," *Control Theory and Multibody Dynamics*, Eds. J. Marsden and P.S. Krishnaprasad, (to appear), Amer. Math. Society.

9. T.A.W. Dwyer, III, F. Karray, and W.H. Bennett, "Bilinear Modeling and Nonlinear Estimation", *Proc. Flight Mechanics/Estimation Theory Symposium*, NASA Goddard Space Flight Center, May 1989.
10. T.A.W. Dwyer, III and J. R. Hoyle, Jr., "Elastically Coupled Precision Pointing by Slew-Induced Deformation Shaping," *Proc. 1989 Amer. Cntrl. Conf.*, Pittsburgh, PA, June 21-23, 1989.
11. T.A.W. Dwyer, III and Jinho Kim, "Bandwidth-Limited Robust Nonlinear Sliding Control of Pointing and Tracking Maneuvers," *Proc. 1989 Amer. Cntrl. Conf.*, Pittsburgh, PA, June 21-23, 1989.
12. T.A.W. Dwyer, III, F. Karray and Jinho Kim, "Sliding Control of Pointing and Tracking with Operator Spline Estimation," *3rd Annual Conf. on Aerospace Computational Control*, Oxnard, CA, Aug. 28-30, 1989.

2 Feedback Linearization and Stabilization of Nonlinear Systems

Conventional techniques for stabilization of nonlinear systems via feedback control are still very limited and tend to be tailored to specific situations. Among the most promising new, general approaches utilize linearization (local or possibly global) by *Exact Feedback Linearization (EFL)* [HSM83, KC87]. EFL methods are based on earlier work of Krener [Kre73] and Brockett [Bro78] which demonstrated that a large class of nonlinear dynamical systems can be exactly (i.e. globally linearized) by a combination of nonlinear transformation of the state coordinates with nonlinear state feedback. More recently, the connection between these methods and the idea of input-output (or *Partial Linearizing Feedback (PLF)*) by construction of a *system inverse* [Hir79] has been articulated in a series of papers by Byrnes and Isidori [BI85, BI84]. These connections have engendered a series of design methods with representative results for specific applications by Kravaris and Chung [KC87] and Fernandez and Hedrick [FH87]. In this section we will show how fundamental these constructions can become in control system design, discuss alternatives for implementation, and suggest some approaches to integrating the nonlinear design philosophy with more conventional approaches. We focus attention in this section on fundamental concepts culminating in the description of the design approach for multibody systems from the perspective of Lagrangian mechanics.

The idea behind feedback linearization is conceptually simple. We start with a nonlinear system model,

$$\dot{x} = f(x) + G(x)u, \quad (2.1)$$

$$y = h(x), \quad (2.2)$$

where $x \in \mathbb{R}^n$, $u, y \in \mathbb{R}^m$ with $G = [g_1, \dots, g_m]$ and assuming the vector fields f, g_i are C^∞ for each $i = 1, \dots, m$ and $f(0) = 0$. The model structure assumes that the control u enters linearly. The feedback linearization problem is to find a change of basis in the state space, $z = T(x)$, with T diffeomorphic and a feedback law,

$$u = \alpha(x) + \beta(x)v,$$

such that in the new (z, v) coordinates the (closed loop) model has the form,

$$\dot{z} = Az + Bv.$$

We remark that if it possible to find such a control law then the linearization is achieved *through the introduction of active control authority*. An important feature for control system design is that the range of validity of the linearization is given by the transformations, $T(x), \alpha(x), \beta(x)$. The functions may be defined locally or globally.

In contrast, the conventional approach to control design would be based on a linear model obtained by Taylor expansion of the vector fields *about given equilibrium conditions*; x_{eq}, u_{eq} , satisfying,

$$0 = f(x_{eq}) + G(x_{eq})u_{eq}.$$

The conventional linear model used for control design represents perturbation dynamics with respect to the equilibrium conditions and assumes the form,

$$\dot{(\Delta x)} = A \Delta x + B \Delta u,$$

$$y = C \Delta x$$

where $\Delta x = x - x_{eq}$, $\Delta u = u - u_{eq}$ and

$$A = \left. \frac{\partial f}{\partial x} \right|_{x=x_{eq}}, \quad B = G(x)|_{x=x_{eq}}, \quad C = \left. \frac{\partial h}{\partial x} \right|_{x=x_{eq}}.$$

A major source of model uncertainty in linear control system design arises from assumptions leading to the linear perturbation model. In many cases it may be difficult to estimate the domain of attraction for the equilibria. Indeed, in aerospace applications the control design is often based on a combination of gain scheduling to take into account the dependence of linear perturbation models on operating point conditions which are subject to variation (e.g. trim conditions in aircraft flight control.) For example, the function of a conventional autopilot for aircraft is to compensate for changes in trim conditions and provide stabilization so that the pilot "feels" a standard, linear response to stick commands.

Although the concept of feedback linearization in control system design is potentially revolutionary, its application has many antecedents in applications. The significance for nonlinear control of flexible space structures is the emerging technology for active control and sensing, the dynamics associated with the CSI technology, and the ability of a comprehensive approach to nonlinear dynamic modeling and control design offered by the approaches discussed in this report. Feedback linearization functions in certain applications in a manner similar to gain scheduling [MC80], however, linearization is achieved about a "nominal model" rather than about an operating point. Thus equilibria conditions do not arise explicitly in linearization. One view of such a controller structure is illustrated in block diagram of Figure 2.1. The process linearization which facilitates the design of the linear controller is obtained by the introduction of an *Inverse Force Model (IFM)* for the nonlinear multibody system. The inverse force model transforms commanded accelerations, a_c , into equivalent system generalized forces, f . Thus the linear controller is designed to yield desired system accelerations given the generalized coordinates, q , and their rates, \dot{q} .

Precursors to the idea of feedback linearization is pervasive in control applications abound. With the development of the geometric theory of nonlinear systems, computational tools and design methods are becoming available to address control system design on a much larger scope. It is clear that the concept of feedback linearization is pervasive in many fundamental control methods. Our study has focused on the considerations for practical implementation of feedback linearization for rapid slewing and precision pointing of aerospace systems with multibody and elastic interactions. Implementation of feedback linearization definitely requires enhanced control authority and issues related to technology for control actuation will either enable or restrict its application.

It is often suggested that controllers designed based on feedback linearization may be sensitive to model assumptions since the linearization is achieved by cancelation of certain nonlinear terms in the system model. Our study of rapid slewing control of a generic

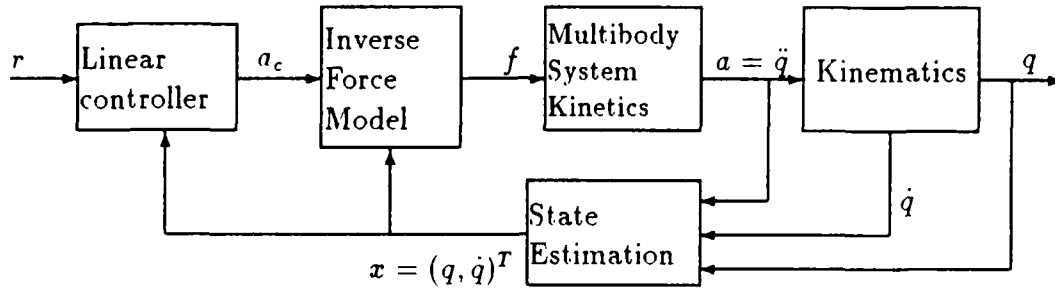


Figure 2.1: Nonlinear Control Concept Using Dynamical System Inverse

space-based laser model has shown that modeling sensitivity and robustness can be obtained through judicious application of control authority. A central issue in nonlinear control design is the limits of available control authority. For example, actuator saturation contributes to limits on control authority. Discontinuous or saturation mode operation of control actuators can often be desirable but such considerations are often not addressed by linear design methods. We have shown that specific consideration for coordination of discontinuous and continuous modes of control actuation in slewing control methods for multibody systems can be readily found. Finally, it is clear that the cost of feedback linearization, in terms of increased control authority, sensor measurement complexity, or computational burden for online implementation may not always be necessary to achieve system performance objectives. We have also demonstrated that such methods can be readily integrated with standard approaches for linear design once a primary system control objective is identified in terms of a primary system output. As we shall show the role of conventional linearization and control design can be relegated to a subsystem whose dynamics are decoupled (by the action of PLF) from a set of system primary outputs.

2.1 Computation of Partial Linearizing Feedback Compensation

Partial linearization derives directly from the Byrnes-Isidori normal form for nonlinear systems. The essentials of the approach are most easily developed for single-input, single output systems and we will present the approach in that context. The theory for extending these results for multi-input, multi-output problems is now complete and references are included.

Consider a nonlinear dynamical system in the form,

$$\dot{x} = f(x) + g(x)u \quad (2.3)$$

$$y = h(x) \quad (2.4)$$

where f, g are smooth C^∞ vector fields on \mathbb{R}^n and h is a smooth function mapping $\mathbb{R}^n \rightarrow \mathbb{R}$. Now if we differentiate (2.4) we obtain

$$\dot{y} = \frac{\partial h}{\partial x}(f(x) + g(x)u). \quad (2.5)$$

In the case that the scalar coefficient of u (viz. $\frac{\partial h}{\partial x}g(x)$) is zero we can differentiate again until a nonzero control coefficient appears. The number of required differentiations is fundamental system invariant which plays a role in constructing a system inverse and therefore in PLF. The Byrnes-Isidori analysis shows that this integer number is analogous to the *relative degree* for a linear system [BI84].

The above construction can be made precise using the notation of differential geometry which has found application in analytical mechanics [Arn78]. We will need only the notion of Lie derivative and Lie bracket. The Lie (directional) derivative of the scalar function h with respect to the vector field f is

$$L_f(h) = \langle dh, f \rangle := \frac{\partial h}{\partial x} f(x). \quad (2.6)$$

Since the above operation results in a scalar function on \mathbb{R}^n , higher order derivatives can be successively defined

$$L_f^k(h) = L_f(L_f^{k-1}(h)) := \langle dL_f^{k-1}(h), f \rangle. \quad (2.7)$$

Then we can write (2.5) as

$$\begin{aligned} \dot{y} &= \langle dh, f \rangle + \langle dh, g \rangle u \\ &= L_f(h) + L_g(h)u. \end{aligned} \quad (2.8)$$

If $L_g(h) = 0$ then we differentiate again to obtain

$$\begin{aligned} \ddot{y} &= \langle dL_f(h), f \rangle + \langle dL_f(h), g \rangle u \\ &= L_f^2(h) + L_g(L_f(h))u. \end{aligned} \quad (2.9)$$

If $L_g(L_f^{k-1}(h)) = 0$ for $k = 1, \dots, r-1$, but $L_g(L_f^{r-1}(h)) \neq 0$ then the process terminates with

$$\frac{d^r y}{dt^r} = L_f^r(h) + L_g(L_f^{r-1}(h))u. \quad (2.10)$$

The system (2.10) can be effectively inverted by introducing a feedback transformation of the form

$$u = \frac{1}{L_g(L_f^{r-1}(h))} [v - L_f^r(h)] \quad (2.11)$$

which results in an input-output response from $v \rightarrow y$ given by

$$\frac{d^r y}{dt^r} = v,$$

a linear system.

The integer $r > 0$ can be viewed as a *relative degree* for the nonlinear system (2.3)–(2.4). Note that if we define new state coordinates $z \in \mathbb{R}^r$ as

$$z_k = L_f^{k-1}(h), \quad k = 1, \dots, r \quad (2.12)$$

for the r -dimensional nonlinear system (2.10), then the system model can be written in state space form as,

$$\dot{z} = \begin{bmatrix} 0 & 1 & 0 & \cdots & 0 \\ 0 & 0 & 1 & \cdots & 0 \\ 0 & 0 & 0 & \cdots & 1 \\ 0 & 0 & 0 & \cdots & 0 \end{bmatrix} z + \begin{bmatrix} 0 \\ 0 \\ \vdots \\ 0 \\ \alpha(x) + \rho(x)u \end{bmatrix}, \quad (2.13)$$

where

$$\alpha(x) = L_f^r(h), \quad \rho(x) = L_g(L_f^{r-1}(h)). \quad (2.14)$$

More generally, using the new coordinates z (2.12) and introducing a nonlinear feedback control of the form

$$u = \frac{(v - \sigma(x))}{\rho(x)} \quad (2.15)$$

where

$$\sigma(x) = \sum_{k=0}^{r-1} \beta_k L_f^k(h) + L_f^r(h), \quad (2.16)$$

$$\rho(x) = L_g(L_f^{r-1}(h)), \quad (2.17)$$

with β_k for $k = 0, \dots, r-1$ real positive coefficients then the equations (2.8)–(2.9) can be written in 'reduced' form;

$$\dot{z} = \begin{bmatrix} 0 & 1 & 0 & \cdots & 0 \\ 0 & 0 & 1 & \cdots & 0 \\ 0 & 0 & 0 & \cdots & 0 \\ -\beta_0 & -\beta_1 & -\beta_2 & \cdots & -\beta_{r-1} \end{bmatrix} z + \begin{pmatrix} 0 \\ 0 \\ \vdots \\ 1 \end{pmatrix} v \quad (2.18)$$

$$y = [1, 0, \dots, 0] z. \quad (2.19)$$

2.2 Nonlinear System Transmission Zeros

Note that the process leading to (2.18)–(2.19) provides an equivalent state space realization for the $v \mapsto y$ input-output response of McMillan degree $r \leq n$ (the dimension of the original state space model (2.3)–(2.4)) *by decoupling a portion of the system dynamics from the output response*. This is depicted in Figure 2.3. Thus the new state coordinates z are a 'partial' state for the system. Thus stabilization of (2.18)–(2.19) cannot guarantee stabilization of the full state model (2.3)–(2.4). We remark that in the case that $h(x)$ is such that the relative degree $r = n$ then the state space transformation (2.12) for $k = 1, \dots, r$ together with the feedback transformation (2.15) exactly linearizes the full system state model (2.3). The methods described in [HSM83] identify necessary and sufficient conditions for the existence of a C^∞ function $h(x)$ such that $r = n$ and provides a computational approach. The necessary and sufficient conditions for (local) EFL are nongeneric and not likely to be satisfied in general. In the sequel we show how that essential property of involutivity of the f and g vector fields will almost never be satisfied for realistic models of flexible space structures due to the infinite dimensional nature of the state space.

Byrnes and Isidori [BI85] describe the transformation of (2.3)–(2.4) to a *normal form* in which the feasibility of PLF control can be assessed. The main result provides the existence of a diffeomorphic transformation of coordinates $T_h : \mathbb{R}^n \rightarrow \mathbb{R}^n$ with $(T_h)(x) \mapsto (\xi, z)$, with the state partition in the new coordinates $\xi \in \mathbb{R}^{n-r}$, $z \in \mathbb{R}^r$ and inverse, $(\hat{T}_h)(x) \mapsto (\xi, z)$, so that the full state representation in the new coordinates is

$$\dot{\xi} = F(\xi, z), \quad (2.20)$$

$$\dot{z} = \begin{bmatrix} 0 & I_{r-1} \\ 0 & 0 \end{bmatrix} z + \begin{bmatrix} 0 \\ 1 \end{bmatrix} [A(\xi, z) + B(\xi, z)u], \quad (2.21)$$

where

$$A(\xi, z) = \alpha(x)|_{x=\hat{T}(\xi, z)}$$

$$B(\xi, z) = \rho(x)|_{x=\hat{T}(\xi, z)}.$$

Definition: The *zero dynamics* of the input-output model (2.3)–(2.4) are given by the autonomous system,

$$\dot{\xi} = F(\xi, 0). \quad (2.22)$$

And the system is *locally minimum phase* if the the diffeomorphic transformation T_h is defined on a neighborhood of the origin and (2.22) is asymptotically stable to the origin; $\xi = 0$.

2.3 PLF Computations for Nonlinear MIMO Systems

The nonlinear input/output model is

$$\dot{x} = f(x) + G(x)u \quad (2.23)$$

$$y = h(x) \quad (2.24)$$

where $x \in \mathbb{R}^n$, $u, y \in \mathbb{R}^m$ and f, g_i (resp. y_i) for $i = 1, \dots, m$ are smooth vector fields defined on \mathbb{R}^n (resp. \mathbb{R}^m). For notational simplicity we write,

$$G(x) = [g_1(x), \dots, g_m(x)].$$

In a process similar to the previous section PLF is determined by transformation of the system model (2.23)–(2.24) to a normal form in which we identify a certain $(m \times m)$ *decoupling matrix* which is locally nonsingular.

The process begins with the computation of an appropriate generalization of the MIMO system relative degrees. Let

$$r_i := \min\{k = 1, 2, \dots : L_{g_j}(L_f^{k-1}(h_i)) \neq 0, \text{ for some } j = 1, \dots, m\}, \quad (2.25)$$

the i^{th} characteristic number [Fre75]. Each r_i is then the minimal relative degree of the set of m individual output responses y_i obtained from each input u_j for $j = 1, \dots, m$. Let

$$A(x) = \begin{bmatrix} \alpha_1(x) \\ \vdots \\ \alpha_m(x) \end{bmatrix}$$

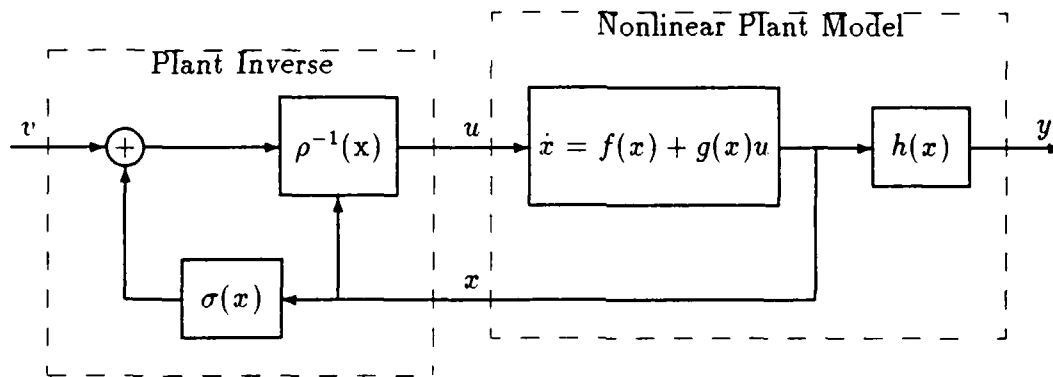


Figure 2.2: Partial Linearizing Feedback via Nonlinear Inverse Model

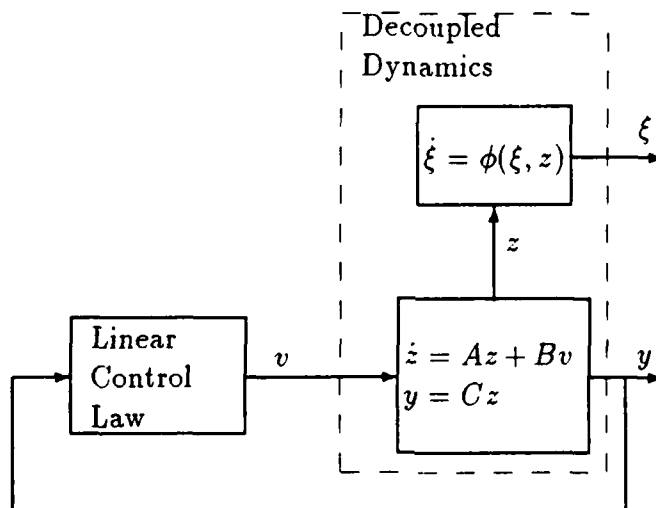


Figure 2.3: Partial Feedback Linearization and Zero Dynamics

where $\alpha_i(x) = L_f^{r_i}(h_i)$ and

$$\mathcal{B}(x) = \begin{bmatrix} \beta_{11}(x) & \cdots & \beta_{m1}(x) \\ \vdots & \ddots & \vdots \\ \beta_{m1}(x) & & \beta_{mm}(x) \end{bmatrix}$$

where $\beta_{ij}(x) = L_{g_j}(L_f^{r_i-1}(h_i))$. Then the desired normal form coordinates are $z \in \mathbb{R}^r$ where $r = \sum_{i=1}^m r_i$, which are obtained as

$$z = \begin{pmatrix} z_1 \\ z_2 \\ \vdots \\ z_m \end{pmatrix} \quad (2.26)$$

with each $z_i \in \mathbb{R}^{r_i}$ for $i = 1, \dots, m$ in the form,

$$z_i = \begin{pmatrix} h_i \\ L_f(h_i) \\ \vdots \\ L_f^{r_i-1}(h_i) \end{pmatrix}. \quad (2.27)$$

Proposition: Given the system (2.23)–(2.24), there exists a diffeomorphic transformation $(T)(x) = (z, \xi)$ to *normal form* coordinates,

$$\dot{z} = Az + E\{\mathcal{A}(z) + \mathcal{B}(z)u\} \quad (2.28)$$

$$\dot{\xi} = F(z, \xi) \quad (2.29)$$

where $A = \text{diag}\{A_1, \dots, A_m\}$ with

$$A_i = \begin{bmatrix} 0 & I_{r_i-1} \\ 0 & 0 \end{bmatrix}$$

of dimension $r_i \times r_i$ for each $i = 1, \dots, m$ and E is an $r \times m$ matrix with elements given as,

$$[E]_{ij} = \begin{cases} 1, & \text{if } i = r_i \text{ and } j = i \\ 0, & \text{otherwise} \end{cases}.$$

Then the *PLF control*,

$$u = -\mathcal{B}^{-1}(x)\{\mathcal{A}(x) - v\}, \quad (2.30)$$

renders the $v \mapsto y$ input/output response in linear form,

$$\dot{z} = Az + Ev, \quad (2.31)$$

$$y = Cz. \quad (2.32)$$

Definition: The system (2.23)–(2.24) (output constrained) *zero dynamics* are given by

$$\dot{\xi} = F(0, \xi). \quad (2.33)$$

Definition: We say the system is locally *minimum phase* if the zero dynamics are asymptotically stable to the origin $\xi = 0$.

Remark: In general the computation of the normal form with (2.29) independent of u is difficult and not required to establish the minimum phase property. Instead, note that the system *zero dynamics* are just the dynamics of (2.23)–(2.24) constrained to the manifold $\mathcal{M}_h \subseteq \mathbb{R}^n$ of dimension $n - m$ given by,

$$\mathcal{M}_h = \{x \in \mathbb{R}^n : h(x) = 0\}.$$

Proposition: The zero dynamics are asymptotically stable if and only if the system,

$$\dot{x} = f(x) - G(x)B^{-1}(x)A(x), \quad x(0) \in \mathcal{M}_h$$

is asymptotically stable to origin. We note that \mathcal{M}_h is an *integral manifold* for (2.23)–(2.24).

2.4 Partial Linearization and Variable Structure Control Systems

The theory of Variable Structure (VS) systems addresses the design of control laws which are discontinuous functions of the system state. VS control offers practical solutions for systems employing actuators which can be efficiently operated in bang-bang and other discontinuous modes. Our interest in VS control for rapid slewing of multibody systems arises from the following observations:

1. Design methods for VS control for output regulation have been shown to effect an implicit partial feedback linearization. The implicit partial linearization is achieved through the use of VS control requires only output feedback.
2. Direct implementations of VS control laws can attain a level of robustness to plant model assumptions which is difficult to achieve with smooth control. Moreover, robustness is achieved without overly conservative restrictions on performance. The limitations of robustness for VS designs are clearly related to the minimum phase conditions for PLF design.
3. The use of discontinuous control and the connections between VS and PLF designs suggest several alternatives for integration of various types of actuators, including both switched and continuous modes of operation. Integration of several control actuation systems will be required for implementation of rapid slewing requirements for several candidate large space platforms.

The general theory of VS control design is well known and we will not attempt to present a complete description of its scope. For details see the survey [DZM88]. However, to focus attention on the concepts we seek to exploit we start with a brief description of the basic ideas.

VS control systems utilize high speed switching control to drive the system trajectories toward a specified manifold called the switching surface. Given the nonlinear system (2.23), the VS control laws are of discontinuous type;

$$u_i = \begin{cases} u_i^+(x), & \text{for } s_i(x) > 0 \\ u_i^-(x), & \text{for } s_i(x) < 0 \end{cases} \quad (2.34)$$

with $s_i(x) = 0$ smooth switching surfaces chosen in the state space for each $i = 1, \dots, m$. The design approach which is preferred is based on the introduction of *sliding modes*.

Definition (sliding modes): A manifold, \mathcal{M}_s , consisting of the intersection of $p < m$ switching surfaces, $s_i(x) = 0$, with the property that $s_i \dot{s}_i < 0$ for each $i = 1, \dots, p$ in the neighborhood of almost every point in \mathcal{M}_s is called a *sliding manifold*. Under these conditions any trajectory of the system which enters \mathcal{M}_s remains confined to the manifold for a finite length of time. We call the motion on \mathcal{M}_s a *sliding mode*.

VS design methods involve a two step process: 1) design the switching surface so that once sliding is achieved the natural sliding mode achieves design objectives such as regulation, stabilization, etc., and 2) design of discontinuous control laws which achieve sliding on desired regions of the switching surfaces. The method of equivalent control is a popular approach for designing the switching surface to achieve desired sliding mode dynamics.

Given the system (2.23) and a manifold, $\mathcal{M}_s = \{x \in \mathbb{R}^n : s(x) = 0\}$, with $s : \mathbb{R}^n \rightarrow \mathbb{R}^m$ then sliding is characterized by satisfaction of the constraint equations,

$$s(x) = 0, \quad \dot{s}(x) = 0 \quad (2.35)$$

over the finite time interval, $t_1 > t > t_2$ where $s(x(t_1)) = 0$. Note that a sliding mode is an instance of an integral manifold for the closed loop system. The *equivalent control*, u_{eq} , is the control required to maintain the system trajectory within the manifold \mathcal{M}_s and is given by the condition,

$$\dot{s} = \nabla s(x) \dot{x} = \nabla s(x) \{f(x) + G(x)u_{eq}\} = 0 \quad (2.36)$$

where $\nabla s(x) = \partial s / \partial x$. Under the assumption that $\det\{\nabla s(x)G(x)\} \neq 0$ for $x \in \mathcal{M}_s$ we have,

$$u_{eq} = -[\nabla s(x)G(x)]^{-1} \nabla s(x)f(x), \quad (2.37)$$

and the motion in sliding is given by,

$$\dot{x} = \{I - G(x)[\nabla s(x)G(x)]^{-1} \nabla s(x)\} f(x), \quad s(x(t_1)) = 0. \quad (2.38)$$

Connections between the design of VS control and feedback linearizing control have received considerable attention [FH87]. The principal focus has been on the problem of synthesis of VS designs for nonlinear systems of the form (2.23) using (exact) feedback linearization. In the sequel we direct attention to the problem of output regulation. The connection we establish with PLF design also illuminates several questions relative to robustness properties of VS designs with sliding modes.

Design objective—Output Regulation. Given the system (2.23)–(2.24) where y indicates a set of regulated outputs, the control problem is to drive the outputs asymptotically to zero.

Since output regulation problem seeks to enforce the set of constraints

$$h_i(x) = 0, \quad i = 1, \dots, m,$$

asymptotically it seems reasonable that VS design could be employed. However, the naive choice $s_i(x) = h_i(x)$ leads to the complication that in general—in fact, most often— $[\nabla h(x)G(x)]$ is singular for almost all $x \in \mathbb{R}^n$. The approach suggested in [KK89] is to design sliding mode via the choice of switching surfaces relative to the normal form coordinates for (2.23)–(2.24) as given by (2.28)–(2.29).

Proposition: Given the system (2.23)–(2.24) obtain the diffeomorphic transformation given by (2.26), (2.27) to the form (2.28)–(2.29). The selection of switching surface,

$$s(z) = Kz \tag{2.39}$$

with K an $m \times m$ constant matrix, solves the output regulation problem if sliding can be achieved. In sliding the equivalent control is,

$$u_{eq} = -B(x)^{-1}KAz - B^{-1}(z)A(z) \tag{2.40}$$

and the sliding dynamics are given by the r linear equations,

$$\dot{z} = [I_r - EK]Az, \quad Kz(0) = 0 \tag{2.41}$$

Proof: The proof is given in detail in [KK89] together with a method for stabilization.

By definition, the transformation $(T)(x) \mapsto (z, \xi)$ is invertible; $(\hat{T})(z, \xi) \mapsto x$, and the switching surface $s(z) = 0$ can be reflected to the original coordinates $s(x) = 0$. The dynamics in the x coordinates are best understood in terms of the geometry. Define the m -dimensional manifolds $\mathcal{M}_s = \{x \in \mathbb{R}^n : s(x) = 0\}$ and $\mathcal{M}_h = \{x \in \mathbb{R}^n : h(x) = 0\}$. The $n - r$ dimensional manifold $\mathcal{M}_z = \{x \in \mathbb{R}^n : x = \hat{T}(0, \xi)\}$ is contained in both \mathcal{M}_s and \mathcal{M}_h .

Assume that in some neighborhood $\mathcal{D} \in \mathbb{R}^n$ a sliding mode exists on $\mathcal{D}_s = \mathcal{D} \cap \mathcal{M}_s$ which is assumed nonempty. Suppose that $\mathcal{D}_z = \mathcal{D}_s \cap \mathcal{M}_z$ is nonempty. Let α denote a bounded, stable attractor of the zero dynamics contained in \mathcal{D}_z . Assume that all trajectories in \mathcal{D}_z converge to α . Then if the initial state is sufficiently close to \mathcal{D} , the trajectory will eventually reach \mathcal{D}_s and sliding will occur. Clearly the stability of the attractor is critical to the stability of the overall design. In the sequel, we establish conditions for output regulation of multibody systems which guarantee that the zero dynamics have well defined local equilibria so that linear stability analysis of the zero dynamics is appropriate. We remark that the problem of establishing estimates for the domain of attraction in the zero dynamics is an open question.

2.5 Robust Stabilization of Nonlinear Systems

For practical implementation of PLF compensation various researchers have focused attention on conditions which guarantee robust stabilization of the nonlinear system (2.3)–(2.4) with feedback transformation of the form (2.11) by introduction of linear feedback $v = Kz$. A brief survey of the wide range of methods which have been proposed is given in [BBKA88]. In this section we focus attention on a ubiquitous assumption in most of the work on robust stabilization of nonlinear systems based on PLF compensation.

Consider the usual case for engineering design where the open loop system dynamics for (2.23)–(2.24) is given by a nominal model of the form

$$\dot{x} = f^o(x) + G^o(x)u \quad (2.42)$$

$$y = h^o(x), \quad (2.43)$$

where f^o, g_i^o are C^∞ vector fields for $i = 1, \dots, m$, defined on a manifold $\mathcal{M} \in \mathbb{R}^n$, with $f^o(0) = 0$. We assume the (true) system response can be modeled via a perturbation of the vector fields;

$$f = f^o + \Delta f, \quad G = G^o + \Delta G$$

with $\Delta f, \Delta g_i$ each C^∞ defined on \mathcal{M} and $\Delta f(0) = 0$. In [AB88] a detailed analysis is given leading to sufficient conditions on $\Delta f, \Delta G$ which—together with the assumption that (2.42) is feedback linearizable—guarantees that (2.23) is also linearizable. The conditions given are less restrictive than the usual structure matching conditions [AB87]. The structure matching conditions also play a role in establishing conditions for robust stabilization and we repeat them for convenience.

The structure matching conditions. Under the assumption that the perturbation vector fields satisfy,

$$\Delta f, \Delta g_i \in \Delta \quad (2.44)$$

where $\Delta = Sp\{g_1, \dots, g_m\}$ then any such model (2.23) is exactly linearizable—in fact, *by the same diffeomorphic transformations*. The above conditions are equivalent to the statement that the perturbations to the vector fields can be factored as:

$$\Delta f(x) = G^o(x)d_f(x), \quad (2.45)$$

$$\Delta G(x) = G^o(x)D_g(x). \quad (2.46)$$

The importance of the structure matching conditions in establishing robust stability is that under these conditions the model uncertainty—after application of PLF compensation—can be equivalently represented by a perturbation (or disturbance) at the compensated system inputs. This facilitates the design of disturbance rejection techniques using either explicitly nonlinear control designs such as Gutman [GL76] or linear control design such as in [Kra87]. To see this we summarize the construction under the assumption that $h(x) = h^o(x)$. Substitute the PLF compensation (2.30) obtained for the nominal model (2.42)–(2.43) into

the model for the true system (2.23) to obtain,

$$\begin{aligned}\dot{x} &= f^o + \Delta f + (G^o + \Delta G)\mathcal{B}^{-1}[v - \mathcal{A}] \\ &= f^o + G^o\Delta d_f + G^o(I + D_g)\mathcal{B}^{-1}[v - \mathcal{A}] \\ &= f^o + G^o\mathcal{B}^{-1}[v - \mathcal{A}] + G^o[d_f + D_g\mathcal{B}(v - \mathcal{A})].\end{aligned}\quad (2.47)$$

The model after nominal PLF compensation can (by the above assumptions) be transformed to z -coordinates defined in (2.26)–(2.27) to obtain,

$$\dot{z} = Az + E\{v + \eta\} \quad (2.48)$$

$$\dot{\xi} = F(z, \xi), \quad (2.49)$$

where

$$\eta(z, \xi, v) = [d_f(x) + D_g(x)\mathcal{B}(x)^{-1}\{v - \mathcal{A}(x)\}]|_{x=T^{-1}(z)} \quad (2.50)$$

$$= [d_f(x) - D_g(x)\mathcal{B}(x)^{-1}\mathcal{A}(x)]|_{x=T^{-1}(z)} + [D_g(x)\mathcal{B}(x)^{-1}v]|_{x=T^{-1}(z)}. \quad (2.51)$$

Thus it is clear that robust stabilization must address the disturbance rejection of the class of input disturbances $d_v(t)$ which bound the model error; $\|\eta\| \leq \|d_v\|$. An effective design approach, in the case when the nominal model is exactly feedback linearizable, is given by Spong and Vidyasagar [SV87]. Their approach utilizes an L_∞ stabilization criterion and obtains a linear, time-invariant feedback control for the v -input.

Remarks: The design methods for robust stabilization of nonlinear systems available in the literature are almost exclusively based on the structure matching conditions. By reflecting the model uncertainty to the system inputs (after nonlinear feedback compensation) they can employ either:

1. linear compensator design which seeks to reduce loop gains consistent with bounded model uncertainty, or
2. nonlinear switching mode compensator design which seeks to over-bound input disturbances by high gain implementations using fast switching control.

Both methods result in essentially conservative designs since the worst case bounds on the input disturbances must be assumed.

In [Akh89] the basis for robust stabilization of nonlinear systems is considered further and new results are obtained for the case of parametric model uncertainty. The new control laws obtained in [Akh89] employ *basic constructions of adaptive control in the context of feedback linearization*. The results show that robust stabilization can be obtained under much less restrictive conditions than the structure matching conditions. Significantly, feedback linearization plays the role of enforcing linearity for subsequent control loop designs. To the extent that this can be achieved in practical applications it can enhance reliability and repeatability thus achieving improved performance prediction—an important feature for space-based systems. Standard constructs in adaptive control can then be applied to

enhance the robustness of feedback linearization with model uncertainty. We emphasize that the constructions described below are new and offer stability results for the nonlinear system under very general assumptions. In the next few paragraphs we briefly review some significant aspects of these results.

Robust Stabilization of Nonlinear Systems by Adaptive Methods. Again, starting with the system model in the form (2.23) we assume the model uncertainty can be represented by parametric dependence of the vector fields so that the model has the form,

$$\dot{x} = f(x, \theta) + G(x, \theta)u, \quad (2.52)$$

with θ a p -vector of unknown parameters. We assume that for every $\theta \in B_\theta$, a closed, compact neighborhood of the nominal parameter θ_o , f and g_i , for $i = 1, \dots, m$, are C^∞ vector fields and $f(0, \theta) = 0$ for $\theta \in B_\theta$. The nominal design model is characterized by the set of nominal parameters and we take $f(x) = f(x, \theta_o)$, $G(x) = G(x, \theta_o)$.

The following assumptions are used in [Akh89] to establish a robust stabilizing controller for the nonlinear system.

Assumption 1: The nominal system is exactly feedback linearizable.¹

It is important to note that assumption 1 is applied only at the nominal plant model with fixed and known parameters θ_o . This is in contrast to the structure matching conditions which are almost universally assumed in the current literature.

Assumption 2: For any $x \in U \subseteq \mathbb{R}^n$ and $\theta \in B_\theta$,

$$\Delta g_i(x, \theta) \in \text{Sp} \{g_1(x, \theta_o), \dots, g_m(x, \theta_o)\}$$

for $i = 1, \dots, m$. This assumption implies that there exists an $m \times m$ matrix valued function, $D(x, \theta)$, with smooth elements such that $\Delta G = G^\circ D$.

Assumption 3: Either there exists an $m \times m$, strictly positive definite matrix, K such that,

$$\forall x \in U, \forall \theta \in B_\theta, \quad 0 \leq D(x, \theta) \leq K,$$

or there exist a K , negative definite, such that,

$$\forall x \in U, \forall \theta \in B_\theta, \quad K \leq D(x, \theta) \leq 0.$$

This assumption (in various forms) is typical in adaptive control stability analysis and design. It says that the "sign" of this term must be definite and known *a priori*.

The design approach is natural and begins with the transformation

$$z = T(x, \theta_o),$$

¹The extension of the results described below to the case of stabilization by PLF is in progress.

to normal form and choice of feedback linearizing compensation (2.30). The v control is chosen in two parts. First, for the nominal design and performance objectives we find $v = Fz$ where $A + EF$ in (2.31) is a stable matrix. In this case, there exists a unique, positive definite, symmetric solution to the Lyapunov equation,

$$(A + EF)^T P + P(A + EF) = -I.$$

The design for the nominal model is now modified by the introduction of adaptation. The control law obtained is described by the following equations;

$$u = -B^{-1}(x)\{A(x) - v\}, \quad (2.53)$$

$$z = T(x, \theta_o), \quad (2.54)$$

$$v = Fz + C(z, \hat{\theta})\hat{\theta}, \quad (2.55)$$

$$\dot{\hat{\theta}} = -\Gamma^{-1}C^T(z, \hat{\theta})E^T Pz, \quad (2.56)$$

$$C(z, \hat{\theta}) = -\mu B(z)G^T(z, \theta_o)Pz\hat{\theta}^T. \quad (2.57)$$

In these control laws the $p \times p$ matrix $\Gamma > 0$ is the "adaptation gain" which is chosen so that the Lyapunov function,

$$V = z^T Pz + \hat{\theta}^T \Gamma \hat{\theta}$$

is positive definite for all $x \in U$ and μ is a positive scalar. The result established in [Akh89] is the following.

Theorem: The adaptive control with feedback linearizing transformation is asymptotically stable to the origin $x = 0$ and $\hat{\theta} \rightarrow \theta$, asymptotically, if for $x \in U$ and $\theta \in B_\theta$ there exists $c_2 > 1$ and

$$2\|T^T(x)P\Psi(x, \theta) - \mu y^T D y\|\|\hat{\theta}\|^2 \leq c_2\|T(x)\|^2,$$

where

$$\Psi(x, \theta) = [\Delta f(z, \theta) + \Delta G(z, \theta)\{A(z) + B^{-1}Fz\}]$$

and

$$y = G^T(z, \theta_o)P^T z.$$

Proof: [Akh89].

2.6 Partial Linearization for Lagrangian Systems

Despite the apparent simplicity of determining the zero dynamics from the normal form as above it is, however, quite complex to compute the complete transformation leading to the full state normal form as given above. One approach (if possible) is to obtain the full state exact linearizing transformation via the procedure given by Hunt, Su, and Meyer [HSM83] which requires the solution of a set of simultaneous partial differential equations. However, in many special cases the zero dynamics as well as the required transformations for partial linearizing control can be obtained more directly. In the sequel we discuss the required constructions for Lagrangian systems.

Consider the case of a square Lagrangian system with inputs $\tau \in \mathbb{R}^m$ and outputs $y \in \mathbb{R}^m$. Suppose that the n generalized coordinates can be partitioned into components $q_1 \in \mathbb{R}^m$ and $q_2 \in \mathbb{R}^{n-m}$ so that the equations of motion take the form

$$\frac{d}{dt} \frac{\partial L}{\partial \dot{q}_1} - \frac{\partial L}{\partial q_1} = \tau, \quad (2.58)$$

$$\frac{d}{dt} \frac{\partial L}{\partial \dot{q}_2} - \frac{\partial L}{\partial q_2} = 0, \quad (2.59)$$

$$y = h(q_1, q_2). \quad (2.60)$$

Assume that the origin is an equilibrium point with $\tau = 0$, $h(0, 0) = 0$, and that the Jacobian $\partial h / \partial q_1$ is nonsingular on some neighborhood of the origin. Furthermore, we assume that the Lagrangian is a positive definite quadratic form in the generalized velocities. Then the input-output map ($\tau \rightarrow y$) has relative degree 2 (locally), a PLF control exists and the zero dynamics may be computed by a relatively simple coordinate transformation applied to (2.58)–(2.60).

In order to demonstrate these properties we introduce a change of coordinates $(q_1, q_2) \mapsto (y, u)$ via the relations

$$y = h(q_1, q_2), \quad u = q_2 \quad (2.61)$$

Note that the assumption $\det \partial h / \partial q_1 \neq 0$ at the origin assures that this is a valid local coordinates transformation and the inverse relations can be given as

$$q_1 = g(y, u), \quad q_2 = u. \quad (2.62)$$

Since any "point" transformation preserves the Lagrangian structure of the equations, in the new coordinates we can write the variational problem in the form

$$\frac{d}{dt} \frac{\partial \hat{L}}{\partial \dot{y}} - \frac{\partial \hat{L}}{\partial y} = \hat{\Gamma}_y \tau, \quad (2.63)$$

$$\frac{d}{dt} \frac{\partial \hat{L}}{\partial \dot{u}} - \frac{\partial \hat{L}}{\partial u} = \hat{\Gamma}_u \tau, \quad (2.64)$$

where

$$\hat{L}(y, \dot{y}, u, \dot{u}) = L(q_1, \dot{q}_1, q_2, \dot{q}_2) \Big|_{\substack{q_1 = g(y, u) \\ q_2 = u}} \quad (2.65)$$

and

$$\hat{\Gamma}_y = \left[\frac{\partial g}{\partial y} \right]^T, \quad \hat{\Gamma}_u = \left[\frac{\partial g}{\partial u} \right]^T. \quad (2.66)$$

Equations (2.63)–(2.64) reduce to the form

$$\hat{J}_y \ddot{y} + \hat{N} \ddot{u} + \hat{K}_y(y, \dot{y}, u, \dot{u}) = \hat{\Gamma}_y \tau, \quad (2.67)$$

$$\hat{N}^T \ddot{y} + \hat{J}_u \ddot{u} + \hat{K}_u(y, \dot{y}, u, \dot{u}) = \hat{\Gamma}_u \tau. \quad (2.68)$$

Let us define the partitioned matrices $\Sigma_y, \Sigma_u, \Phi_y, \Phi_u$, via the relations

$$\begin{pmatrix} \Sigma_y \\ \Sigma_u \end{pmatrix} = \begin{bmatrix} \hat{J}_y & \hat{N} \\ \hat{N}^T & \hat{J}_u \end{bmatrix}^{-1} \begin{pmatrix} \hat{K}_y \\ \hat{K}_u \end{pmatrix} \quad (2.69)$$

and

$$\begin{pmatrix} \Phi_y \\ \Phi_u \end{pmatrix} = \begin{bmatrix} \hat{J}_y & \hat{N} \\ \hat{N}^T & \hat{J}_u \end{bmatrix}^{-1} \begin{pmatrix} \hat{\Gamma}_y \\ \hat{\Gamma}_u \end{pmatrix}. \quad (2.70)$$

Note the choice of control

$$\tau = \Phi_y^{-1} \{ \Sigma_y + v \} \quad (2.71)$$

reduces (2.67)-(2.68) to

$$\ddot{y} = v \quad (2.72)$$

$$\hat{N}^T(y, u) \ddot{y} + \hat{J}_u(y, u) \ddot{u} + \hat{K}(y, \dot{y}, u, \dot{u}) = \hat{\Gamma}_u(y, u) \Phi_y^{-1}(y, u) \{ \Sigma_y(y, u) + v \} \quad (2.73)$$

where we have explicitly displayed the dependence of the model parameters on the generalized coordinates. Equation (2.72) provides the linearized input-output dynamics and the zero dynamics are obtained from (2.73) upon setting $y(t) = 0$, which implies $\dot{y} = 0, \ddot{y} = 0$, and $v = 0$. Thus, we obtain the zero dynamics in the form

$$\hat{J}_u(0, u) \ddot{u} + \hat{K}(0, 0, u, \dot{u}) - \hat{\Gamma}_u(0, u) \Phi_y^{-1}(0, u) \Sigma_y(0, u) = 0 \quad (2.74)$$

which represents an autonomous nonlinear dynamical system in the state coordinates u, \dot{u} . We say the system is *locally minimum phase* if the origin in the (u, \dot{u}) coordinates is a stable equilibrium for (2.74). If the system is minimum phase then selecting the control v to stabilize the origin of (2.72) guarantees stability of the origin of the dynamical system (2.58)-(2.60). Thus the computational complexity of obtaining the zero dynamics depends on the complexity of the required inverse relation g in (2.62).

3 Reduced Order Modeling of Multibody Systems and Nonlinear Control Design

The approach described in [BBKA88] to obtain finite dimensional models for multibody systems with elastic interactions utilizes *Finite Element Methods (FEM)* based on the method of collocation by splines. In this section we focus attention on a system model for attitude re-orientation including a primary set of rigid bodies whose attitude relative to an inertial frame is given by a set of attitude parameters $x_r = \xi_b \in \mathbb{R}^{n_b}$. The system model includes spatially distributed elastic interactions with FEM deformation coordinates, $x_s = (\bar{\eta}^T, \bar{\xi}^T)^T \in \mathbb{R}^{2n_s}$.

After some manipulation, the general class of multibody systems we will consider can be written in the generic form,

$$M_r(x_r, x_s)\ddot{x}_r + N\ddot{x}_s + K_r(x_r, \dot{x}_r, x_s, \dot{x}_s) = \tau_b \quad (3.1)$$

$$M_s(x_r, x_s)\ddot{x}_s + N^T\ddot{x}_r + K_s(x_r, \dot{x}_r, x_s, \dot{x}_s) = Gf_s, \quad (3.2)$$

where $\tau_b \in \mathbb{R}^{n_b}$ are independent torques applied to rigid bodies and $f_s \in \mathbb{R}^{2k}$ are generalized forces acting on the flexible structure. By virtue of the collocation FEM model coordinates we note that the influence of structural control enters through the $2n_s \times 2k$ matrix,

$$G = \begin{bmatrix} G_f & 0 \\ 0 & G_m \end{bmatrix}$$

where G_f, G_m are $n_s \times k$ with elements given by,

$$[G_f]_{ij} = \begin{cases} 1 & \text{if at } z = z_i \text{ control force } f_j \text{ is applied,} \\ 0 & \text{else} \end{cases} \quad (3.3)$$

$$[G_m]_{ij} = \begin{cases} 1 & \text{if at } z = z_i \text{ control moment } m_j \text{ is applied,} \\ 0 & \text{else} \end{cases} \quad (3.4)$$

As a result there exists a $n_s \times n_s$ nonsingular permutation V_s such that

$$V_s G = \begin{bmatrix} I_{2k} \\ 0 \end{bmatrix},$$

which defines a change of basis for the structural deformation coordinates,

$$\bar{x}_s := V_s^T x_s = \begin{pmatrix} \bar{x}_{s,1} \\ \bar{x}_{s,2} \end{pmatrix},$$

with $\bar{x}_{s,1} \in \mathbb{R}^{2k}$, $\bar{x}_{s,2} \in \mathbb{R}^{2(n_s-k)}$. The model can then be decomposed as,

$$M_r(x_r, \bar{x}_s)\ddot{x}_r + \bar{N}_1\ddot{\bar{x}}_{s,1} + \bar{N}_2\ddot{\bar{x}}_{s,2} + \bar{K}_r(x_r, \dot{x}_r, \bar{x}_s, \dot{\bar{x}}_s) = \tau_b, \quad (3.5)$$

$$\bar{M}_{s,11}\ddot{\bar{x}}_{s,1} + \bar{M}_{s,12}\ddot{\bar{x}}_{s,2} + \bar{N}_1^T\ddot{x}_r + \bar{K}_{s,1}(x_r, \dot{x}_r, \bar{x}_s, \dot{\bar{x}}_s) = f_s, \quad (3.6)$$

$$\bar{M}_{s,21}\ddot{\bar{x}}_{s,1} + \bar{M}_{s,22}\ddot{\bar{x}}_{s,2} + \bar{N}_2^T\ddot{x}_r + \bar{K}_{s,2}(x_r, \dot{x}_r, \bar{x}_s, \dot{\bar{x}}_s) = 0. \quad (3.7)$$

Let $m = n_b + 2k$ and introduce the definitions,

$$f := \begin{pmatrix} \tau_b \\ f_s \end{pmatrix}, \quad \xi_1 := \begin{pmatrix} x_r \\ \bar{x}_{s,1} \end{pmatrix}, \quad \xi_2 := \bar{x}_{s,2}.$$

Then we can write the model (3.5)–(3.7) in the simplified form,

$$M_{11}\ddot{\xi}_1 + M_{12}\ddot{\xi}_2 + K_1(\xi, \dot{\xi}) = f, \quad (3.8)$$

$$M_{21}\ddot{\xi}_1 + M_{22}\ddot{\xi}_2 + K_2(\xi, \dot{\xi}) = 0. \quad (3.9)$$

To illustrate the practical simplicity of decoupling control computations and the fundamental design issues we focus attention on a m -vector of *independent* system outputs consisting of linear combination of deformation coordinates,

$$y = [C_1, C_2] \begin{pmatrix} \xi_1 \\ \xi_2 \end{pmatrix}, \quad (3.10)$$

where $C = [C_1, C_2]$ is constant, $m \times n$ matrix with $n = n_b + 2n_s$. Without loss of generality we assume the $m \times m$ matrix C_1 is nonsingular. To identify the specific form of decoupling control for this special case we rewrite (3.8)–(3.9) in y -coordinates (3.10);

$$M_{11}C_1^{-1}\ddot{y} + (M_{12} - M_{11}C_1^{-1}C_2)\ddot{\xi}_2 + K_y(y, \dot{y}, \xi_2, \dot{\xi}_2) = f, \quad (3.11)$$

$$M_{21}C_1^{-1}\ddot{y} + (M_{22} - M_{21}C_1^{-1}C_2)\ddot{\xi}_2 + K_2(y, \dot{y}, \xi_2, \dot{\xi}_2) = 0. \quad (3.12)$$

It is then straightforward to identify the required decoupling control;

$$f = K_y + (M_{12} - M_{11}C_1^{-1}C_2)\ddot{\xi}_2 + M_{11}C_1^{-1}u. \quad (3.13)$$

Applying the decoupling control (3.13) obtains the first m degrees of freedom (3.11) in decoupled, linearized coordinates with synthetic control in 'acceleration coordinates';

$$\ddot{y} = u. \quad (3.14)$$

The remaining $n - m$ degrees of freedom (3.12) comprise the dynamics which are then decoupled from the output. We note that the ξ_2 coordinates will be driven by the synthetic control u . However, for most practical designs the principal consideration is for the stability of the zero-output constrained dynamics in ξ_2 ; i.e., the *system zero dynamics*. Here the zero dynamics are readily identified from (3.12) with $\ddot{y} = \dot{y} = y = 0$;

$$(M_{22} - M_{21}C_1^{-1}C_2)\ddot{\xi}_2 + K_2(0, 0, \xi_2, \dot{\xi}_2) = 0. \quad (3.15)$$

The form of (3.15) is significant since PFL/decoupling is feasible only if the zero dynamics are stable in an appropriate sense. In this study we take rapid slewing to be a 'rest-to-rest' maneuver. At the end of the maneuver we will require precision pointing; i.e., structural alignment. Thus we focus attention on asymptotic stability of the structural alignment state; i.e., $\xi_2 = 0, \dot{\xi}_2 = 0$ in (3.15). As seen from (3.15), a general choice of outputs as linear combination of the deformation coordinates together with the primary body attitude coordinates may lead to nonlinear, possibly unstable zero dynamics.

For various practical considerations we focus attention on implementation of decoupling control for the special choice of *outputs collocated with the control forces*; i.e.,

$$y = [I_{n_b}, C^T] \begin{pmatrix} x_r \\ x_s \end{pmatrix} = [I_m, 0] \begin{pmatrix} \xi_1 \\ \xi_2 \end{pmatrix}. \quad (3.16)$$

This choice of outputs for decoupling will obtain the zero dynamics in the form,

$$M_{22}\ddot{\xi}_2 + K_2(0, 0, \xi_2, \dot{\xi}_2) = 0. \quad (3.17)$$

More importantly, our assumptions on elastic potential energy for the structural deformation [BBKA88] focuses attention on small amplitude deformation dynamics and we have,

$$K_s(x_r, \dot{x}_r, x_s, \dot{x}_s) = B_c \dot{x}_s + K_c x_s + D(x_r, \dot{x}_r, x_s, \dot{x}_s) \quad (3.18)$$

with $D : \mathbb{R}^n \rightarrow \mathbb{R}^N$ with $D = 0$ for $\dot{x}_r = 0$ (i.e., when the rigid body is at rest), and B_c, K_c constant, positive semidefinite matrices (see Section 5.1). Under these assumptions it is easy to show that (3.17) is a set of $n - m$ linear, second order equations for the structural deformation dynamics constrained at the physical output locations given by (3.10); i.e., the structural dynamics with certain combinations of localized pinned and/or cantilevered supports. Thus stability properties of the zero dynamics for the case of outputs collocated with the control forces follow from the natural structural properties of stiffness and damping.

3.1 PFL with Reduced Order Models

In this section we will outline general considerations for implementation of PFL via nonlinear partial state feedback. Considerations for rapid slewing of flexible space structures suggest that the relative stiffness of the structure by comparison with the severity of the maneuver dynamics will dominate the complexity of the process model for control design. In addition to nonlinear couplings the distributed parameter nature of the structural deformation suggests that time scaling via singular perturbation methods be applied. In the previous section we described nonlinear controller realization which achieves exact decoupling using full state feedback. We remark that considerations for good mechanical design suggest that space systems designed for rapid slewing maneuvers will be structurally stiff [Le87]. Considerable attention has been given to the use of composite material for enhanced damping and stiffness properties of such structures [RR87]. However, a primary system cost for any space system is mass and the resulting constraints on system mass will ultimately limit structural stiffness. Our models have been configured to represent generic considerations for rapid slewing of space structures but have been scaled to focus dynamic effects expected to dominate behavior of optical systems such as the SBL.

In previous studies where the singular perturbation approach was used [Dwy88, KO88], a scaling parameter ϵ was introduced as a measure of the system compliance; for example, Dwyer [Dwy88] considers $\epsilon = \frac{1}{\omega_1^2}$ while dimensionless scaling of the form $\epsilon = \frac{\omega_0^2}{\omega_n^2}$ [KO88], is more often chosen. In both cases, scaling is chosen relative to ω_1 , the lowest modal frequency due to the structural flexure, and ω_0 , the natural frequency of the rigid system. For relatively stiff systems the scaling leads to $\epsilon < 1$. Using standard singular perturbation approach, the dynamics of the system can then be approximated by the dynamics of the reduced slow subsystem (i.e., rigid body dynamics).

We have considered a slightly different time scale separation which identifies a reduced order model; viz., a *quasi-rigid model*. The dynamics of the quasi-rigid model do not coincide necessarily (as in previous time scale separations) with the rigid body dynamics. The *slow*

modes will consist of the rigid body modes together with an arbitrary number, p , of low frequency flexure modes. The *fast* modes will consist of the remaining (higher frequency) flexure modes. Thus we can study the tradeoff of model order reduction vs. decoupling performance directly.

We assume that any structure designed for repeated rapid slewing will be relatively stiff and we investigate the obvious time scale decomposition of (3.1)–(3.2) as follows. We assume that M_s is positive definite and K_c , B_c in (3.18) are each positive semidefinite. To obtain appropriate time scaling we transform (3.1)–(3.2) to modal coordinates as follows. Under the above assumptions there exists a nonsingular matrix P such that:

$$P^T M_s P = I_{n_s} \quad \text{and} \quad P^T K_c P = \bar{K}$$

where $\bar{K} = \text{diag}(\omega_1^2, \dots, \omega_{n_s}^2)$ with $\omega_1 < \omega_2 < \dots < \omega_{n_s}$. We also assume P is such that

$$P^T B_c P = \bar{B}$$

where \bar{B} is a diagonal matrix.

Note that $\bar{x}_f = P^T x_s$ transforms (3.1), (3.2) from displacement coordinates x_s into modal coordinates \bar{x}_f ;

$$\bar{M}(x_r, \bar{x}_f) \ddot{x}_r + \bar{N}^T \ddot{\bar{x}}_f + \bar{K}_r(x_r, \dot{x}_r, \bar{x}_f, \dot{\bar{x}}_f) = \tau_b \quad (3.19)$$

$$\ddot{\bar{x}}_f + \bar{N} \ddot{x}_r + \bar{B}_c \dot{\bar{x}}_f + \bar{K}_c \bar{x}_f + \bar{D}(x_r, \dot{x}_r, \bar{x}_f, \dot{\bar{x}}_f) = \bar{G} f_s \quad (3.20)$$

where

$$\begin{aligned} \bar{D} &= P^T D(x_r, \dot{x}_r, P^T x_s, P^T \dot{x}_s) P, \\ \bar{N} &= NP, \quad \bar{G} = P^T G, \quad \bar{M}(x_r, \bar{x}_f) = M_r(x_r, P^T x_s) \end{aligned}$$

and

$$\bar{K}_r(x_r, \dot{x}_r, \bar{x}_f, \dot{\bar{x}}_f) = K_r(x_r, \dot{x}_r, P^T x_s, P^T \dot{x}_s). \quad (3.21)$$

In the sequel the overbars will be omitted and we assume the model is given in modal coordinates, (3.19)–(3.20).

Time scale decomposition is obtained by identifying a separation between the first p low order modes, $\omega_1^2, \dots, \omega_p^2$ from the remaining higher modal frequencies $\omega_{p+1}^2, \dots, \omega_{n_s}^2$. The separation above induces a decomposition of the state x_f as:

$$x_f = \begin{bmatrix} x_f^0 \\ x_f^1 \end{bmatrix}, \quad x_f^0 \in R^p, \quad x_f^1 \in R^{n_s-p},$$

with the corresponding decomposition for the matrices N , G , K_c , B_c and D being

$$N = [N_0^T, N_1^T]^T, \quad \text{with} \quad N_0 \in R^p, \quad N_1 \in R^{n_s-p} \quad (3.22)$$

$$G = [G_0^T, G_1^T]^T, \quad \text{with} \quad G_0 \in R^{p \times 2k}, \quad G_1 \in R^{(n_s-p) \times m} \quad (3.23)$$

$$K_c = \begin{pmatrix} K_0 & 0 \\ 0 & K_1 \end{pmatrix}, \quad \text{with} \quad K_0 \in R^{p \times p}, \quad K_1 \in R^{(n_s-p) \times (n_s-p)} \quad (3.24)$$

$$B_c = \begin{pmatrix} B_0 & 0 \\ 0 & B_1 \end{pmatrix}, \quad \text{with} \quad B_0 \in R^{p \times p}, \quad B_1 \in R^{(n_s-p) \times (n_s-p)} \quad (3.25)$$

$$D(x_r, \dot{x}_r, x_f, \dot{x}_f) = \begin{pmatrix} D_1 \\ D_2 \end{pmatrix} (x_r, \dot{x}_r, x_f, \dot{x}_f), \quad (3.26)$$

with $D_1: \mathbb{R}^n \rightarrow \mathbb{R}^p$, $D_2: \mathbb{R}^n \rightarrow \mathbb{R}^{n*}$.

With this decomposition, (3.20) becomes:

$$\ddot{x}_f^0 + N_0 \ddot{x}_r + B_0 \dot{x}_f^0 + K_0 x_f^0 + D_1(x_f^0, \dot{x}_f^1) = G_1 f_s, \quad (3.27)$$

$$\ddot{x}_f^1 + N_1 \ddot{x}_r + B_1 \dot{x}_f^1 + K_1 x_f^1 + D_2(x_f^0, \dot{x}_f^1) = G_2 f_s. \quad (3.28)$$

By assumption the modal frequencies $\omega_{p+1}^2, \dots, \omega_n^2$ are of the same (large) order of magnitude and we can express them as multiples of $1/\epsilon$ with $\epsilon = \frac{\omega_1^2}{\omega_{p+1}^2}$. Thus the stiffness, $K_1 = \text{diag}(\omega_{p+1}^2, \omega_{p+2}^2, \dots)$, can be scaled as:

$$K_1 = \frac{1}{\epsilon} K_{10}, \quad (3.29)$$

and the "fast time" state, x_f^1 , will satisfy,

$$x_f^1 = \epsilon z \quad \text{where} \quad z \sim O(1). \quad (3.30)$$

Substituting (3.27), (3.28), (3.29) and (3.30) into (3.19), (3.20) yields the standard form for singular perturbation analysis;

$$M_r(x_r, x_f^0, \epsilon z) \ddot{x}_r + N_0^T \ddot{x}_f^0 + \epsilon N_1^T \ddot{z} + K_r(x_r, \dot{x}_r, x_f^0, \dot{x}_f^0, \epsilon z, \epsilon \dot{z}) = \tau_b \quad (3.31)$$

$$\ddot{x}_f^0 + N_0 \ddot{x}_r + B_0 \dot{x}_f^0 + K_0 x_f^0 + D_1(x_r, \dot{x}_r, x_f^0, \dot{x}_f^0, \epsilon z) = G_1 f_s, \quad (3.32)$$

$$\epsilon[\ddot{z} + B_1 \dot{z}] + N_1 \ddot{x}_r + D_2(x_r, \dot{x}_r, x_f^0, \dot{x}_f^0, \epsilon z) + K_{10} z = G_2 f_s. \quad (3.33)$$

The reduced state consists of the rigid state, x_r , and a p -dimensional part of the flexible state for the elastic structural deformation.

3.1.1 Quasi-Rigid Model

The singular perturbation approach models the time responses as decomposed into slow time or quasi-steady state and boundary layer terms. Neglecting the boundary layer amounts to letting $\epsilon \rightarrow 0$ and the resulting *slow subsystem* is:

$$M_0(x_r, x_f^0) \ddot{x}_r + N_0^T \ddot{x}_f^0 + K_r^0(x_r, \dot{x}_r, x_f^0, \dot{x}_f^0) = \tau_b, \quad (3.34)$$

$$\ddot{x}_f^0 + N_0 \ddot{x}_r + B_0 \dot{x}_f^0 + K_0 x_f^0 + D_1^0(x_r, \dot{x}_r, x_f^0, \dot{x}_f^0) = G_1 f_s, \quad (3.35)$$

$$N_1 \ddot{x}_r + K_{10} z + D_2^0(x_r, \dot{x}_r, x_f^0, \dot{x}_f^0) = G_2 f_s, \quad (3.36)$$

where

$$M_0(x_r, x_f^0, \epsilon z) = M(x_r, x_f^0, 0)$$

and

$$K_r^0(x_r, \dot{x}_r, x_f^0, \dot{x}_f^0, \epsilon z, \epsilon \dot{z}) = K_r(x_r, \dot{x}_r, x_f^0, \dot{x}_f^0, 0, 0).$$

The dimension of the state space is thus reduced from $2(n_r + n_s)$ to $2(n_r + p)$ and we identify the *quasi-rigid model* in the form

$$\mathcal{M}_0(x_r, x_f^0) \begin{pmatrix} \ddot{x}_r \\ \ddot{x}_f^0 \end{pmatrix} + C_0(x_r, \dot{x}_r, x_f^0, \dot{x}_f^0) = E \begin{pmatrix} \tau_b \\ f_s \end{pmatrix} \quad (3.37)$$

where

$$\mathcal{M}_0(x_r, x_f^0) = \begin{pmatrix} M_0(x_r, x_f^0) & N_0^T \\ N_0 & I_p \end{pmatrix}, \quad (3.38)$$

$$C_0(x_r, \dot{x}_r, x_f^0, \dot{x}_f^0) = \begin{pmatrix} K_r^0(x_r, \dot{x}_r, x_f^0, \dot{x}_f^0) \\ B_0 \dot{x}_f^0 + K_0 x_f^0 + D_1^0(x_r, \dot{x}_r, x_f^0, \dot{x}_f^0) \end{pmatrix}, \quad (3.39)$$

$$E = \begin{pmatrix} I_n & 0 \\ 0 & G_1 \end{pmatrix}. \quad (3.40)$$

By assumption K_{10} is nonsingular and the $n_s - p$ algebraic equations (3.36) yields the following expression for z in terms of $x_r, \dot{x}_r, x_f^0, \dot{x}_f^0$ and τ_b :

$$\begin{aligned} z &= -K_{10}^{-1} [D_2^0(x_r, \dot{x}_r, x_f^0, \dot{x}_f^0) + N_1 \ddot{x}_r - G_2 f_s], \\ &= -K_{10}^{-1} [D_2^0(x_r, \dot{x}_r, x_f^0, \dot{x}_f^0) + N_1 (M_0 - N_0 N_0^T)^{-1} \{ \tau_b - K_r^0(x_r, \dot{x}_r, x_f^0, \dot{x}_f^0) \\ &\quad + N_0^T (B_0 \dot{x}_f^0 + K_0 x_f^0 + D_1^0(x_r, \dot{x}_r, x_f^0, \dot{x}_f^0) - G_1 f_s) \} - G_2 f_s]. \end{aligned} \quad (3.41)$$

Equation (3.41) defines a $2(n_r + p)$ -dimensional manifold M_0 in the $2(n_r + n_s)$ dimensional state space called the *slow manifold*.

The quasi-rigid model (3.37) approximates the slow response as a *quasi-steady-state* for the full model (3.31)–(3.33). The difference between the response of the quasi-rigid model and that of the full model (3.31)–(3.33) is given by a *boundary-layer system* which is obtained as follows. Let z_f be the fast time scale part of z (i.e., in the *stretched* time scale $\tau = \frac{t}{\sqrt{\epsilon}}$). Then the *fast time scale system* is;

$$\frac{d^2 z_f}{d\tau^2} + B_{10} \frac{dz_f}{d\tau} + K_{10} z_f = G_2 f_s^f \quad (3.42)$$

where the B_{10} is obtained via the appropriate scaling of the damping; $B_1 = \sqrt{\epsilon} B_{10}$.

The trajectories of the full system (3.31)–(3.33) can be approximated by examining the solutions of the quasi-rigid model (3.37). The approximation is $O(\epsilon)$ under the assumption that the fast subsystem (3.42) is asymptotically stable. For ϵ small (i.e., sufficient separation of adjacent modal frequencies) stability of the boundary layer must be obtained by inherent damping or by the introduction of fast time scale (wide bandwidth) control f_s^f . This analysis suggests the alternatives for material damping vs. active control will be significant in achieving robust high performance nonlinear decoupling control. The role of stabilization of the boundary layer is in improving the approximation offered by model order reduction. The forces required are relatively weak but of wide bandwidth. They can, in principle, be generated by internal material properties deliberately introduced through the use of passive damping or by active control using imbedded actuators.

3.1.2 The reduced flexible model

In analyzing the qualitative robustness of nonlinear decoupling and PFL we may require refinements of the quasi-steady state analysis described above. In this section, we describe alternatives for refined reduced order modeling by application of the method of integral manifolds. Following [KKO86], we note that the solutions $x(t, \epsilon), z(t, \epsilon)$ of (3.30)–(3.32) consist of a fast boundary layer and a slow quasi-steady-state. The boundary layer is significant only in $z(t, \epsilon)$ since $x(t, \epsilon)$ is predominantly slow and its boundary layer is no larger than $O(\epsilon)$. As we have seen in the previous section, (3.41), obtained for $\epsilon = 0$, defines a $2(n_s + p)$ -dimensional manifold, $M_0 \subseteq \mathbb{R}^n$. For nonzero ϵ , we define a $2(n_s + p)$ -dimensional manifold, $M_\epsilon \subseteq \mathbb{R}^n$, depending on the scalar parameter ϵ by

$$M_\epsilon = \left\{ \begin{pmatrix} z \\ \dot{z} \end{pmatrix} \in \mathbb{R}^n : z = h(x, \dot{x}, \tau_b, f_s, \epsilon), \dot{z} = \dot{h}(x, \dot{x}, \tau_b, f_s, \epsilon) \right\}, \quad (3.43)$$

where it is assumed that h is continuously differentiable sufficiently many times in all of its arguments. The manifold M_ϵ is said to be an *integral manifold* for the system (3.44)–(3.30) if, for given initial conditions $x(0), \dot{x}(0), z(0), \dot{z}(0)$ in M_ϵ , then the trajectories $x(t), z(t)$ are in M_ϵ for all $t > 0$. Following [KKO86], it follows that the existence of a stable equilibrium manifold M_0 of (3.34)–(3.36) for $\epsilon = 0$ (since K_{10} is nonsingular), implies the existence of an integral manifold M_ϵ of (3.31)–(3.33). When the fast dynamics (3.42) are asymptotically stable, then if $z(0), \dot{z}(0)$ are not initially in M_ϵ , z will converge to M_ϵ after the decay of a fast transient; z_f . Thus the response $x(t)$ of the full system (3.31)–(3.33) will rapidly approach M_ϵ and then flow along M_ϵ . As $\epsilon \rightarrow 0$, the manifold M_ϵ converges to M_0 .

By definition, the function h defining the integral manifold in (3.43), satisfies (3.33)—the manifold condition;

$$\epsilon [\ddot{h} + B_1 \dot{h}] + N_1 \ddot{x}_r + K_{10} h + D_2(x_r, \dot{x}_r, x_f^0, \dot{x}_f^0, \epsilon h, \epsilon \dot{h}) = G_2 f_s. \quad (3.44)$$

Solving for h in (3.44), then by replacing z by h and \dot{z} by \dot{h} in (3.31)–(3.32), we obtain the *reduced flexible model* [SKK87]:

$$M_r(x_r, \epsilon h) \ddot{x}_r + N_0^T \ddot{x}_f^0 + \epsilon N_1^T \ddot{h} + K_r(x_r, \dot{x}_r, \epsilon h, \epsilon \dot{h}) = \tau_b \quad (3.45)$$

$$\ddot{x}_f^0 + N_0 \ddot{x}_r + B_0 \dot{x}_f^0 + K_0 x_f^0 + D_1(x_f^0, \dot{x}_f^0, \epsilon h, \epsilon \dot{h}) = G_1 f_s. \quad (3.46)$$

We remark that although this model has the same dimension as the quasi-rigid model (3.37) it is not an approximation to the singularly perturbed model (3.31)–(3.33); instead, it represents the exact system (3.1)–(3.2) restricted to the manifold M_ϵ . The reduced flexible model (3.45)–(3.46) therefore models the flexible system more accurately than does the quasi-rigid model (3.37). Unfortunately, to construct the reduced flexible model (3.45)–(3.46), one needs (in general) to solve a partial differential equation for h . The approach presented in [SKK87], is to approximate the manifold M_ϵ and the reduced flexible model up to any order in ϵ . The first step consists of expanding $h(x, \dot{x}, \epsilon)$ in a power series;

$$h(x, \dot{x}, \epsilon) = h_0(x, \dot{x}) + \epsilon h_1(x, \dot{x}) + \dots \quad (3.47)$$

and substituting into the manifold condition (3.33) to obtain the coefficients. Then the control is synthesized via an expansion;

$$\tau_b(x, \dot{x}, \epsilon) = \tau_b^0(x, \dot{x}) + \epsilon \tau_b^1(x, \dot{x}) + \dots \quad (3.48)$$

$$f_s(x, \dot{x}, \epsilon) = f_{s0}(x, \dot{x}) + \epsilon f_{s1}(x, \dot{x}) + \dots \quad (3.49)$$

which highlights the importance of the relatively weak forces in the refined analysis. To compute the h_i 's, we equate terms in like powers of ϵ in the manifold condition (3.33) from which we obtain

$$h_0 = -K_{10}^{-1}[D_2(x_r, \dot{x}_r, x_f^0, \dot{x}_f^0) + N_1 \ddot{x}_r - G_2 f_{s0}] \quad (3.50)$$

$$h_1 = -K_{10}^{-1}[D_2(x_r, \dot{x}_r, h_0, \dot{h}_0) + B_1 \dot{h}_0 + \ddot{h}_0 - G_2 f_{s1}]. \quad (3.51)$$

⋮

As expected, h_0 has the same expression as (3.41). We can also write:

$$M(x, \epsilon h) = M_0(x) + \epsilon M_1(x, h_0) + \dots \quad (3.52)$$

$$K_r(x, \dot{x}, \epsilon h, \epsilon \dot{h}) = K_r^0(x, \dot{x}) + \epsilon K_r^1(x, \dot{x}, h_0, \dot{h}_0) + \dots \quad (3.53)$$

Substituting (3.47)–(3.49), (3.52), (3.53) in (3.45)–(3.46) obtains a reduced flexible model up to any desired degree of accuracy in ϵ . Let the m -dimensional control vector $f = (\tau^T, f_s^T)^T$ and recall that $x = [x_r^T, x_f^0]^T$. The reduced flexible model (3.45)–(3.46) can then be written

$$\begin{aligned} & [\mathcal{M}_0(x_r) \ddot{x}_r + C_0(x_r, \dot{x}_r) - E f_0] \\ & + \epsilon [\mathcal{M}_1(x_r, h_0) \ddot{x}_r + C_1(x_r, \dot{x}_r, h_0, \dot{h}_0, \ddot{h}_0) - E f_1] + O(\epsilon^2) = 0 \end{aligned} \quad (3.54)$$

where $\mathcal{M}_0(x_r)$, $C_0(x_r, \dot{x}_r)$ and E are as defined in (3.38)–(3.40). The order 1 correction terms \mathcal{M}_1 and C_1 are

$$\mathcal{M}_1(x_r, h_0) = \begin{pmatrix} M_1(x_r, h_0) & 0 \\ 0 & 0 \end{pmatrix}, \quad (3.55)$$

$$C_1(x_r, \dot{x}_r, h_0, \dot{h}_0, \ddot{h}_0) = \begin{pmatrix} K_r^1(x_r, \dot{x}_r, h_0, \dot{h}_0) + N_1^T \ddot{h}_0 \\ D_1(h_0) \end{pmatrix}. \quad (3.56)$$

Thus neglecting terms of order ϵ^2 and higher in (3.54), we obtain the *First-Order Corrected Model (FOCM)*;

$$[\mathcal{M}_0 + \epsilon \mathcal{M}_1](x_r, h_0) \ddot{x}_r + [C_0 + \epsilon C_1](x_r, \dot{x}_r, h_0, \dot{h}_0, \ddot{h}_0) = E(f_0 + \epsilon f_1), \quad (3.57)$$

an $O(\epsilon)$ improved approximation to the reduced flexible model.

3.1.3 Feedback linearization and decoupling of the quasi-rigid model

Recall the quasi-rigid model (3.37):

$$\mathcal{M}_0(x) \ddot{x} + C_0(x, \dot{x}) = E f_0 \quad (3.58)$$

where $x = [x_r^T, x_f^0]^T$ and $f_0 = [\tau_b^0{}^T, f_{s0}^T]^T$. Depending on the number, $2k$, of structural controllers available and the number p of flexible states available for feedback, the controls, τ_b^0 and f_{s0} , can be synthesized using feedback linearization to completely, or partially, decouple the quasi-rigid model (3.58) from the deformation z . We consider three cases as follows.

Case 1 ($m < p$): An important question which we first consider concerning the approximating model (3.58) is whether it is exactly feedback linearizable? That is, can the linearization be performed by identifying a critical set of outputs for which the input/output relation is invertible? If such a set of outputs can be found then no further consideration for decoupling and/or stability of system zero dynamics is required. To answer this question, let us write the model in state space form with $x_1 = x = [x_r^T, x_f^{0T}]^T \in R^{n+p}$,

$$\begin{pmatrix} \dot{x}_1 \\ \dot{x}_2 \end{pmatrix} = d(x_1, x_2) + \mathcal{G}(x_1, x_2)f \quad (3.59)$$

where

$$d(x_1, x_2) = \begin{pmatrix} x_2 \\ -\mathcal{M}_0^{-1}(x_1)\mathcal{C}_0(x_1, x_2) \end{pmatrix}, \quad \mathcal{G}(x_1) = \mathcal{M}_0^{-1}(x_1)E. \quad (3.60)$$

Conditions for exact linearization are well known but can be tedious to check. The required computations are straightforward and can be performed using a symbolic algebra system. We utilized CONDENS, a symbolic manipulation package for analysis and design of nonlinear control systems using geometric methods, to check the feedback linearizability conditions [?]. Checking the conditions for each $p = 0, 1, 2, \dots$, we find that the first condition (i.e., controllability) is generically satisfied; i.e.,

$$\dim\{\mathcal{G}, [f, \mathcal{G}], ad_f^2 \mathcal{G}, \dots, ad_f^{2p+1} \mathcal{G}\} = 2p + 2.$$

However, as we suspected, if $m < p$ the second condition of linearizability—the involutivity condition [Isi85]—is not satisfied. This means that the distribution

$$\text{Sp}\{\mathcal{G}, [f, \mathcal{G}], \dots, ad_f^{2p} \mathcal{G}\}$$

is not involutive and hence, that the system (3.58) is not exactly feedback linearizable in the case $m < p$. This is the generic case for control of distributed parameter systems with a finite number of localized controls.

To consider PFL we identify a set of m system outputs for the inverse dynamics computations. A natural choice which guarantees the minimum phase property is to identify collocated outputs as:

$$y = E^T x.$$

In this case the decoupled, quasi-steady state zero dynamics include the dynamics of the last $p - m$ modes of the structure with additional boundary conditions arising from $y = 0$. After the decay of the fast transients, the uncontrolled deformation z approaches the slow manifold M_0 defined by (3.41) with the controls τ_b and f , replaced by the resulting linearizing input-output controls.

Case 2 ($m = p$): In this case, the reduced order model (3.58) is exactly feedback linearizable with the linearizing control

$$f_0 = E^{-1}(\mathcal{C}_0(x, \dot{x}) + \mathcal{M}_0(x)v). \quad (3.61)$$

where $v = (v_1^T, v_2^T)^T \in R^m$. The effective quasi-steady state response from the synthetic control v to output y is given by:

$$\ddot{x} = v. \quad (3.62)$$

As in the previous case, the deformation z approaches the slow manifold M_0 defined by (3.41) with τ_b^0 and f_s^0 , the components of f_0 are as in (3.61).

Case 3 ($m > p$): If the number of dominant flexible modes p we choose to incorporate in the reduced-order model is smaller than the number of available structural controls, then p of these controllers can be used for decoupling and linearization of the reduced order model (3.58), while the remaining $m - p$ controllers can be used to *shape* the slow manifold, M_0 , as well as to compensate for the structural elastic response, z , within reasonable limits. The idea is due to Dwyer [Dwy88] who studied the method of *deformation shaping* in the particular case $p = 0$; i.e., when the reduced order model (quasi-rigid model) coincides with the rigid body dynamics and the "fast" subsystem coincides with the dynamics of the whole flexible appendage.

In the case $m > p$, the structural control forces, f_s , can be decomposed as

$$f_s = \begin{pmatrix} f_{s,1} \\ f_{s,2} \end{pmatrix}, \quad f_{s,1} \in R^p, \quad f_{s,2} \in R^{2k-p}.$$

The $p \times m$ full rank matrix G_1 in the slow subsystem (3.34)-(3.36) can be put in the form $[G_{11} \ 0]$ using elementary permutations, where G_{11} is a $p \times p$ and nonsingular matrix. Similarly, the $(2k - p) \times m$ matrix G_2 takes the form $[0 \ G_{22}]$ with the $(2k - p) \times (m - p)$ matrix G_{22} having full rank $(m - p)$. The reduced order model (3.58) can then be written as

$$\mathcal{M}_0(x)\ddot{x} + C_0(x, \dot{x}) = E_1 f_p^0 \quad (3.63)$$

where $f_p^0 = (\tau_b^0{}^T, f_s^0{}^T)^T \in R^{n+p}$ and

$$E_1 = \begin{pmatrix} I & 0 \\ 0 & G_{11} \end{pmatrix}. \quad (3.64)$$

The model (3.63) is exactly feedback linearizable with the linearizing feedback as in (3.61) but with E_1 replacing E . The algebraic constraint (3.41) defining the slow manifold M_0 becomes in this case

$$z = -K_{10}^{-1} [D_2(x_r, \dot{x}_r, x_f^0, \dot{x}_f^0) + N_1 \ddot{x}_r + G_{22} f_{s_{m-p}}], \quad (3.65)$$

where the acceleration \ddot{x}_r can be replaced by the synthetic control v_1 . Contrary to the previous cases, the deformation z can be controlled or compensated (completely in the case $m = q$) by the structural controllers $f_{s_{m-p}}$ which will require high bandwidth, but "low-authority" (i.e. relatively weak) actuators for implementation.

3.1.4 Partial feedback linearization of the Reduced Flexible Model

In some applications, and depending upon the choice of the scaling, ϵ may not be "small" enough relative to the decoupling requirement. In this case, it is necessary to replace the quasi-rigid model (3.58) by the more accurate FOCM (3.57) for control design. The application of feedback linearization to the FOCM introduces a correction term in the controls which improves the decoupling (and thus linearization) of the system by an order of ϵ . The corrected controls are obtained via an expansion;

$$f = f^0 + \epsilon f^1, \quad (3.66)$$

where f^0 is the linearizing torque for the quasi-rigid (zero-order approximation) model.

Design of the corrective control f^1 : The corrective control f^1 is designed to improve the decoupling by annihilating the $O(\epsilon)$ terms in (3.57), i.e.,

$$[\mathcal{M}_1(x, h_0)\ddot{x} + C_1(x, \dot{x}, h_0, \dot{h}_0, \ddot{h}_0) - E f^1] = 0. \quad (3.67)$$

The construction will depend, as in the previous section, on the values of p and m . In the case $m < p$ the corrective control, f^1 , can be constructed to annihilate part of (3.67). In the case $m = p$, (3.67) can be exactly annihilated by:

$$f^1 = E^{-1} (C_1(x, \dot{x}, h_0, \dot{h}_0, \ddot{h}_0) + \mathcal{M}_1(x, h_0)v). \quad (3.68)$$

If we apply the control, $f = f^0 + \epsilon f^1$, to the reduced flexible model (3.54), where τ_b^0 , τ_b^1 , f_s^0 and f_s^1 are as designed above, we obtain:

$$\ddot{x} = v + O(\epsilon^2) \quad (3.69)$$

which linearizes the reduced flexible system up to order ϵ^2 .

3.2 Conclusions and Directions

The results described in this section represent a preliminary analysis of the problem of PLF compensation for multibody system with flexible interactions. (A preliminary version of the analysis was presented at the 1989 American Control Conference in Pittsburgh, PA [ABB89]. Our interest in this phase of the research was primarily motivated by concerns for the complexity of implementation of PLF compensation required for high order FEM models of the elastic response of a multibody system. The primary objective was to demonstrate rapid slewing and precision pointing of the system attitude as defined relative to a body-fixed frame attached to the primary system body. The analytical approach based on integral manifold methods offers a refinement of the standard singular perturbation approach which suggests that higher order corrections applied to the rigid body torques can improve performance of PLF compensation for relatively low order models of structural flexure. Simulation studies performed during this study did not reveal substantial improvement from such corrections.

In response to the observed responses of simulation studies we can draw several conclusions. The SBL system model developed in this study consists of a multibody system with

primary system outputs to be regulated consisting of rigid body positions and parasitics arising from low mass structural interactions. Primary system controls are collocated with the position coordinates for regulation. Singular perturbation analysis reveals that the system flexure dynamics in such cases are only weakly controllable in the sense that control of the fast time scale enters only through the slow time system. As is well known, such system will require additional control authority to affect control of the fast time scale response. For the problem of rapid slewing and precision pointing this means that active structural control which interacts with the low mass density, structural components may be important in achieving enhanced robustness of the system slewing and alignment responses. This observation is potentially important given the increasing reliance on passive damping methods for space structure applications [RR87]. Unfortunately a comprehensive study will require some analysis of emerging technology for imbedded actuation and sensing of flexible structure response. This was viewed outside the scope of the second year effort on the subject contract.

4 Some Design Approaches for Combined Rapid Slewing and Precision Pointing

Consider the general form of the equations of motion for a multibody system undergoing attitude reorientation. The model includes n degrees of freedom (including elastic degrees of freedom retained from a FEM expansion) with position coordinates $q \in \mathbb{R}^n$ and velocities $p \in \mathbb{R}^n$. The model has the form,

$$\dot{q} = \tilde{\Gamma}(q)p \quad (4.1)$$

$$M(q)\dot{p} + B(q,p)p + K(q,p)q = Gf \quad (4.2)$$

where M, B, K are $n \times n$ symmetric, matrix-valued functions and G is an $n \times m$ matrix. The m -vector f includes generalized forces (and torques) acting on the multibody system. For simplicity we assume the position coordinates are ordered as: $q = [\gamma^T, u^T]^T$ where $\gamma \in \mathbb{R}^3$ parametrizes the rotation of the body fixed frame of the system principal body. Also, $p = [\omega^T, \dot{u}^T]^T$, where ω is the body angular rates. The general model includes nonlinear kinematics (4.1) which is assumed to have the form,

$$\tilde{\Gamma}(q) = \begin{bmatrix} \Gamma(\gamma) & 0 \\ 0 & I_{n-3} \end{bmatrix}$$

where the 3×3 matrix is defined previously depending on the parametrization of $SO(3)$.

The general problem of control of system pointing and multibody alignment is addressed by establishing a set of m principal system outputs taken as an m -vector of position coordinates,

$$y = C'q. \quad (4.3)$$

Claim 1: The decoupling/PLF control

$$f = (C\tilde{\Gamma}M^{-1}G)^{-1}v - (C\tilde{\Gamma}M^{-1}G)^{-1}C\tilde{\Gamma}M^{-1}[(MD - B)p - Kq], \quad (4.4)$$

with

$$D(\gamma) = \begin{bmatrix} \gamma^T \omega I_3 & 0_{3,n-3} \\ 0_{n-3,3} & 0_{n-3,n-3} \end{bmatrix},$$

renders the input/output response from $v \rightarrow y$ as a linear, $2m$ -dimensional system of the form,

$$\ddot{y} = v.$$

Proof: To obtain (4.4) we proceed by direct computation of the normal form coordinates for the general model (4.1)-(4.2) with outputs (4.3). First, identify a change of state coordinates, $(T)(\dot{q}, q) \mapsto (z, \xi)$,

$$\begin{pmatrix} z_1 \\ z_2 \\ \xi \end{pmatrix} = T \begin{pmatrix} q \\ \dot{q} \end{pmatrix}$$

$$= \begin{bmatrix} C' & 0_{m,n} \\ 0_{m,n} & C' \\ Z_1 & Z_2 \end{bmatrix} \bar{\Gamma}(q) \begin{pmatrix} q \\ p \end{pmatrix} \quad (4.5)$$

with Z_1, Z_2 chosen so that T has rank $2n$. Thus a direct computation yields,

$$z_1 = C'q \quad (4.6)$$

$$z_2 = C'\dot{q} = C'\bar{\Gamma}(q)p \quad (4.7)$$

$$\xi = Z_1q + Z_2\Gamma(\gamma)p \quad (4.8)$$

an invertible transformation.

Before we obtain the system model in the (z, ξ) coordinates we express the accelerations in a convenient form. From (4.1)–(4.2) we have,

$$\ddot{q} = \frac{d}{dt}\dot{q} = \frac{\partial}{\partial q}\{\bar{\Gamma}(q)p\}\dot{q} + \bar{\Gamma}(q)\dot{p}. \quad (4.9)$$

Note that the n -vector valued function,

$$\frac{\partial}{\partial q}\{\bar{\Gamma}(q)p\}\dot{q} = \frac{\partial}{\partial q}\{\bar{\Gamma}(q)p\}\bar{\Gamma}(q)p \quad (4.10)$$

$$= \begin{bmatrix} \frac{\partial}{\partial \gamma}\{\Gamma(\gamma)\omega\} & 0 \\ 0 & 0 \end{bmatrix} \begin{bmatrix} \Gamma(\gamma) & 0 \\ 0 & I_{n-3} \end{bmatrix} \begin{pmatrix} \omega \\ \dot{u} \end{pmatrix}. \quad (4.11)$$

A principal advantage of the use of the Gibbs vector parametrization for attitude position is the simple algebraic form of the kinematic relation. Appendix A establishes the following based on the Gibbs vector parametrization,

$$\frac{\partial}{\partial \gamma}\{\Gamma(\gamma)\omega\}\Gamma(\gamma)\omega = \gamma^T\omega\Gamma(\gamma)\omega.$$

Using this relation we obtain,

$$\ddot{q} = \begin{bmatrix} \gamma^T\omega\Gamma(\gamma)\omega \\ 0 \end{bmatrix} - \begin{bmatrix} \Gamma(\gamma) & 0 \\ 0 & I_{n-3} \end{bmatrix} M(q)^{-1}\{Bp + Kq - Gf\} \quad (4.12)$$

$$= \bar{\Gamma}(\gamma)M(q)^{-1}\{[M(q)D(q) - B(q, p)]p - K(q, p)q + Gf\} \quad (4.13)$$

where,

$$D(q) = \begin{bmatrix} \gamma^T\omega I_3 & 0 \\ 0 & 0 \end{bmatrix}.$$

The model can be expressed in normal form coordinates as,

$$\dot{z}_1 = z_2, \quad (4.14)$$

$$\dot{z}_2 = \mathcal{A}(z, \xi) + \mathcal{B}(z, \xi)f, \quad (4.15)$$

$$\dot{\xi} = F(z, \xi). \quad (4.16)$$

From (4.5), (4.13) we have,

$$\mathcal{A}(q, p) = \tilde{\Gamma}(\gamma)M(q)^{-1}\{(M(q)D(q) - B(q, p))p - K(q, p)q\} \quad (4.17)$$

$$\mathcal{B}(q, p) = \tilde{\Gamma}(\gamma)M(q)^{-1}G. \quad (4.18)$$

The decoupling control is then,

$$f = \mathcal{B}(p, q)^{-1}\{v - \mathcal{A}(p, q)\},$$

and (4.4) follows. □

Claim 2: Given the model (4.1)-(4.3) we can find $(n-m) \times n$ valued functions $Z_1(q), Z_2(q)$ such that

$$Z_1\tilde{\Gamma}(q)M(q)^{-1}C^T = 0, \quad (4.19)$$

$$Z_2\tilde{\Gamma}(q)M(q)^{-1}C^T = 0, \quad (4.20)$$

and

$$T(q) = \begin{bmatrix} C & 0 \\ 0 & C \\ Z_1(q) & Z_2(q) \end{bmatrix}$$

is nonsingular.

Claim 3: In the case that outputs for regulation, linearization, and decoupling defined by (4.3) are *collocated* with the generalized control forces; i.e.,

$$\text{span}\{G\} = \text{span}\{C^T\}$$

then the (output-constrained) *zero dynamics* are given as,

$$\dot{\xi} = F(z, \xi)|_{z=0} \quad (4.21)$$

where $F(z, \xi) = \Phi(p, q)$ with (p, q) such that

$$T(q)\tilde{\Gamma}(q) \begin{pmatrix} p \\ q \end{pmatrix} = \begin{pmatrix} z \\ \xi \end{pmatrix} \quad (4.22)$$

and

$$\begin{aligned} \Phi(p, q) = & \dot{Z}_1(q)q + Z_1(q)\tilde{\Gamma}(q)p + \dot{Z}_2(q)\tilde{\Gamma}(\gamma)p \\ & + Z_2(q)\tilde{\Gamma}(q)M^{-1}\{[M(q)D(q) - B(q, p)]p + K(p, q)q\}. \end{aligned} \quad (4.23)$$

Proof: From (4.13) and (4.5) we obtain $\xi = Z_1 q + Z_2 \dot{q}$. Direct evaluation of (4.16) obtains,

$$\dot{\xi} = \dot{Z}_1(q)q + Z_1(q)\dot{q} + \dot{Z}_2(q)\bar{\Gamma}(\gamma)p \quad (4.24)$$

$$+ Z_2(q)\bar{\Gamma}(\gamma)M(q)^{-1}\{[M(q)D(q) - B(q,p)]p - K(q,p)q + Gf\}. \quad (4.25)$$

Then by Claim 2 and the assumption we have,

$$Z_2(q)\bar{\Gamma}(\gamma)M(q)^{-1}G = 0.$$

□

4.1 Practical Implementation of Time-optimal Slewing for an Inertial Load

The advantage of the PLF control which implements the system inverse is the slewing control can now be implemented in the new coordinates. A switching control law is designed for the independent decoupled axis motions in acceleration coordinates. The decoupled single axis response obtained after PLF compensation is:

$$\ddot{\theta}(t) = \alpha(t) \quad (4.26)$$

where θ is the attitude parameter for i^{th} axis (subscripts suppressed) and α (the acceleration) is the control. Requirements for rapid slewing suggest a minimum time criterion is appropriate for the design of control laws.

Necessary conditions for a control law, optimal with respect to a minimum time objective, can be obtained directly from the maximum principle. Under magnitude constraint on the available acceleration,

$$|\alpha(t)| < \alpha_{\max} \quad (4.27)$$

the optimal control is of bang-bang type with switching strategy described by a switching surface in the state space \mathfrak{R}^2 with coordinates $x = [\theta, \dot{\theta}]^T$. For the double integrator plant the optimal control involves determining a single switch point. Briefly, the optimal switching surface is a quadratic curve in \mathfrak{R}^2 which can be obtained as follows. For constant accelerations, $\alpha(t) = \alpha_{\max}$, the natural trajectories are,

$$\dot{\theta}(t) = \xi_1 + \alpha_{\max} t, \quad (4.28)$$

$$\theta(t) = \xi_0 + \xi_1 t + \frac{1}{2} \alpha_{\max} t^2, \quad (4.29)$$

where $\theta(0) = \xi_0$ and $\dot{\theta}(0) = \xi_1$ are initial conditions. The optimal trajectory reaches the equilibrium at the origin in minimum time. To identify the required switching surface choose the trajectories which reach the origin at time t_f by solving the above equations simultaneously and eliminating dependence on t_f , to obtain,

$$\xi_1^2 = 2\alpha_{\max} \xi_0. \quad (4.30)$$

It is easy to see that the required switching surface in the state space \mathfrak{R}^2 with coordinates $z = [\theta, \dot{\theta}]^T$ is

$$s(z) = f(z_2) + 2\alpha_{\max} z_1 = 0, \quad (4.31)$$

with $f(z_2) = z_2|z_2|$ and the time-optimal control is bang-bang;

$$\alpha(t) = -\alpha_{\max} \operatorname{sgn}\{s(z)\}. \quad (4.32)$$

However, any practical implementation of the time-optimal control law will involve an approximation of the ideal discontinuous actuation. Most realistic actuators have slew rate limits, dead zones, delays, or other dynamics which may play a role in implementation dynamics. A simple example of the difficulty of implementing time-optimal control can be illustrated if we replace the ideal signum function with a saturating element. In this case it can be shown that the origin is not an asymptotically stable equilibrium. To see this consider a Lyapunov function,

$$V(z) = \frac{1}{2} z^T z,$$

defined on \mathbb{R}^2 with coordinates as given above. For the practical control law,

$$\alpha(t) = -\alpha_{\max} \operatorname{sat}\{s(z)\}, \quad (4.33)$$

where

$$\operatorname{sat}(\xi) := \begin{cases} 1, & \text{for } \xi \geq 1/g_1 \\ g_1 \xi, & \text{for } |\xi| < 1/g_1 \\ -1, & \text{for } \xi \leq -1/g_1 \end{cases} \quad (4.34)$$

where g_1 is a positive constant gain representing slew rate limiting in the actuator.

In a neighborhood of the origin such that $|z_2| < 1/g_1$ we can evaluate the time derivative of the Lyapunov function along trajectories of the closed loop system;

$$\dot{V} = z^T \dot{z} \quad (4.35)$$

$$= z^T \left\{ \begin{bmatrix} 0 & 1 \\ 0 & 0 \end{bmatrix} z - \begin{bmatrix} 0 \\ 1 \end{bmatrix} \operatorname{sat}\{2\alpha_{\max} z_1 + z_2|z_2|\} \right\} \quad (4.36)$$

$$= z^T \begin{bmatrix} 0 & 1 \\ -2\alpha_{\max} & -|z_2| \end{bmatrix} z. \quad (4.37)$$

The V -function is positive definite, decreasent, and radially unbounded. In the neighborhood of the origin we have $\dot{V} \leq 0$ for $|z_2| < 1/g_1$. Any finite precision implementation of $f(z_2)$ will ultimately become negligible near the origin and the closed loop system response will ultimately oscillate with frequency $\sqrt{2\alpha_{\max}}$ and amplitude given by the precision of f near the origin.

The above limitations are simple examples of the general tradeoffs involved in design of nonlinear control systems where dual mode operation must be considered to resolve the tradeoffs between requirements for *static accuracy* such as local stability, noise rejection, etc. and *dynamic accuracy* such as speed of response. These issues are well known to control engineers but do not receive a lot of attention in the theoretical literature. Considerations for dual mode operation in this case suggest that the optimal switching function be replaced with a dual mode version which approximates time optimal operation for large signal motion but achieves asymptotic stability of the origin for small angle displacements. Additionally, considerations for small signal overshoot, stability margins, etc. can be included without sacrifice of the large signal response.

A dual mode version of the time-optimal control law can be obtained by replacing the nonlinear function f with a peicewise continuous modification with finite slope near $z_2 = 0$. The choice,

$$f(z_2) := \begin{cases} z_2^2 + \frac{g_2^2}{4}, & \text{for } z_2 \geq g_2/2 \\ g_2 z_2, & \text{for } |z_2| < g_2/2 \\ -z_2^2 - \frac{g_2^2}{4}, & \text{for } z_2 \leq -g_2/2 \end{cases} \quad (4.38)$$

obtains asymptotic stability of the origin for any $g_2 > 0$ with closed loop control (4.33).

The resulting practical implementation of the time-optimal servo control law is shown in Figure 4.1. Here θ_c is the commanded attitude angle. To the extent that practical limits of actuators permit, the gains g_1 and g_2 should be chosen to satisfy local stability and overshoot as well as large angle rapid (time-optimal) slewing. These tradeoffs can be reconciled by appealing to the ideal bang-bang control law (4.32) with the modified f . With ideal switching the surface, $s(z) = 0$, (4.31) is an integral manifold for the closed loop system. From the theory of discontinuous differential equations we can obtain stability analysis by decomposition of the closed loop system dynamics into two phases: 1) reaching to the switching surface and 2) ideal sliding on the switching surface.

Assume the closed loop system achieves ideal sliding condition $s(z) = 0$ for $t > t_s$. Then the sliding dynamics are obtained from the constraint $\dot{s}(z) = 0$ for $t > t_s$;

$$\dot{s}(z) = f'(z_2)\dot{z}_2 + 2\alpha_{\max}\dot{z}_1 = 0$$

where $f' = \partial f / \partial z_2$. In the linear region of the peicewise function f —namely, when $|z_2| < g_2/2$ —we obtain,

$$\dot{s}(z) = g_2\alpha + 2\alpha_{\max}z_2 = 0. \quad (4.39)$$

The *equivalent control* in sliding is

$$\alpha_{eq} = -\frac{2\alpha_{\max}}{g_2}z_2. \quad (4.40)$$

The sliding dynamics on the manifold $\mathcal{M}_s = \{z \in \mathbb{R}^2 : s(z) = 0\}$ are then obtained by substitution of the equivalent control in the closed loop equations. In the linear region we obtain,

$$\dot{z}_1 = z_2 \quad (4.41)$$

$$\dot{z}_2 = -\frac{2\alpha_{\max}}{g_2}z_2 \quad (4.42)$$

and together with the constraint $s(z) = 0$ the ideal sliding dynamics reduce to

$$\dot{z}_2 = -\frac{2\alpha_{\max}}{g_2}z_2 \quad (4.43)$$

which are asymptotically stable to $z_2 = 0$ for any $g_2 > 0$. The local time constant in sliding is

$$\tau = \frac{g_2}{2\alpha_{\max}} \quad (4.44)$$

To choose the gain g_2 we take θ_1 as the desired tolerance for large angle slewing; i.e., for any initial offsets exceeding θ_1 we want to apply large angle, time-optimal slewing control, but for any offsets smaller than θ_1 we want linear mode action. Then the required gain is obtained by substituting $z_1 = \theta_1$ into (4.31);

$$g_2 = \sqrt{2\alpha_{\max}\theta_1} \quad (4.45)$$

The resulting linear mode time constant is

$$\tau = \frac{\theta_1}{\sqrt{\alpha_{\max}}}.$$

Note that the ideal sliding dynamics retain the feature of no overshoot characteristic of time-optimal slewing into the linear mode operation.

To implement the time-optimal servo we need to understand the limits of saturation mode operation of the actuator and the effect of available torque. From the theory of sliding mode design it remains to show in what region sliding will be achieved. A straightforward application of the reaching analysis of [DZM88] follows. From (4.31) let $V(z) = \frac{1}{2}s^2$. To achieve sliding we need to show that $\dot{s}s < 0$. Here

$$\dot{s}(z) = f'(z_2)\dot{z}_2 + 2\alpha_{\max}\dot{z}_1 \quad (4.46)$$

where

$$f' = \frac{\partial f}{\partial z_2} = \begin{cases} 2z_2, & \text{for } z_2 \geq g_2/2 \\ g_2, & \text{for } |z_2| < g_2/2 \\ -2z_2, & \text{for } z_2 \leq -g_2/2 \end{cases} \quad (4.47)$$

A necessary and sufficient condition for sliding to be achieved globally with the ideal switching control law

$$\alpha(t) = -\bar{\alpha}_{\max}\text{sgn}\{s(z)\},$$

is

$$\bar{\alpha}_{\max} > \alpha_{\max}.$$

Within the linear region sliding is achieved when

$$\bar{\alpha}_{\max} \geq \alpha_{\max}.$$

For practical implementation of time-optimal slewing the choice of actuator slew rate g_1 is critical. With the (practical) closed loop control (4.33) the dynamics in a neighborhood of the origin are given by

$$\dot{z} = \begin{bmatrix} 0 & 1 \\ -2\alpha_{\max}^2 g_1 & -\alpha_{\max} g_1 g_2 \end{bmatrix} z. \quad (4.48)$$

Sensitivity of the stability properties can be determined from a root locus analysis with respect to g_1 (see Figure 4.2). The characteristic equation of the closed loop system is

$$\lambda^2 + \alpha_{\max} g_1 g_2 \lambda + 2\alpha_{\max}^2 g_1 = 0$$

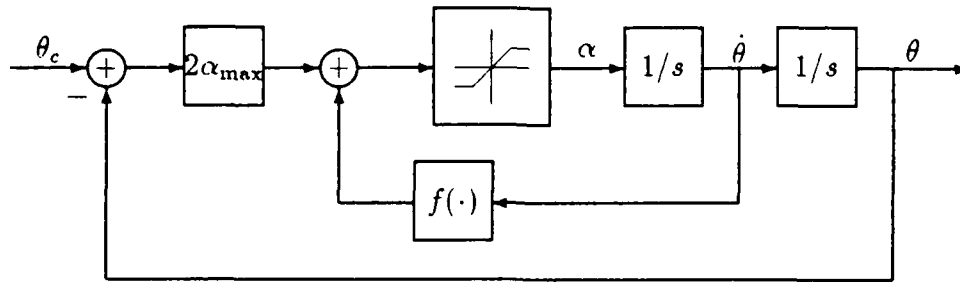


Figure 4.1: Implementation of Time-Optimal Servo

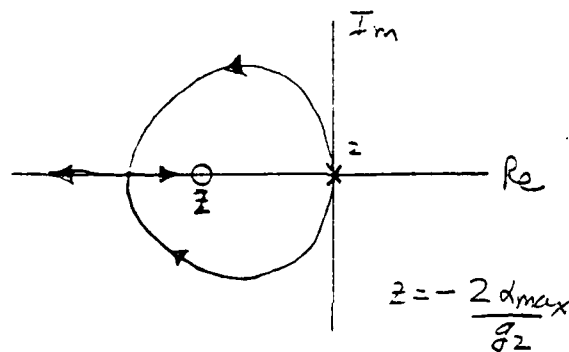


Figure 4.2: Root Locus for Linear Mode Sensitivity of Saturation Mode Slewing

which we write in the form

$$\lambda^2 + k(g_2\lambda + 2\alpha_{\max}) = 0$$

with $k = \alpha_{\max}g_1$. To approximate ideal sliding in the linear region we require

$$g_1 > \frac{8}{g_2^2}$$

which guarantees that the roots are real and stable. As $g_1 > 0$ is increased the small signal response is dominantly a single time constant which approaches the ideal sliding mode response in the limit as $g_1 \rightarrow \infty$ [SS83].

4.2 Implementation of Rapid Slewing with Coordinated Modes of Actuation

In this section we describe the basis for design of coordinated use of different modes of actuation for rapid slewing. The idea is to utilize the smooth (or continuous) mode actuators (such as AMED's) to implement a component of the PLF compensation. This implementation permits a simple decomposition of the slewing control into individual single axis commands. The slewing control is implemented using discrete (discontinuous) mode actuation (such as reaction jets). This is consistent with the very large torque requirements for large angle, rapid slewing of significant system inertias. Bang-bang mode operation of high

torque AMED's (such as reaction wheels and CMG's) is inconsistent with (or at least technically very challenging for) the state-of-the-art. Whereas reaction jets can—depending on physical placement issues—generate very large torques with rapid, discontinuous action; but their use in throttled (continuous) mode is technically challenging. The decomposition of control authority suggested in the following design approach is chosen to exploit the benefits of current actuation technology for attitude control.

One design approach for rapid slewing focuses on controlling the dynamics of the rigid body motion. We discuss the implications of dynamic reaction from the elastic appendage in the context of robust control performance. Recall that the rigid body dynamics can be given in the form,

$$\dot{\gamma} = \Gamma(\gamma)\omega_b \quad (4.49)$$

$$\dot{\omega}_b = I_b^{-1}(I_b\omega_b \times \omega_b) + I_b^{-1}\tau_b \quad (4.50)$$

where $\gamma, \omega_b \in \mathbb{R}^3$ are respectively the vector attitude parameters and angular rates referenced to the body fixed frame.

To control the vehicle attitude we now design an implementation of PLF compensation for the system outputs,

$$y = \gamma,$$

given the external torques, τ_b , applied to the rigid body. We remark that the assumptions leading to the model (4.50) together with the choice of primary system outputs, y , indicate that the relative degree from each input/output pair, $\tau_{b,i} \mapsto y_i$ is 2. Transformations obtained as in (2.27) indicate that the system can be *exactly* linearized by feedback (i.e., no zero dynamics are obtained in the transformation to the normal form).

The computation of the normal form coordinates is obtained as in section 2 by differentiation of the output. In this case,

$$z_1 = y = \gamma \quad (4.51)$$

$$z_2 = \dot{y} = \Gamma(\gamma)\omega \quad (4.52)$$

and since the 3×3 matrix Γ is nonsingular for almost all γ the transformation is invertible. A straightforward computation obtains the normal form as,

$$\begin{aligned} \dot{z}_1 &= z_2 \\ \dot{z}_2 &= \mathcal{A}(z_1, z_2) + \mathcal{B}(z_1, z_2)\tau_b \end{aligned} \quad (4.53)$$

where

$$\mathcal{B}(z_1) = \Gamma(z_1)I_b^{-1} \quad (4.54)$$

$$\mathcal{A}(z_1, z_2) = \left[\gamma^T \omega \Gamma(\gamma) \omega + \Gamma(\gamma) I_b^{-1} (I_b \omega \times \omega) \right] \Big|_{\gamma=z_1, \omega=\Gamma(z_1)z_2} \quad (4.55)$$

Thus the feedback compensation which linearizes the system (4.50) for large angle motion is [Dwy84],

$$\begin{aligned} \tau_b &= \mathcal{B}(z_1)^{-1} \{ \alpha(t) - \mathcal{A}(z_1, z_2) \} \\ &= -I_b \omega \omega^T \gamma - I_b \omega \times \omega + I_b \Gamma(\gamma) \alpha(t) \end{aligned} \quad (4.56)$$

where $\alpha \in \mathbb{R}^3$ is the "synthetic control" (in acceleration coordinates). To implement the rapid, large angle slewing control we apply the bang-bang, time-optimal switching logic to each axis; i.e.,

$$\alpha_i = -\alpha_{\max} \operatorname{sgn}\{f(z_{2,i}) + 2\alpha_{\max} z_{1,i}\}$$

as in (4.32) with $f(\cdot)$ as in (4.38). This form assumes identical acceleration limiting is desired in each axis.

A straightforward computation reveals that we can write,

$$\mathcal{A}(z_1, z_2) = \mathcal{B}(z_1)d(z_1, z_2), \quad (4.57)$$

with

$$d(z_1, z_2) = [\gamma^T \omega I_b \omega + I_b \omega \times \omega] \Big|_{\gamma=z_1, \omega=\Gamma(z_1)z_2} \quad (4.58)$$

The normal form equations can be written,

$$\dot{z}_1 = z_2 \quad (4.59)$$

$$\dot{z}_2 = \mathcal{B}(z_1, z_2)\{d(z_1, z_2) + \tau_b\}. \quad (4.60)$$

Note that the factorization obtained in (4.57) indicates that the matching condition for robust feedback linearization is valid for the model terms contributing to $d(z_1, z_2)$.

One approach to implementation of feedback linearizing control for rapid slewing is to implement the compensation in two components;

$$\tau_b = \tau^c + \tau^s, \quad (4.61)$$

where the continuous mode torque component is,

$$\begin{aligned} \tau^c &= -d(z_1, z_2) \Big|_{z_1=\gamma, z_2=\Gamma(\gamma)\omega} \\ &= -[\gamma^T \omega I_b \omega + I_b \omega \times \omega]. \end{aligned} \quad (4.62)$$

This component compensates by decoupling the Coriolis and centripetal accelerations arising from large angle, rapid, rigid body rotations. Note a typical source of model uncertainty arises due to asymmetries in system inertia properties which are typically not considered in control system design studies. Such asymmetries arise in the SBL system with the addition of trackers or additional mirror components. We see that the smooth control is not directly driven by the subsequent synthetic control which obtains the desired slewing maneuver. Thus the smooth control functions to reliably achieve linearization.

The second component, τ^s , will be implemented by discontinuous or *saturation mode actuation*. We shall now indicate a simple approach to identify a switching control law for τ^s based on VS control design. After application of the control (4.61) to (4.60) we obtain the design system for the choice of the saturation mode control law,

$$\begin{aligned} \dot{z}_1 &= z_2 \\ \dot{z}_2 &= \mathcal{B}(z_1, z_2)\tau^s \end{aligned} \quad (4.63)$$

For design of VS control we follow the method described in section 2. Thus we choose the switching surface in the normal form, z -coordinates. The choice of the switching surface establishes the ideal dynamic behavior in sliding and its design should embody the system design goals. In section 2 and [KK89] we outlined options for stabilization of the origin. In the present design the large angle slewing motion is critical and the design goal is time optimal motion. Solution of the general problem of time-optimal attitude control for the rigid body equations (4.50) with independent saturation constraints on the available torques, $|\tau_i| < \tau_{\max}$ is an open problem [AF66]. The formal time-optimal control problem does not embody considerations for robustness or implementation issues as described above and we will not consider it further. Our approach is to develop requirements for the torque authority of the saturation mode control, τ^s , so that decoupled, independent single axis slewing is obtained.

In section 2 we showed that, in sliding, the inverse dynamic control which linearizes the system response is obtained implicitly. The PLF also obtains decoupling of the individual response of the motion about each axis. Our approach is to choose the switching surfaces for independent axis slewing by applying the modified, quadratic switching surfaces for time-optimal servocontrol (4.31) to each axis.

To make these statements precise we introduce the following notation. In the normal form coordinates we decompose the positions and rates in terms of decoupled axis motions as,

$$z_k = \begin{pmatrix} z_{k,1} \\ z_{k,2} \\ z_{k,3} \end{pmatrix}$$

for $k = 1, 2$. Then in the normal form coordinates we establish three switching surfaces,

$$s_i(z) = f(z_{2,i}) + 2\alpha_{\max} z_{1,i}$$

for $i = 1, \dots, 3$. Let $s(z) = [s_1, s_2, s_3]^T$.

It is easy to see that if we can enforce the sliding mode over a significant region of the switching manifold, \mathcal{M} , then the independent axis, time-optimal slewing will be obtained. The design of the required switching control to achieve sliding on \mathcal{M} , and to guarantee reaching the manifold from the expected region of operation after a sufficiently small transient can be based on Lyapunov stability arguments as follows.

Consider a V -function,

$$V = \frac{1}{2} s^T(z) s(z)$$

defined in the normal form coordinates. The time derivative of V along trajectories of (4.63) is,

$$\begin{aligned} \dot{V} &= s^T(z) \dot{s}(z) = s^T(z) \frac{\partial s}{\partial z} \dot{z} \\ &= s^T(z) [2\alpha_{\max} I_3, F'(z)] \begin{bmatrix} z_2 \\ B(z_1) \tau^s \end{bmatrix} \\ &= s^T(z) \{2\alpha_{\max} z_2 + F'(z) B(z_1) \tau^s\}, \end{aligned} \quad (4.64)$$

where

$$F'(z_2) := \text{diag}\{f'(z_{2,i}), i = 1, 2, 3\}, \quad (4.65)$$

and

$$f'(\xi) := \begin{cases} 2\xi, & \text{for } \xi \geq g_2/2 \\ g_2, & \text{for } |\xi| < g_2/2 \\ -2\xi, & \text{for } \xi \leq -g_2/2 \end{cases} \quad (4.66)$$

To guarantee that the switching manifold is reached in finite time and that sliding is achieved we seek the control law which satisfies,

$$\min_{\tau \in T_{ad}} s^T(z) F'(z) \mathcal{B}(z) \tau^s \leq -\mu \quad (4.67)$$

for $\mu > 0$ with admissible controls

$$T_{ad} = \{\tau \in \mathbb{R}^3 : |\tau_i| \leq T_{\max}, \quad i = 1, 2, 3\}. \quad (4.68)$$

Claim 4: The saturation mode control law which is optimal for (4.67)-(4.68) is,

$$\tau_i^s = -T_{\max} \operatorname{sgn}\{\mathcal{B}^T(z_1)[F'(z_2)]^T s(z)\} \quad (4.69)$$

for $i = 1, 2, 3$. Together with the optimal switching strategy (4.69) a sufficient condition for the required saturation mode control authority to guarantee that $\dot{V} \leq 0$ in a given closed set, $\gamma \in \mathcal{B}_\gamma \subseteq \mathbb{R}^3$, containing the origin is

$$T_{\max} \geq \alpha_{\max} \max_{i=1,2,3} \max_{\gamma \in \mathcal{B}_\gamma} |\sum_{j=1}^3 [\Gamma(\gamma) I_b^{-1}]_{ij}|^{-1} \quad (4.70)$$

Proof: From (4.64) it is sufficient to show that

$$T_{\max} \geq \max_{i=1,2,3} \max_{\gamma \in \mathcal{B}_\gamma} \frac{2\alpha_{\max}|z_{2,i}|}{|\sum_{j=1}^3 [F'(z_2)\mathcal{B}(z_1)]_{ij}|}.$$

From (4.65)-(4.66) and (4.54) we can simplify the ratio for each i as,

$$\frac{2\alpha_{\max}|z_{2,i}|}{|\sum_{j=1}^3 [F'(z_2)\mathcal{B}(z_1)]_{ij}|} = \frac{2\alpha_{\max}|z_{2,i}|}{|\sum_{j=1}^3 f'(z_{2,i})[\Gamma(z_1)I_b^{-1}]_{ij}|}.$$

To find the worst case for each i from the discontinuous definition (4.66) we note that for $|z_{2,i}| > g_2/2$,

$$\frac{2\alpha_{\max}|z_{2,i}|}{|f'(z_{2,i})|} = \frac{2\alpha_{\max}|z_{2,i}|}{2|z_{2,i}|} = \alpha_{\max},$$

and for the case $|z_{2,i}| \leq g_2/2$,

$$\max_{|z_{2,i}| \leq g_2/2} \frac{2\alpha_{\max}|z_{2,i}|}{|f'(z_{2,i})|} = \frac{2\alpha_{\max}|z_{2,i}|}{g_2} \Big|_{z_{2,i} = \pm g_2/2} = \alpha_{\max}.$$

□

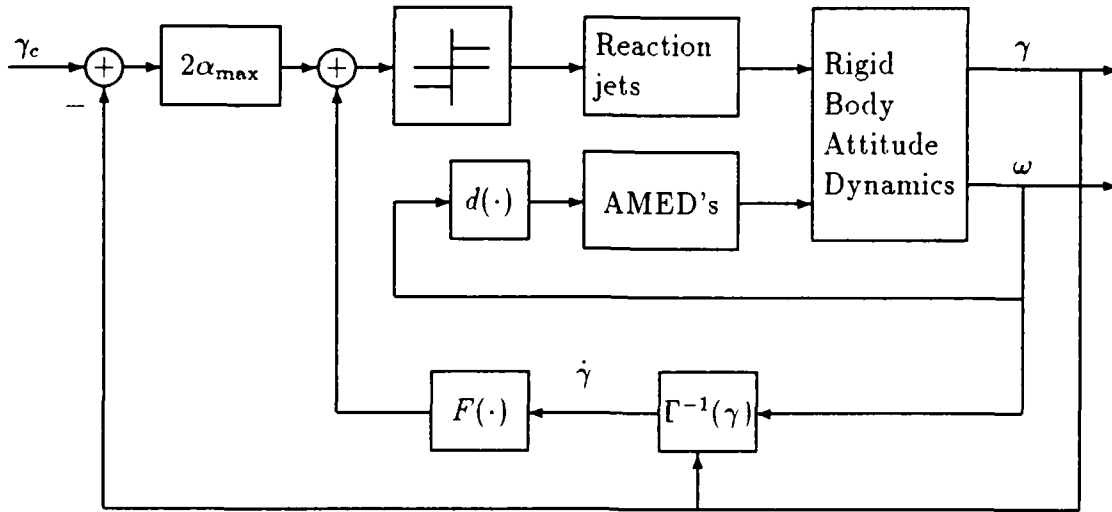


Figure 4.3: Coordinated Rapid Slewing Control Implementation

To obtain the required strict negative requirement $\dot{V} < -\mu$ similar relations can be developed which involve assumptions on the a priori maximal rates, $|z_2| < \dot{\gamma}_{\max}$. Our principal concern is in implementing the bang-bang control with sufficient control authority T_{\max} such that reaction of the flexible appendage response will be effectively decoupled from the rigid body attitude so that time-optimal slewing can be obtained. Note that the control law (4.69) can be implemented independently of state measurements associated with the flexible appendage deformation. The overall control structure is illustrated in Figure 4.3. From the above analysis we see that robustness to model uncertainty can be obtained if sufficient control authority in slewing torque τ^s (in particular T_{\max} is large enough) is available so that (4.70) is satisfied for all model variations [GP82].

4.3 Coordinating Control for System Slewing and Multibody Alignment

Throughout the modeling and control development for multibody slewing we have emphasized the importance of establishing a body fixed coordinate system attached to a system primary body. The dominant system nonlinearities arise from the introduction of nonlinear kinematics and dynamics of large angle rotations. We have implicitly assumed that structural deformation contributing to multibody misalignment dynamics are small and therefore linear when referenced to the body fixed frame. Our approach for coordinating multibody alignment and rapid slewing will be based on these assumptions. We now show that application of PLF compensation for linearizing and decoupling the natural nonlinear response of rapid, large angle slewing motions of the system primary body results in decoupling the multibody alignment problem from the slewing problem.

Referring the general multibody dynamics model (4.1)–(4.2), consider now the special case of (5.47)–(5.52). Let $q = [\gamma^T, u^T]^T$, $p = [\omega^T, \dot{u}^T]^T$, and $u = [\bar{\eta}^T, \xi^T]^T$. Then the SBL

model for multiaxis slewing developed in section 5.1 can be written in the form,

$$\begin{aligned} & \begin{bmatrix} M_{11}(q) & M_{12}(q) \\ M_{12}^T(q) & M_{22}(q) \end{bmatrix} \begin{pmatrix} \dot{\omega}_b \\ \ddot{u} \end{pmatrix} + \begin{bmatrix} B_{11}(q, p) & B_{12}(q, p) \\ B_{12}^T(q, p) & B_{22}(q, p) \end{bmatrix} \begin{pmatrix} \omega_b \\ \dot{u} \end{pmatrix} \\ & + \begin{bmatrix} K_{11}(q, p) & K_{12}(q, p) \\ K_{12}^T(q, p) & K_{22}(q, p) \end{bmatrix} \begin{pmatrix} \gamma \\ u \end{pmatrix} = \begin{bmatrix} G_b \\ 0 \end{bmatrix} \tau_b. \end{aligned} \quad (4.71)$$

We focus attention on the regulation of the primary system body frame attitude and take as primary system outputs,

$$y = [C_\gamma, 0]q = C_\gamma \gamma,$$

where we assume that y and τ_b are 3-vectors and the 3×3 matrix C_γ is full rank. We further assume that the regulated outputs (note that these outputs do not necessarily coincide with sensor locations) are collocated with the primary body torques;

$$C_\gamma = G_b^T.$$

Under these assumptions it is by now easy to see that the zero dynamics resulting from PLF compensation are given by,

$$M_{22}\ddot{u} + B_{22}\dot{u} + K_{22}u = 0. \quad (4.72)$$

Note that (4.72) is linear time invariant equation of the free response of the multibody alignment and structural vibration with

$$\gamma = \omega = 0.$$

Stability of the zero dynamics is a prerequisite for stabilization using PLF, but for practical implementations the degree of stability may be an important factor. For the SBL rapid slewing and pointing problem this decomposition of control problems is critical to system performance.

Decomposition of Control Authority and Stabilization of the Zero Dynamics.

Consider the general model of (4.1)–(4.2) modified to include additional controls,

$$\dot{q} = \tilde{\Gamma}(q)p \quad (4.73)$$

$$M(q)\dot{p} + B(q, p)p + K(q, p)q = \underbrace{G_b \tau_b}_{\text{primary control}} + \underbrace{G_s f_s}_{\text{alignment control}} \quad (4.74)$$

A direct computation based on (4.4) indicates that the required PLF compensation for the output (4.3) includes feedforward from the structural controls;

$$\tau_b = (C\tilde{\Gamma}M^{-1}G_b)^{-1}v - (C\tilde{\Gamma}M^{-1}G_b)^{-1}C\tilde{\Gamma}M^{-1}[(MD - B)p - Kq + G_s f_s], \quad (4.75)$$

and the resulting zero dynamics are

$$M_{22}\ddot{u} + B_{22}\dot{u} + K_{22}u = G_s f_s. \quad (4.76)$$

For application to rapid slewing of the multibody system the primary system output will be taken to be $y = \xi_b$ (or in terms of the Gibbs vector $y = \gamma$). Referring to the equations of motion for the generic multibody system derived in Section 5.1 we see that the zero dynamics (4.76) are merely the linear dynamics of the flexible structure with cantilevered boundary conditions. The structure controls effect multibody alignment and vibration suppression relative to the system body fixed frame.

The design approach we suggest is the integration of precision multibody alignment and vibration suppression based on robust stabilization of (4.76) together with the PLF compensation and slewing design described above. We remark that the design approach is predicated on the fact that multibody alignment for precision pointing and tracking is required at the termination of the slewing maneuver. Stabilization of (4.76) by the introduction of local feedback will effect transient responses during the slewing maneuver but the principal concern is stabilization at the end of the slew.

Remark: The decomposition for coordination of multibody alignment with rapid slewing can be viewed as a generalization of implementations commonly used for vibration suppression in flexible space structures. As described in [Jos89] implementation of feedback control for active vibration damping commonly uses pairs of actuators and sensors symmetrically located so as to eliminate sensitivity to rigid body modes. Such configurations are required since the low levels of control authority typically available for structural damping are too small to effect attitude and translation of the space vehicle. If the response of the rigid body modes are not decoupled from these control loops the actuators would saturate during any maneuver. Although the approach based on PLF for decoupling clarifies the role of local linear mode vibration damping in the context of the nonlinear system dynamics. Note however that in general, stabilization of the local linearization of the zero dynamics may not guarantee global stabilization with feedback linearizing control [KS89].

5 Simulation Tradeoff Studies for Multiaxis Slewing of SBL System Model

In this section we develop a model for generic SBL system beam expander as a two body system with elastic support structure. The model is refined from that developed and reported in [BBKA88] by:

- 3 rotational degrees-of-freedom included in system primary rigid body motion,
- area moments of attached structure modified to represent tripod metering truss,
- system inertias and slewing requirements scaled to represent capabilities of ASTREX facility and initial test article.

5.1 Multibody System Model for Multiaxis Slewing and Precision Alignment

The modeling method of Lagrange's equations, as described in the report [BBKA88], along with spatial discretization via collocation by splines to develop a finite dimensional model suitable for simulation of large angle, multiaxis motion of a generic, two-body model of a SBL system beam expander is described in this section. Beginning with the generic flexible spacecraft model [BBKA88, sec 4] the following model assumptions are made:

1. axial appendage deformations are negligible, $\eta_3 \approx z$,
2. translation velocity of the system primary body is negligible, $\dot{R} \approx 0$,
3. torsional appendage deformations are negligible, $\psi(z) \approx 0$.

Thus, following the DPS modeling approach discussed in [BBKA88, sec 3], the configuration space for the distributed parameter model is $SO(3) \times H_G^1$, where H_G^1 is the set of continuously differentiable functions, $\chi(z) = [\eta_1, \eta_2, \theta, \phi]^T \in H_G^1$ defined on the interval $z \in [0, \ell]$, and which satisfy the geometric boundary conditions :

$$\mathcal{G} : \quad \eta_1(z) = 0, \eta_2(z) = 0, \theta(z) = 0, \phi(z) = 0, \text{ at } z = 0.$$

With the notational conventions in [BBKA88], the model will be described by the appendage lateral deformation, $\eta(t, z) = [\eta_1, \eta_2]^T$, along the body-fixed x and y axes, respectively, and appendage angular deformation, $\xi(z, t) = [\theta(z), \phi(z)]^T$. The attitude angular rates referenced to the body fixed frame are denoted, ω_b .

The potential functions for the variational analysis leading to the dynamic equations of motion reduce in this case to:

$$\begin{aligned} T = & \frac{1}{2} \omega_b^T I_b \omega_b \\ & + \frac{1}{2} \int_0^\ell \|\Omega_b \eta(z) + \eta_t(z)\|^2 \rho A \, dz \\ & + \frac{1}{2} \int_0^\ell [\omega_b + P \xi_t(z)]^T I [\omega_b + P \xi_t(z)] \rho \, dz, \end{aligned} \tag{5.1}$$

Notation	Explanation
ρ	mass density
A	cross section area
E	elasticity
κG	effective shear modulus
I	area moment of inertia
$\dot{x} = \frac{dx}{dt}$	time differentiation
$x_z(t, z) = \frac{\partial x}{\partial z}(z, t)$	partial differentiation

Table 5.1: Standard Notation for Lagrangian Mechanics

$$V(\eta, \xi) = \frac{1}{2} \int_0^\ell \{EI_\theta \theta_z^2(z) + EI_\phi \phi_z^2(z) \quad (5.2)$$

$$+ \kappa_1 GA[(\eta_1(z))_z - \theta(z)]^2 + \kappa_2 GA[(\eta_2(z))_z - \phi(z)]^2\} dz, \quad (5.3)$$

$$R(\dot{\eta}, \dot{\xi}) = \frac{1}{2} \int_0^\ell \{\eta_t^T \Xi_1 \eta_t + \xi_t^T \Xi_2 \xi_t + (\eta_{tz})^T \Xi_3 \eta_{tz} + (\xi_{tz})^T \Xi_4 (\xi_{tz})\} dz, \quad (5.4)$$

where

$$P = \begin{bmatrix} 0 & 0 & 1 \\ 0 & 1 & 0 \\ 1 & 0 & 0 \end{bmatrix},$$

T is the kinetic energy, V the potential energy, and R the Rayleigh dissipation function. The notation used is standard in continuum mechanics of beams and is summarized in Table 5.1. The area moment tensor is assumed to have the form²,

$$I(z) = \begin{bmatrix} I_{xx} & 0 & 0 \\ 0 & I_{yy} & 0 \\ 0 & 0 & I_{zz} \end{bmatrix}.$$

For simulation studies contained in this report we utilize a simple damping model given by the assumption that the matrix coefficients in the dissipation function are of the form,

$$\Xi_i = \begin{bmatrix} \zeta_{1,i} & 0 \\ 0 & \zeta_{2,i} \end{bmatrix}.$$

Note that Ξ_1, Ξ_2 model *external dissipation* while Ξ_3, Ξ_4 model *internal dissipation* [BK89].

The control forces acting on the system primary body are modeled as external torques and enter the variational setup through a virtual work expression of the form,

$$\delta W = \tau_b^T \delta \xi_b$$

²We use the so-called NASA standard or 321 convention [Gol82].

In the sequel, we refer to the kinetic energy expression in terms of three components;

$$T_{\text{rigid body}} = \frac{1}{2} \omega_b^T I_b \omega_b, \quad (5.5)$$

$$T_{\text{flex}_1} = \frac{1}{2} \int_0^\ell \|\Omega_b \eta(z) + \eta_t(z)\|^2 \rho A \, dz, \quad (5.6)$$

$$T_{\text{flex}_2} = \frac{1}{2} \int_0^\ell [\omega_b + \xi_t(z)]^T I [\omega_b + \xi_t(z)] \rho \, dz. \quad (5.7)$$

5.1.1 FEM: Collocation by Splines

A model based on the Finite Element Method (FEM) is obtained by spatial discretization via collocation by splines. The use of splines for such purposes is described in [BBKA88]. Given the geometric boundary conditions described above the discrete approximations of the scalar valued functions, $\eta_1(z)$, $\eta_2(z)$, $\theta(z)$, $\phi(z)$, are decoupled and reduce to approximation of a single scalar function, say $\gamma(z)$, on the interval $z \in [0, \ell]$ with boundary condition, $\gamma(0, t) = 0$. Dividing the interval $[0, \ell]$ into N uniform subintervals and using first-order B-splines we obtain the approximation:

$$\gamma(z, t) \approx \sum_{i=0}^N \hat{\gamma}_i(t) B_{i-1}^1(z) \quad (5.8)$$

with the boundary condition,

$$\sum_{i=0}^N \hat{\gamma}_i(t) B_{i-1}^1(0) = 0.$$

Then following the reduction procedure described in [BBKA88, §4.4.2] we obtain the FEM approximations with $\Phi(z)$ as given in [BBKA88, Eqn. (4.47)],

$$\eta_1(z, t) \approx \Phi^T(z) \bar{\eta}_1(t) \quad (5.9)$$

$$\eta_2(z, t) \approx \Phi^T(z) \bar{\eta}_2(t) \quad (5.10)$$

$$\theta(z, t) \approx \Phi^T(z) \bar{\theta}(t) \quad (5.11)$$

$$\phi(z, t) \approx \Phi^T(z) \bar{\phi}(t). \quad (5.12)$$

5.1.2 Reduction of the Kinetic Energy Function

Using the FEM approximations of order N we obtain the spatial discretization of the kinetic energy terms,

$$T_{\text{flex}_1} \approx \frac{1}{2} \{ \omega_b^T I_{\omega\omega}(\bar{\eta}) \omega_b + 2 \omega_b^T I_{\omega\eta}(\bar{\eta}) \dot{\bar{\eta}} + \dot{\bar{\eta}}^T I_{\eta\eta} \dot{\bar{\eta}} \} \quad (5.13)$$

$$T_{\text{flex}_2} \approx \frac{1}{2} \{ \omega_b^T J_{\omega\omega} \omega_b + 2 \omega_b^T J_{\omega\xi} \dot{\bar{\xi}} + \dot{\bar{\xi}}^T J_{\xi\xi} \dot{\bar{\xi}} \} \quad (5.14)$$

where

$$I_{\omega\omega}(\bar{\eta}) = \begin{bmatrix} \bar{\eta}_2^T N_{\eta\eta} \bar{\eta}_2 + \sigma & -\bar{\eta}_1^T N_{\eta\eta} \bar{\eta}_2 & -\bar{\eta}_1^T N_{\eta} \\ -\bar{\eta}_1^T N_{\eta\eta} \bar{\eta}_2 & \bar{\eta}_1^T N_{\eta\eta} \bar{\eta}_1 + \sigma & -\bar{\eta}_2^T N_{\eta} \\ -\bar{\eta}_1^T N_{\eta} & -\bar{\eta}_2^T N_{\eta} & \bar{\eta}_2^T N_{\eta\eta} \bar{\eta}_2 + \bar{\eta}_1^T N_{\eta\eta} \bar{\eta}_1 \end{bmatrix}, \quad (5.15)$$

$$N_{\eta\eta} = \int_0^\ell \rho A \Phi(z) \Phi^T(z) dz, \quad (5.16)$$

$$N_\eta^T = \int_0^\ell \rho A z \Phi^T(z) dz, \quad (5.17)$$

$$\sigma = \int_0^\ell \rho A z^2 dz = \frac{\rho A \ell^3}{3}, \quad (5.18)$$

$$I_{\omega\eta} = \begin{bmatrix} 0 & -N_\eta^T \\ N_\eta^T & 0 \\ -\bar{\eta}_2^T N_{\eta\eta} & \bar{\eta}_1^T N_{\eta\eta} \end{bmatrix}, \quad (5.19)$$

$$I_{\eta\eta} = \begin{bmatrix} N_{\eta\eta} & 0 \\ 0 & N_{\eta\eta} \end{bmatrix}, \quad (5.20)$$

$$J_{\omega\omega} = \int_0^\ell \rho I(z) dz, \quad (5.21)$$

$$J_{\omega\xi} = \begin{bmatrix} 0 & N_\phi^T \\ N_\theta^T & 0 \\ 0 & 0 \end{bmatrix}, \quad (5.22)$$

and

$$J_{\xi\xi} = \begin{bmatrix} N_{\theta\theta} & 0 \\ 0 & N_{\phi\phi} \end{bmatrix}. \quad (5.23)$$

The following terms are used in the above expressions,

$$N_\psi^T = \int_0^\ell \rho I_{zz} \Phi^T(z) dz, \quad (5.24)$$

$$N_\theta^T = \int_0^\ell \rho I_{yy} \Phi^T(z) dz, \quad (5.25)$$

$$N_\phi^T = \int_0^\ell \rho I_{xx} \Phi^T(z) dz, \quad (5.26)$$

$$N_{\phi\phi} = \int_0^\ell \rho I_{xx} \Phi(z) \Phi^T(z) dz, \quad (5.27)$$

$$N_{\theta\theta} = \int_0^\ell \rho I_{yy} \Phi(z) \Phi^T(z) dz. \quad (5.28)$$

Note that the total kinetic energy can be written in the standard form,

$$T \approx \frac{1}{2} [\omega_b^T, \dot{\bar{\eta}}^T, \dot{\bar{\xi}}^T] M(\xi_b, \bar{\eta}, \bar{\xi}) \begin{pmatrix} \omega_b \\ \dot{\bar{\eta}} \\ \dot{\bar{\xi}} \end{pmatrix} \quad (5.29)$$

where

$$M(\xi_b, \bar{\eta}, \bar{\xi}) = \begin{bmatrix} I_b + I_{\omega\omega}(\bar{\eta}) + J_{\omega\omega} & I_{\omega\eta}(\bar{\eta}) & J_{\omega\xi} \\ I_{\omega\eta}^T(\bar{\eta}) & I_{\eta\eta} & 0 \\ J_{\omega\xi}^T & 0 & J_{\xi\xi} \end{bmatrix}. \quad (5.30)$$

5.1.3 Reduction of the Potential Energy and Dissipation Functions

As above, the potential energy and dissipation functions are reduced by substitution of the FEM approximations. For the potential energy we obtain,

$$V = \frac{1}{2} \{ \bar{\theta}^T K_{\theta} \bar{\theta} + \bar{\phi}^T K_{\phi} \bar{\phi} + \bar{\eta}_1^T K_{\eta_1} \bar{\eta}_1 + \bar{\eta}_2^T K_{\eta_2} \bar{\eta}_2 + 2 \bar{\theta}^T K_{\theta \eta_1} \bar{\eta}_1 + 2 \bar{\phi}^T K_{\phi \eta_2} \bar{\eta}_2 \}, \quad (5.31)$$

where

$$K_{\theta} = \int_0^{\ell} \{ E I_{yy} \Phi_z(z) \Phi_z^T(z) + \kappa_1 G A \Phi(z) \Phi^T(z) \} dz \quad (5.32)$$

$$K_{\phi} = \int_0^{\ell} \{ E I_{xx} \Phi_z(z) \Phi_z^T(z) + \kappa_2 G A \Phi(z) \Phi^T(z) \} dz \quad (5.33)$$

$$K_{\eta_1} = \int_0^{\ell} \{ \kappa_1 G A \Phi_z(z) \Phi_z^T(z) \} dz \quad (5.34)$$

$$K_{\eta_2} = \int_0^{\ell} \{ \kappa_2 G A \Phi_z(z) \Phi_z^T(z) \} dz \quad (5.35)$$

$$K_{\theta \eta_1} = -\frac{1}{2} \int_0^{\ell} \{ \kappa_1 G A \Phi(z) \Phi_z^T(z) \} dz \quad (5.36)$$

$$K_{\phi \eta_2} = -\frac{1}{2} \int_0^{\ell} \{ \kappa_2 G A \Phi(z) \Phi_z^T(z) \} dz. \quad (5.37)$$

Similarly, the dissipation function reduces to the form,

$$R = \frac{1}{2} \{ \dot{\bar{\eta}}_1^T B_{\eta_1} \dot{\bar{\eta}}_1 + \dot{\bar{\eta}}_2^T B_{\eta_2} \dot{\bar{\eta}}_2 + \dot{\bar{\theta}}^T B_{\theta} \dot{\bar{\theta}} + \dot{\bar{\phi}}^T B_{\phi} \dot{\bar{\phi}} + 2 \dot{\bar{\theta}}^T B_{\theta \eta_1} \dot{\bar{\eta}}_1 + 2 \dot{\bar{\phi}}^T B_{\phi \eta_2} \dot{\bar{\eta}}_2 \}, \quad (5.38)$$

where given the expressions,

$$R_0 := \int_0^{\ell} \Phi(z) \Phi^T(z) dz, \quad (5.39)$$

$$R'_0 := \int_0^{\ell} \Phi_z(z) \Phi^T(z) dz, \quad (5.40)$$

$$R''_0 := \int_0^{\ell} \Phi_z(z) \Phi_z^T(z) dz, \quad (5.41)$$

we find it convenient to express the individual matrix coefficients in R (arising from the FEM approximation) as:

$$B_{\eta_i} = \zeta_{i1} R_0 + \zeta_{i3} R''_0 \quad \text{for } i = 1, 2, \quad (5.42)$$

$$B_{\theta} = (\zeta_{12} + \zeta_{13}) R_0 + \zeta_{14} R'_0, \quad (5.43)$$

$$B_{\phi} = (\zeta_{22} + \zeta_{23}) R_0 + \zeta_{24} R'_0, \quad (5.44)$$

$$B_{\eta_1 \theta} = -\zeta_{13} R'_0, \quad (5.45)$$

$$B_{\eta_2 \phi} = -\zeta_{23} R'_0. \quad (5.46)$$

Finally, we summarize the model stiffness and damping using the expressions,

$$K_{\eta} = \begin{bmatrix} K_{\eta_1} & 0 \\ 0 & K_{\eta_2} \end{bmatrix}, \quad K_{\eta \xi} = \begin{bmatrix} K_{\theta \eta_1} & 0 \\ 0 & K_{\phi \eta_2} \end{bmatrix}, \quad K_{\xi} = \begin{bmatrix} K_{\theta} & 0 \\ 0 & K_{\phi} \end{bmatrix},$$

$$B_{\eta} = \begin{bmatrix} B_{\eta_1} & 0 \\ 0 & B_{\eta_2} \end{bmatrix}, \quad B_{\eta \xi} = \begin{bmatrix} B_{\theta \eta_1} & 0 \\ 0 & B_{\phi \eta_2} \end{bmatrix}, \quad B_{\xi} = \begin{bmatrix} B_{\theta} & 0 \\ 0 & B_{\phi} \end{bmatrix}.$$

5.1.4 Lagrange's Equations

Finally, we compute the equations of motion using Lagrange's equations in the form:

$$\dot{q} = \tilde{\Gamma}(q)p \quad (5.47)$$

$$M(q)\dot{p} + \left[\frac{\partial M(q)p}{\partial q} \right] p - \frac{1}{2} \left[\frac{\partial M(q)p}{\partial q} \right]^T p + \frac{\delta V}{\delta q} = -\frac{\delta R}{\delta p} + Q_q \quad (5.48)$$

with generalized coordinates $q = \{\xi_b, \bar{\eta}, \bar{\xi}\}$, and velocities, $p = \{\omega_b, \dot{\bar{\eta}}, \dot{\bar{\xi}}\}$.

Equations of Motion for Multiaxis Slewing Applying Lagrange's equation results (after some simplification) in the equations of motion with kinematics of the system attitude expressed in terms of the Gibbs vector, γ ;

$$\dot{\gamma} = \Gamma(\gamma)\omega_b, \quad (5.49)$$

and kinetics,

$$[I_b + I_{\omega\omega} + J_{\omega\omega}]\dot{\omega}_b + I_{\omega\eta}\ddot{\eta} + J_{\omega\xi}\ddot{\xi} + \Omega_b\{[I_b + I_{\omega\omega} + J_{\omega\omega}]\omega_b + I_{\omega\eta}\dot{\eta} + J_{\omega\xi}\dot{\xi}\} + H\dot{\eta} = \tau_b \quad (5.50)$$

$$I_{\omega\eta}^T\dot{\omega}_b + I_{\eta\eta}\ddot{\eta} - \frac{1}{2}H^T\omega_b + R\dot{\eta} + K_{\eta}\bar{\eta} + K_{\eta\xi}\bar{\xi} + B_{\eta}\dot{\eta} + B_{\eta\xi}\dot{\xi} = G_{\eta}f, \quad (5.51)$$

$$J_{\omega\xi}^T\dot{\omega}_b + J_{\xi\xi}\ddot{\xi} + K_{\xi}\bar{\xi} + K_{\eta\xi}^T\bar{\eta} + B_{\xi}\dot{\xi} + B_{\eta\xi}^T\dot{\eta} = G_{\xi}\tau, \quad (5.52)$$

where

$$H(\bar{\eta}, \omega_b, \dot{\eta}) = \begin{bmatrix} -\omega_2\bar{\eta}_2^T N_{\eta\eta}^T - \omega_3 N_{\eta}^T & 2\bar{\eta}_2^T N_{\eta\eta}\omega_1 \\ -\omega_1\bar{\eta}_2^T N_{\eta\eta}^T + 2\omega_2\bar{\eta}_1^T N_{\eta\eta} & -\omega_1\bar{\eta}_1^T N_{\eta\eta}^T - 2\omega_3 N_{\eta}^T \\ -\omega_1 N_{\eta}^T + \omega_3 2\bar{\eta}_1^T N_{\eta\eta} + \dot{\eta}_1^T N_{\eta\eta} & -\omega_2 N_{\eta}^T + \omega_3 2\bar{\eta}_2^T N_{\eta\eta} + \dot{\eta}_2^T N_{\eta\eta} \end{bmatrix}, \quad (5.53)$$

$$R(\omega_b) = \begin{bmatrix} 0 & \omega_3 N_{\eta\eta} \\ \omega_3 N_{\eta\eta} & 0 \end{bmatrix}. \quad (5.54)$$

5.2 Computer Simulation Model for Nonlinear Control Law Tradeoff Studies

A computer simulation model was developed and coded based on the above FEM model for attitude slewing of a flexible space craft (5.49)–(5.52). The model parameters and geometry was chosen to represent the dynamics of a SBL system beam expander with structural flexure arising from the flexure response of the metering truss. A goal of the second year effort was to develop concepts for experimental testing of nonlinear control concepts for flexible space structures. A suitable facility for testing large angle, multiaxis slewing and precision pointing is currently under construction at the Astronautics Laboratory. The ASTREX facility will include 3 axis slewing and the initial test article is a scaled model of a SBL beam expander. We have adapted our nonlinear slewing control simulation model to represent available parameters and geometry of the ASTREX test article. Details of the modeling assumptions and geometry are given below.

5.2.1 Simulation model geometry assumptions and parameters

The objective of the simulation model design was to generate a simplified model that would duplicate, as closely as possible, the geometry and dynamics of the ASTREX test article. Information describing the test article was sparse, therefore, the following assumptions were required to develop a working simulation model:

1. The basic configuration of the model consisted of a rigid body, representing the main mirror assembly and associated structure, and an attached tripod structure, representing the flexible metering truss with secondary mirror, see Figure 5.1.

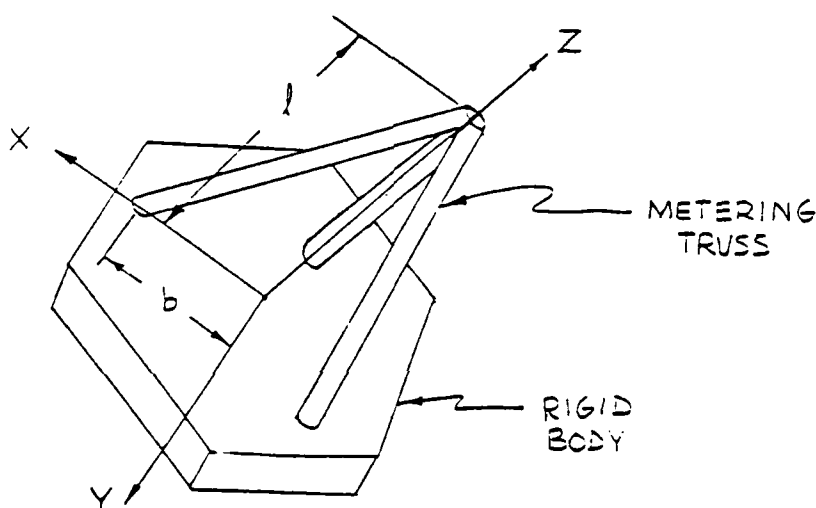


Figure 5.1: Simulation model.

2. The metering truss geometry consisted of a tripod of tubes located at the corners of an equilateral triangular base. The generic model discussed above was readily adapted to represent this geometry by including spatial variation of the area moments $I_{xx}(z)$ and $I_{yy}(z)$ based on this geometry. Details of the computation of the area moments and the resulting FEM model approximations are given in Appendix A.
3. The dimensions of the metering truss model were as follows:

Length, l	-	5.0 m
Base width, b	-	3.8 m
Tube inner dia.	-	8.0 cm
Tube outer dia.	-	12.7 cm
Mass of secondary mirror	-	190 kg (5 % of total sys. mass)
4. The overall system characteristics were as follows:

Mass moments of inertia	I_{xx}	=	16640 kg m ²
	I_{yy}	=	16590 kg m ²
	I_{zz}	=	11660 kg m ²
System mass	m	=	3810 kg
First modal freq. of metering truss		=	12.2 Hz

5. The dynamics of the secondary mirror were neglected and it was modeled as a point mass at the end of the truss.
6. The modulus of elasticity of the truss material was chosen so that its first modal frequency matched that of the ASTREX test article.

5.3 Simulation Results for PLF Control with Rapid Slewing and Precision Pointing

Based on the above simulation model a digital simulation was developed using PC-Matlab to perform tradeoff studies for implementation rapid slewing and precision pointing of an SBL beam expander with PLF compensation.

The model equations (5.49)–(5.52) with position coordinates, $q = [\gamma_b^T, \bar{\eta}^T, \bar{\xi}^T]^T$, and velocities, $p = [\omega_b^T, \dot{\bar{\eta}}^T, \dot{\bar{\xi}}^T]^T$, can be reduced to the generic form (4.1)–(4.2). The simulation models and parameters assumed for the tradeoff studies are summarized in Table 5.2. Simulated time responses for each model with several different control laws are displayed in the figures contained in Appendix C. Each simulated maneuver is summarized in a set of figures including the responses of position γ , attitude rates, $\dot{\gamma}$, system torques applied to the primary body, τ_b , and deformations at the apex of the truss, $\eta(\ell), \xi(\ell)$. Table 5.3 describes the simulation runs performed and illustrates the relationship between system models and control laws used.

Slewing with Smooth PLF Compensation. For precision pointing of the system attitude we take the primary system outputs as $y = \gamma_b$. PLF compensation for the resulting system is given by the formula, (4.4). Multiaxis slewing and pointing control was implemented on an independent axis basis subsequent to PLF compensation. Thus the PLF Slewing control is obtained by setting the v controls appearing in (4.4) as,

$$v_i = \alpha_i, \quad \text{for } i = 1, 2, 3$$

where the commanded accelerations, α_i are generated by the independent axis, time-optimal slewing control,

$$\alpha_i(t) = -\alpha_{\max} \text{sat}\{f(\dot{\gamma}_i) + 2\alpha_{\max}\gamma_i\},$$

as described in Section 4.1.

Simulation tradeoff studies completed this year focused on the implementation of PLF compensation for various reduced-order models of the metering truss flexure. The reduction methods described in Section 3 were used to obtain implementation alternatives for PLF compensation in terms of the quasi-rigid model with DOF, $r = 3, 4, 5, 11$. The case $r = 11$

Parameter	Simulation Model									
	MOD1	MOD2	MOD3	MOD4	MOD5	MOD6	MOD7	MOD8	MOD9	
SBL beam expander model parameters										
ρ - mass density	1520	-	-	-	-	-	-	-	-	
E - elasticity	200	-	-	-	-	-	-	-	-	
N - # finite elements	2	-	-	-	-	-	-	-	-	
ϵ damping factor	.001	.001	.004	.004	.001	.001	.001	.001	.001	
m_t/m_{tot}	0.05	0.0	0.05	0.0	0.0	0.0	0.05	0.0	0.05	
Control/Actuator parameters										
α_{max} [rad/sec ²]	.349	-	-	-	-	-	-	-	-	
T_{max} Peak Torque ($\times 10^3$)	N/A	N/A	N/A	N/A	9.3	1.4	27.0	22.	22.	
g_1 - control gain ($\times 10^3$)	6.477	6.477	6.477	6.477	5.E6	5.E6	5.E6	5.E6	5.E6	
g_2 - control gain	0.0374	-	-	-	-	-	-	-	-	
Simulation Solution Precision										
ODE tolerance	0.001	-	-	-	-	-	-	-	-	

Table 5.2: Matrix of Simulation Models Considered

Models	Control Laws					
	Continuous PLF/Slewing				Discontinuous PLF/Slewing	
	$r = 3$	$r = 4$	$r = 5$	$r = 11$	Slew rate limited torque	Discontinuous torque
Multiaxis Slew						
MOD1	SIM11	SIM12	SIM13	SIM14		
MOD2	SIM21	SIM22	SIM23	SIM24		
MOD3	SIM31	SIM32	SIM33			
MOD4	SIM41	SIM42	SIM43			
MOD5					SIM51	SIM62 SIM72
MOD6					SIM61	
MOD7						
MOD8					SIM81	
MOD9					SIM91	
Multiaxis Large Angle Slew						
MOD1	SIM15		SIM16			
MOD2	SIM25		SIM26			

Table 5.3: Matrix of PLF/Slewing Control Implementations

Slew Times (sec) to $ \gamma_i < .001$				
$r =$	PLF Model DOF			
	3	4	5	11
Model MOD1				
Axis 1	.8005	.8218	.8268	.8258
2	.6709	.6725	.6933	.6930
3	.5145	.5162	.5241	.5223
Model MOD2				
Axis 1	> 1.00	.8257	.8246	.8296
2	.8402	.8335	.6868	.6872
3	.5145	.5168	.5189	.5183
Model MOD3				
Axis 1	> 1.00	.8260	.8273	
2	.8497	.8494	.6892	
3	.5172	.5193	.5227	
Model MOD4				
Axis 1	.8094	.8277	.8302	
2	.6732	.6920	.6888	
3	.5184	.5136	.5191	

Table 5.4: Slewing Times for Standard 3-axis Maneuver

corresponds to compensation for all the simulated elastic degrees of freedom of the flexible structure response and was included as a baseline for ideal PLF compensation.

Simulation runs SIM11—SIM43 were made to compare slewing time and peak torque requirements for implementation of PLF compensation for multiaxis slewing. For comparison of subsequent time responses, a nominally small angle, multiaxis maneuver was considered with desired system attitude given by $\gamma = 0$ and initial orientation given by $\gamma = [.07, .05, .03]^T$. This attitude maneuver can be expressed in Euler angles as,

$$[\psi, \theta, \phi] = [1.4^\circ, -1.7^\circ, 2.3^\circ].$$

Performance results for continuous mode PLF implementation are summarized in Table 5.4 and 5.5. The performance sensitivity to the presence of a significant mass (approximately 5 % of the system mass) at the apex of the truss was also examined. Despite the relative stiffness of the structure the multibody coupling is evident in the attitude overshoot for the small angle maneuver. (All simulation runs are included in Appendix C.) Implementation of the PLF compensation for multiaxis slewing requires increased bandwidth and peak torques on the system rigid body. The importance of damping in the appendage can be seen in Tables 5.4–5.5. With increased damping peak torque required for PLF compensation will decrease.

To illustrate the large angle response with PLF compensation we also simulated a ma-

Peak Torque $\Delta T_{pk}(r)/T_{pk}(3)$ Relative to rigid body case				
simulation model $r =$	PLF Model DOF			
	3	4	5	11
MOD1	0	1.11	1.10	1.12
MOD2	0	.278	.282	.293
MOD3	0	.848	.842	
MOD4	0	.238	.243	

Table 5.5: Relative Peak Torque Increase with PLF Compensation DOF

maneuver characterized by $\gamma = [.5, .4, .3]^T$, which can be expressed in Euler angles as,

$$[\psi, \theta, \phi] = [45.^\circ, -19.5^\circ, 61.3^\circ].$$

The simulated time responses with PLF compensation for the rigid body modes only reveals significant overshoot and in the case of a mass at the apex significant torque switching activity is generated. The addition of PLF compensation for the rigid body plus first two elastic modes of the beam recovers ideal time-optimal attitude orientation. This also noticeably reduces chattering activity near the time-optimal switching surface. For these large angle maneuvers (probably difficult to test experimentally at the ASTREX facility) the lateral deformation of the apex (with tip mass) is less than 1 cm. indicating the stiffness of this structure.

Slewing with Discontinuous/Continuous Actuation. Simulation studies SIM51-SIM91 were performed using coordination of discontinuous and continuous modes of actuation for PLF compensation and rapid slewing as described in section 4.2. The simulation trade-off studies for this case focused on the requirements for increased peak torque to recover near ideal time-optimal, independent axis slewing using only the rigid body attitude output information for control law implementation.

As discussed in Section 4.1 actuators are often subject to slew rate limits which will limit switching response for on-line implementation of discontinuous mode control laws of the form (4.69). Simulation runs were completed with slew rate limited implementation of the discontinuous controls, τ^s , by replacing the sgn function with a saturation function with linear slope, g_1 (cf. Table 5.2).

The significance of implicit PLF compensation achieved in sliding is apparent by comparison of the time responses of SIM13 and SIM72. In both cases the models include a secondary body at the apex of the metering truss which involves significant multibody dynamic response. Using continuous mode actuation, PLF compensation is maintained during the entire slewing transient by control torques applied to the primary body. Using discontinuous actuation PLF compensation is achieved after an initial transient—once the sliding condition is attained. Thus during the acceleration phase of system slewing the action of the continuous compensation component, τ^c does not compensate for multibody dynamics. It

is also clear that increased torque authority, T_{\max} , is necessary to maintain sliding over that required for purely continuous mode PLF compensation of SIM13. The primary difference is that the continuous mode PLF compensation achieves decoupling by 'in-phase' compensation of the multibody motion while the discontinuous/continuous mode approach of SIM72 is achieved without explicit feedback of the motion of the secondary body.

It is not clear at this point in our study how significant it is to maintain PLF compensation during initial transients. For system slewing the total slew time and terminal pointing accuracy are clearly dominant concerns. However, it is possible to include compensation for multibody motion in the combined implementation and we hope to investigate this further in the next year.

Our simulation studies of the method of PLF compensation and slewing by coordinated discontinuous and continuous modes of actuation should be viewed as preliminary. A goal of the next years activities will be to further investigate implementation alternatives and performance tradeoffs in this area. The simulation results obtained to date reveal that implicit PLF compensation and near time optimal slewing can be obtained with increased system torques. We believe that the peak torque requirements for slewing can be relaxed using dual mode actuation if the secondary body motion can be taken into account in the continuous mode component τ^c of the torque acting on the rigid body.

6 Conclusions and Directions

The second year study has provided some new insights in implementation alternatives for coordinated multiple actuation mechanisms for achieving rapid, large angle, multiaxis slewing control of multibody systems. The simulation studies illustrate several important design issues in implementation of PLF control for slewing and pointing. Implementation of PLF control by continuous mode actuation enforces decoupling during system transient responses by additional control authority. Its implementation will require available measurements of structural flexure. Implementation using discontinuous mode actuation, based on sliding mode control, enforces feedback linearization implicitly and only after an initial transient. An open question is the importance of enforcing feedback linearization during such transients for retargeting and pointing maneuvers.

Simulation studies have been scaled as much as possible based on available data and system parameters for the ASTREX test article. It is hoped that the control concepts for nonlinear PLF compensation and slewing can be tested experimentally on the ASTREX or similar facility. A goal of the third year effort is to develop designs for control law validation using laboratory simulations and experiments for the control concepts developed in this study. Although detailed designs and laboratory simulations are outside the scope of the present study we hope to describe a framework for an experimental test plan which will identify significant nonlinear dynamic responses and validate the importance of feedback linearization for their compensation. We feel that the presence of such nonlinear dynamical interactions can be an important limiting factor in predicting the responses of control system designs for multibody systems. It is widely recognized that such nonlinear dynamics will be evident in rapid, large angle, multiaxis slewing. We feel that in the presence of significant multibody coupling that pointing and tracking precision may also be limited by weak nonlinear interactions. If such limitations are significant they can best be demonstrated in laboratory simulations.

References

- [AB87] O. Akhrif and G.L. Blankenship. Using computer algebra in the design of nonlinear control systems. *Proc. ACC*, 1987.
- [AB88] O. Akhrif and G. L. Blankenship. Robust stabilization of feedback linearizable systems. In *Proc. 27th IEEE Cont. Dec. Conf.*, 1988.
- [ABB89] O. Akhrif, G.L. Blankenship, and W.H. Bennett. Robust control for rapid reorientation of flexible structures. In *Proc. 1989 ACC*, pages 1142-1147, 1989.
- [AF66] M. Athans and P. L. Falb. *Optimal Control*. McGraw-Hill, 1966.
- [Akh89] O. Akhrif. *Nonlinear Adaptive Control with Application to Flexible Structures*. PhD thesis, University of Maryland, College Park, MD, 1989.
- [Arn78] V.I. Arnold. *Mathematical Methods of Classical Mechanics*. Springer-Verlag, New York, 1978.
- [BBKA88] W. H. Bennett, G. L. Blankenship, H. G. Kwatny, and O. Akhrif. Nonlinear dynamics and control of flexible structures. Technical Report SEI-88-11-15-WB, SEI, November 1988. AFOSR/AFSC contract F49620-87-C-0103.
- [BI84] C.I. Byrnes and A. Isidori. A frequency domain philosophy for nonlinear systems, with application to stabilization and adaptive control. In *Proc. IEEE CDC*, Las Vegas, NV, 1984.
- [BI85] C. I. Byrnes and A. Isidori. Global feedback stabilization of nonlinear systems. In *Proc. 24th IEEE CDC*, pages 1031-1037, Dec. 1985.
- [BK89] W.H. Bennett and H.G. Kwatny. Continuum modeling of flexible structures with application to vibration control. *AIAA J.*, 27(9):1264-1273, September 1989.
- [BL87] J. Baillieul and M. Levi. Rotational elastic dynamics. *Physica 27D*, 27:43-62, 1987.
- [Bro78] R.W. Brockett. Feedback invariants for nonlinear systems. In *Proc. 6th IFAC World Congress*, pages 1115-1120, Helsinki, 1978.
- [Dwy84] T. A. W. Dwyer. Exact nonlinear control of large angle rotational maneuvers. *IEEE Trans. on Auto. Control*, AC-29(9):760-764, 1984.
- [Dwy88] T.A.W. Dwyer. Slew-induced deformation shaping. In *Proc. 27th IEEE CDC*, 1988.
- [DZM88] R. A. DeCarlo, S. H. Zak, and G.P. Matthews. Variable structure control of nonlinear multivariable systems: A tutorial. *Proc. IEEE*, 76(3):212-232, 1988.

- [FH87] R. B. Fernandez and J. K. Hedrick. Control of multivariable nonlinear systems by the sliding mode method. *Int. J. Control*, 46(3):1019-1040, 1987.
- [Fre75] E. Freund. The structure of decoupled nonlinear systems. *Int. J. Control*, 21(3):443-450, 1975.
- [GL76] S. Gutman and G. Leitman. Stabilizing control for linear systems with bounded parameter and input uncertainty. In *Proc. 7th IFIP Conf. on Optimization Techniques*, page 729. Springer-Verlag, 1976.
- [Gol82] H. Goldstein. *Classical Mechanics*. Addison-Wesley, Reading, MA, 1982.
- [GP82] S. Gutman and Z. Palmor. Properties of min-max controllers in uncertain dynamical systems. *SIAM J. Control*, 20(6):850-861, 1982.
- [Hir79] R. M. Hirschorn. Invertibility of nonlinear control systems. *SIAM J. Optim. and Control*, 17(2):289-297, 1979.
- [HSM83] R. Hunt, R. Su, and G. Meyer. Global transformation of nonlinear systems. *IEEE Trans. Automatic Control*, AC-28:24-31, 1983.
- [Isi85] A. Isidori. *Nonlinear Control Systems: An Introduction*. Springer-Verlag, 1985.
- [Jos89] S. M. Joshi. *Control of Large Flexible Space Structures*. Springer-Verlag, 1989.
- [KC87] C. Kravaris and C-B Chung. Nonlinear state feedback synthesis by global input/output linearization. *AIChE Journal*, 33(4):592-603, April 1987.
- [KK89] H.G. Kwatny and H. Kim. Variable structure control of partially linearizable dynamics. In *Proc. 1989 ACC*, pages 1148-1153, 1989.
- [KKO86] P.V. Kokotovic, H. Khalil, and J. O'Reilly. *Singular Perturbation Methods in Control: Analysis and Design*. Academic Press, New York, 1986.
- [KO88] F. Khorrami and U. Ozguner. Singular perturbation analysis of a distributed parameter model of a flexible manipulators. In *Proc. 1988 ACC*, pages 1701-1709, 1988.
- [Kra87] C. Kravaris. On the internal stability and robust design of globally linearizing control systems. In *Proc. ACC*, pages 270-279, 1987.
- [Kre73] A. J. Krener. On the equivalence of control systems and linearization of nonlinear systems. *SIAM J. Cont. and Optim.*, 11:670, 1973.
- [KS89] P. V. Kokotovic and H. J. Sussman. A positive real condition for global stabilization of nonlinear systems. *Syst. Cntrl. Letters*, 13:125-133, 1989.
- [Le87] M. Lock and et al. Structural dynamic response of a space based laser system. Technical Report AD-B109 212, February 1987.

- [MC80] G. Meyer and L. Cicolani. Applications of nonlinear system inverses to automatic flight control design—systems concepts and flight evaluations. In P. Kent, editor, *Theory and Applications of Optimal Control in Aerospace Systems*, pages 10–1–29. NATO AGARD, 1980. AGARDograph 251.
- [RR87] L. C. Rogers and K. E. Richards. Pacoss program status and results. Technical report, Air Force Wright Aeronautical Laboratory, 1987.
- [SKK87] M. W. Spong, K. Khorasani, and P. V. Kokotovic. An integral manifold approach to the feedback control of flexible joint robots. *IEEE J. Robotics and Auto.*, RA-3(4):291–299, 1987.
- [SS83] J.J. Slotine and S.S. Sastry. Tracking control of nonlinear systems using sliding surfaces with application to robot manipulators. *Int. J. Control*, 38(2):465–492, 1983.
- [SV87] M. W. Spong and M. Vidyasagar. Robust linear compensator design for nonlinear robotic control. *IEEE J. Robotics Auto.*, RA-3(4):345–351, 1987.
- [Wer78] J.R. Wertz, editor. *Spacecraft Attitude Determination and Control*. D. Reidel, Dordrecht, Holland, 1978.

A Advantages of Gibbs vector description of nonlinear kinematics.

Dwyer [Dwy84] uses the Gibbs vector parametrization of the rigid body attitude to compute an exact feedback linearizing transformation for rigid body attitude dynamics. The simple, algebraic form of the resulting kinematic relations aid in the computation of PLF compensation. In this appendix we review the basis for certain relations useful in the general case.

Euler's theorem says that a general rotation between three dimensional orthogonal frames can be described by rotation through an angle θ about a unit vector \vec{e} . Thus any $L \in SO(3)$ can be given by,

$$L(\vec{e}, \theta) = \cos \theta I_3 + \sin \theta \Omega(\vec{e}) + (1 - \cos \theta) \vec{e} \vec{e}^T$$

where

$$\Omega(x) := \begin{bmatrix} 0 & -x_3 & x_2 \\ x_3 & 0 & -x_1 \\ -x_2 & x_1 & 0 \end{bmatrix}. \quad (\text{A.1})$$

In terms of the Gibbs vector [Wer78, pp. 416], $\gamma \in \mathbb{R}^3$, given by,

$$\gamma := \tan\left(\frac{\theta}{2}\right) \vec{e}, \quad (\text{A.2})$$

the general rotation (or *direction cosine matrix* [Wer78]) can be expressed,

$$L(\gamma) = \frac{(1 - \gamma^T \gamma) I_3 + 2\gamma \gamma^T - \Omega(\gamma)}{1 + \gamma^T \gamma}.$$

In terms of the Gibbs vector the kinematic relation for rigid body rotation [Wer78, pp. 513] can be expressed as,

$$\begin{aligned} \dot{\gamma} &= \Gamma(\gamma) \omega \\ &= \frac{1}{2} [\omega - \omega \times \gamma + (\omega \cdot \gamma) \gamma], \end{aligned} \quad (\text{A.3})$$

where,

$$\Gamma(\gamma) = \frac{1}{2} [I_3 + \gamma \gamma^T + \Omega(\gamma)]. \quad (\text{A.4})$$

Facts about skew symmetric matrices. The following relations summarize the salient geometric properties of $SO(3)$. Let $\Omega : \mathbb{R}^3 \rightarrow SO(3)$ (as defined above) and take $\hat{\Omega}$ as the inverse map. Let $A \in SO(3)$ and $u, v \in \mathbb{R}^3$. Then the following relations hold.

1. $v \times u = \hat{\Omega}([\Omega(v), \Omega(u)])^3$
2. $v \times u = \hat{\Omega}(uv^T - vu^T)$
3. $Au = \hat{\Omega}(A) \times u$
4. $\frac{\partial}{\partial u}(u \times v) = \Omega(-v)$

³Here $[A, B] = AB - BA$, the matrix commutator.

Proof: See Baillieul and Levi [BL87] for proofs of (i)–(iii). To show (4) note that from (3)

$$u \times v = \begin{bmatrix} 0 & -u_3 & u_2 \\ u_3 & 0 & -u_1 \\ -u_2 & u_1 & 0 \end{bmatrix} \begin{pmatrix} v_1 \\ v_2 \\ v_3 \end{pmatrix} = \begin{pmatrix} u_2 v_3 - u_3 v_2 \\ u_3 v_1 - u_1 v_3 \\ u_1 v_2 - u_2 v_1 \end{pmatrix}$$

, and we have,

$$\frac{\partial}{\partial u}(u \times v) = \frac{\partial}{\partial u}\{\Omega(u)v\} \quad (\text{A.5})$$

$$= \begin{bmatrix} 0 & v_3 & -v_2 \\ -v_3 & 0 & v_1 \\ v_2 & -v_1 & 0 \end{bmatrix}. \quad (\text{A.6})$$

□

Lemma: Using the Gibbs vector (A.2) the following kinematic relations hold;

$$\frac{\partial}{\partial \gamma} \{\Gamma(\gamma)\omega\} = \frac{1}{2}[\gamma^T \omega I_3 + \gamma \omega^T + \Omega(-\omega)], \quad (\text{A.7})$$

$$\frac{\partial}{\partial \gamma} \{\Gamma(\gamma)\omega\} \Gamma(\gamma)\omega = \gamma^T \omega \Gamma(\gamma)\omega. \quad (\text{A.8})$$

Proof: To show (A.7) compute the indicated differentiation of (A.3) using fact (4). To show (A.8) use (A.7) and (A.3) and expand term by term in vector notation,

$$\frac{\partial}{\partial \gamma} \{\Gamma(\gamma)\omega\} \Gamma(\gamma)\omega = \frac{1}{4}[\gamma^T \omega I_3 + \gamma \omega^T + \Omega(-\omega)][\omega + \gamma \gamma^T \omega + \gamma \times \omega] \quad (\text{A.9})$$

$$= \frac{1}{4}[(\gamma \cdot \omega)\omega + \gamma(\omega \cdot \omega) - \omega \times \omega] \quad (\text{A.10})$$

$$+ (\gamma \cdot \omega)\gamma(\gamma \cdot \omega) + \gamma(\gamma \cdot \omega)^2 - \omega \times \gamma(\gamma \cdot \omega) \quad (\text{A.11})$$

$$+ (\gamma \cdot \omega)(\gamma \times \omega) + \gamma(\omega \cdot (\gamma \times \omega)) - \omega \times (\gamma \times \omega)]. \quad (\text{A.12})$$

Recalling the basic vector relations;

$$\omega \cdot (\gamma \times \omega) = \gamma \cdot (\omega \times \omega) = 0,$$

$$\omega \times (\gamma \times \omega) = (\omega \cdot \omega)\gamma - (\omega \cdot \gamma)\omega,$$

then the right hand side of (A.12) simplifies to:

$$= \frac{1}{4} \{ 2(\gamma \cdot \omega)^2 \gamma + 2(\gamma \cdot \omega)[\omega + \gamma \times \omega] \} \quad (\text{A.13})$$

$$= \frac{1}{2}(\gamma^T \omega)[(\gamma^T \omega)\gamma + \omega + \gamma \times \omega] \quad (\text{A.14})$$

$$= \gamma^T \omega \Gamma(\gamma)\omega. \quad (\text{A.15})$$

□

B Supporting Computations for area moment of inertia and B-spline model for 3-axis slewing with tripod shaped appendage

In this appendix we summarize the computation of the area moments of inertia of the tripod metering truss model and the computation by explicit integration of the required matrix parameters obtained from the B-spline finite element model for 3-axis slewing of a rigid body with attached appendage consisting of a tripod with equilateral triangular base. Only those matrix parameters that are a function of the area moments are presented here. The supporting computations for the matrix parameters that are not a function of the area moments can be found in [BBKA88].

Computation of area moments As described earlier, the metering truss was modeled as a tripod of tubes located at the vertices of an equilateral triangle. A cross-section of the structure appears in Figure 2.1. The area moments of inertia can be computed using the following relations:

$$I_x = 3I_{cir} + I_{x||axis} \quad (B.1)$$

$$I_y = 3I_{cir} + I_{y||axis} \quad (B.2)$$

$$I_z = I_x + I_y, \quad (B.3)$$

where I_{cir} is the area moment of inertia of a circle and is given by

$$I_{cir} = \frac{\pi r^4}{4}, \quad (B.4)$$

and $I_{x||axis}$, $I_{y||axis}$ are additional terms that are a consequence of the axis of rotation being translated from an axis through the centroid of the circle to the x or y axis respectively.

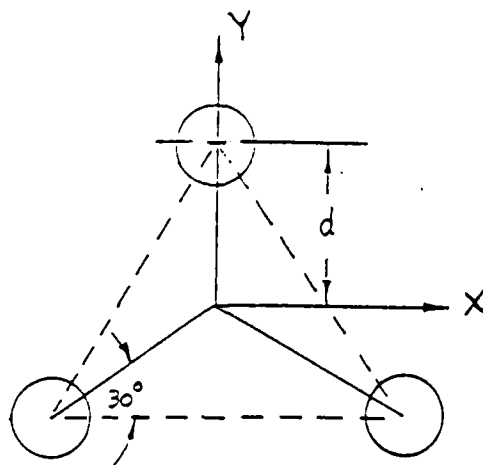


Figure 2.1: Cross-section of tripod metering truss.

Beginning with the x-axis, the area moment associated with the axis translation can be computed as,

$$I_{x||axis} = \pi r^2 d^2 + 2 \frac{\pi r^2 d^2}{4}. \quad (B.5)$$

From the truss geometry it can be shown that,

$$d = b(1 - \frac{z}{l}), \quad (B.6)$$

where b is the distance from the center of the tripod base to the center of one of the tubes, and l is the distance from the base of the tripod to the end of the truss. Using (B.6), (B.5) becomes,

$$I_{x||axis} = \pi r^2 b^2 (1 - \frac{z}{l})^2 + \frac{\pi r^2 b^2}{2} (1 - \frac{z}{l})^2 \quad (B.7)$$

$$= \frac{3}{2} \pi r^2 b^2 - \frac{3\pi b^2}{l} z + \frac{3\pi r^2 b^2}{2l^2} z^2. \quad (B.8)$$

Finally, substituting (B.4) and (B.8) into (B.1) gives,

$$I_x = \frac{3\pi r^4}{4} + \frac{3\pi r^2 b^2}{2} - \frac{3\pi r^2 b^2}{l} z + \frac{3\pi r^2 b^2}{2l^2} z^2. \quad (B.9)$$

Next, the area moment of inertia for the y-axis is computed similarly as the sum of the moments of inertia of three circles about their centroids and the additional moments of inertia of two circles whose rotational axes have been translated (see Figure 2.1). The latter term is given by,

$$I_{y||axis} = \frac{3\pi r^2 d^2}{2}, \quad (B.10)$$

substituting (B.6) into (B.10) and simplifying we obtain,

$$I_{y||axis} = \frac{3\pi r^2 b^2}{2} - \frac{3\pi r^2 b^2}{l} z + \frac{3\pi r^2 b^2}{2l^2} z^2. \quad (B.11)$$

Finally, I_y is computed from (B.2) using (B.11) and (B.4) as,

$$I_y = \frac{3\pi r^4}{4} + \frac{3\pi r^2 b^2}{2} - \frac{3\pi r^2 b^2}{l} z + \frac{3\pi r^2 b^2}{2l^2} z^2. \quad (B.12)$$

The area moment of inertia for the z-axis is obtained by substituting (B.8) and (B.11) into (B.3) which gives,

$$I_z = \frac{3\pi r^4}{2} + 3\pi r^2 b^2 - \frac{6\pi r^2 b^2}{l} z + \frac{3\pi r^2 b^2}{l^2} z^2. \quad (B.13)$$

Computation of matrix FEM parameters In [BBKA88] the flexible appendage was modeled as a beam with uniform cross-section and with corresponding constant area moments of inertia along its length. However, in this report, the tripod shaped appendage has area moments of inertia that vary along its length according to (B.9), (B.12), and (B.13). Therefore, it is necessary to recompute the four matrix parameter relations which are a function of the area moments using the new relations. The affected integral equations are:

$$N_{\omega_h} = \int_0^\ell \{z^2 \rho A + \rho I(z)\} dz, \quad (\text{B.14})$$

$$N_\theta = \int_0^\ell \rho I(z) \Phi(z) \Phi^T(z) dz, \quad (\text{B.15})$$

$$N_{\omega_h \theta}^T = \int_0^\ell \rho I(z) \Phi^T(z) dz, \quad (\text{B.16})$$

$$K_\theta = \int_0^\ell \{EI(z) \Phi_z(z) \Phi_z^T(z) + \kappa GA \Phi(z) \Phi^T(z)\} dz. \quad (\text{B.17})$$

Computation of N_{ω_h}

According to (B.9) and (B.12) $I_x = I_y$. Therefore, let

$$I(z) = I_x = I_y = c_1 + c_2 z + c_3 z^2 \quad (\text{B.18})$$

where

$$\begin{aligned} c_1 &= \frac{3\pi r^4}{4} + \frac{3\pi r^2 b^2}{2}, \\ c_2 &= \frac{-3\pi r^2 b^2}{l}, \\ c_3 &= \frac{3\pi r^2 b^2}{2l^2}. \end{aligned}$$

Substituting (B.18) into (B.14) gives,

$$N_{\omega_h} = \int_0^\ell \{z^2 \rho A + \rho(c_1 + c_2 z + c_3 z^2)\} dz. \quad (\text{B.19})$$

By direct integration of (B.19) we obtain,

$$N_{\omega_h} = \rho \left[\frac{l^3}{3} (A + c_3) + \frac{l^2}{2} c_2 + l c_1 \right].$$

Computation of N_θ

By definition the right hand side of (B.15) has elements given in terms of linear B-splines as

$$N_\theta = \int_0^\ell I(z) B_{i-1}^1(z) B_{j-1}^1(z) dz \quad (\text{B.20})$$

for $i, j = 1, \dots, N$. Given the "hat" shaped, linear B-spline,

$$B_i^1(z) := \left(\frac{N}{\ell}\right) \left[z - i\left(\frac{\ell}{N}\right)\right] B_i^0(z) + \left(\frac{N}{\ell}\right) \left[(i+2)\frac{\ell}{N} - z\right] B_{i+1}^0(z)$$

where the zero order B-spline is chosen with continuity from the left; i.e.,

$$B_i^0(z) := \begin{cases} 1, & \text{if } x_i \leq z < x_{i+1} \\ 0, & \text{else} \end{cases}$$

Substituting (B.18) into (B.20) we obtain,

$$N_\theta = \rho \int_0^l (c_1 + c_2 z + c_3 z^2) B_{i-1}^1(z) B_{j-1}^1(z) dz$$

Then we have three nonzero cases to consider.

Case 1: $i = j = N$. Then

$$\begin{aligned} [N_\theta]_{ij} &= \rho \int_{z_{N-1}}^{z_N} (c_1 + c_2 z + c_3 z^2) \left(\frac{N}{l}\right)^2 (z_N - z)^2 dz \\ &= \rho \left[\frac{l}{3N} (c_1 + c_2 z_N + c_3 z_N^2) - \frac{l^2}{4N^2} (c_2 + 2c_3 z_N) + \frac{l^3}{5N^3} c_3 \right]. \end{aligned}$$

Case 2: $i = j \pm 1$. Here we obtain a simple form for the integral by transformation of the variable and limits of integration;

$$\begin{aligned} [N_\theta]_{ij} &= \rho \int_0^l (c_1 + c_2 z + c_3 z^2) B_{i-1}^1(z) B_{j-1}^1(z) dz \\ &= \rho \int_{z_{j-1}}^{z_j} (c_1 + c_2 z + c_3 z^2) \left(\frac{N}{l}\right)^2 (z - z_{j-1})(z_j - z) dz \\ &= \rho \left(\frac{N}{l}\right)^2 \int_0^{\frac{l}{N}} [(c_1 + c_2(z_j - x) + c_3(z_j - x)^2) \left(\frac{l}{N} - x\right)x] dx \\ &= \rho \left[\frac{l}{6N} (c_1 + c_2 z_j + c_3 z_j^2) - \frac{l^2}{12N^2} (c_2 + 2c_3 z_j) + \frac{l^3}{20N^3} c_3 \right]. \end{aligned}$$

Case 3: $i = j < N$.

$$\begin{aligned} [N_\theta]_{ij} &= \rho \int_0^l (c_1 + c_2 z + c_3 z^2) B_{i-1}^1(z) B_{j-1}^1(z) dz \\ &= \rho \int_{z_{j-2}}^{z_{j-1}} (c_1 + c_2 z + c_3 z^2) \left(\frac{N}{l}\right)^2 (z - z_{j-2})^2 dz \\ &\quad + \rho \int_{z_{j-1}}^{z_j} (c_1 + c_2 z + c_3 z^2) \left(\frac{N}{l}\right)^2 (z_j - z)^2 dz \\ &= \rho \int_{\frac{l}{N}}^{\frac{2l}{N}} (c_1 + c_2(z_j - x) + c_3(z_j - x)^2) \left(\frac{N}{l}\right)^2 (2\frac{l}{N} - x)^2 dx \\ &\quad + \rho \int_0^{\frac{l}{N}} (c_1 + c_2(z_j - x) + c_3(z_j - x)^2) \left(\frac{N}{l}\right)^2 x^2 dx \\ &= \rho \left[\frac{2l}{3N} (c_1 + c_2 z_j + c_3 z_j^2) - \frac{2l^2}{3N^2} (c_2 + 2c_3 z_j) + \frac{11l^3}{15N^3} c_3 \right]. \end{aligned}$$

Computation of $N_{\omega, \theta}$

Under the assumptions of the 3-axis slewing model, the $1 \times N$ coupling coefficient matrix $N_{\omega, \theta}$ has elements

$$[N_{\omega, \theta}]_i = \rho \int_0^l (c_1 + c_2 z + c_3 z^2) B_i^1(z) dz,$$

for $i = 1, \dots, N$. There are two cases of interest.

Case 1: $i < N$. Then

$$\begin{aligned} \int_0^l (c_1 + c_2 z + c_3 z^2) B_i^1(z) dz &= \int_{z_i}^{z_{i+1}} \left(\frac{N}{l}\right) (c_1 + c_2 z + c_3 z^2) [z - i(\frac{l}{N})] dz \\ &\quad + \int_{z_{i+1}}^{z_{i+2}} \left(\frac{N}{l}\right) (c_1 + c_2 z + c_3 z^2) [(i+2)(\frac{l}{N}) - z] dz. \end{aligned}$$

Changing limits of integration by the transformation $x = z - z_i$ in the first integral gives

$$\begin{aligned} &\int_{z_i}^{z_{i+1}} \left(\frac{N}{l}\right) (c_1 + c_2 z + c_3 z^2) [z - i(\frac{l}{N})] dz \\ &= \left(\frac{N}{l}\right) \int_0^{\frac{l}{N}} [c_1 + c_2(x + z_i) + c_3(x + z_i)^2] x dx \\ &= \frac{l}{2N} (c_1 + c_2 z_i + c_3 z_i^2) + \frac{l^2}{3N^2} (c_2 + 2c_3 z_i) + \frac{l^3}{4N^3} c_3 \end{aligned}$$

Changing variables (and limits) of integration in the second integral yields

$$\begin{aligned} &\int_{z_{i+1}}^{z_{i+2}} \left(\frac{N}{l}\right) (c_1 + c_2 z + c_3 z^2) [(i+2)(\frac{l}{N}) - z] dz \\ &= \left(\frac{N}{l}\right) \int_{\frac{l}{N}}^{\frac{2l}{N}} [c_1 + c_2(x + z_i) + c_3(x + z_i)^2] (2\frac{l}{N} - x) dx \\ &= \frac{l}{2N} (c_1 + c_2 z_i + c_3 z_i^2) + \frac{2l^2}{3N^2} (c_2 + 2c_3 z_i) + \frac{11l^3}{12N^3} c_3. \end{aligned}$$

From which we can obtain

$$\int_0^l (c_1 + c_2 z + c_3 z^2) B_i^1(z) dz = \frac{l}{N} (c_1 + c_2 z_i + c_3 z_i^2) + \frac{l^2}{N^2} (c_2 + 2c_3 z_i) + \frac{7l^3}{6N^3} c_3.$$

Case 2: $i = N$.

$$\begin{aligned} \int_0^l (c_1 + c_2 z + c_3 z^2) B_i^1(z) dz &= \int_{z_{N-1}}^{z_N} (c_1 + c_2 z + c_3 z^2) \left(\frac{N}{l}\right) [z - z_{N-1}] dz \\ &= \int_{-\frac{l}{N}}^0 \left(\frac{N}{l}\right) [c_1 + c_2(x + z_N) + c_3(x + z_N)^2] (x + \frac{l}{N}) dx \\ &= \frac{l}{N} (c_1 + c_2 z_N + c_3 z_N^2) + \frac{l^2}{6N^2} (c_2 + 2c_3 z_N) + \frac{l^3}{12N^3} c_3 \end{aligned}$$

Computation of K_θ

Under the assumptions of the 3-axis slewing model, the $N \times N$ coefficient matrix K_θ has elements

$$\begin{aligned} [K_\theta]_{ij} &= \int_0^l \{EI(z) \Phi_i(z) \Phi_j^T(z) + \kappa GA \Phi_i(z) \Phi_j^T(z)\} dz, \\ &= EIN'' + \kappa GAN'. \end{aligned}$$

where N'' has elements

$$[N'']_{ij} = \int_0^l \frac{\partial}{\partial z} B_{i-1}^1(z) B_{j-1}^1(z) (c_1 + c_2 z + c_3 z^2) dz$$

and \tilde{N} is given in [BBKA88]. For the $N \times N$ tridiagonal matrix N'' and $i, j = 1, \dots, N$ we obtain three nonzero cases.

Case 1: $i = j < N$.

$$\begin{aligned} [N'']_{ij} &= \int_0^{\frac{l}{N}} \left(\frac{N}{l}\right)^2 (c_1 + c_2 z + c_3 z^2) dz + \int_0^{\frac{l}{N}} \left(\frac{N}{l}\right)^2 (c_1 + c_2 z + c_3 z^2) dz \\ &= \frac{2N}{l} c_1 + c_2 + \frac{2l}{3N} c_3. \end{aligned}$$

Case 2: $i = j = N$.

$$\begin{aligned} [N'']_{ij} &= \int_0^{\frac{l}{N}} \left(\frac{N}{l}\right)^2 (c_1 + c_2 z + c_3 z^2) dz \\ &= \frac{N}{l} c_1 + \frac{1}{2} c_2 + \frac{l}{3N} c_3. \end{aligned}$$

Case 3: $i = j \pm 1$. For $i = j + 1$ we obtain,

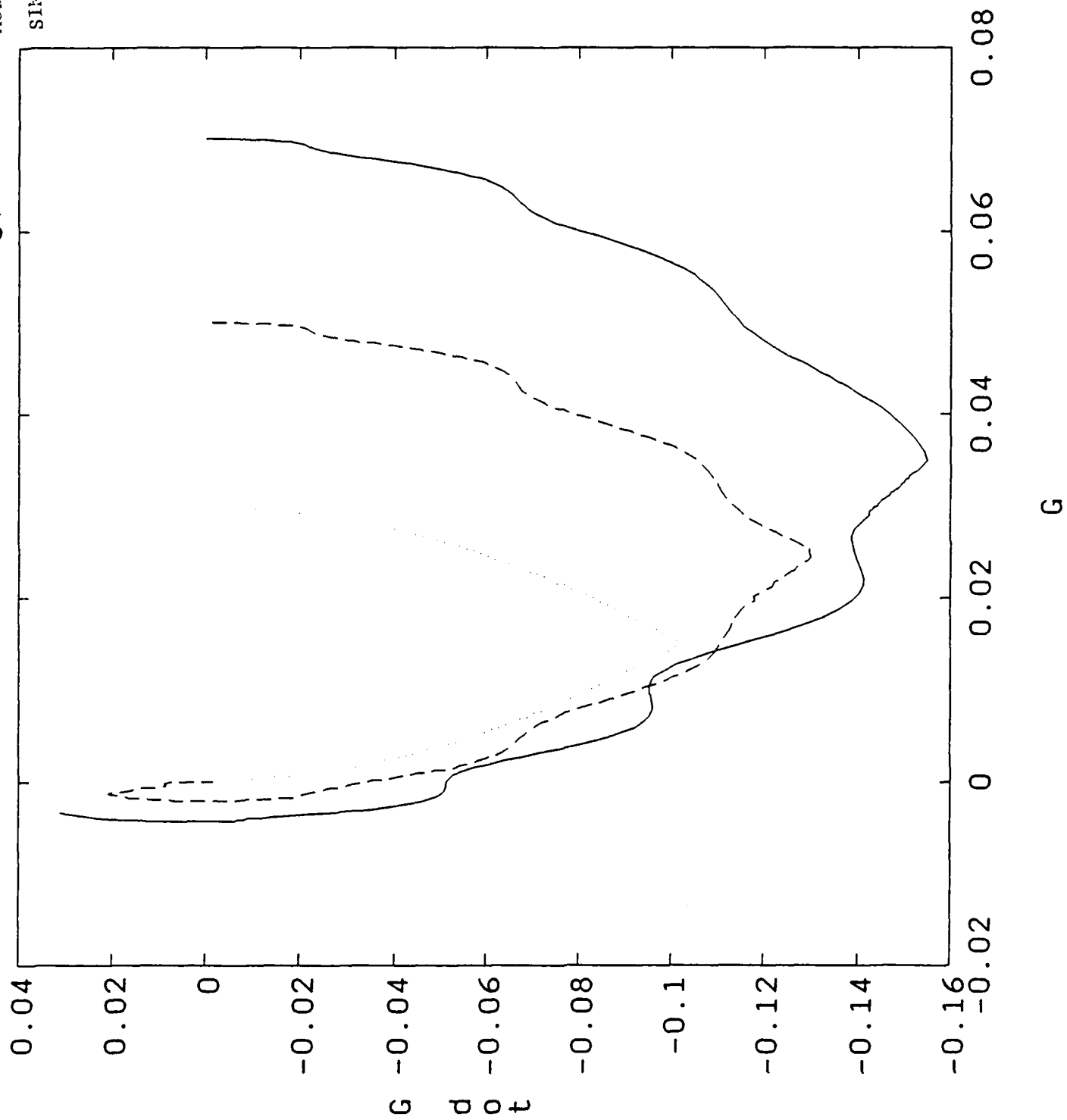
$$\begin{aligned} [N'']_{ij} &= \int_{z_{i+1}}^{z_{i+2}} -\left(\frac{N}{l}\right)^2 (c_1 + c_2 z + c_3 z^2) dz \\ &= \int_{\frac{l}{N}}^{\frac{2l}{N}} -\left(\frac{N}{l}\right)^2 (c_1 + c_2(x + z_i) + c_3(x + z_i)^2) dz \\ &= -\frac{N}{l} (c_1 + c_2 z_i + c_3 z_i^2) - \frac{3}{2} (c_2 + 2c_3 z_i) - \frac{7l}{3N} c_3. \end{aligned}$$

Similarly, for $i = j - 1$.

TSI-89-12-12-WB

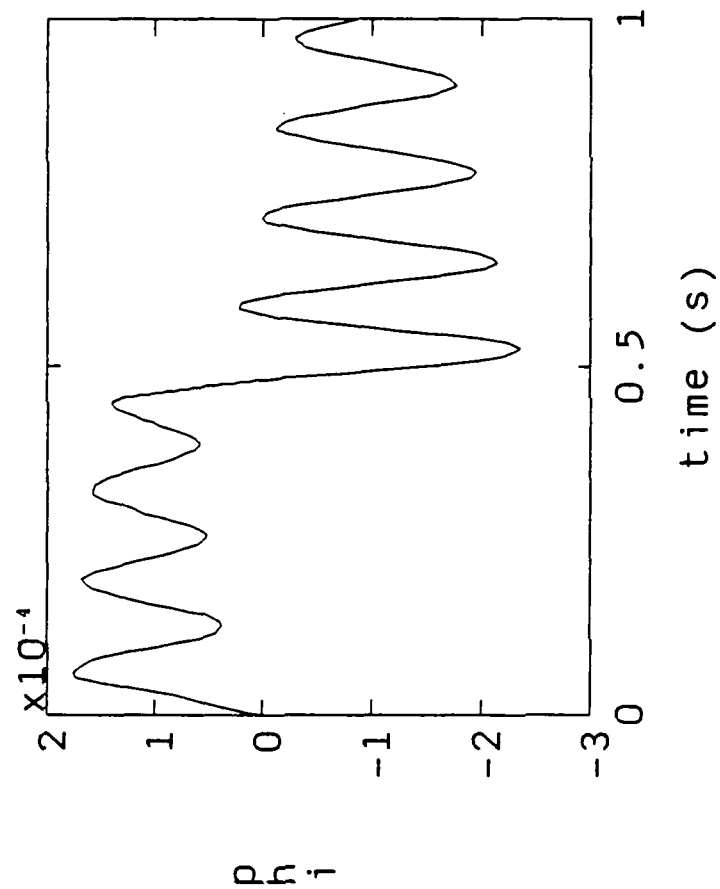
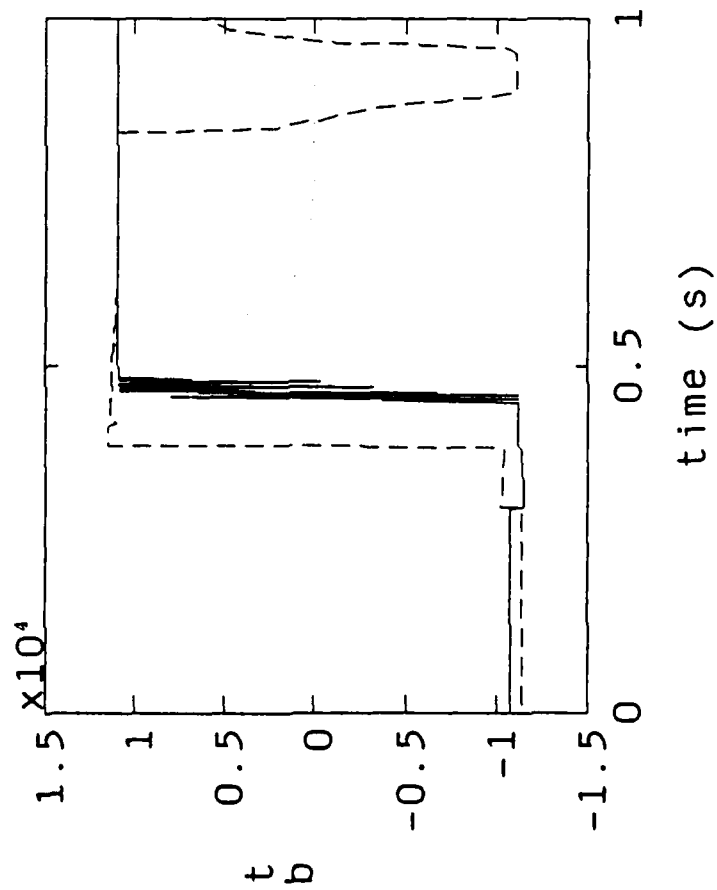
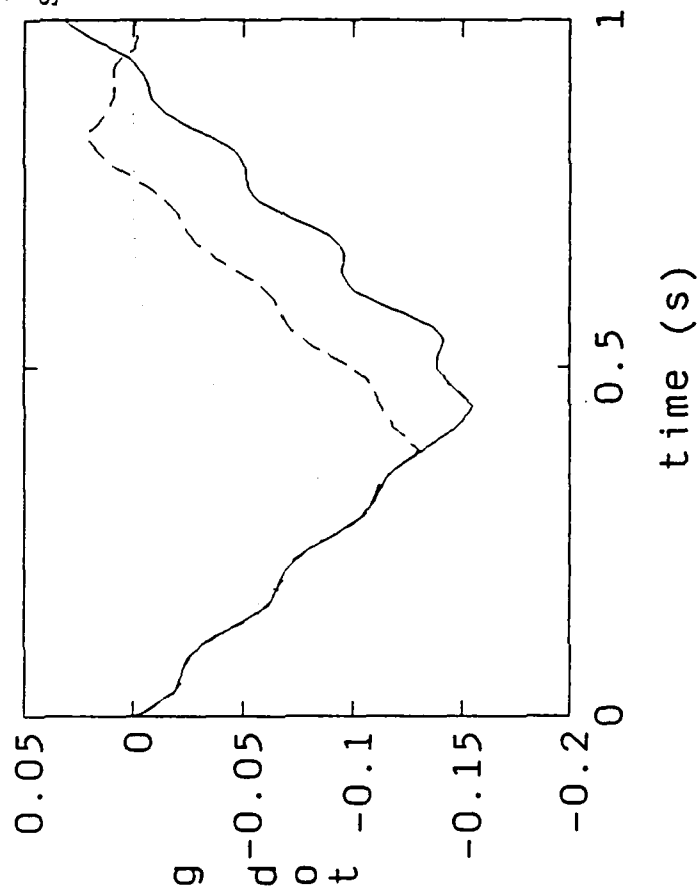
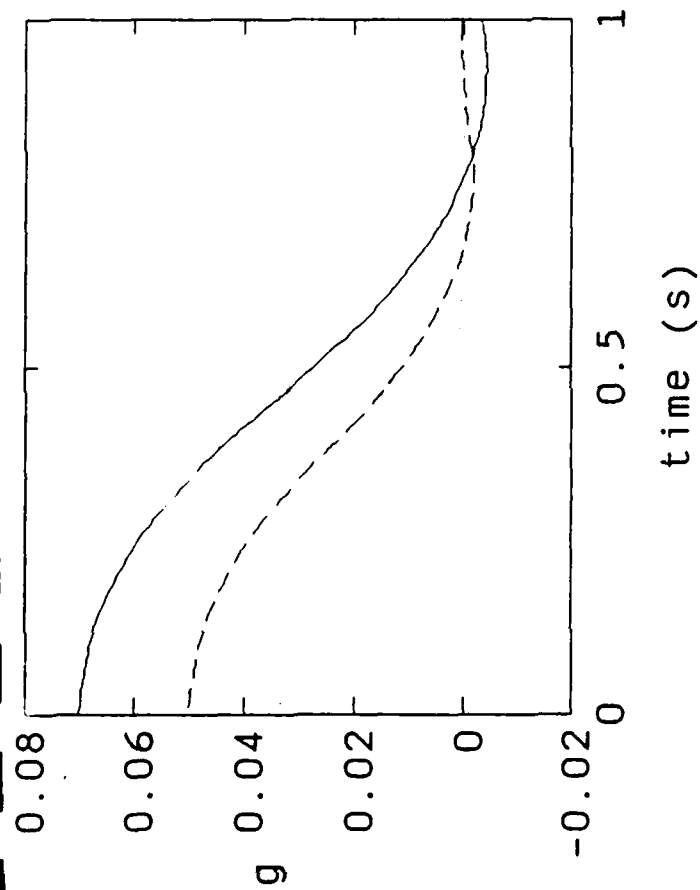
73

C Simulated Time Responses for Multiaxis Slewing



MOD1

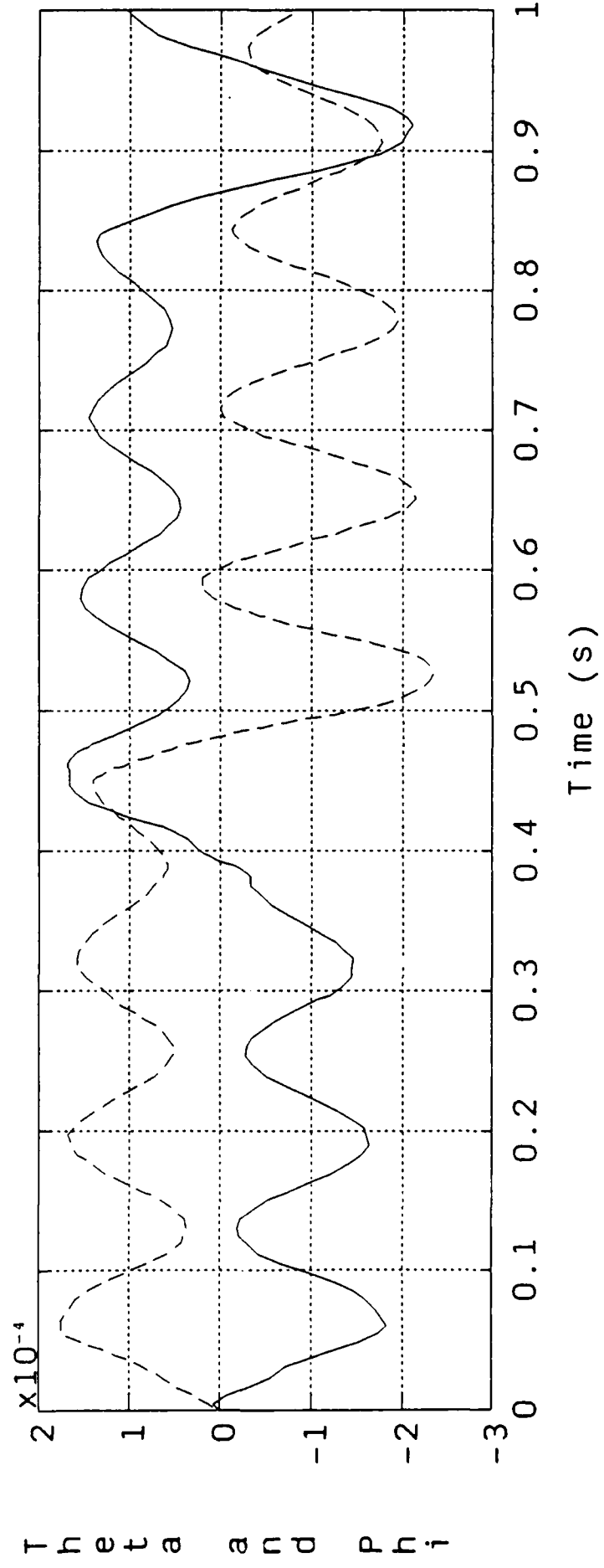
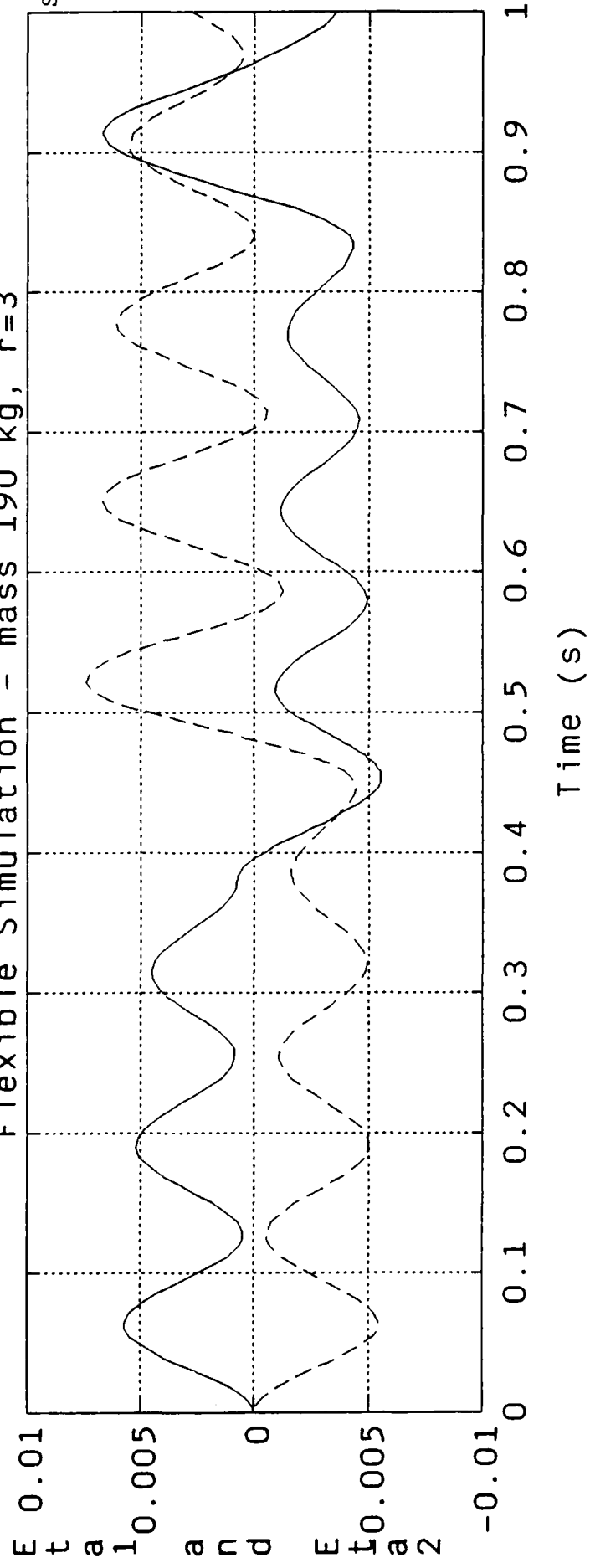
SIM11



Flexible Simulation - mass 190 kg, r=3

MOD1

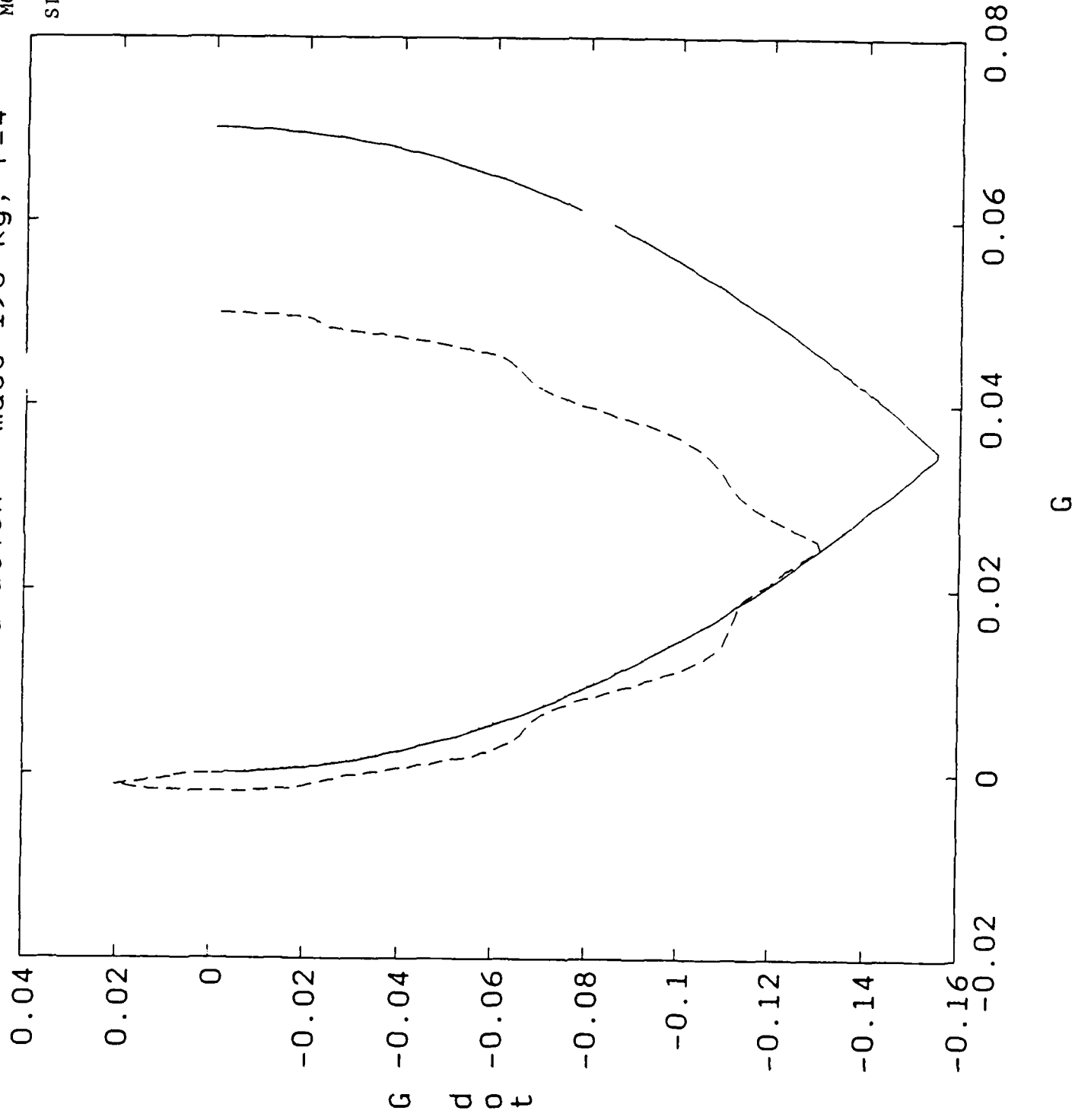
SIM11



Flexible Simulation - mass 190 kg, r=4

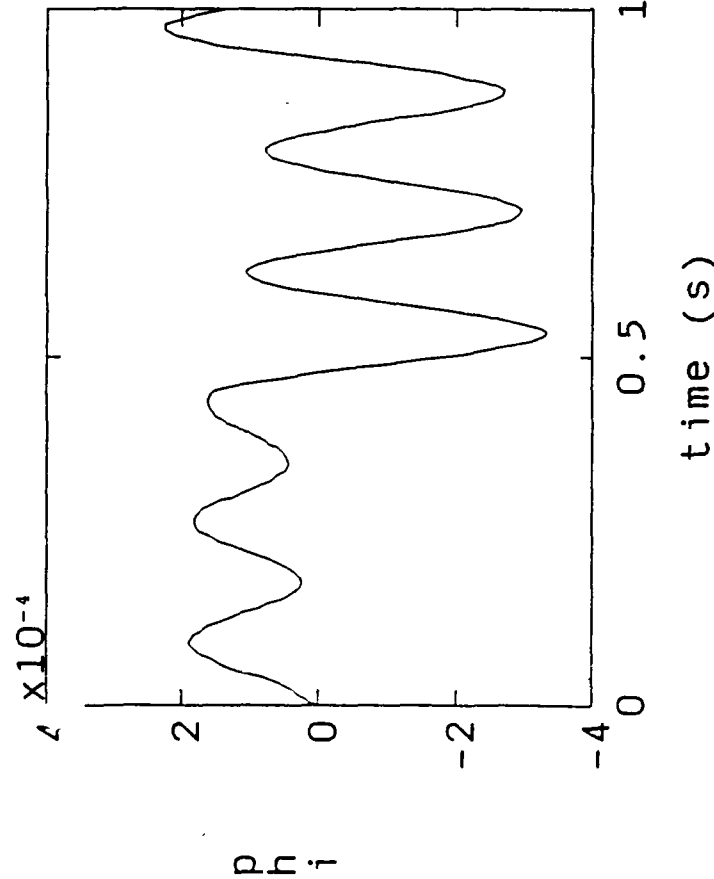
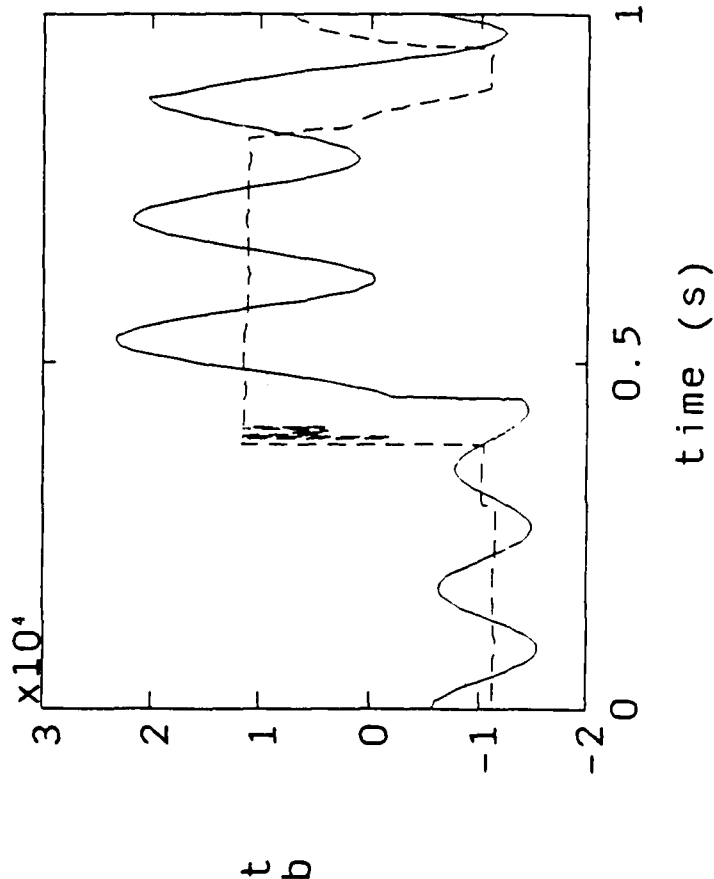
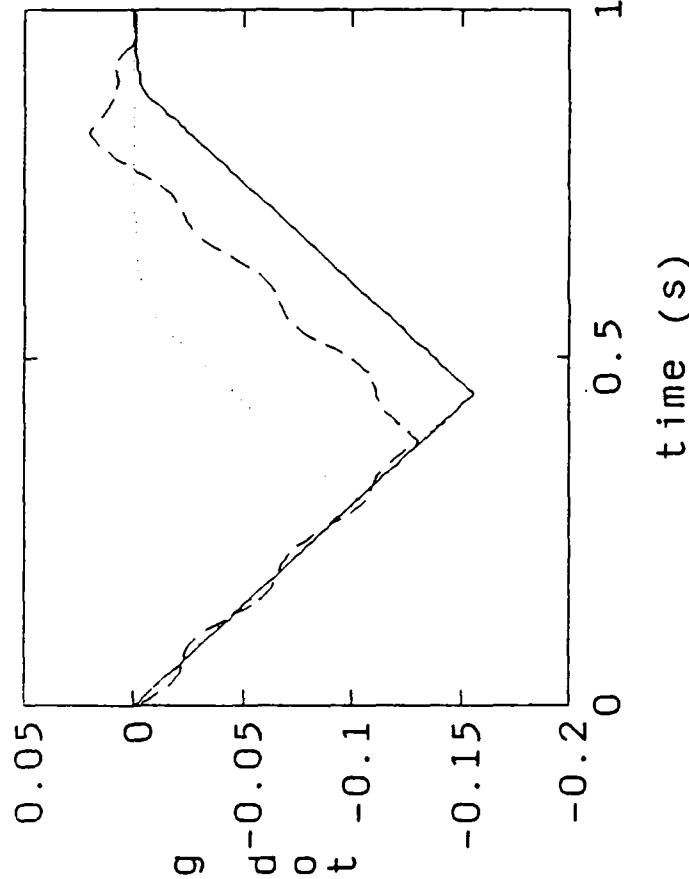
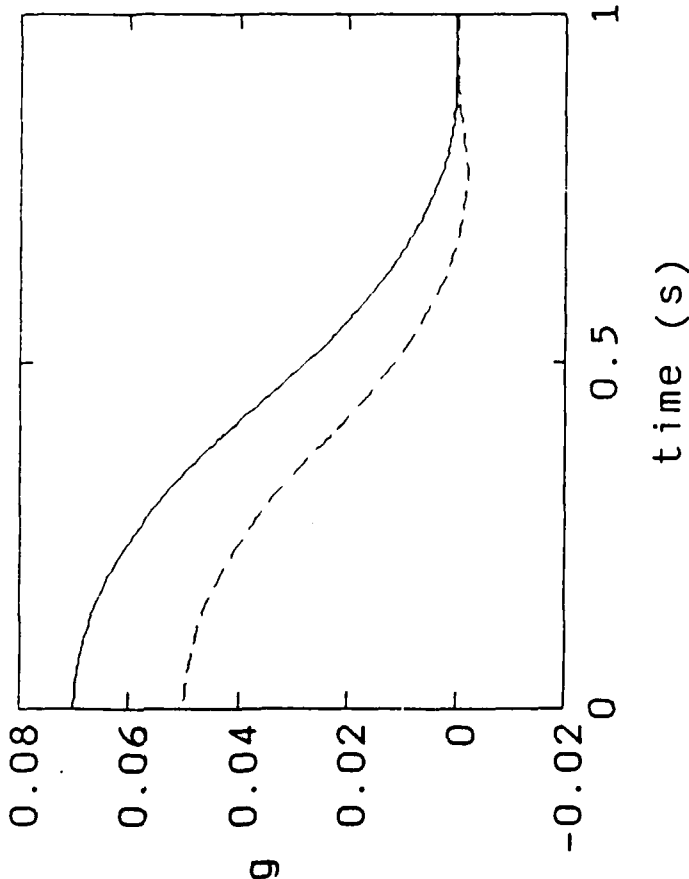
MOD1

SIM12



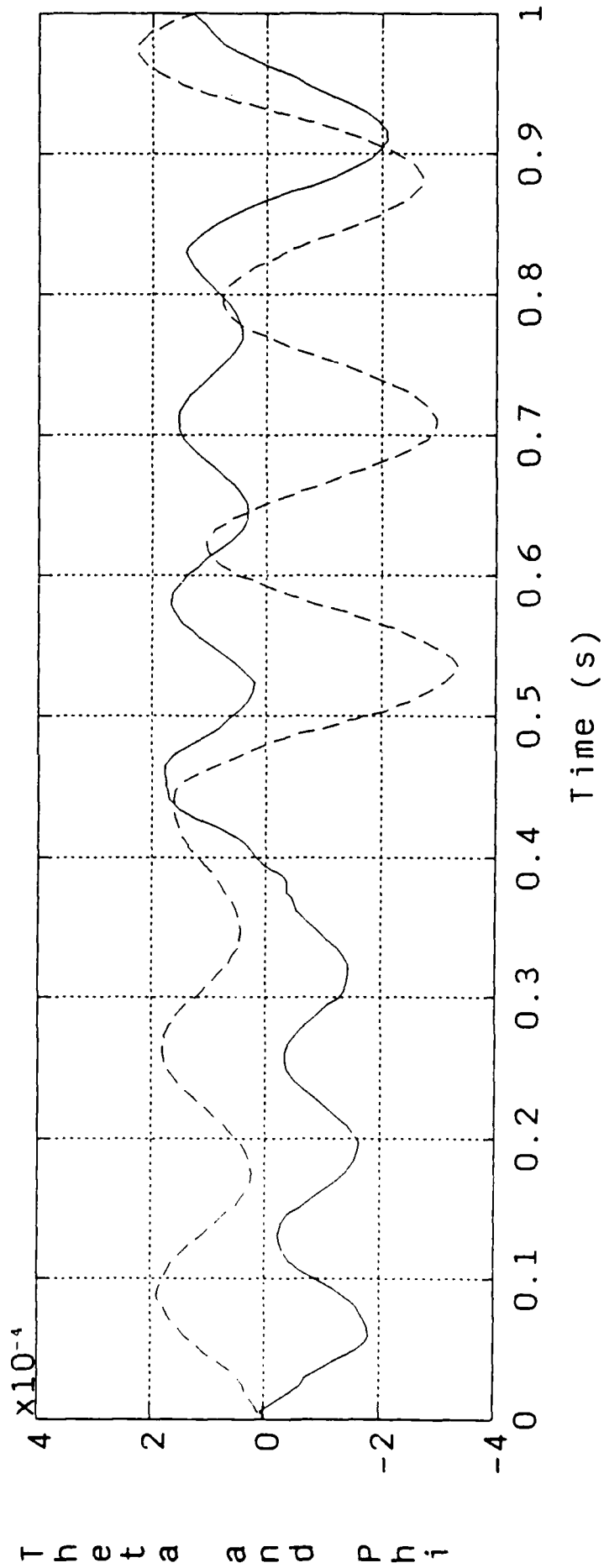
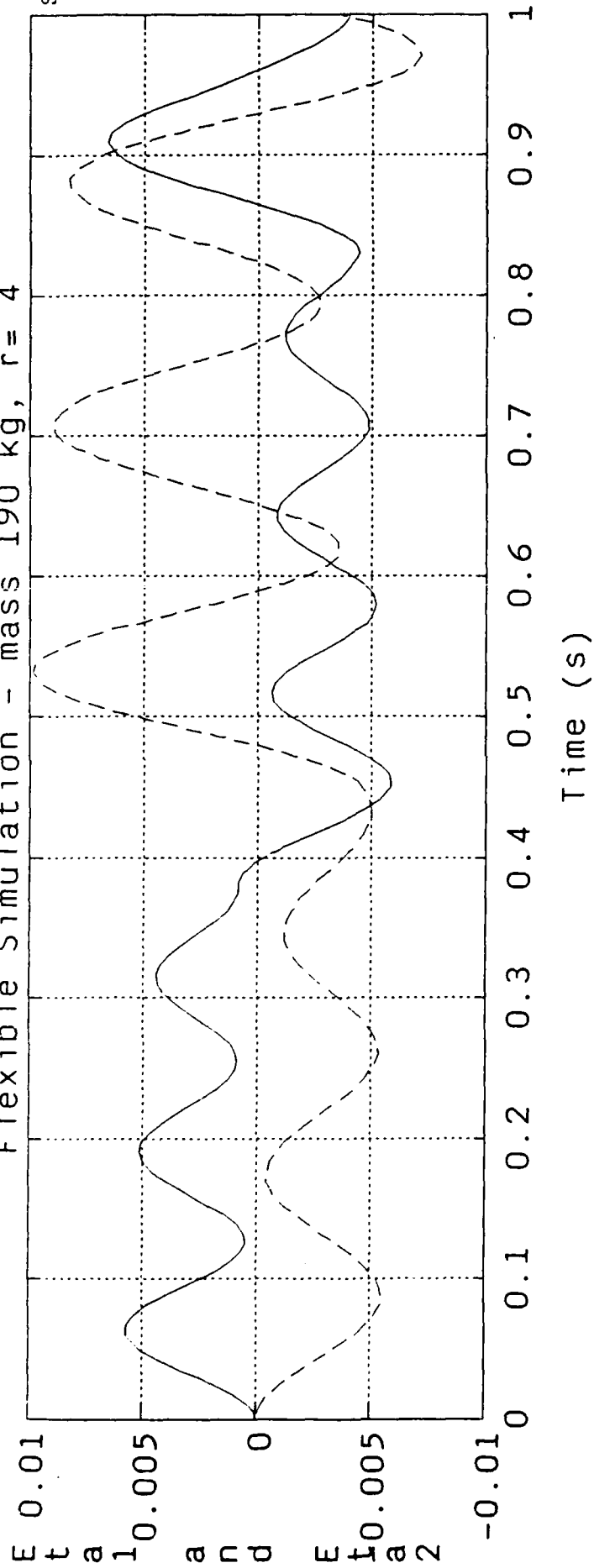
MOD1

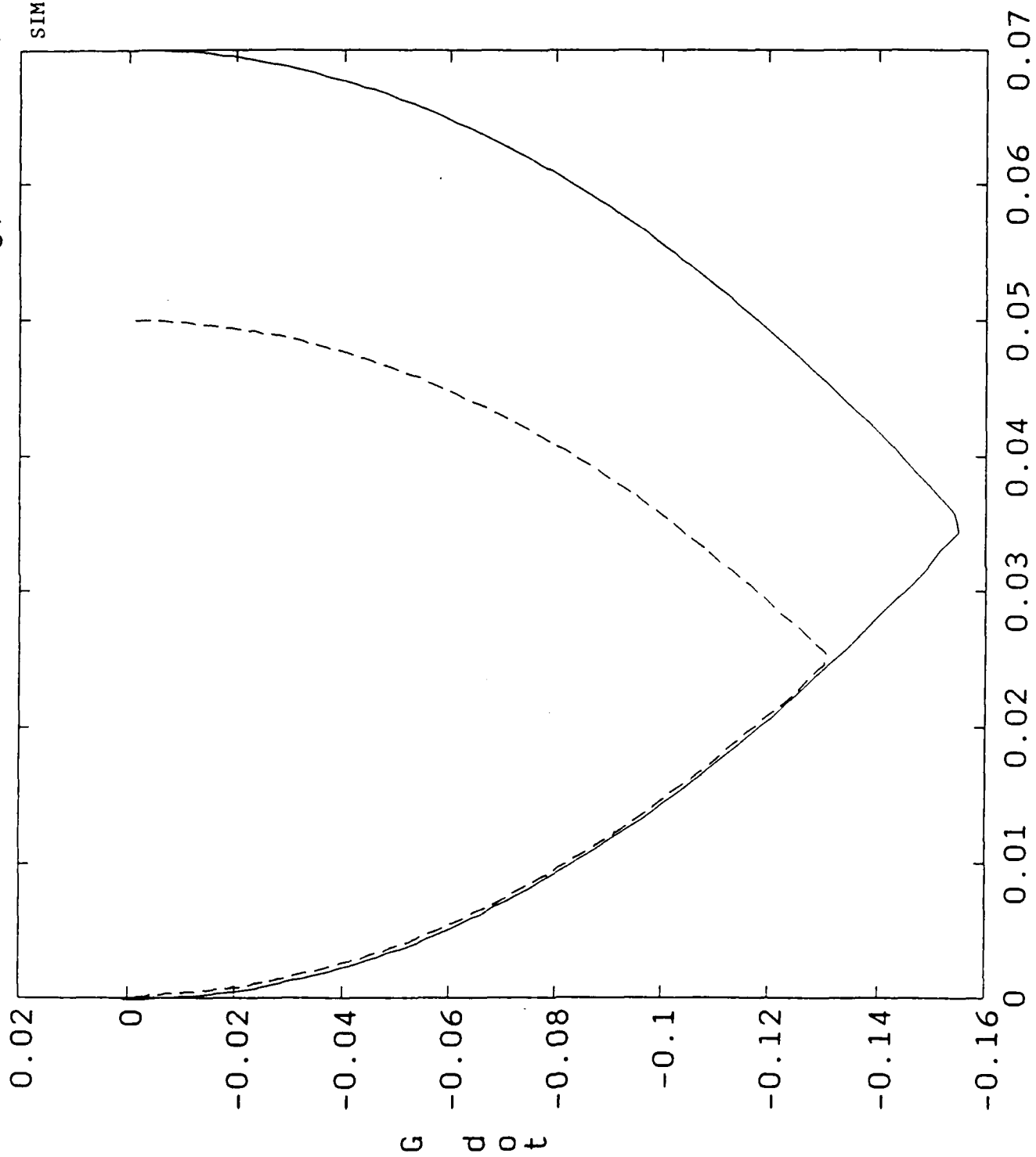
SIM12

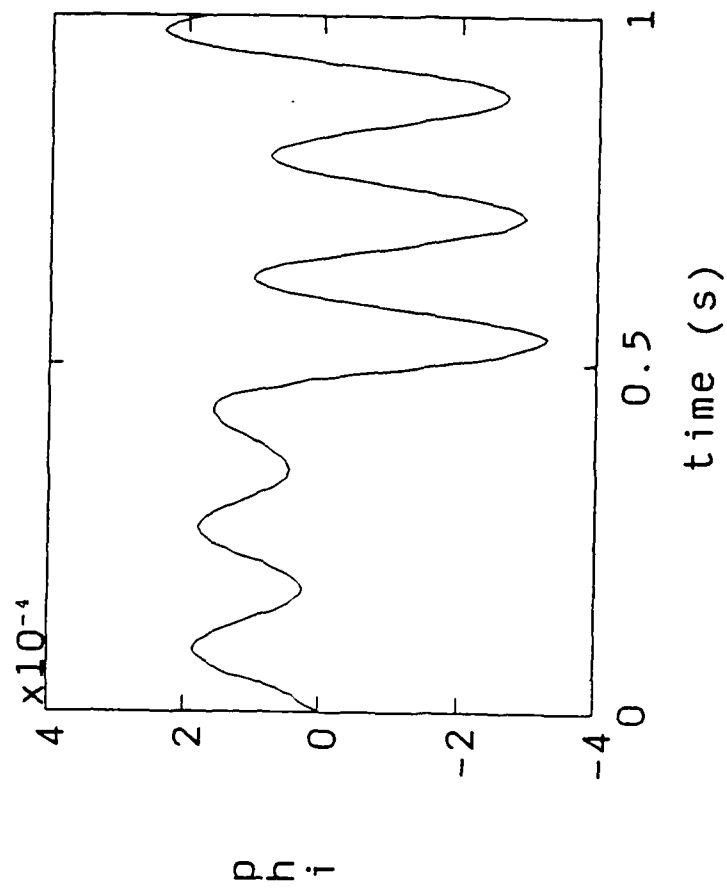
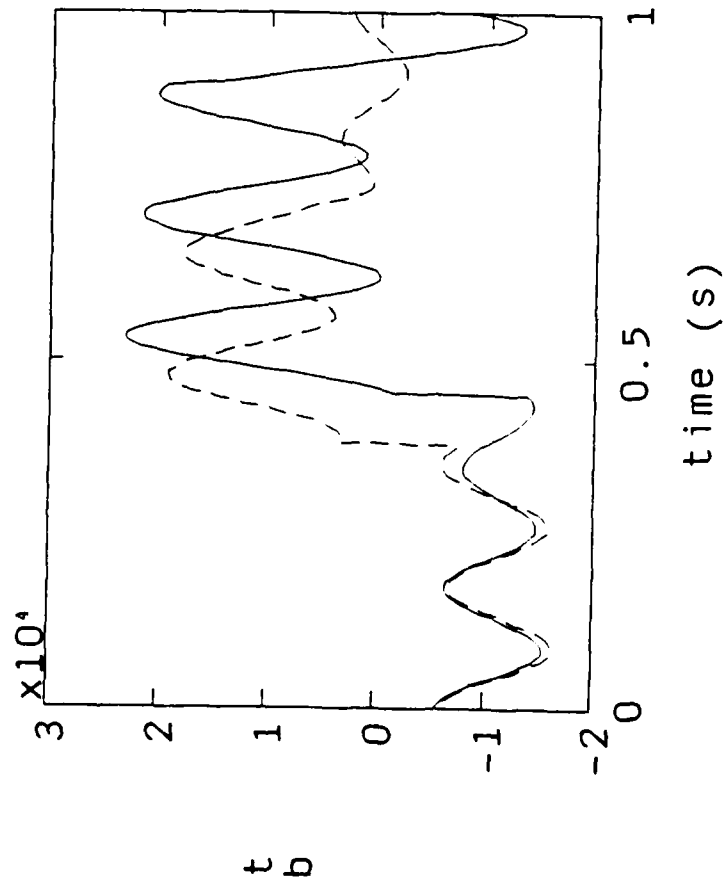
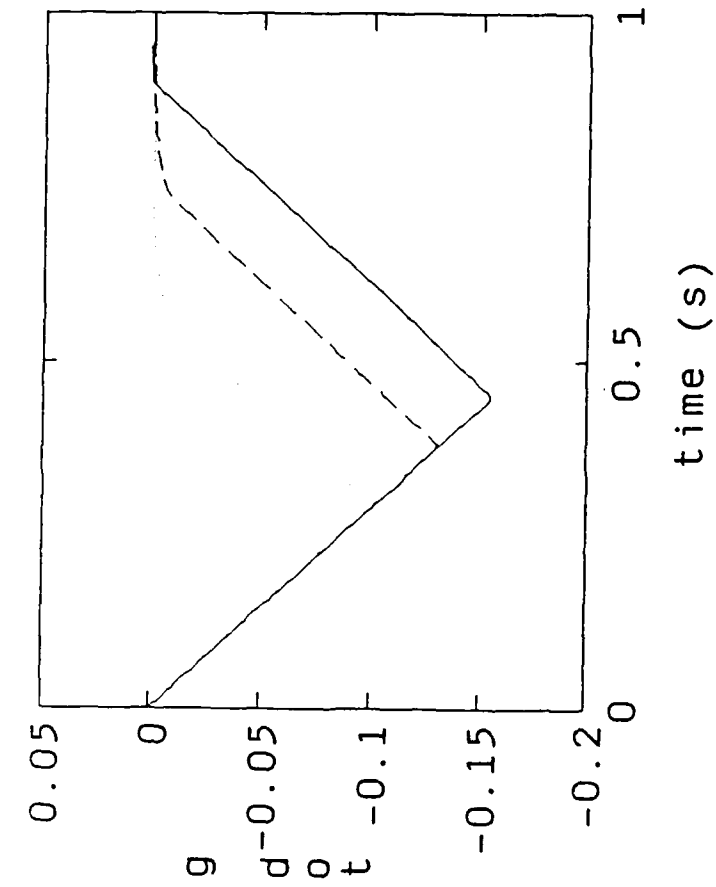
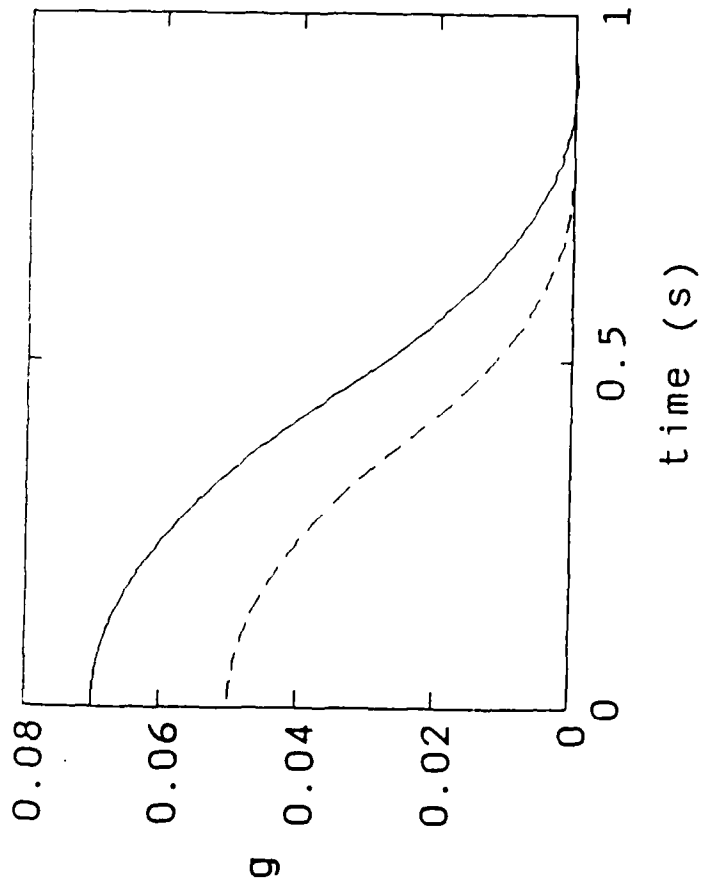


MOD1

SIM12

Flexible Simulation - mass 190 kg, $r = 4$ 

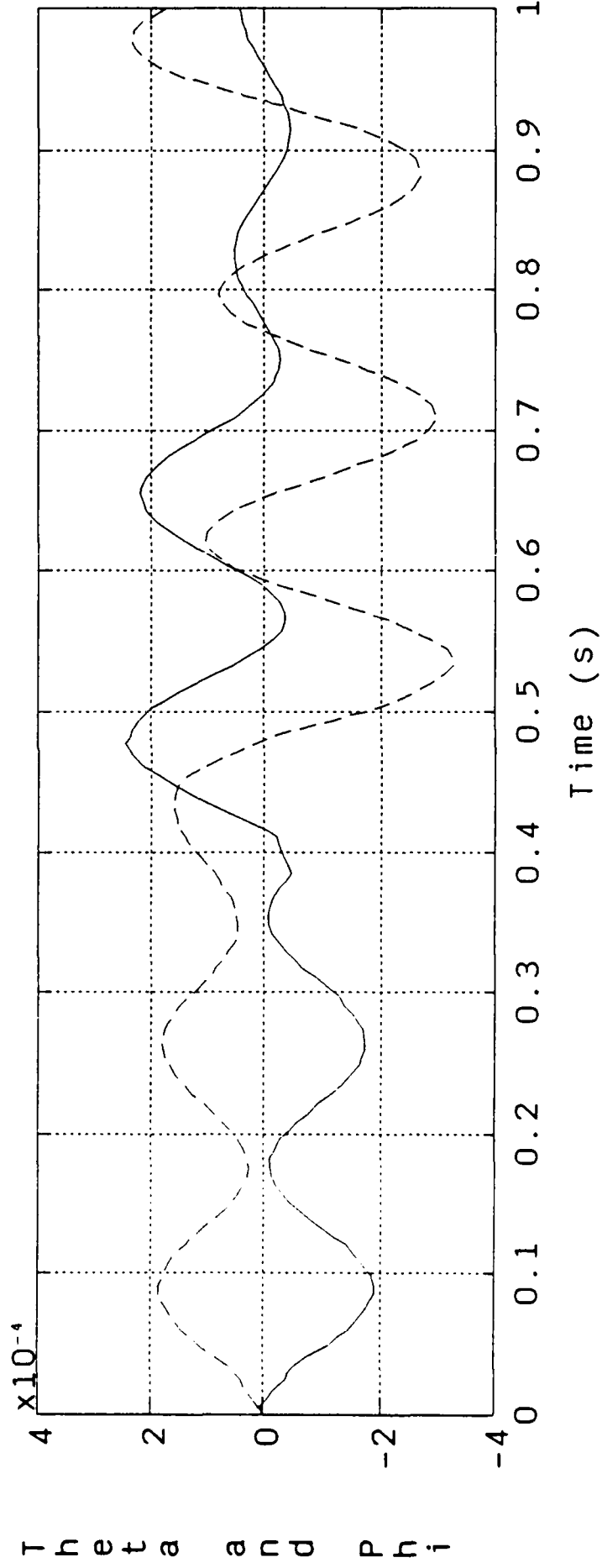
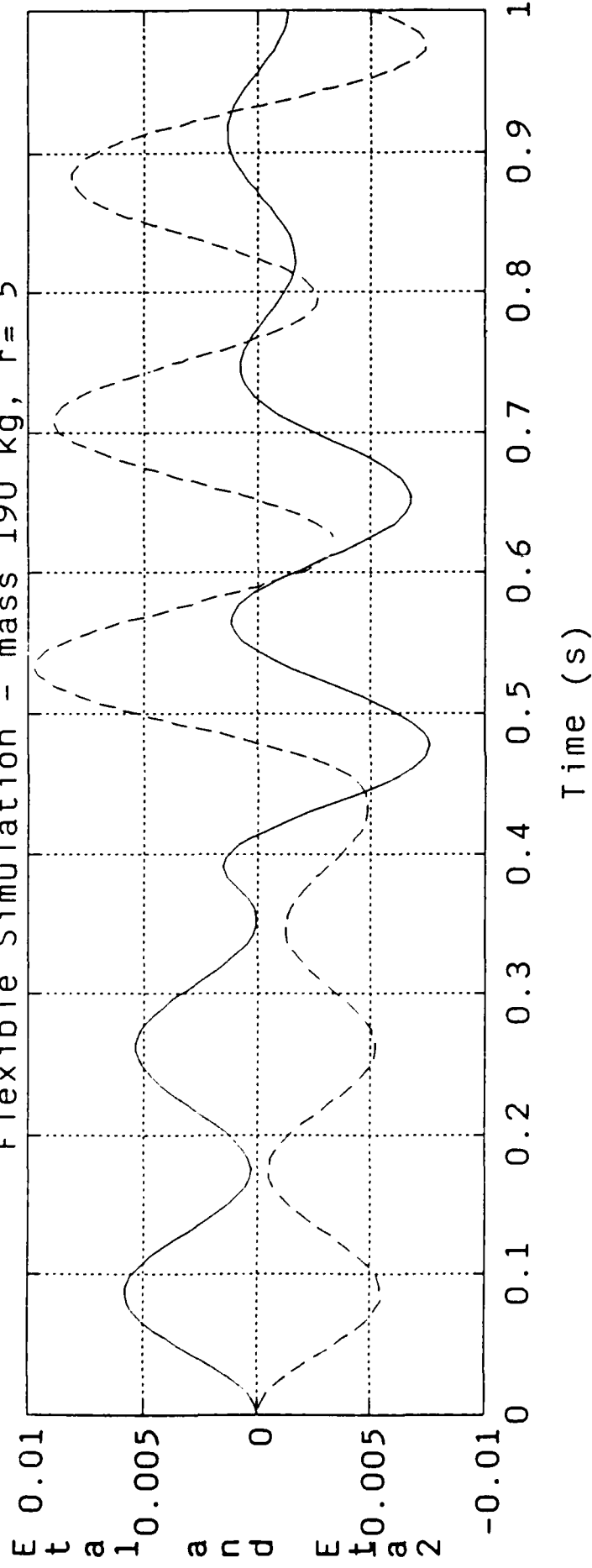


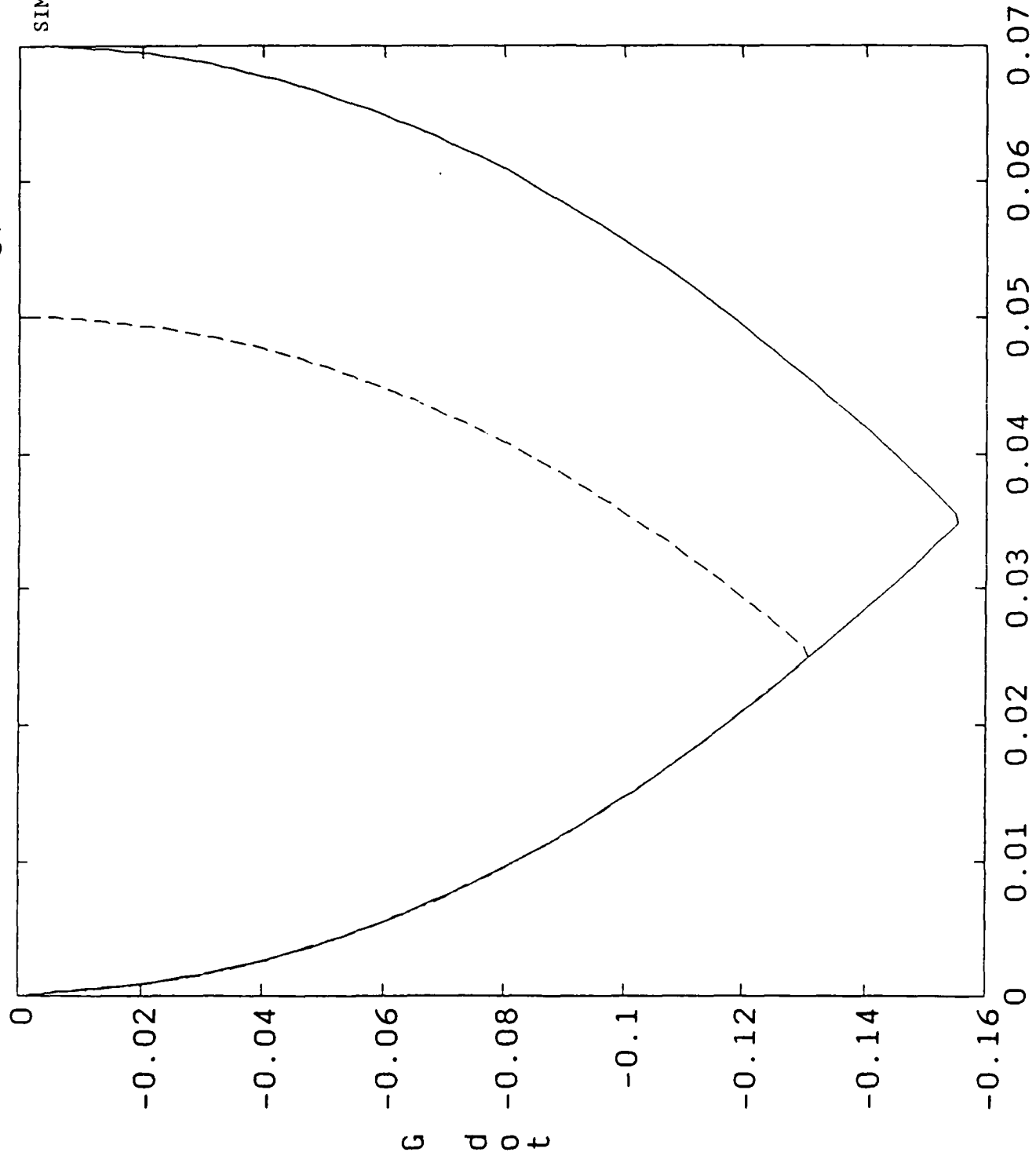


Flexible Simulation - mass 190 kg, $r = 5$

MOD1

SIM13

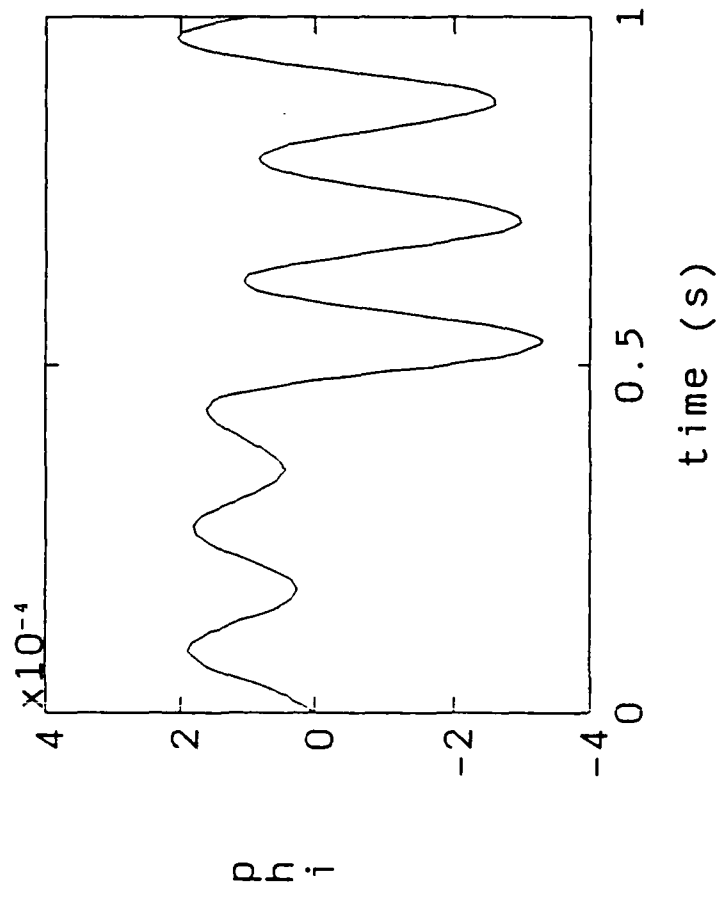
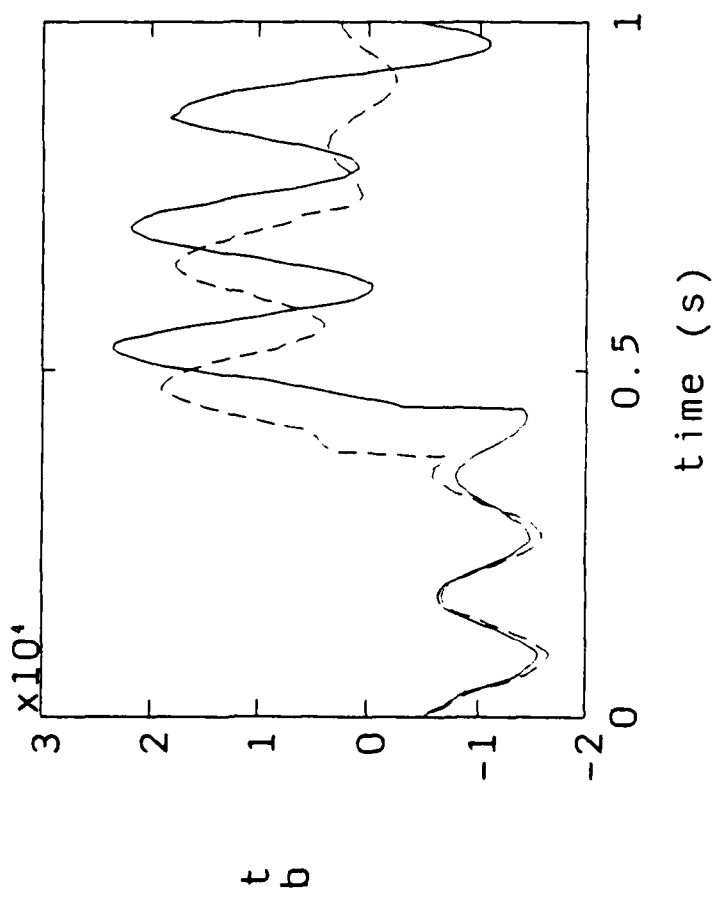
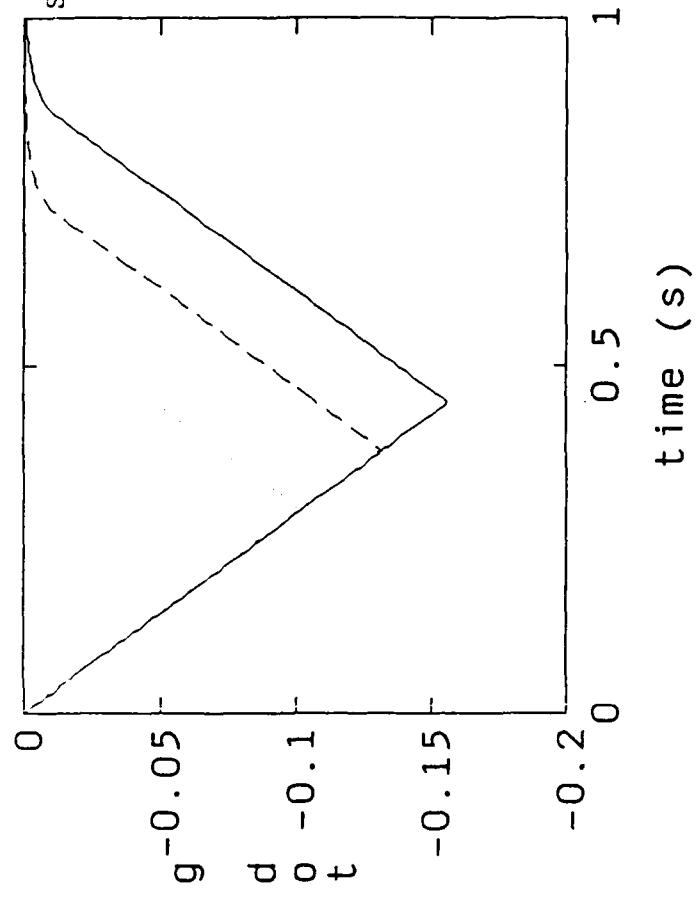
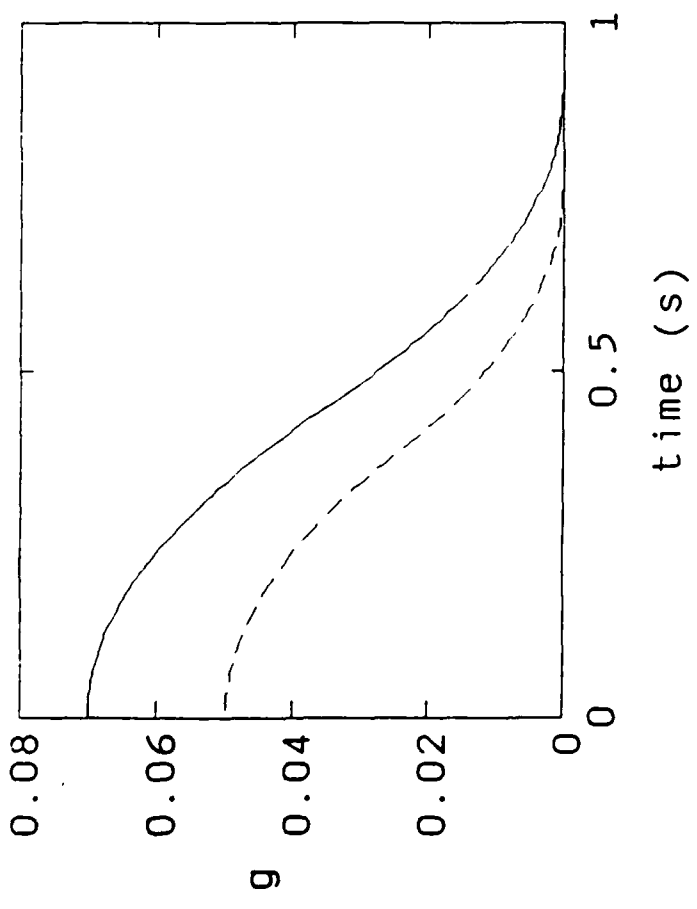




G

MOD1

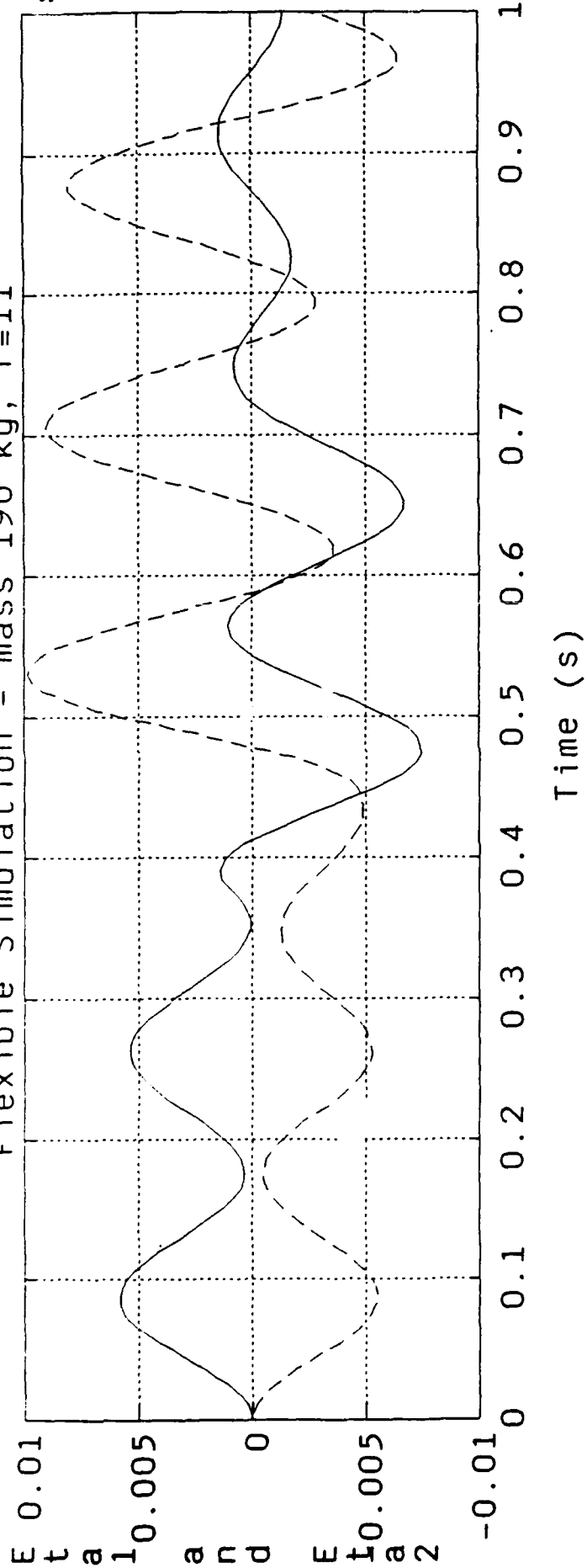
SIM14



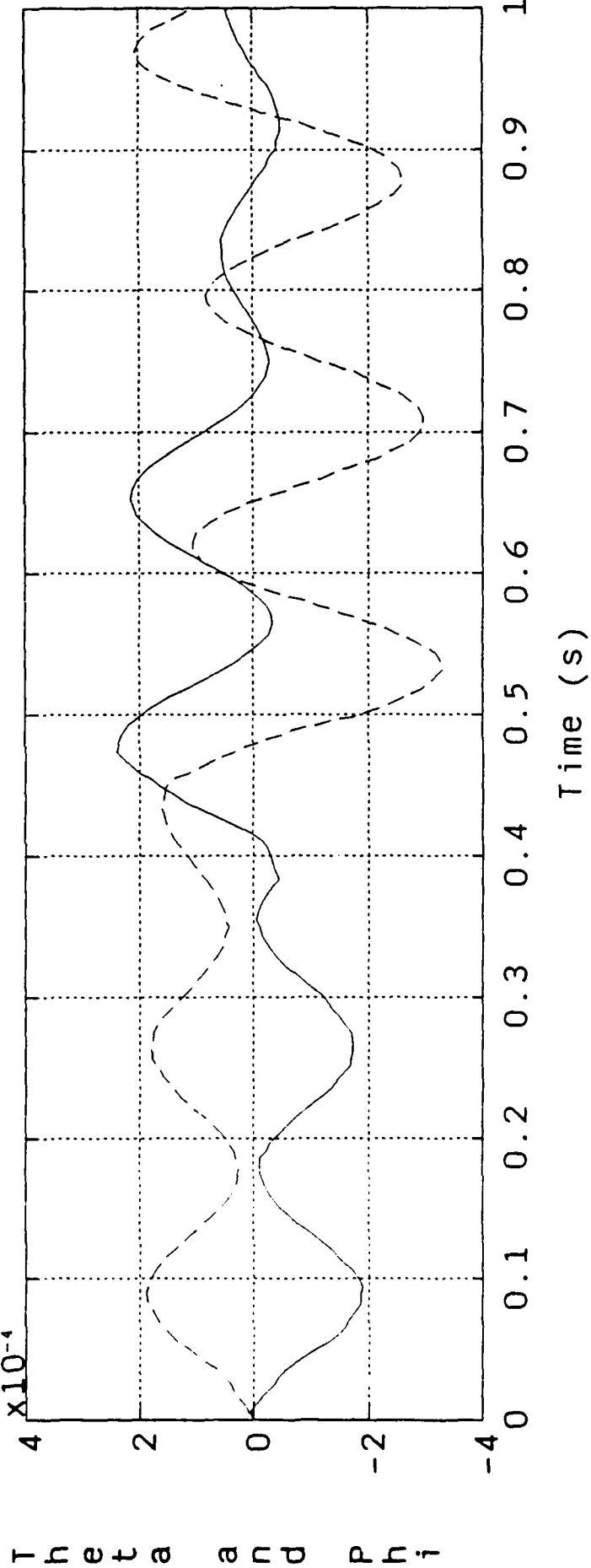
MOD1

SIM14

Flexible Simulation - mass 190 kg, r=11



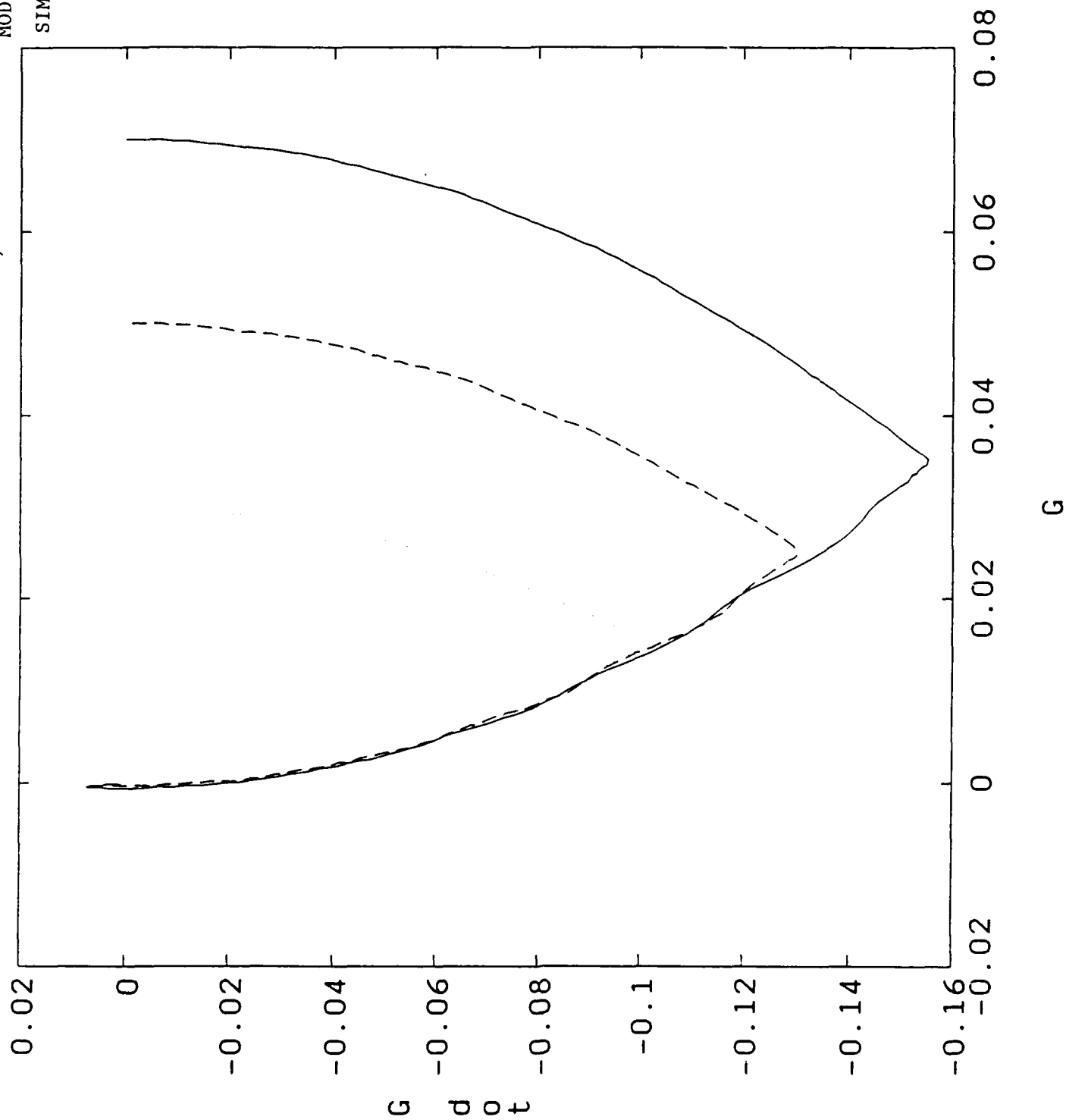
$\times 10^{-4}$



Flexible Simulation - no mass, $r=3$

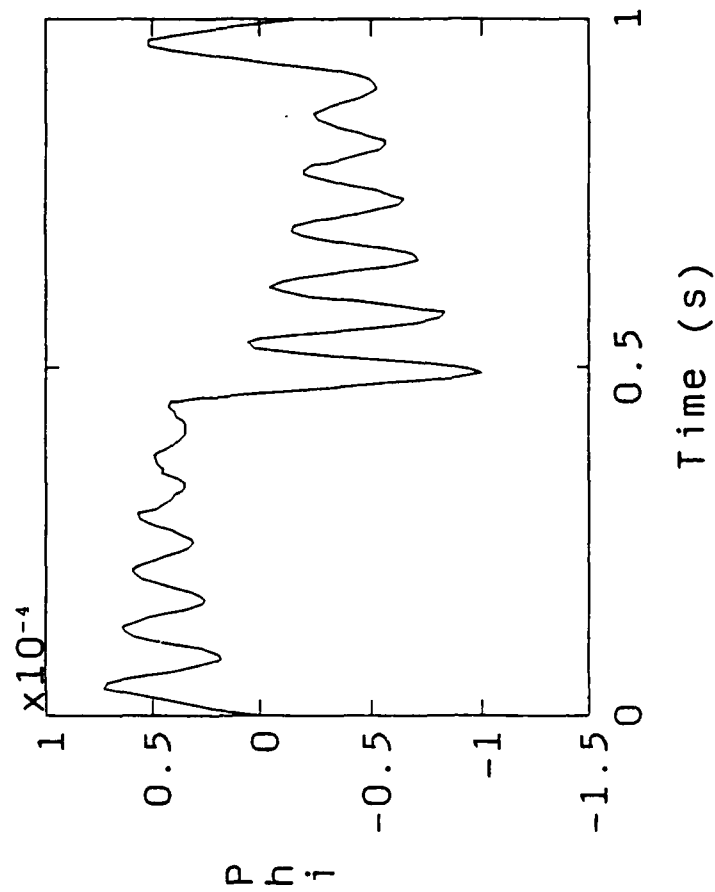
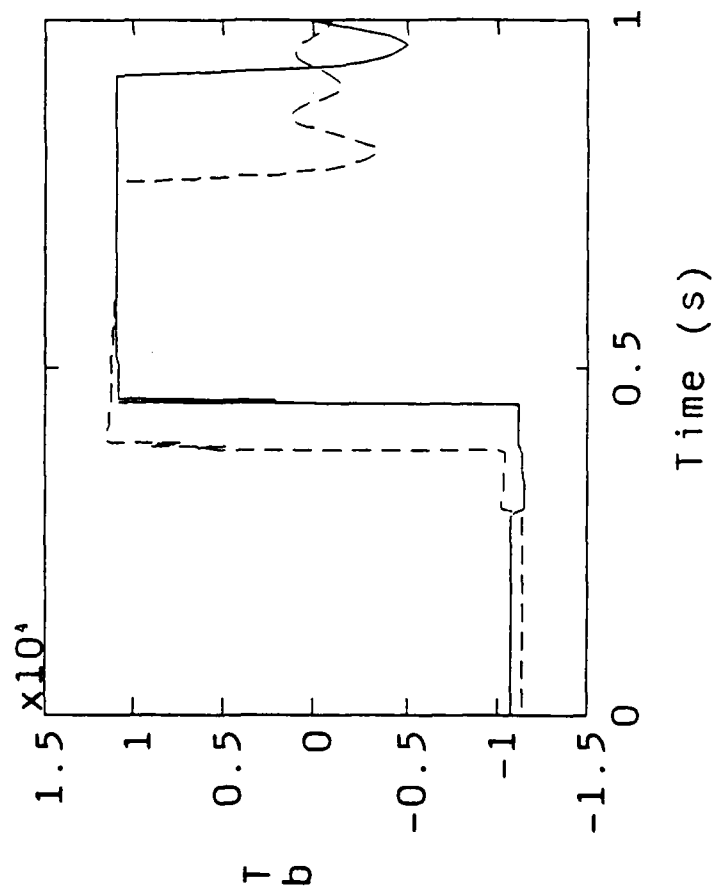
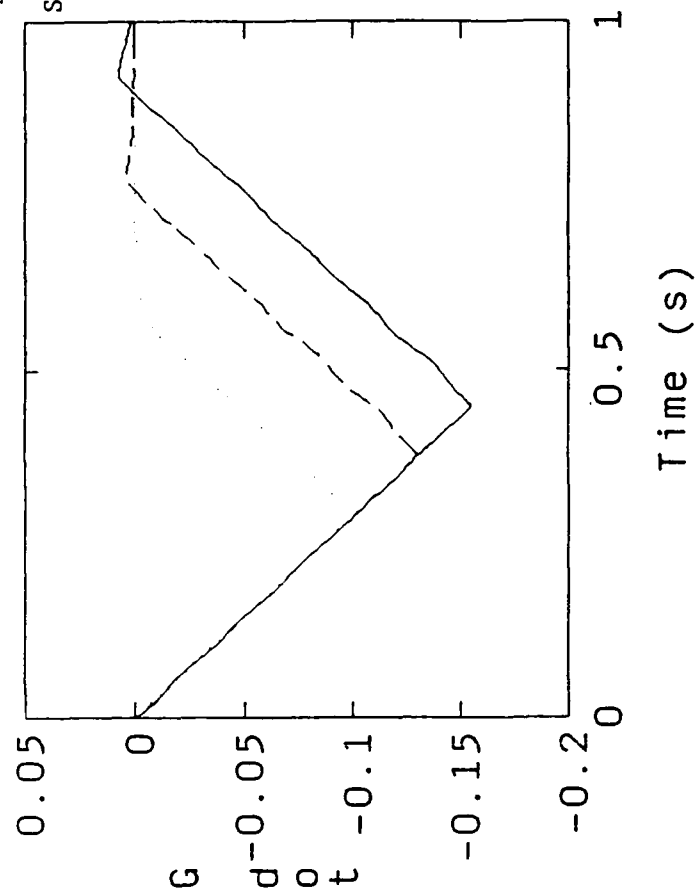
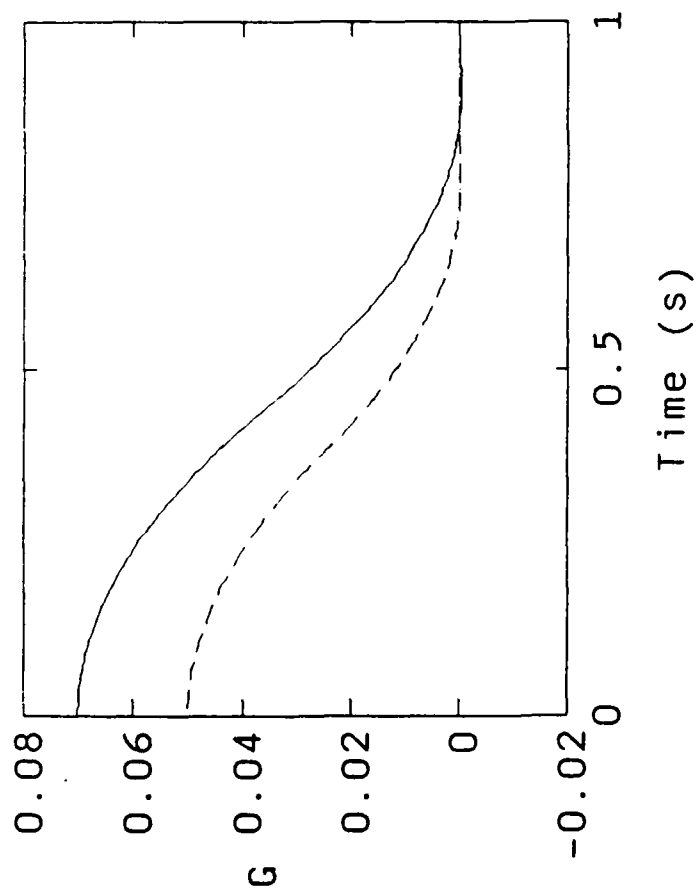
MOD2

SIM21



MOD2

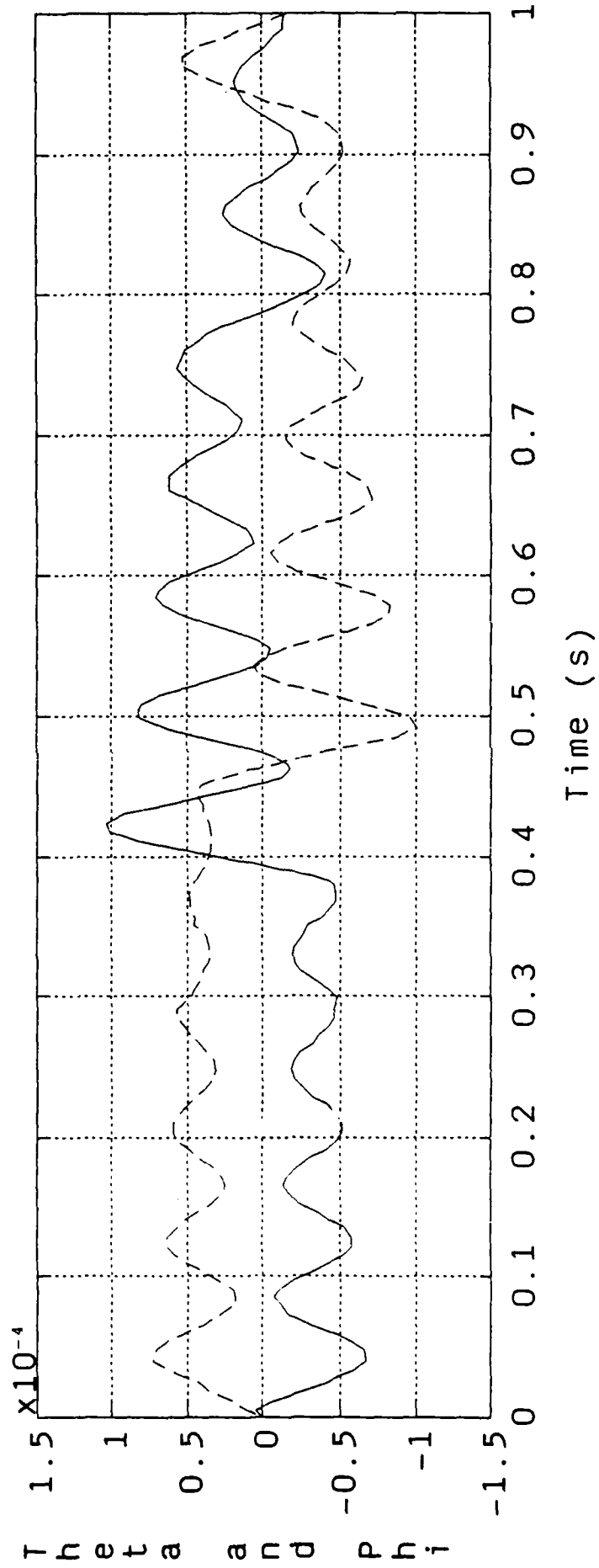
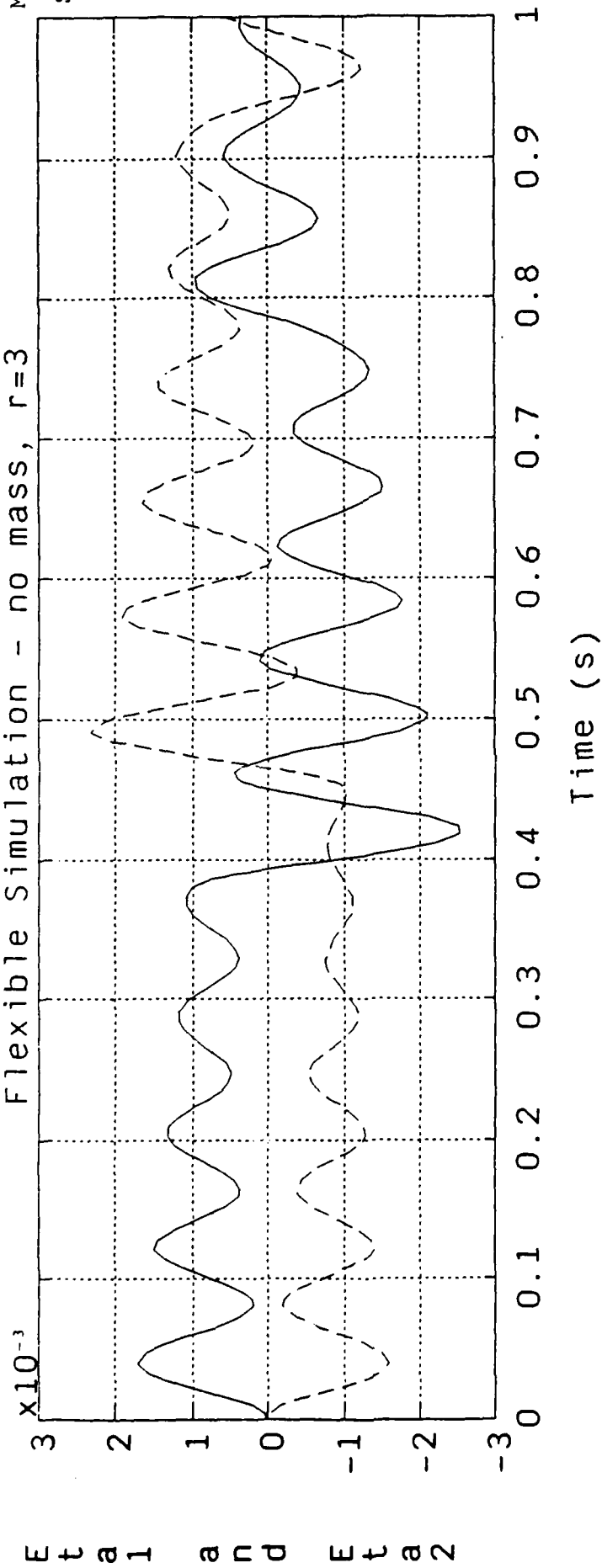
SIM21



Flexible Simulation - no mass, r=3

MOD2

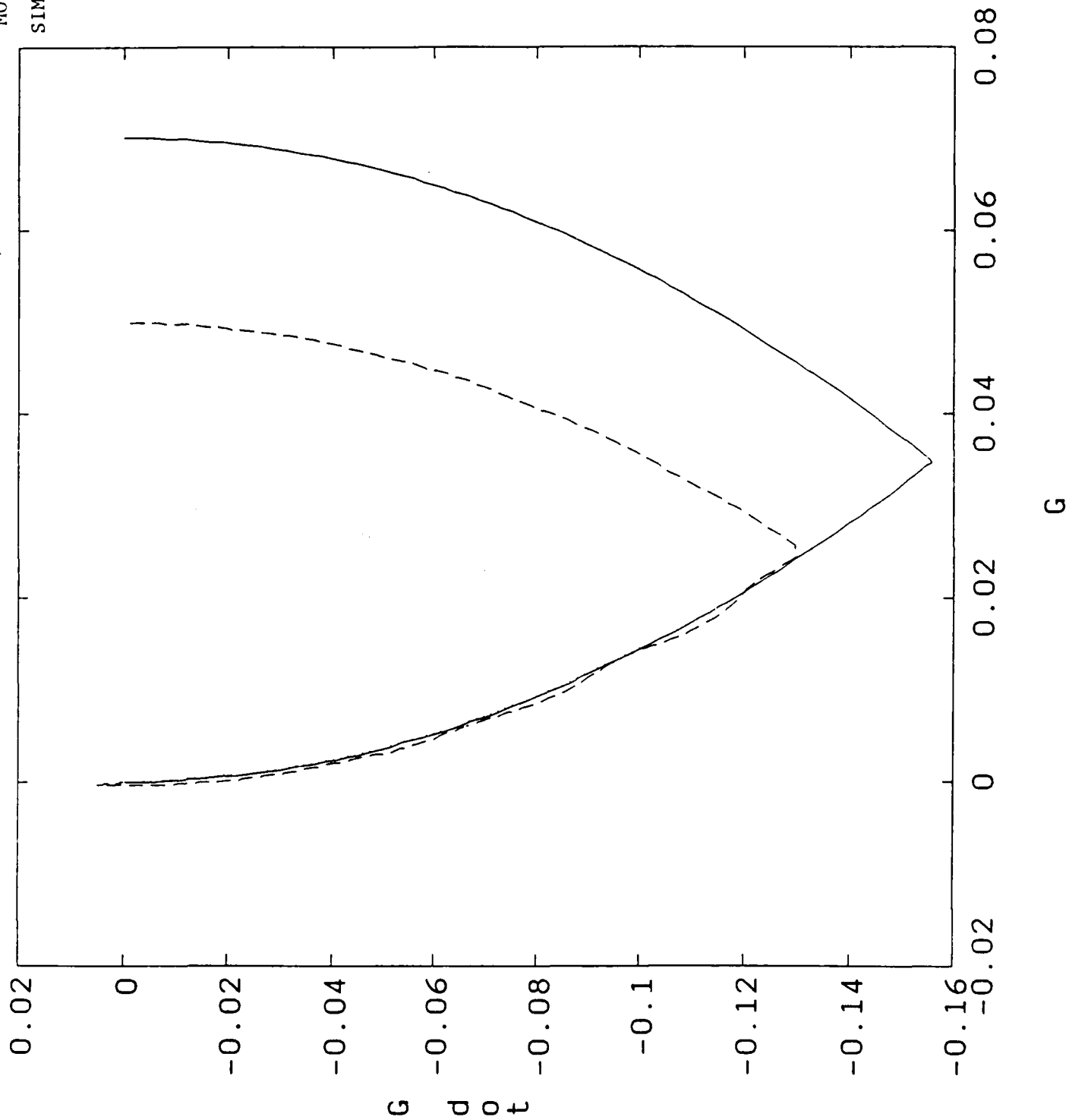
SIM21



Flexible Simulation - no mass, $r=4$

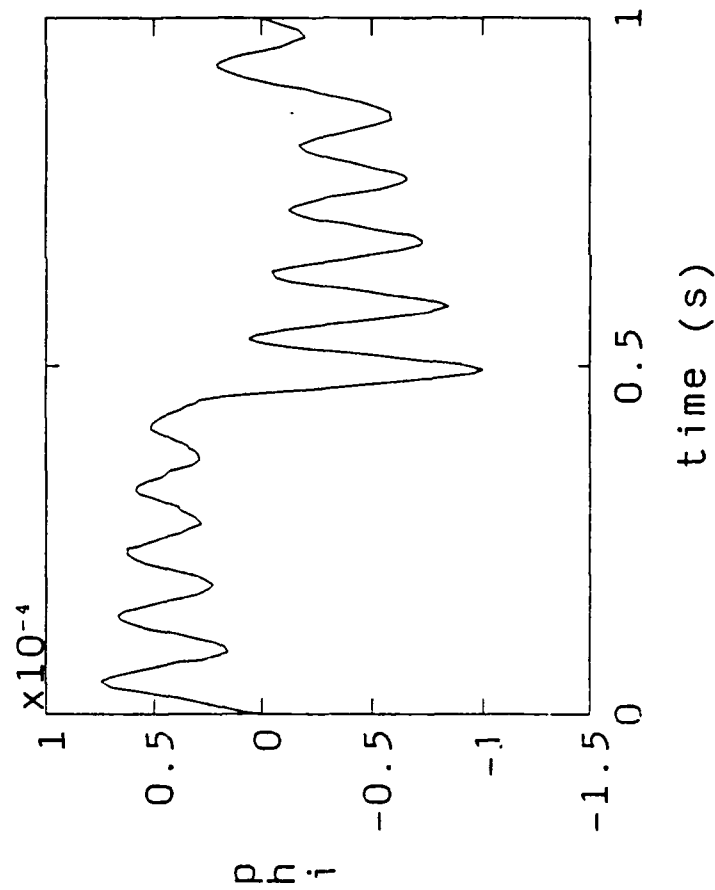
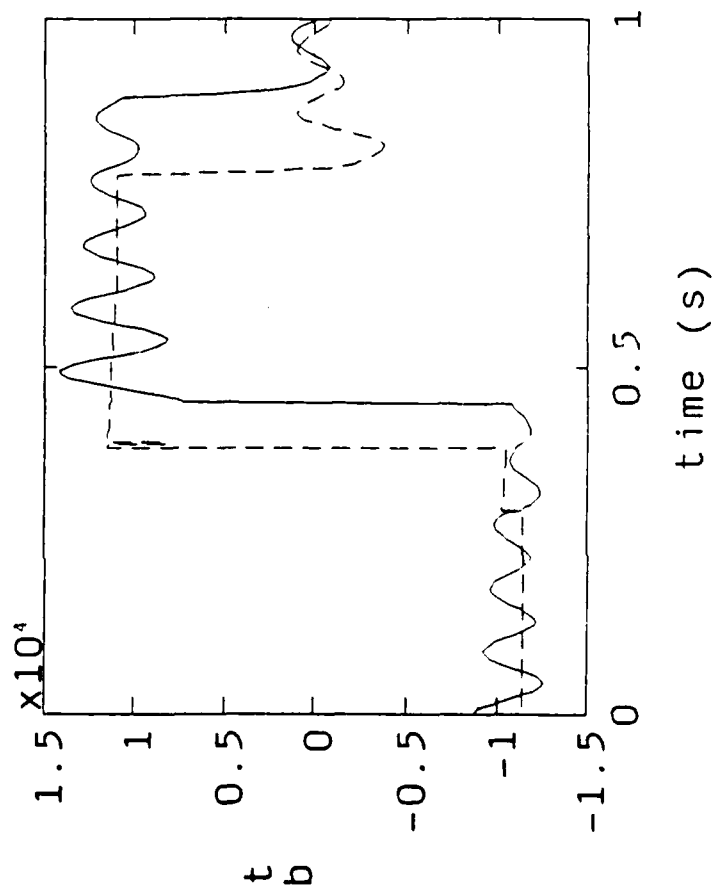
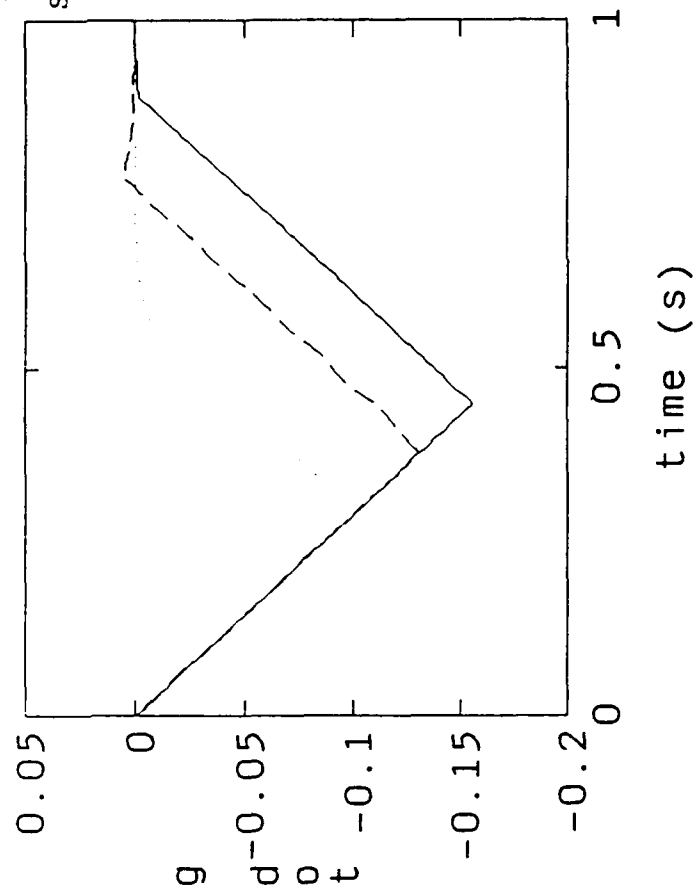
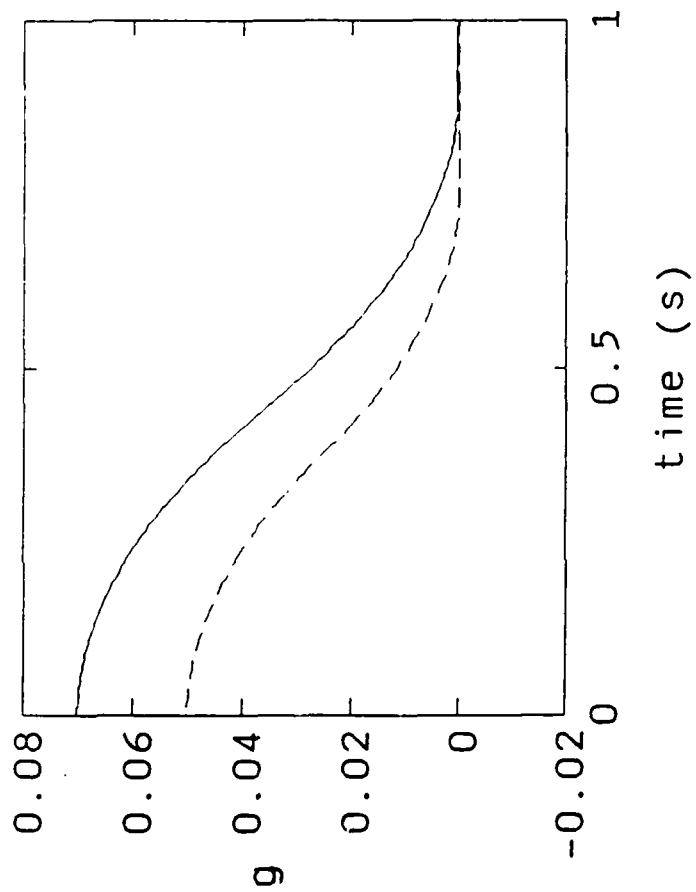
MOD2

SIM22



MOD2

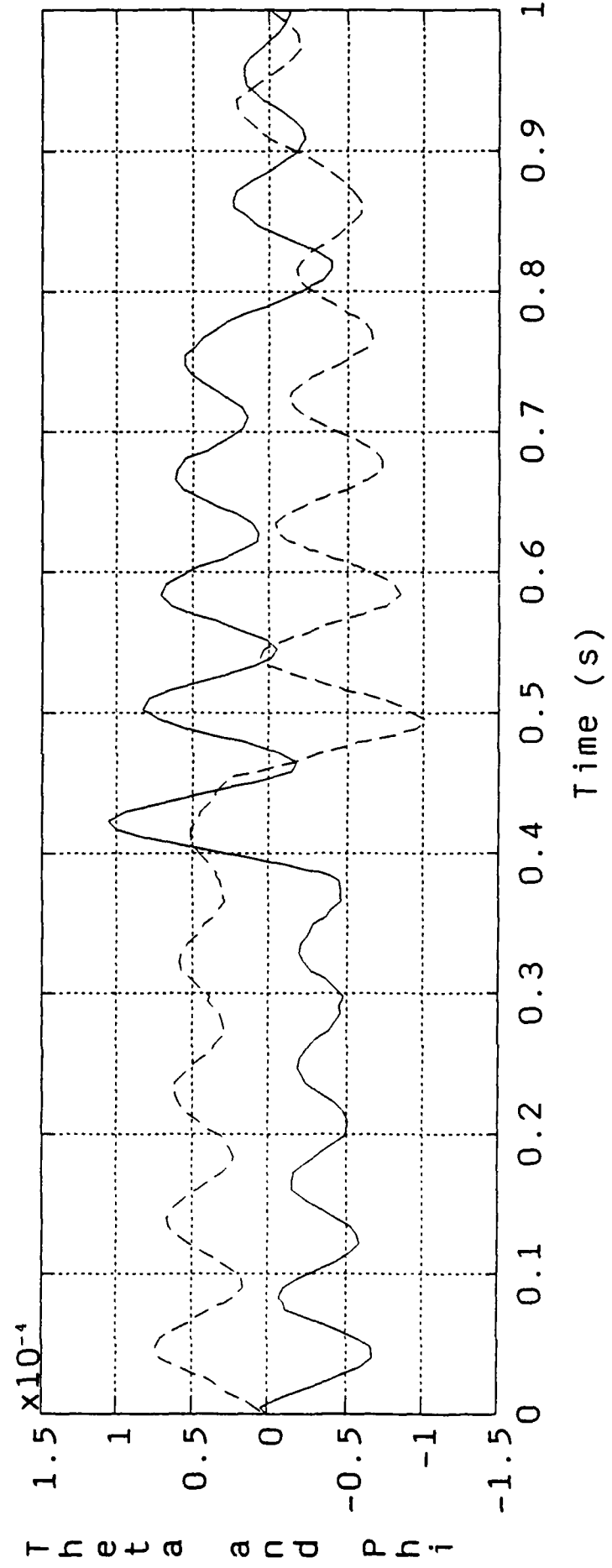
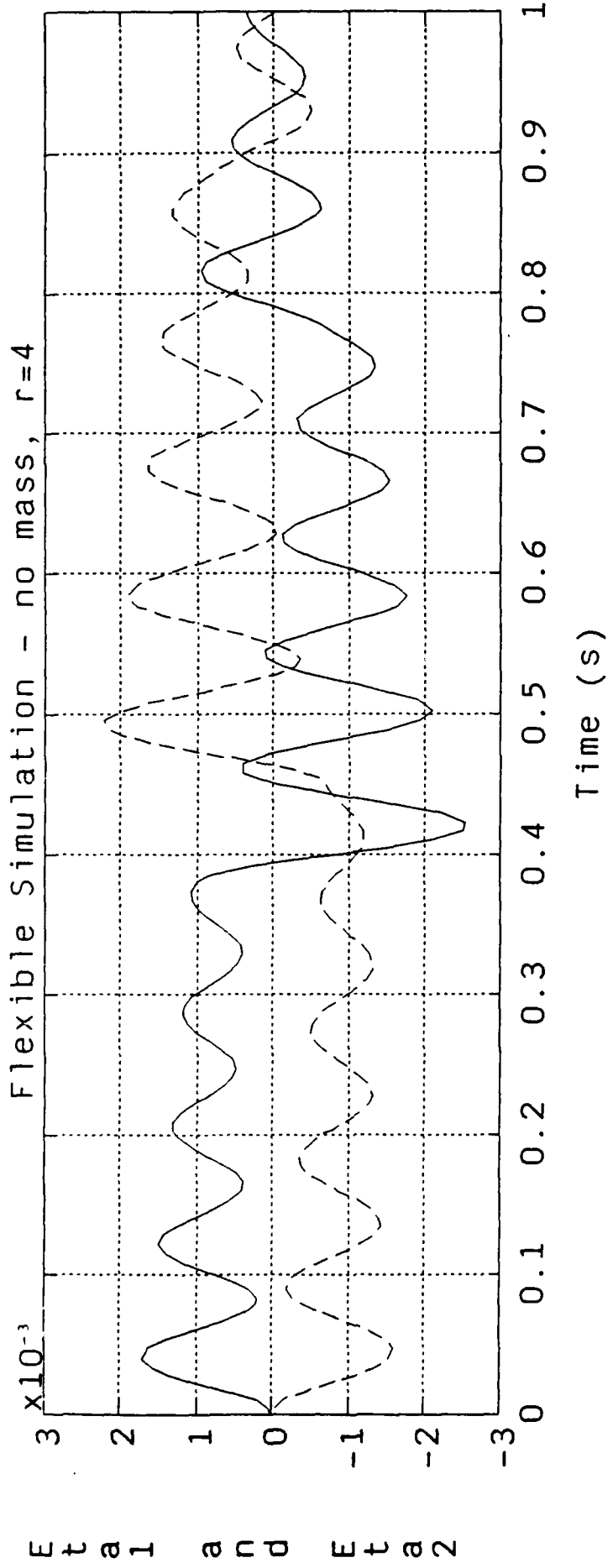
SIM22



Flexible Simulation - no mass, r=4

MOD2

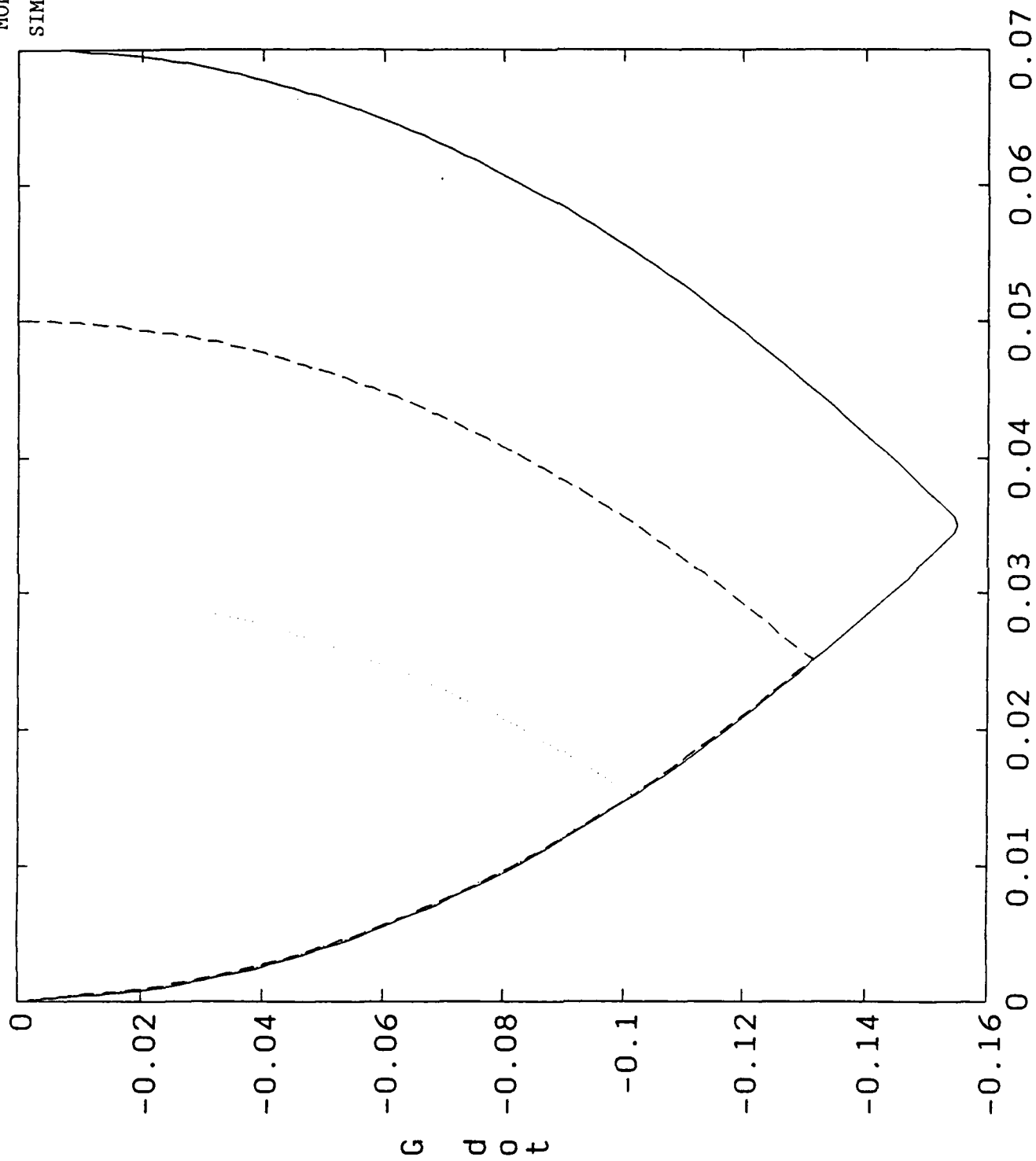
SIM22



Flexible Simulation - no mass, $r=5$

MOD2

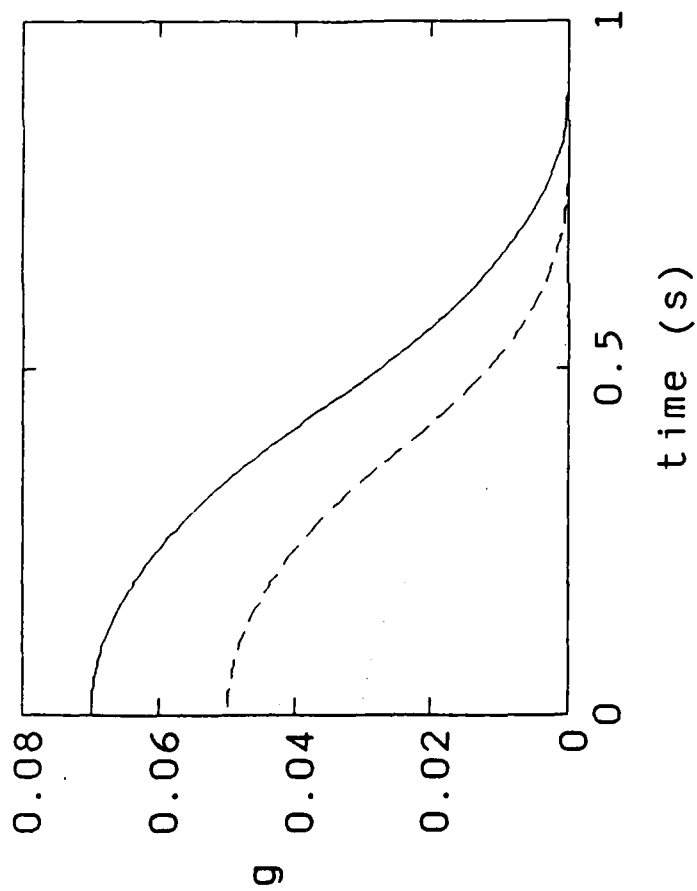
SIM23



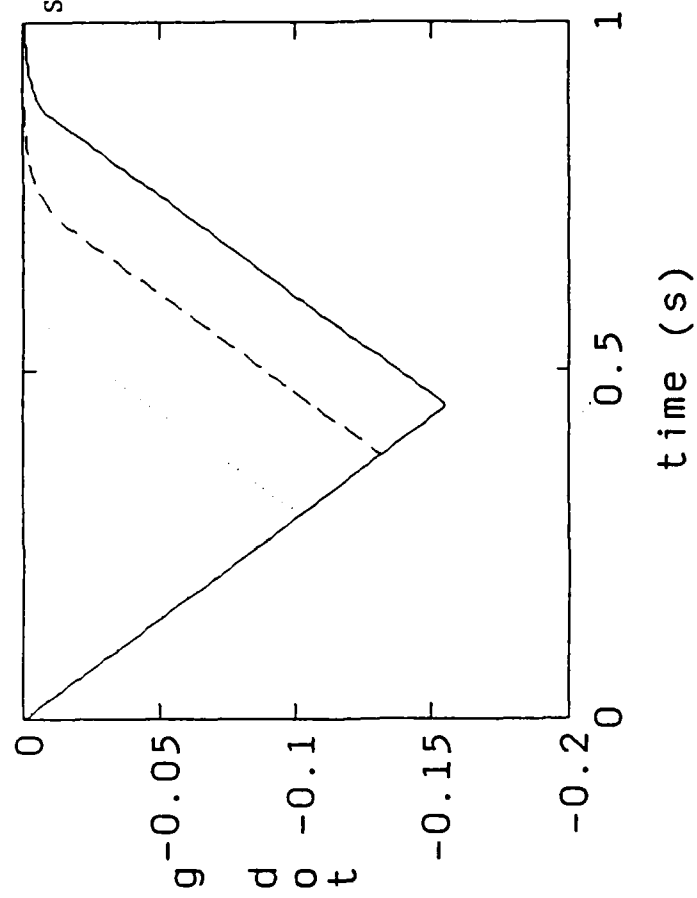
G

MOD2

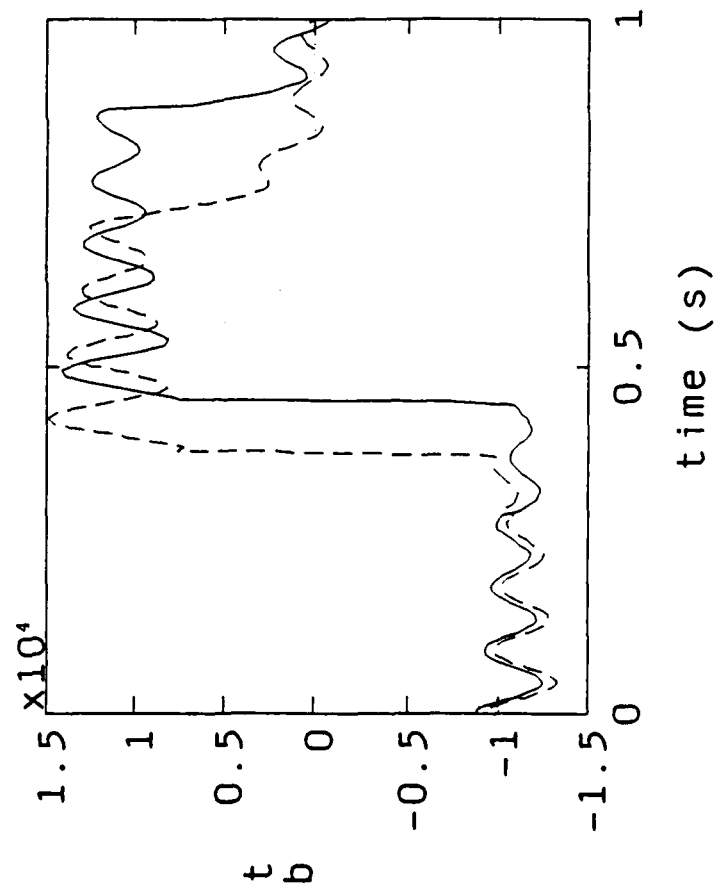
SIM23



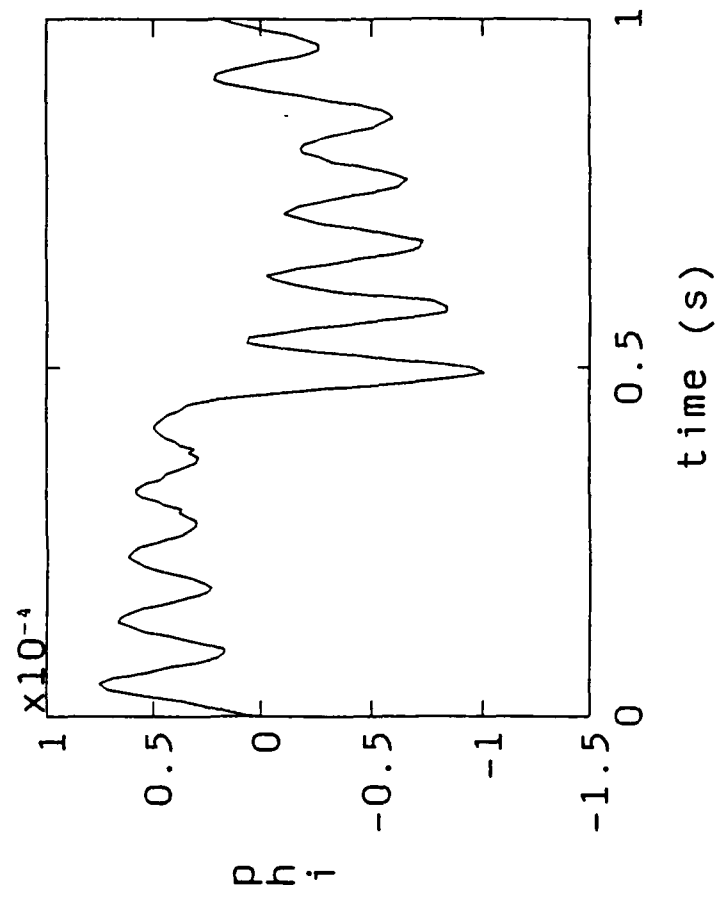
time (s)



time (s)



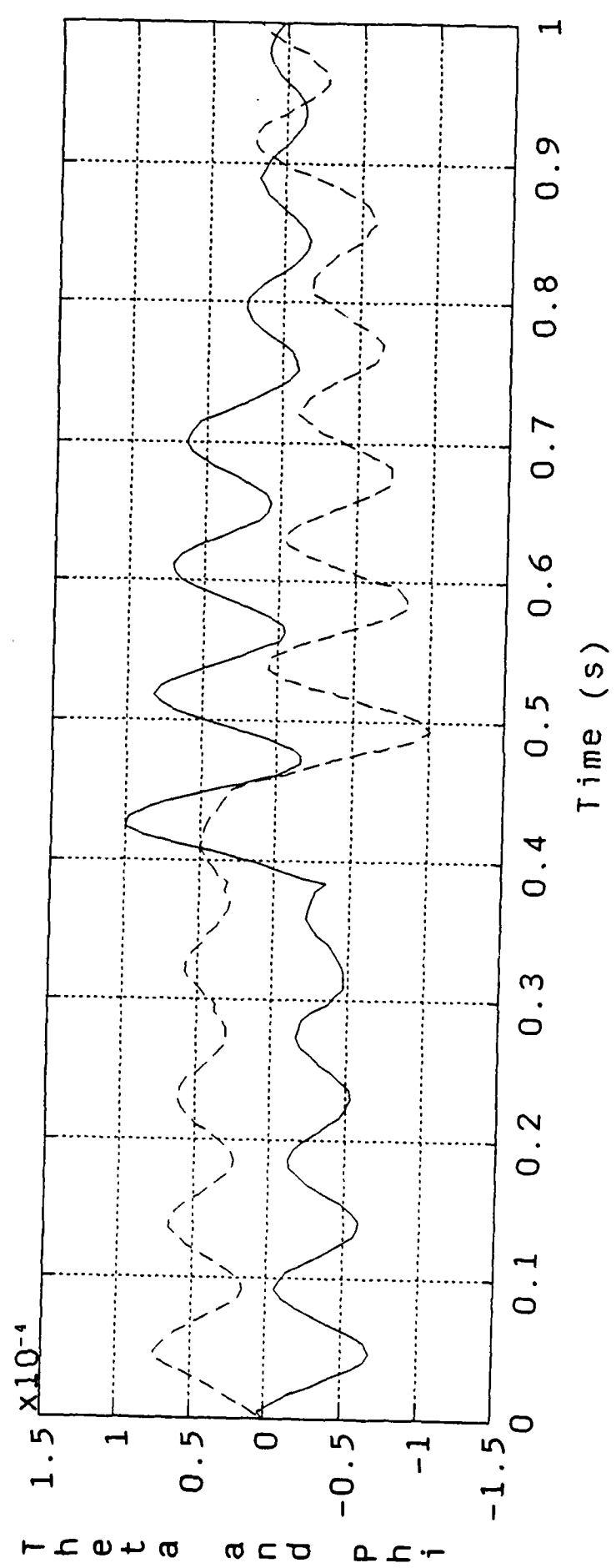
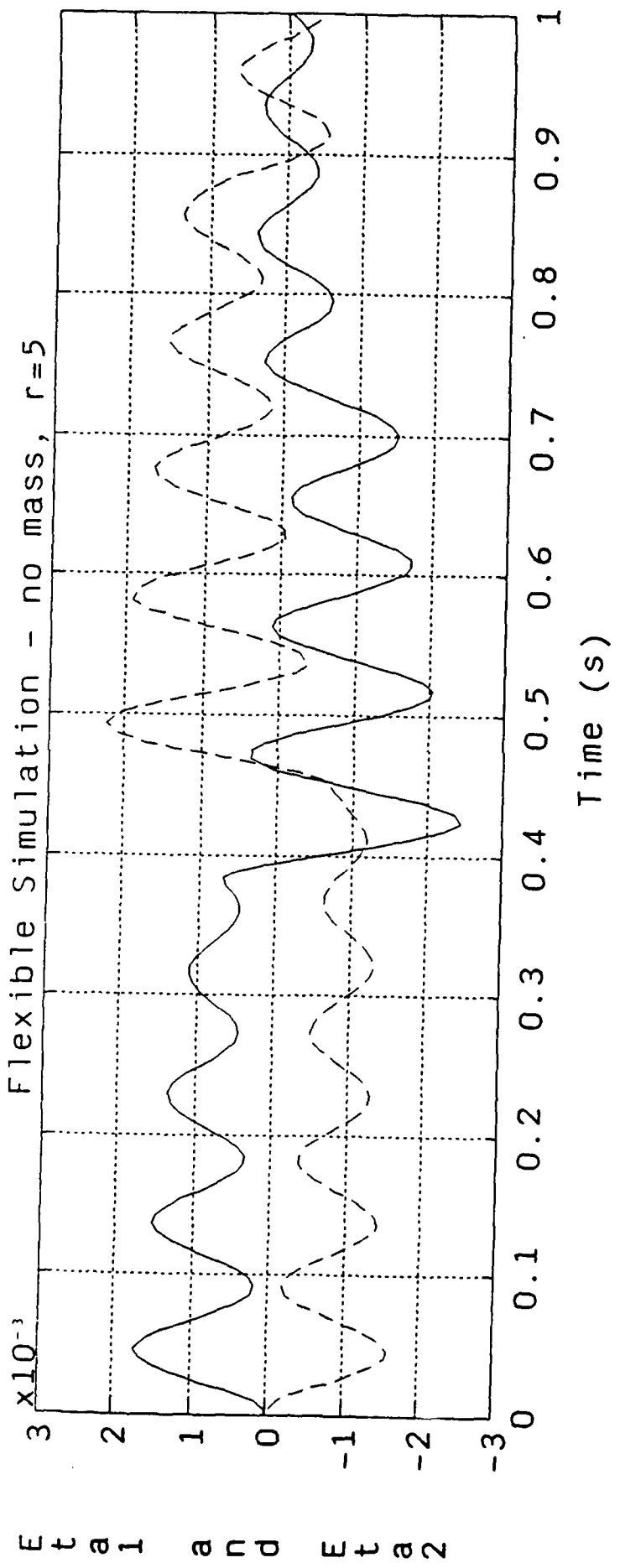
time (s)



time (s)

Flexible Simulation - no mass, $r=5$

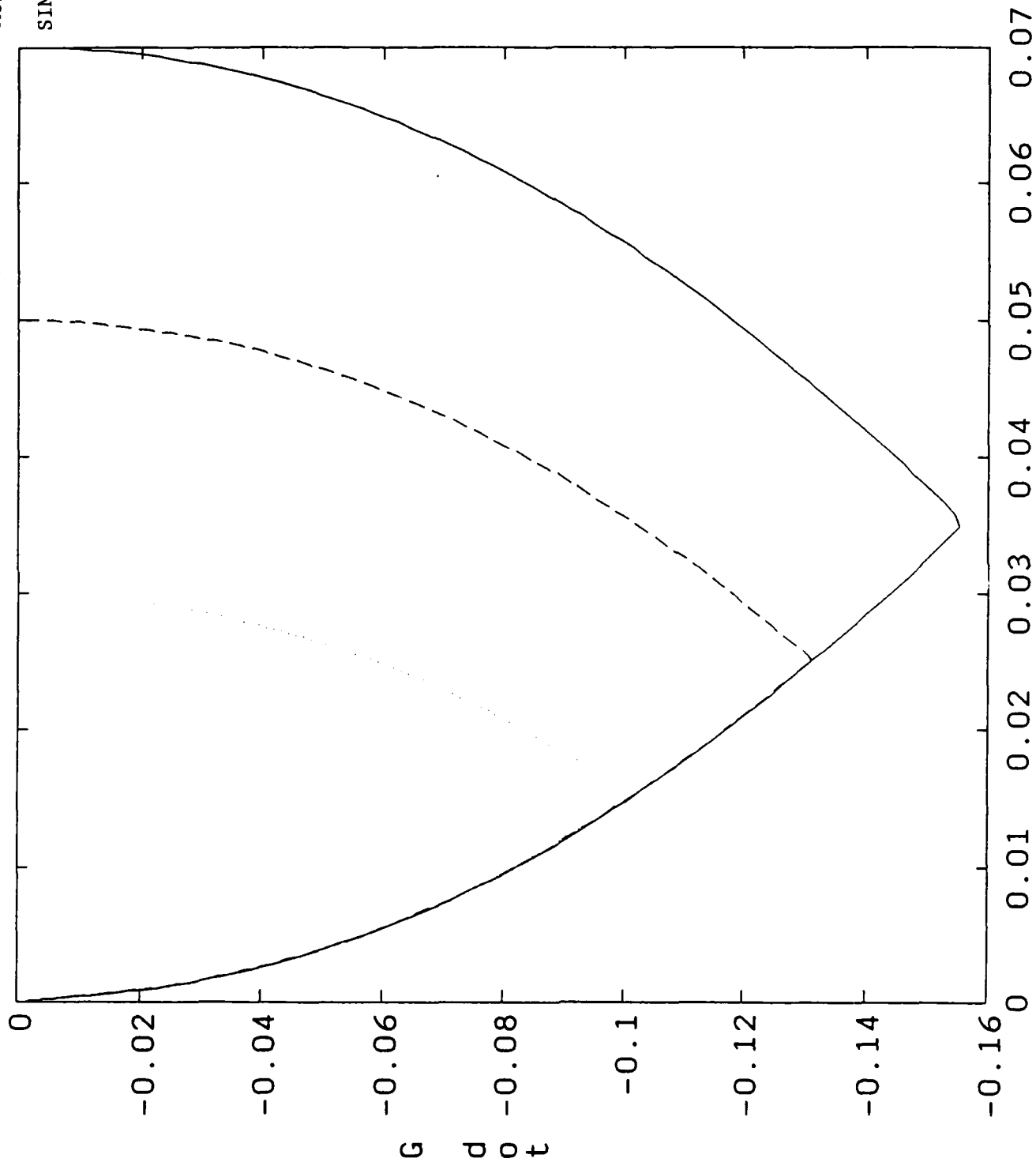
MOD2
SIM23



Flexible Simulation - no mass, $r=11$

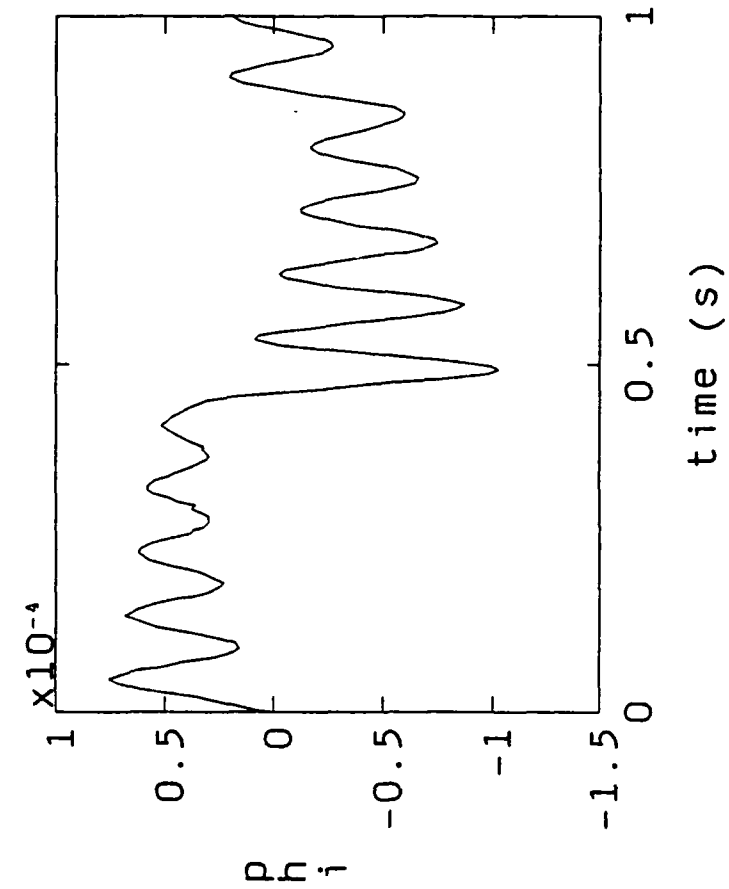
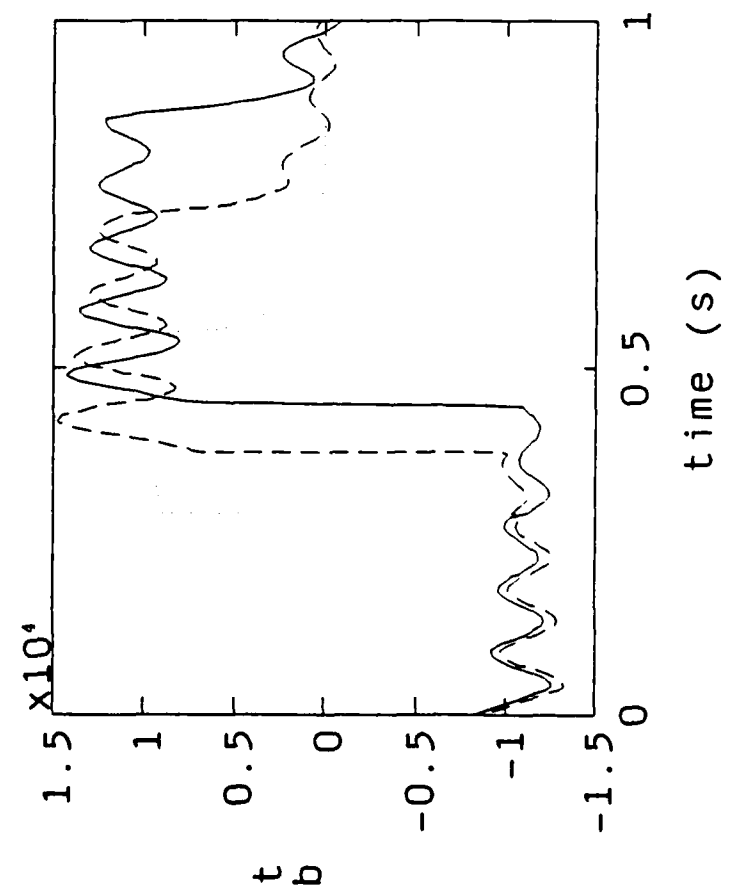
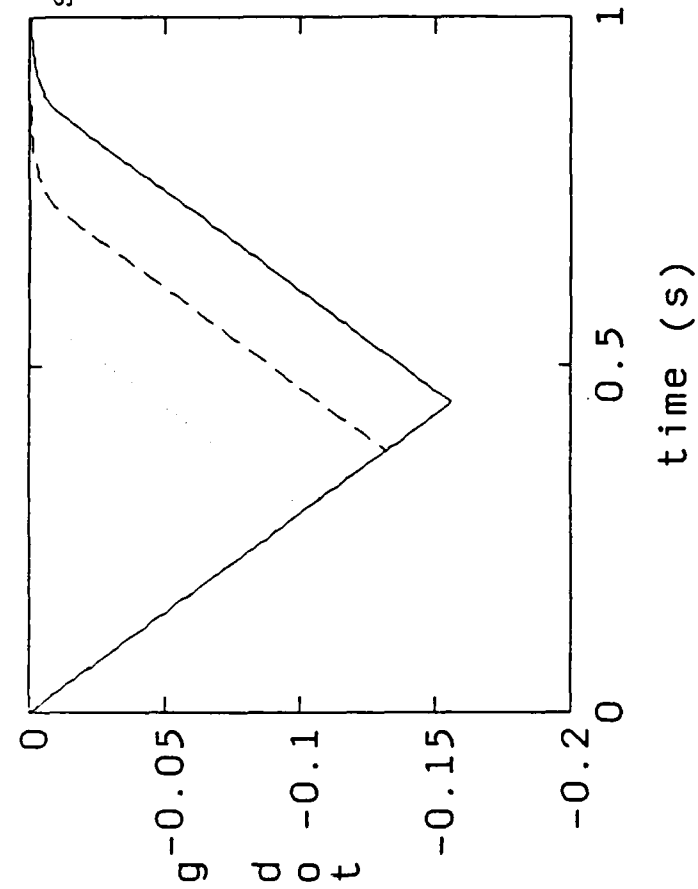
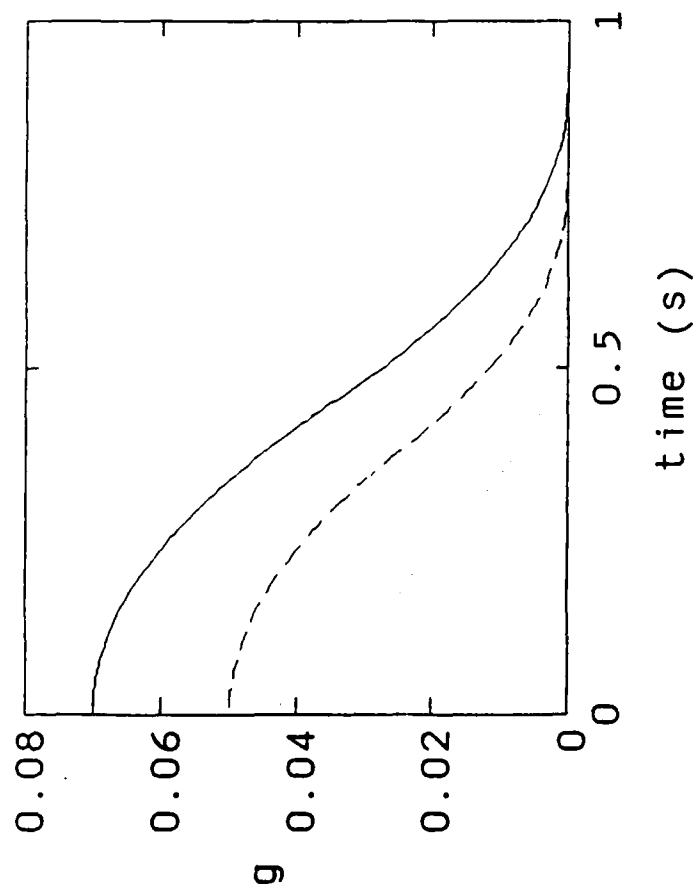
MOD2

SIM24



MOD2

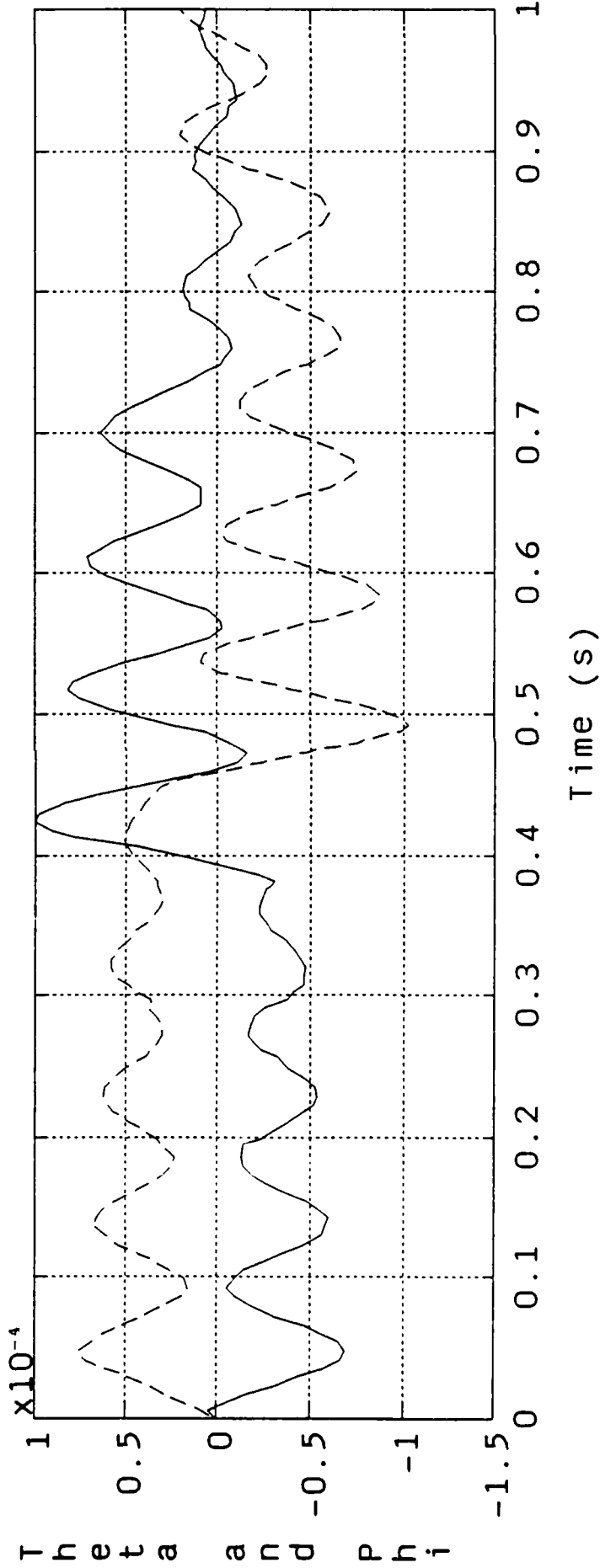
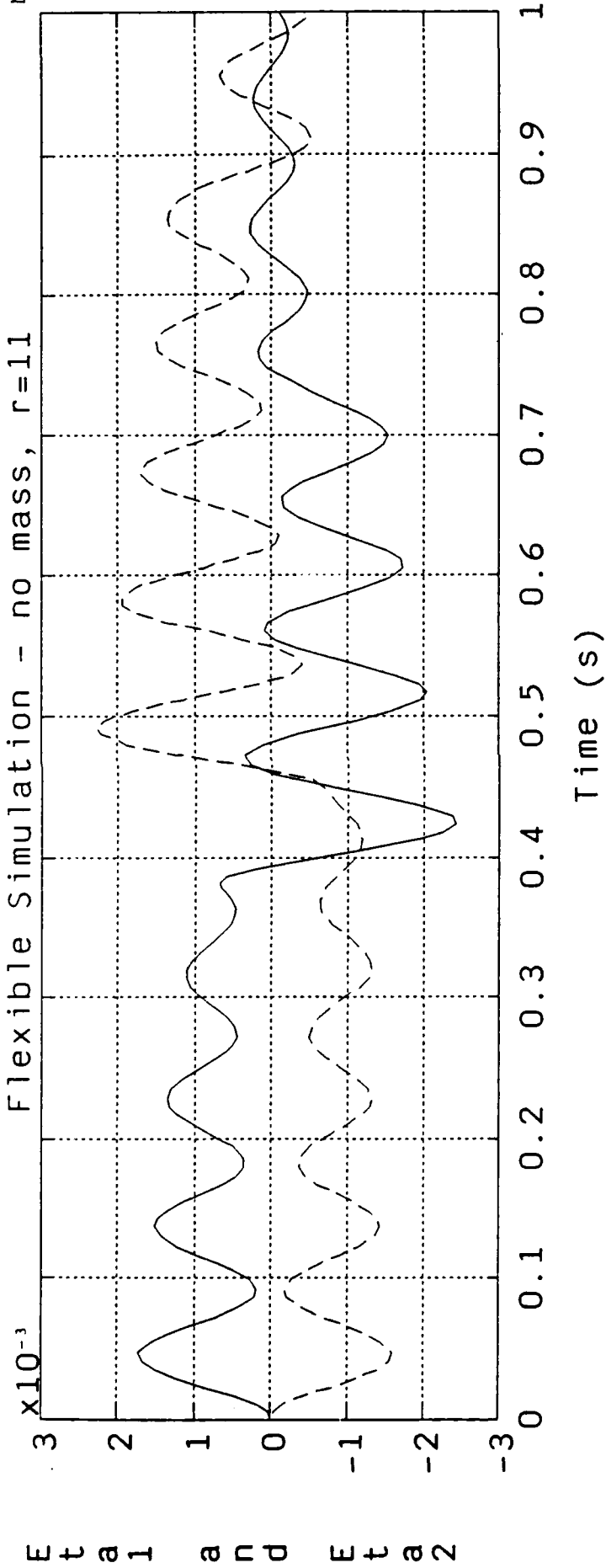
SIM24

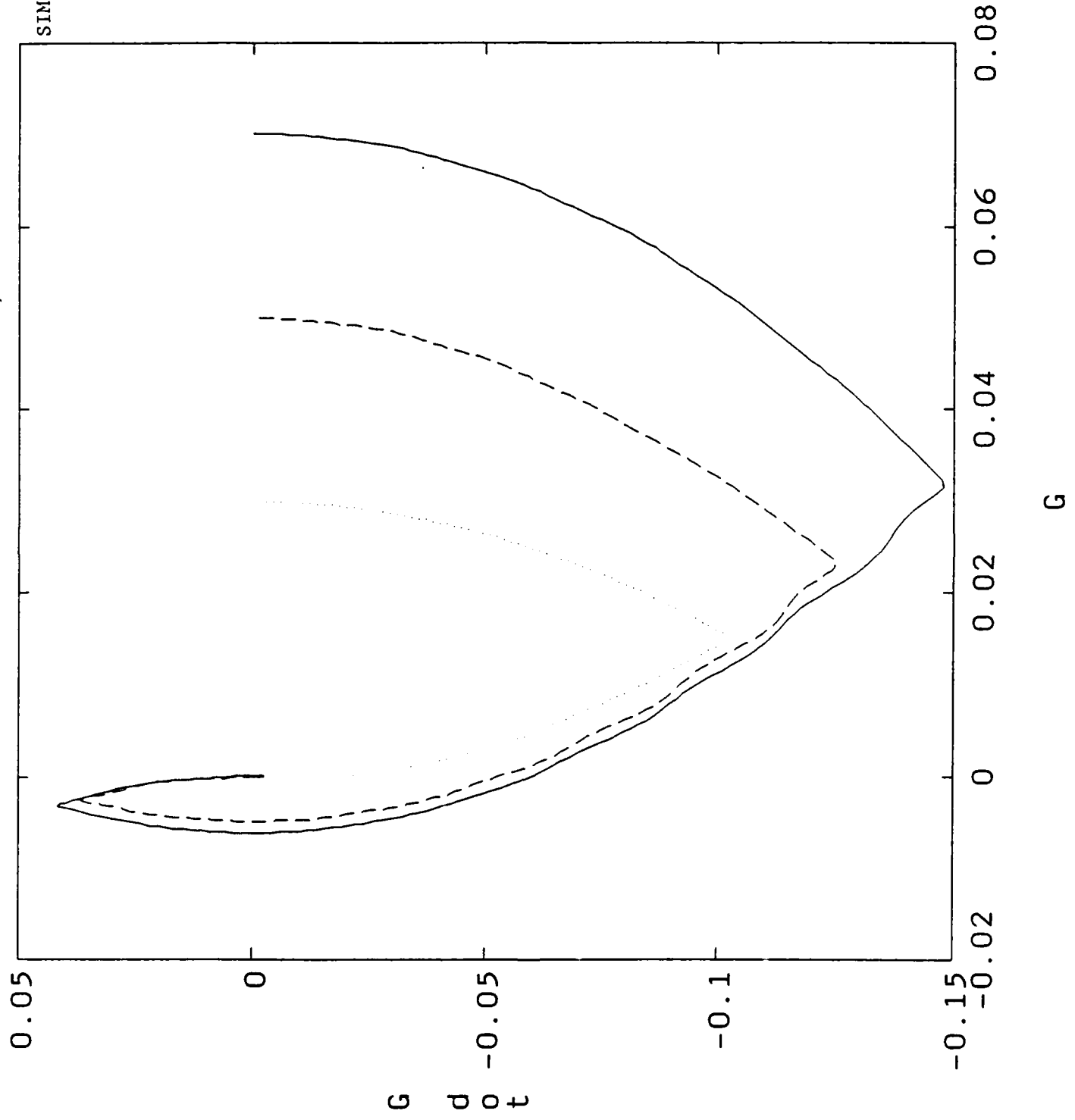


Flexible Simulation - no mass, r=11

MOD2

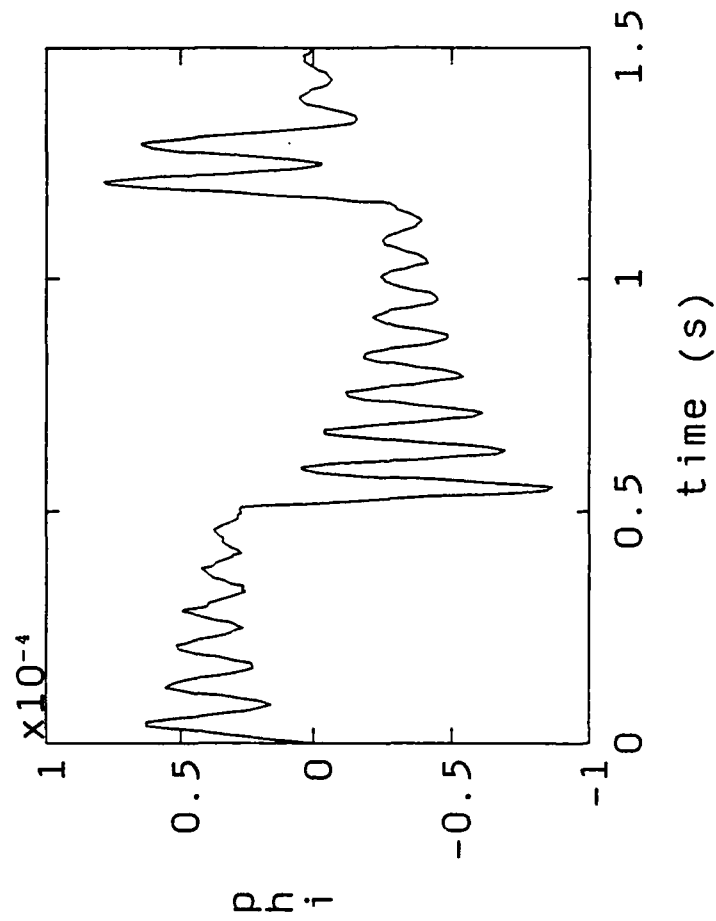
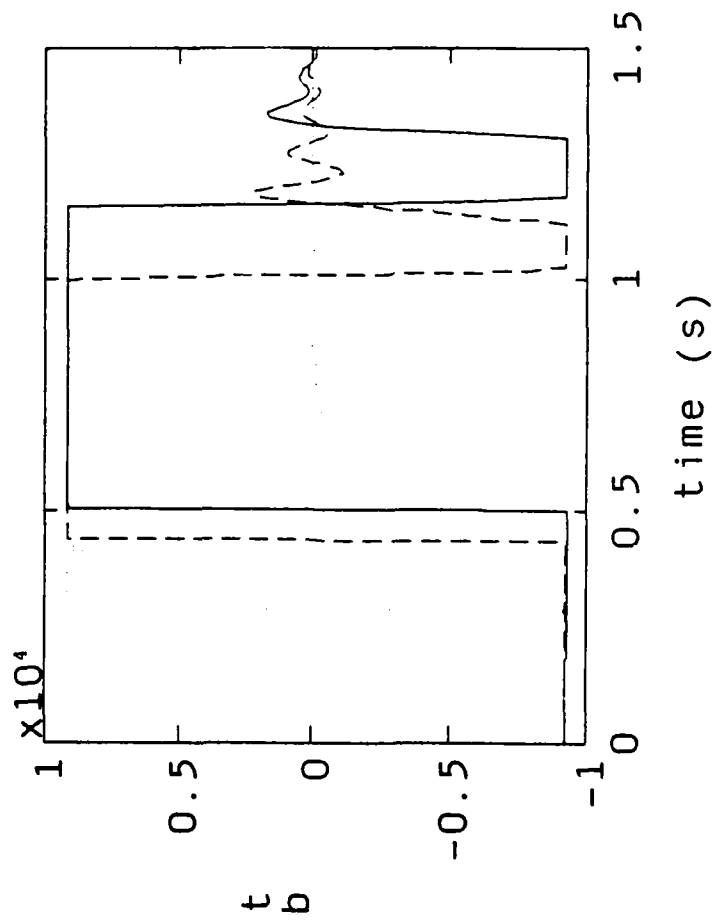
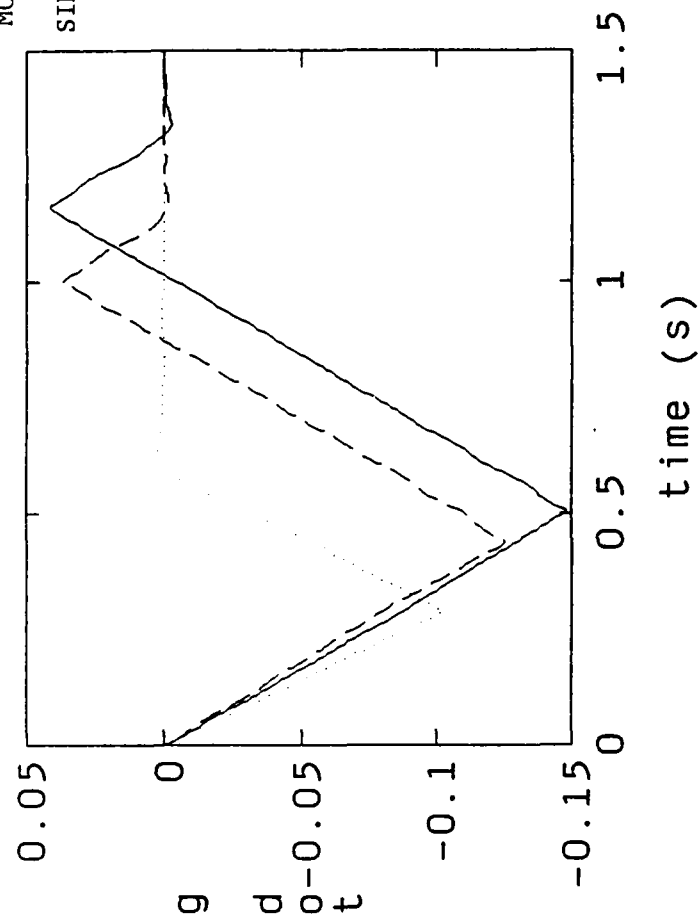
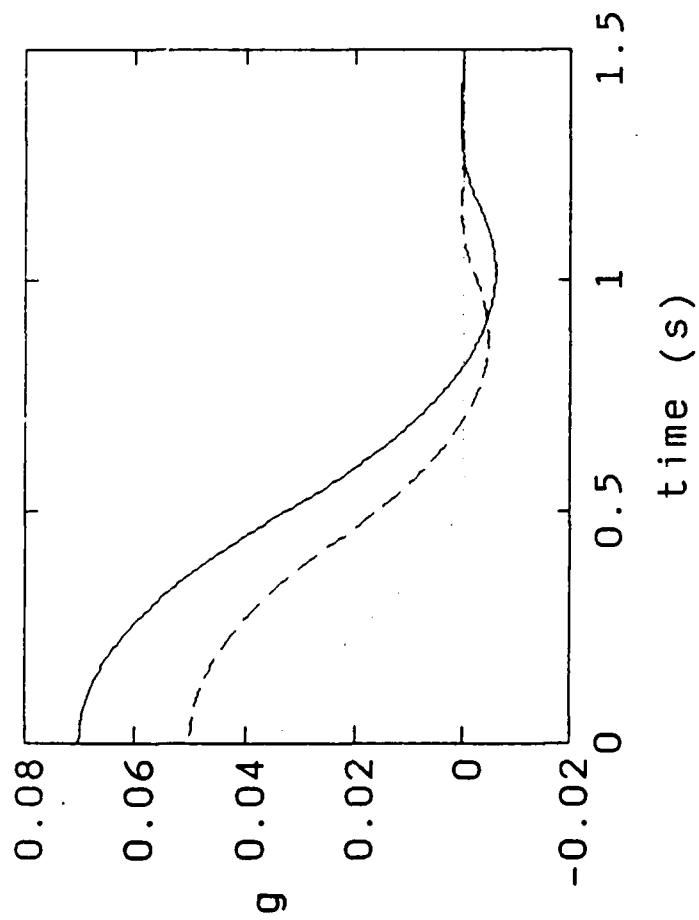
SIM24

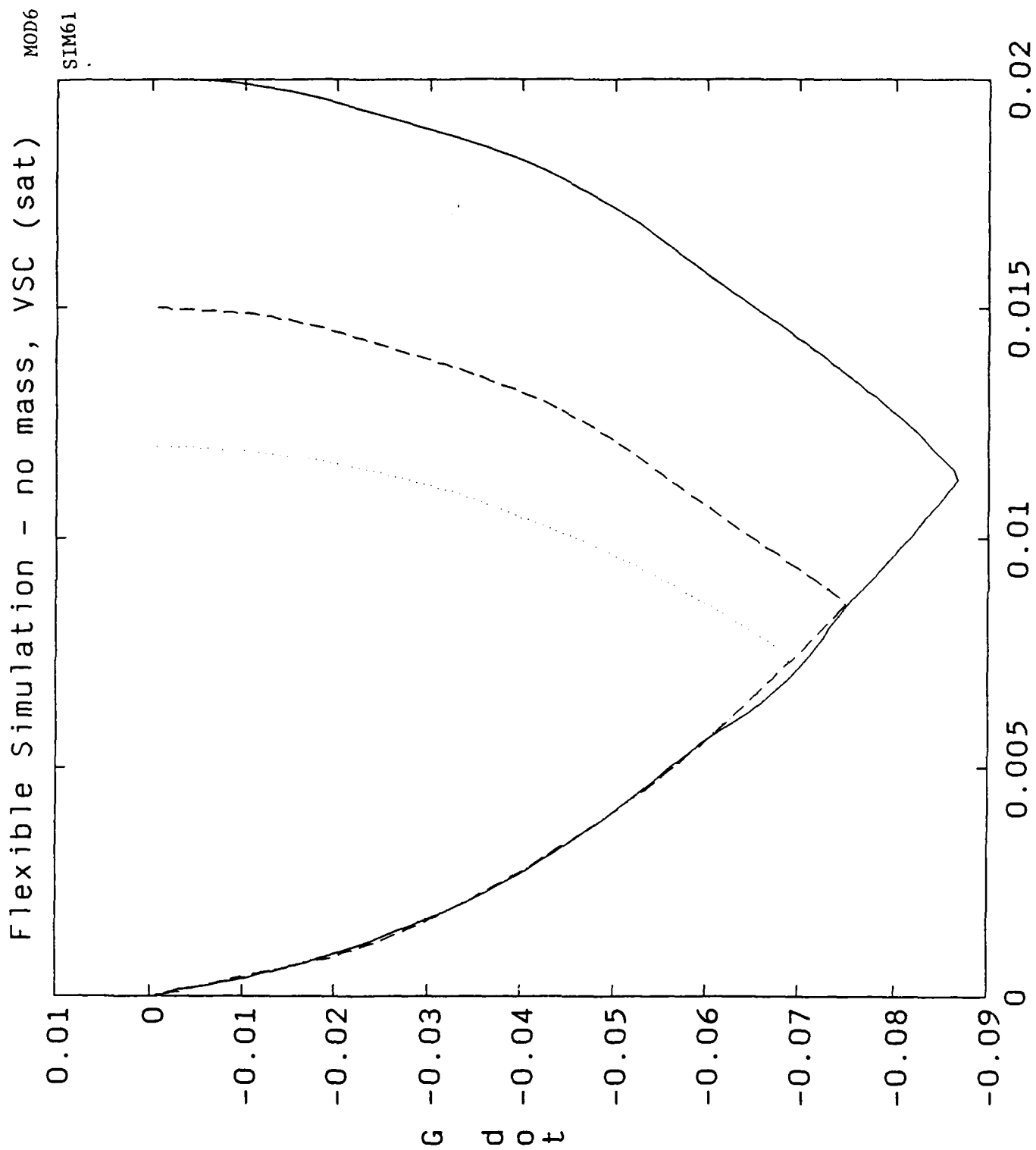




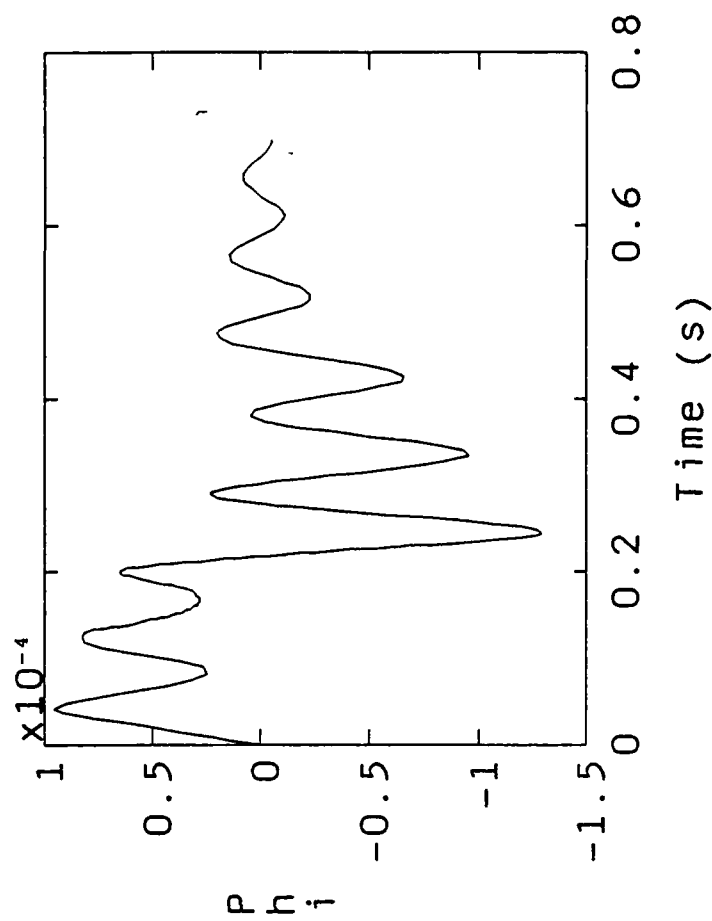
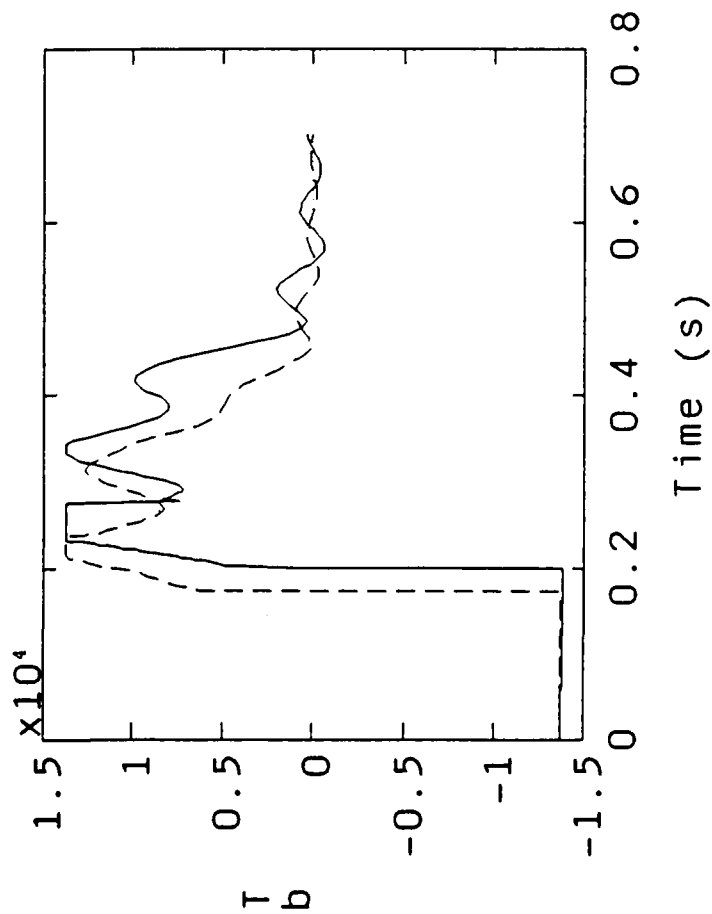
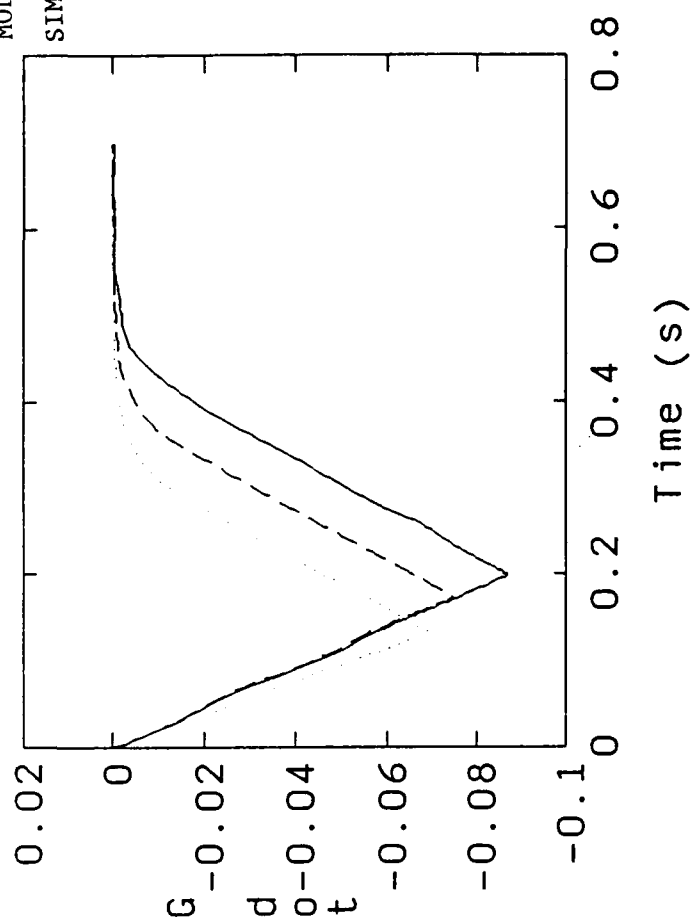
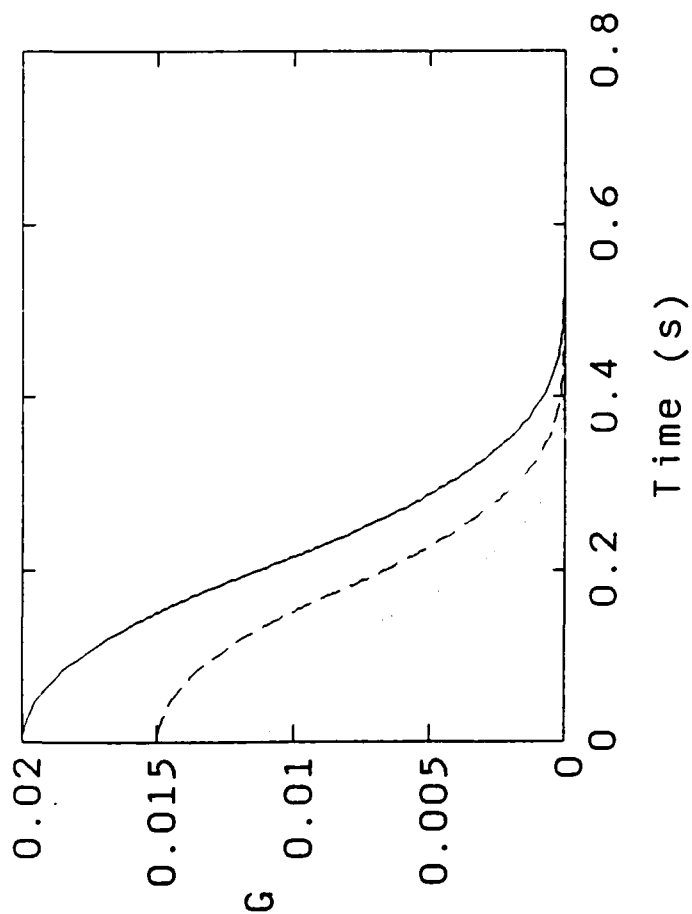
MOD5

SIM51



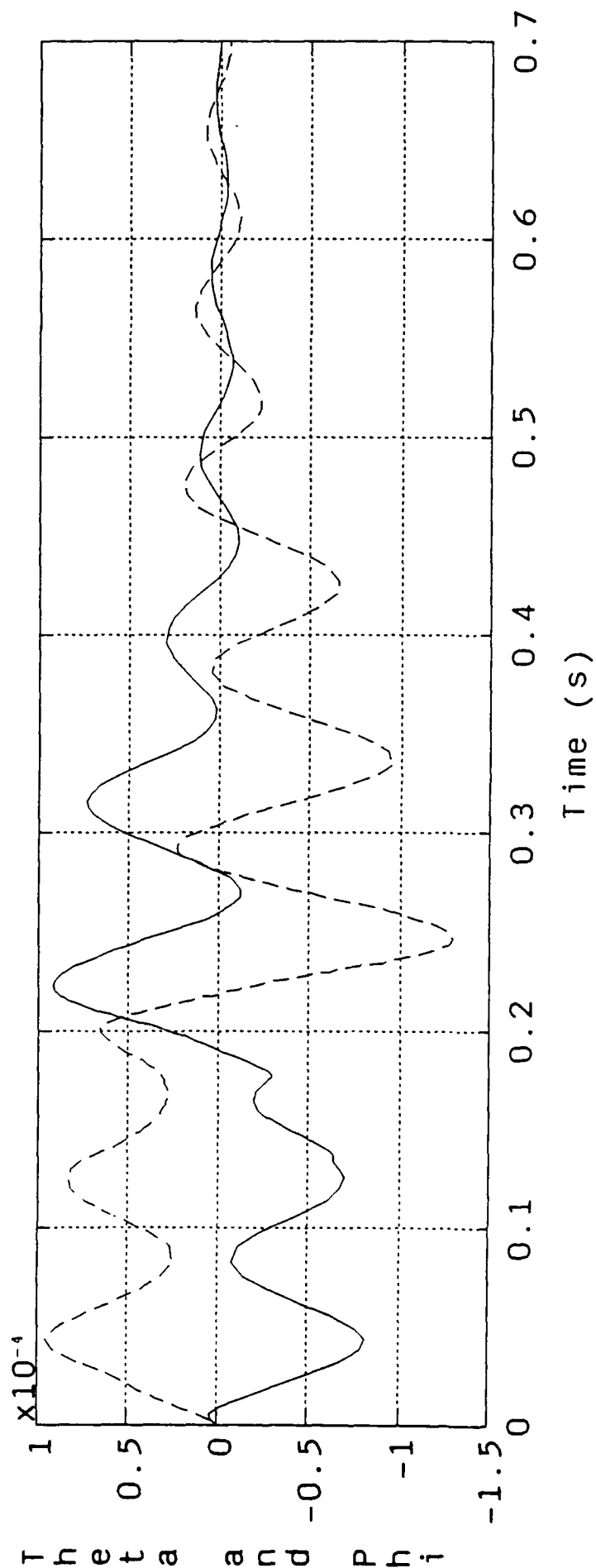
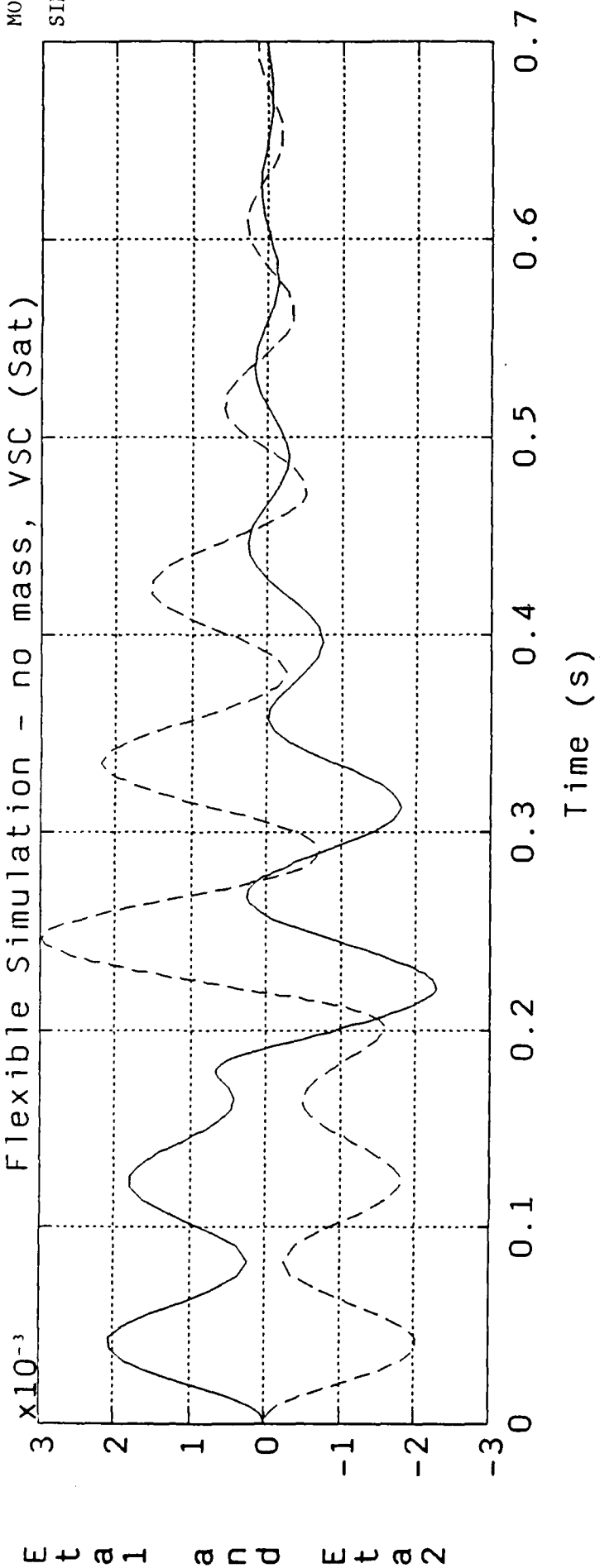


MOD6
SIM61

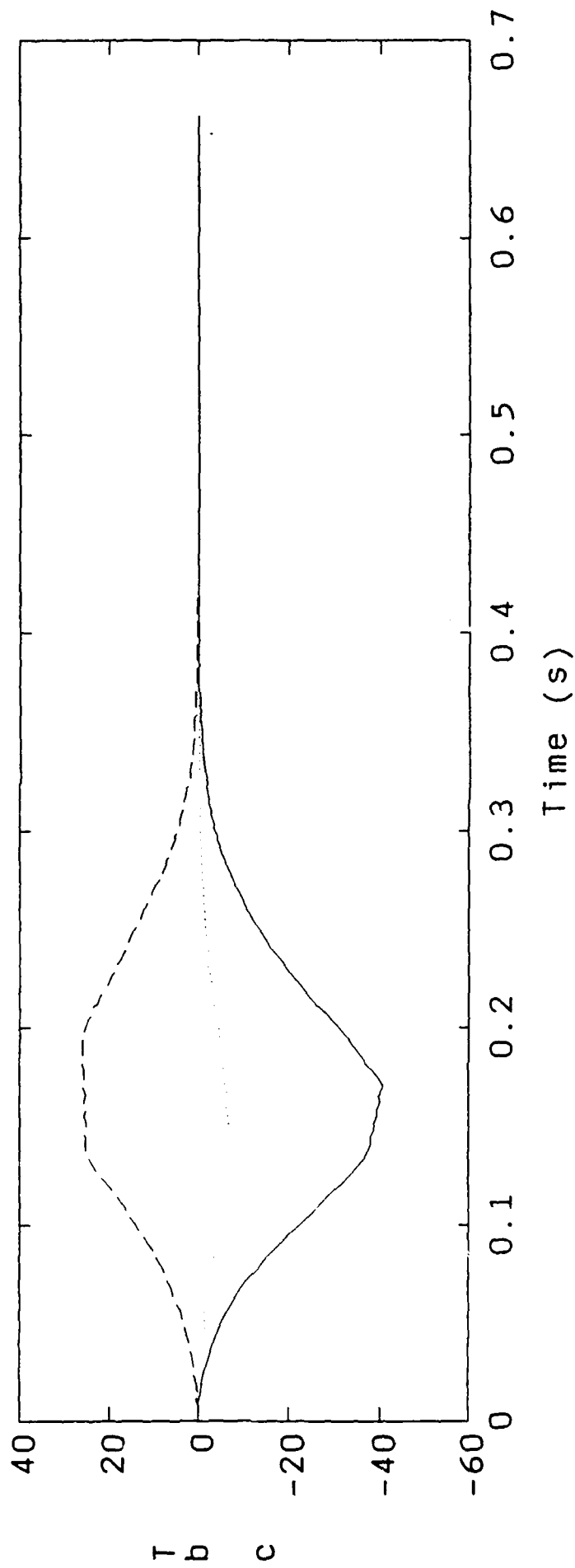
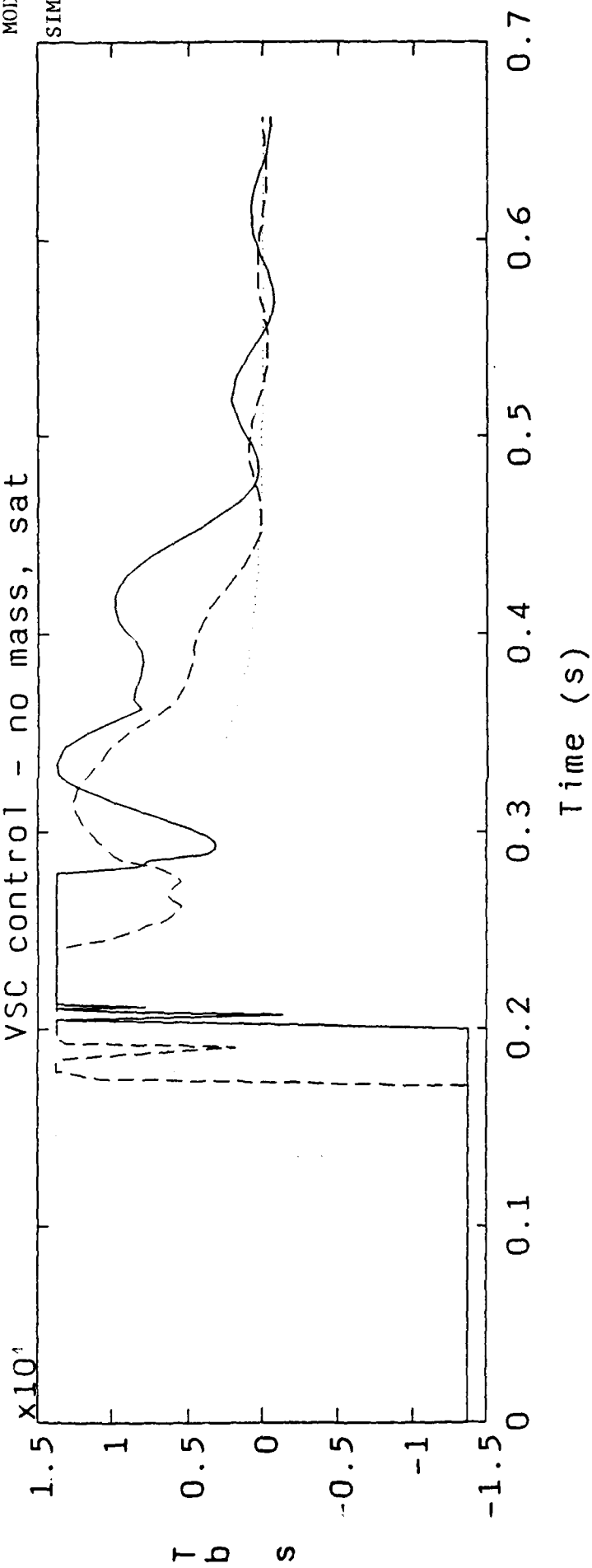


Flexible Simulation - no mass, VSC (Sat)

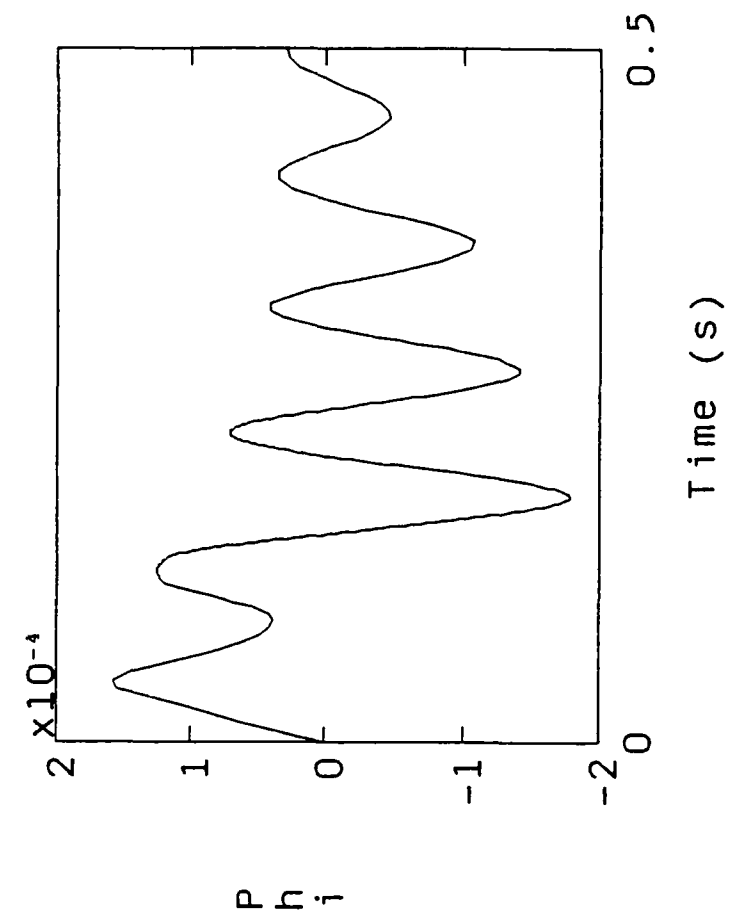
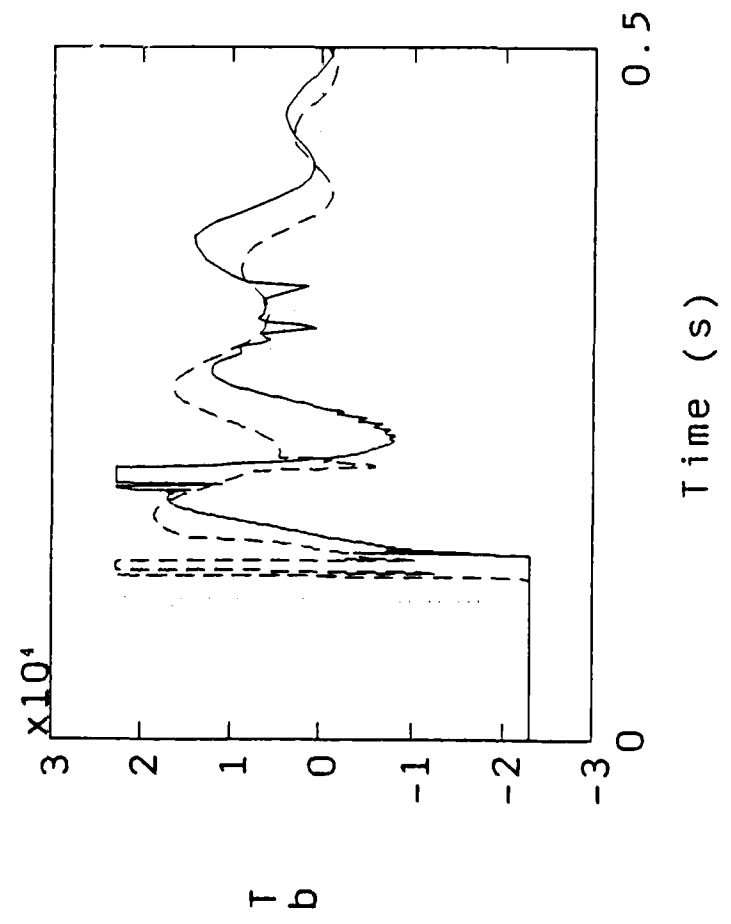
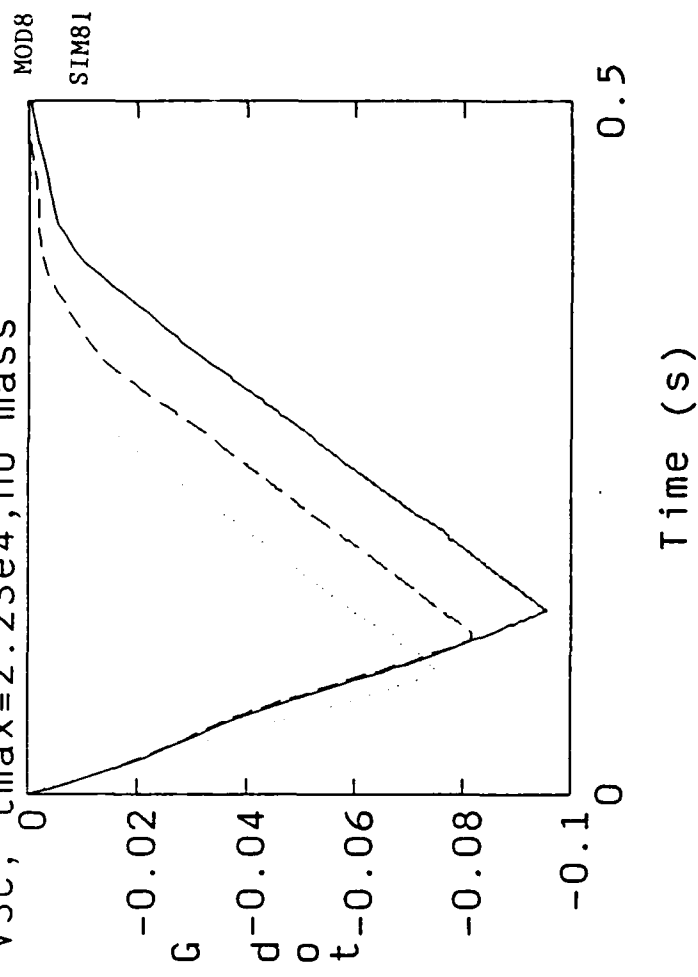
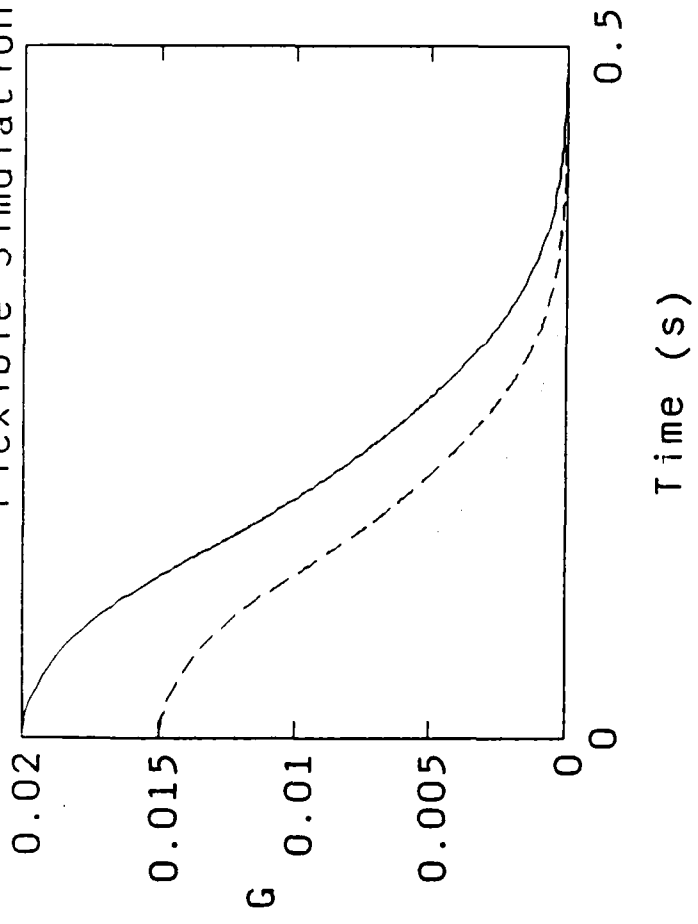
MOD6
SIM61

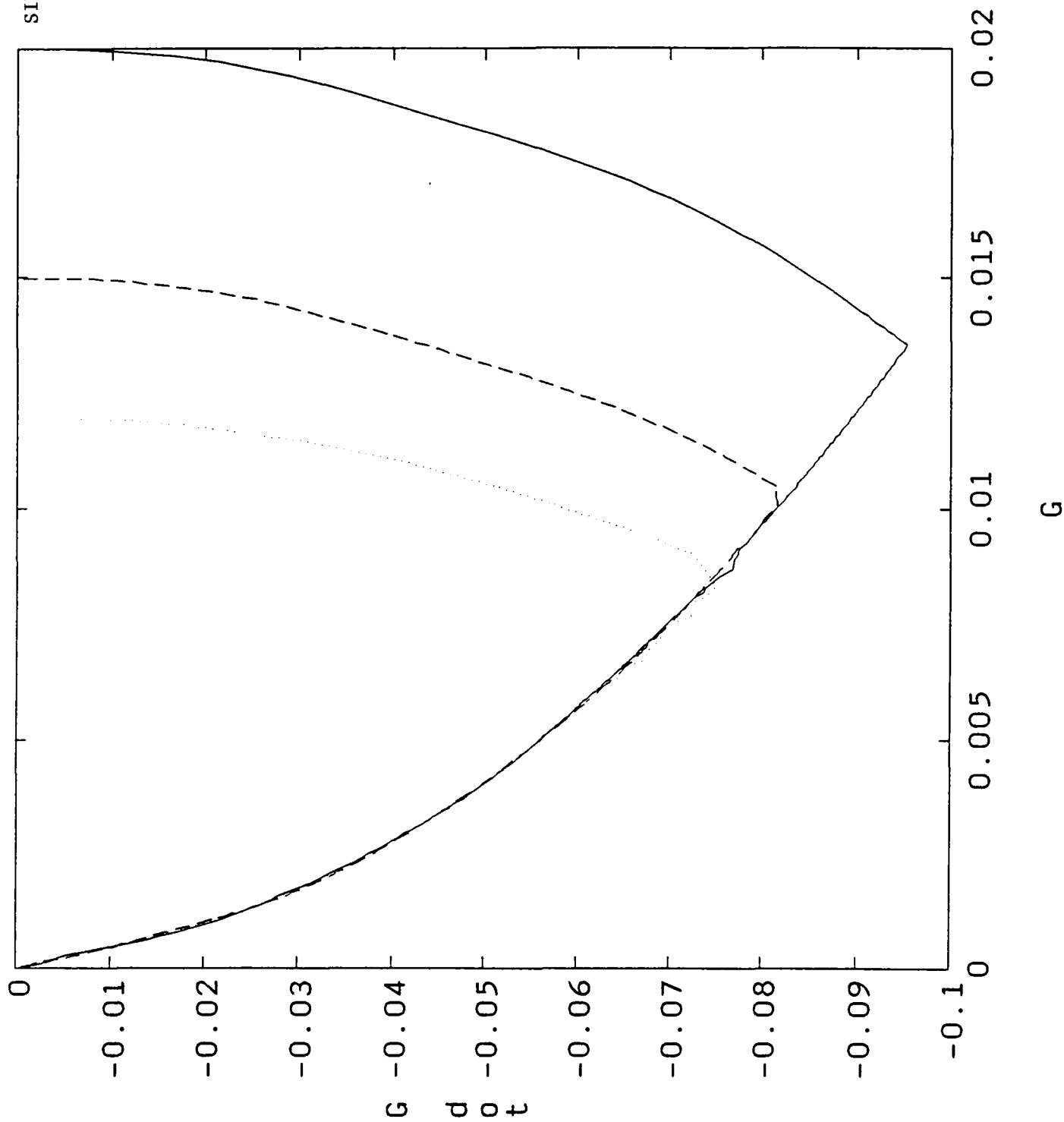


VSC control - no mass, sat



Flexible Simulation - VSC, $t_{max}=2.23e4$, no mass



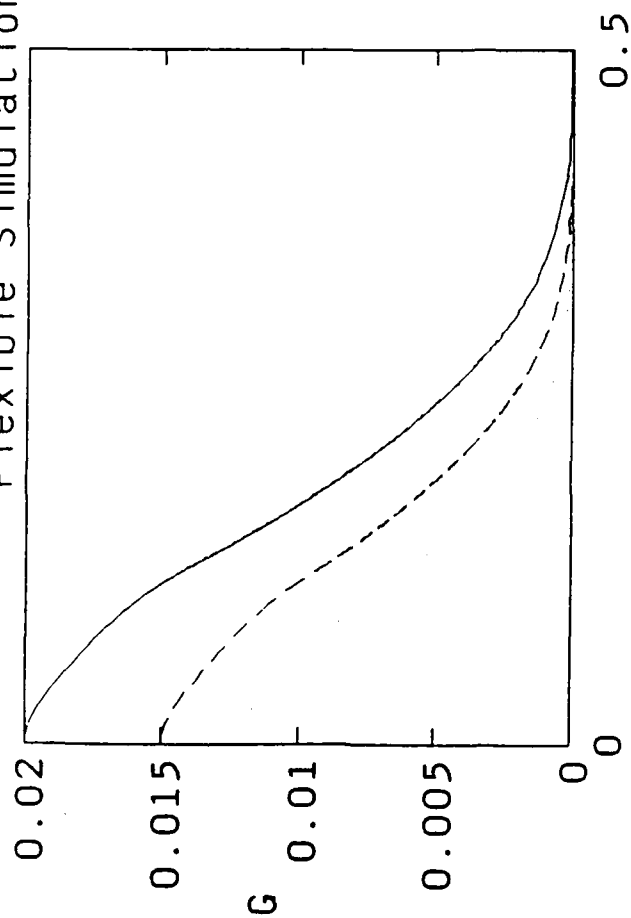


Flexible Simulation - VSC

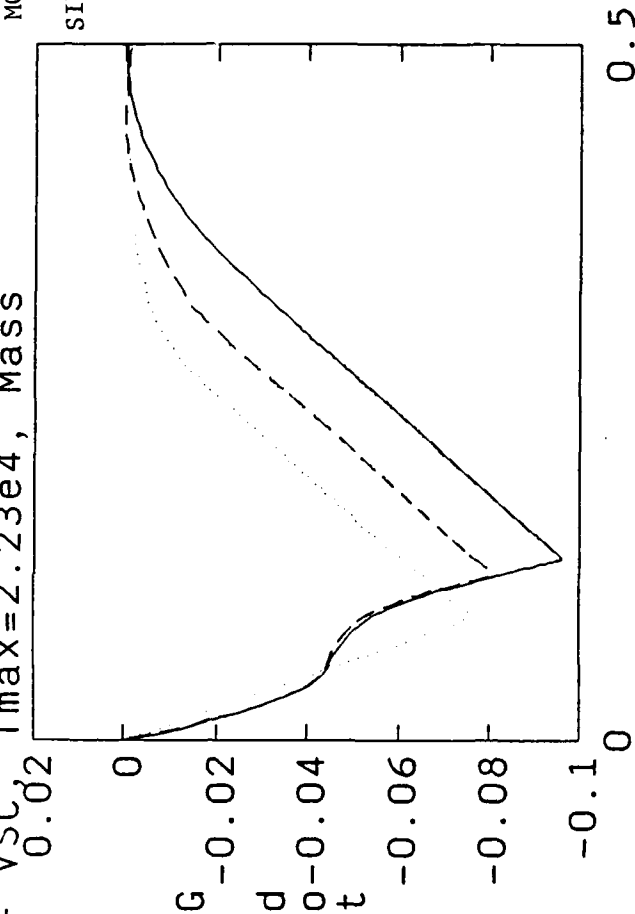
MOD9

Tmax=2.23e4, Mass

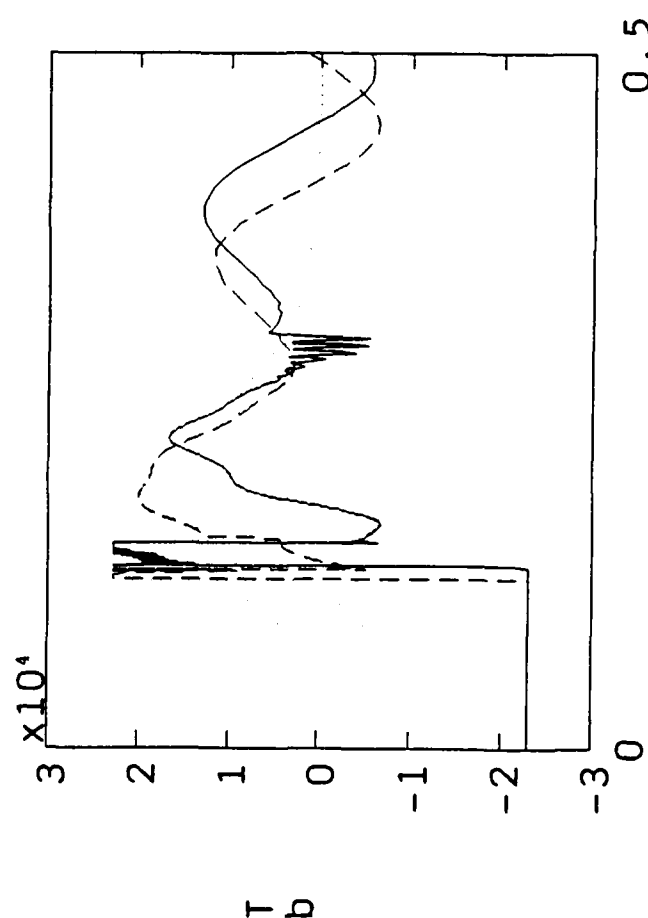
SIM91



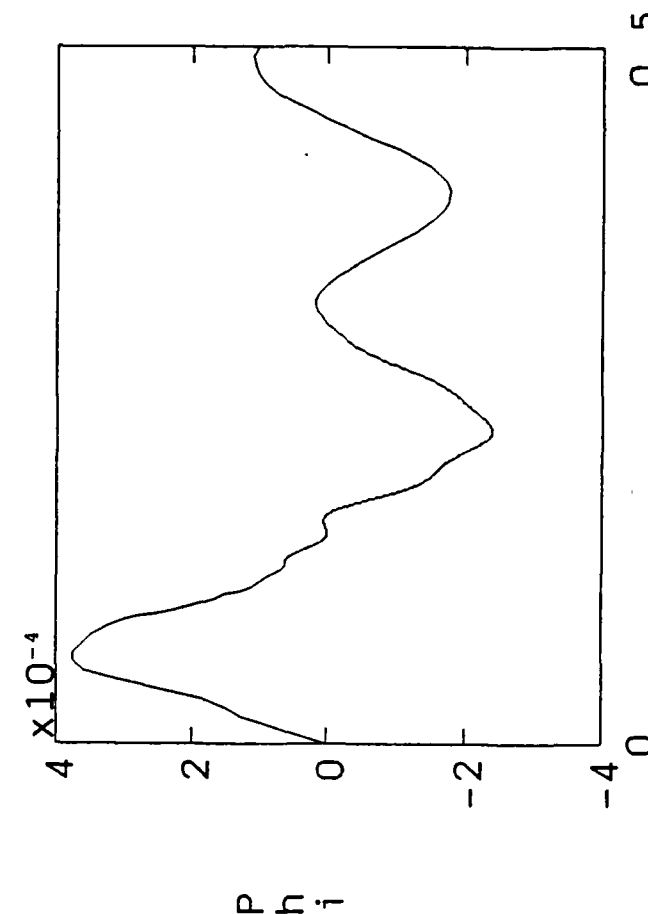
Time (s)



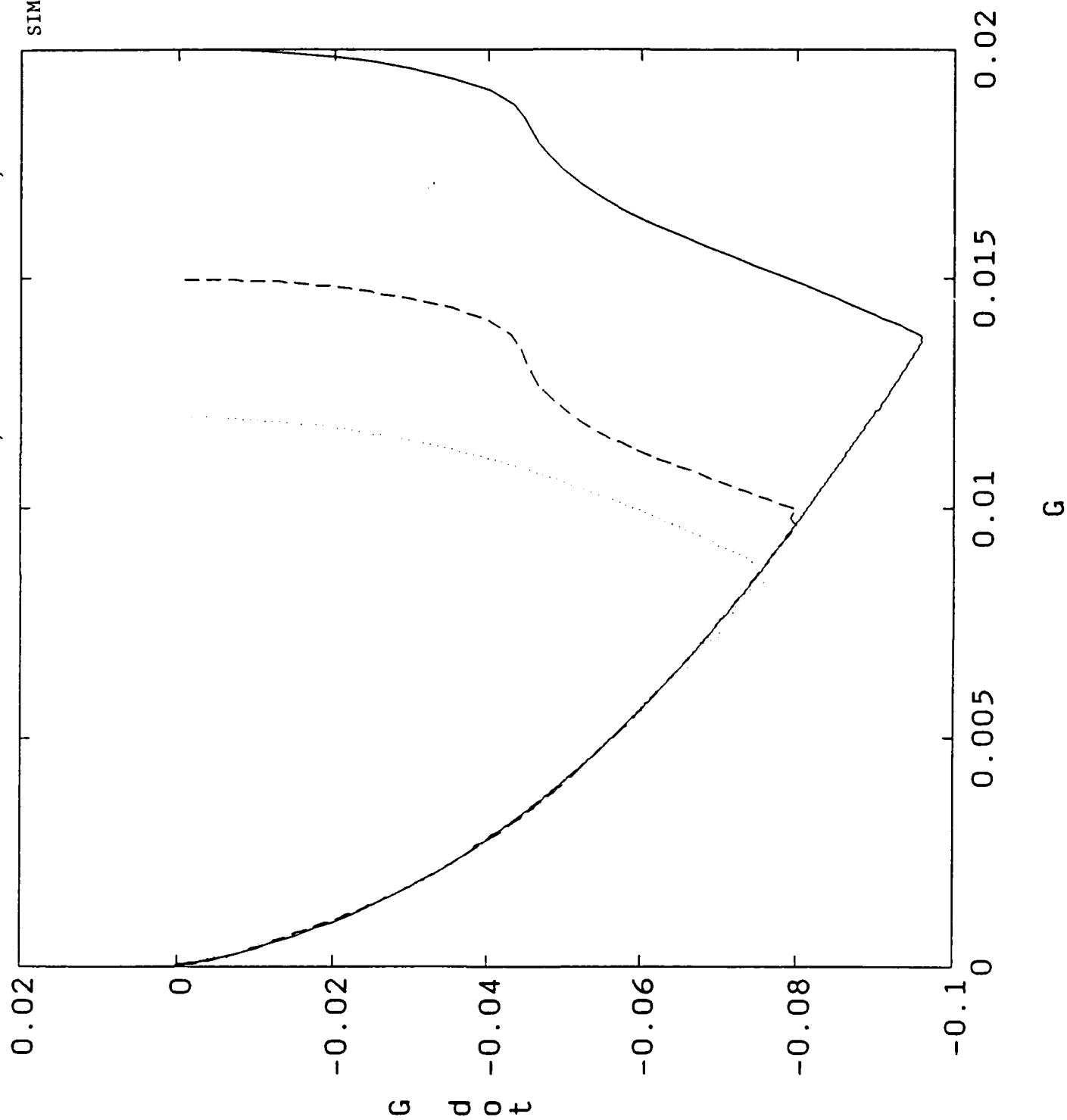
Time (s)



Time (s)



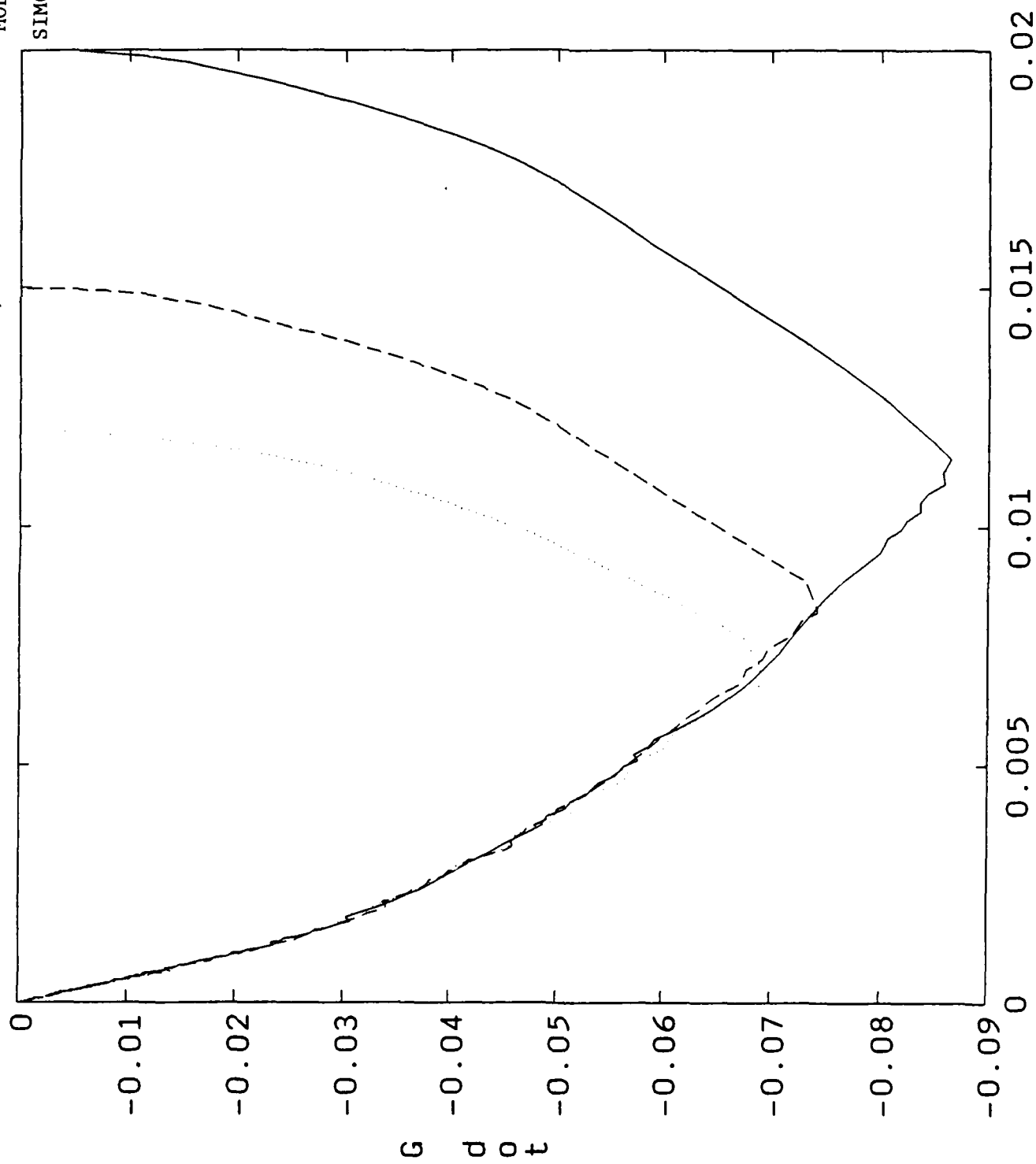
Time (s)



Flexible Simulation - no mass, VSC Ctrl

MOD6

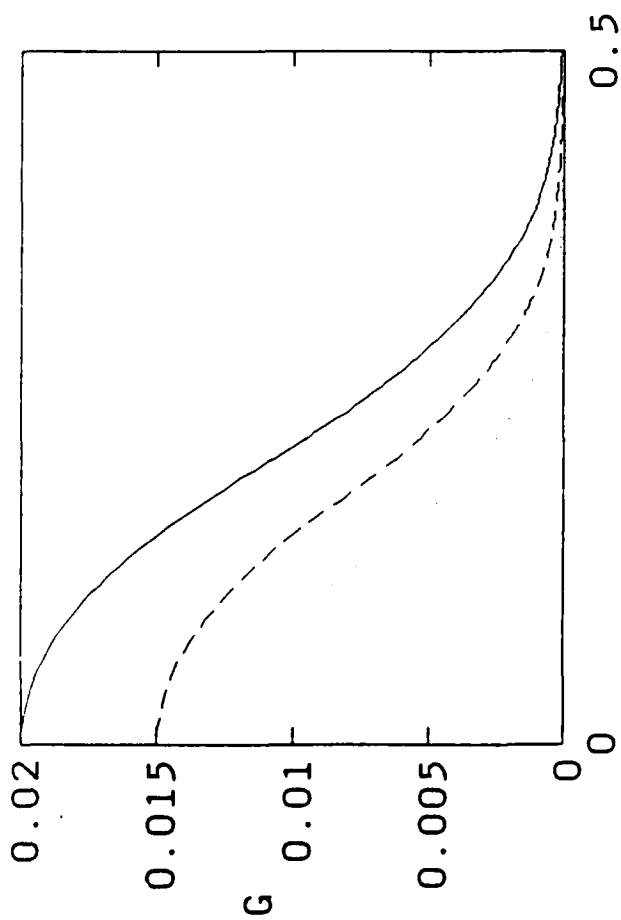
SIM62



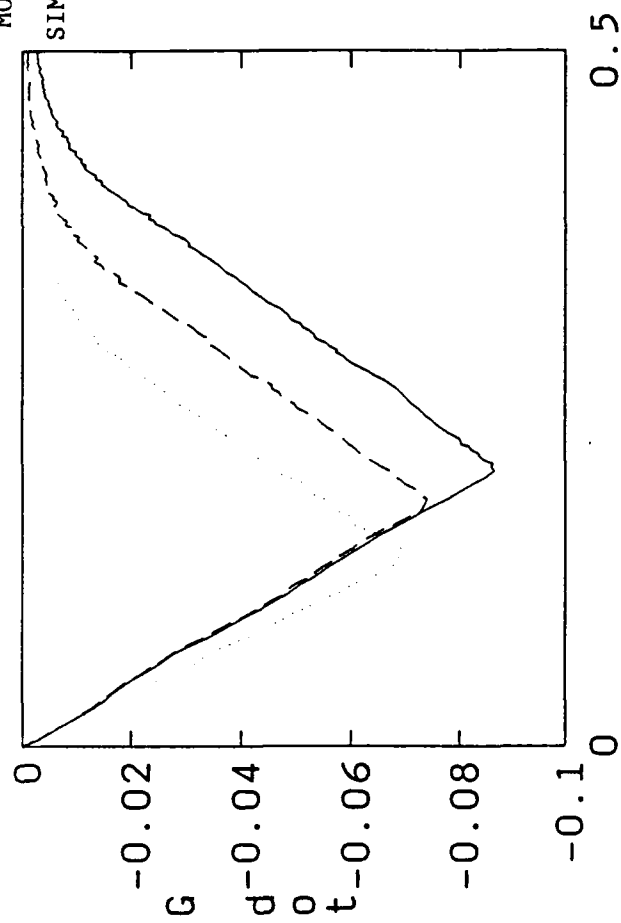
G

MOD6

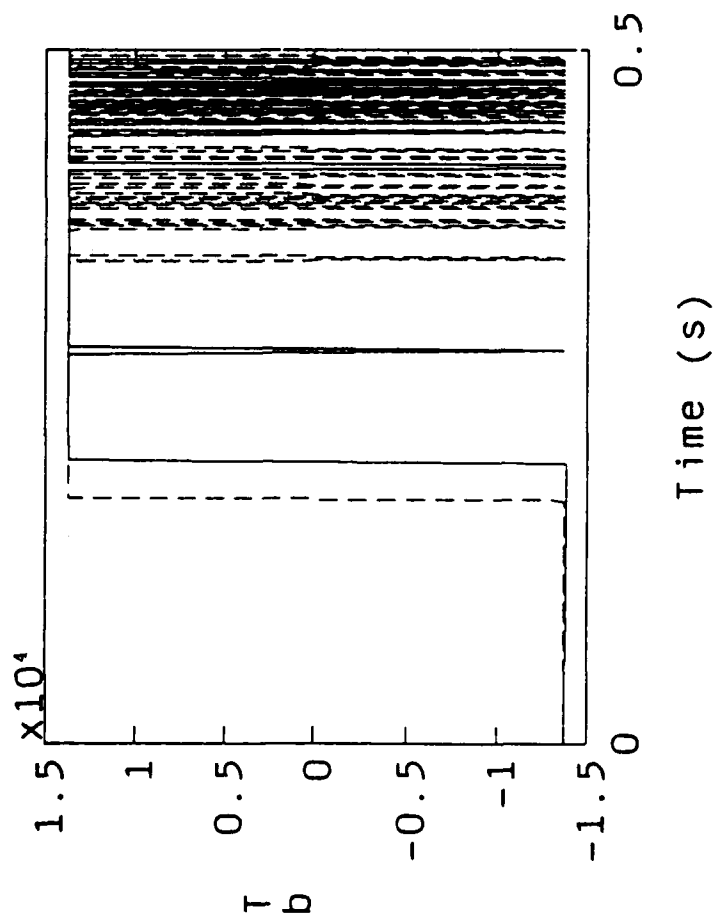
SIM62



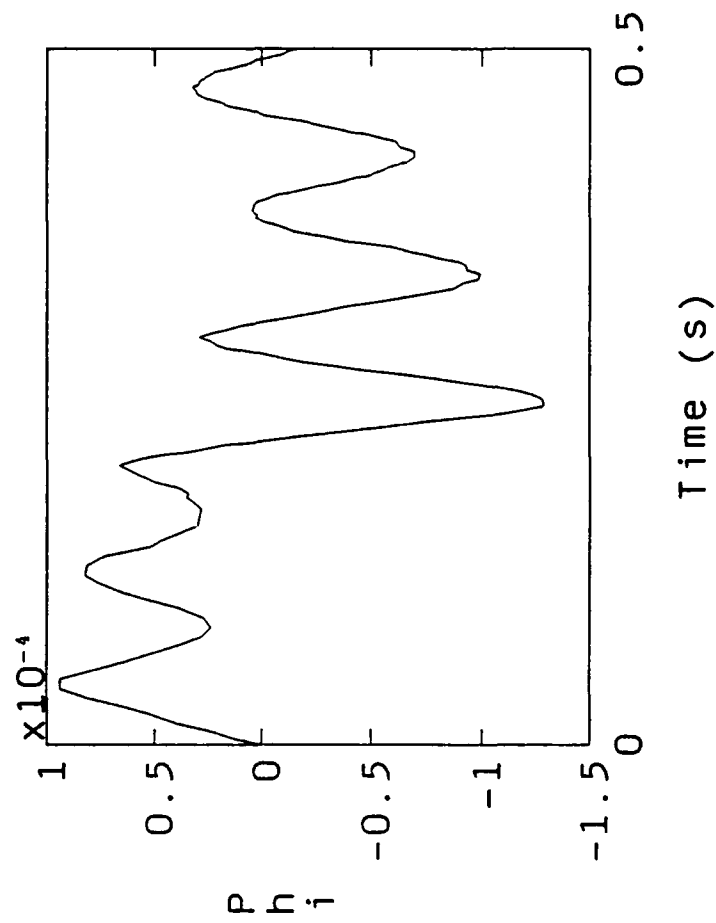
Time (s)



Time (s)



Time (s)



Time (s)

VSc control - no mass sgn

MOD6
SIM62

Time (s)

1.5 x10⁴

1

0.5

0

-0.5

-1

-1.5

0

0.1

0.2

0.3

0.4

0.5

0.6

0.7

T
b
s

Time (s)

1.5 x10⁴

1

0.5

0

-0.5

-1

-1.5

0

0.1

0.2

0.3

0.4

0.5

0.6

0.7

T
b
s

Time (s)

1.5 x10⁴

1

0.5

0

-0.5

-1

-1.5

0

0.1

0.2

0.3

0.4

0.5

0.6

0.7

T
b
s

Time (s)

1.5 x10⁴

1

0.5

0

-0.5

-1

-1.5

0

0.1

0.2

0.3

0.4

0.5

0.6

0.7

T
b
s

Time (s)

1.5 x10⁴

1

0.5

0

-0.5

-1

-1.5

0

0.1

0.2

0.3

0.4

0.5

0.6

0.7

T
b
s

Time (s)

1.5 x10⁴

1

0.5

0

-0.5

-1

-1.5

0

0.1

0.2

0.3

0.4

0.5

0.6

0.7

T
b
s

Time (s)

1.5 x10⁴

1

0.5

0

-0.5

-1

-1.5

0

0.1

0.2

0.3

0.4

0.5

0.6

0.7

T
b
s

Time (s)

1.5 x10⁴

1

0.5

0

-0.5

-1

-1.5

0

0.1

0.2

0.3

0.4

0.5

0.6

0.7

T
b
s

Time (s)

1.5 x10⁴

1

0.5

0

-0.5

-1

-1.5

0

0.1

0.2

0.3

0.4

0.5

0.6

0.7

T
b
s

Time (s)

1.5 x10⁴

1

0.5

0

-0.5

-1

-1.5

0

0.1

0.2

0.3

0.4

0.5

0.6

0.7

T
b
s

Time (s)

1.5 x10⁴

1

0.5

0

-0.5

-1

-1.5

0

0.1

0.2

0.3

0.4

0.5

0.6

0.7

T
b
s

Time (s)

1.5 x10⁴

1

0.5

0

-0.5

-1

-1.5

0

0.1

0.2

0.3

0.4

0.5

0.6

0.7

T
b
s

Time (s)

1.5 x10⁴

1

0.5

0

-0.5

-1

-1.5

0

0.1

0.2

0.3

0.4

0.5

0.6

0.7

T
b
s

Time (s)

1.5 x10⁴

1

0.5

0

-0.5

-1

-1.5

0

0.1

0.2

0.3

0.4

0.5

0.6

0.7

T
b
s

Time (s)

1.5 x10⁴

1

0.5

0

-0.5

-1

-1.5

0

0.1

0.2

0.3

0.4

0.5

0.6

0.7

T
b
s

Time (s)

1.5 x10⁴

1

0.5

0

-0.5

-1

-1.5

0

0.1

0.2

0.3

0.4

0.5

0.6

0.7

T
b
s

Time (s)

1.5 x10⁴

1

0.5

0

-0.5

-1

-1.5

0

0.1

0.2

0.3

0.4

0.5

0.6

0.7

T
b
s

Time (s)

1.5 x10⁴

1

0.5

0

-0.5

-1

-1.5

0

0.1

0.2

0.3

0.4

0.5

0.6

0.7

T
b
s

Time (s)

1.5 x10⁴

1

0.5

0

-0.5

-1

-1.5

0

0.1

0.2

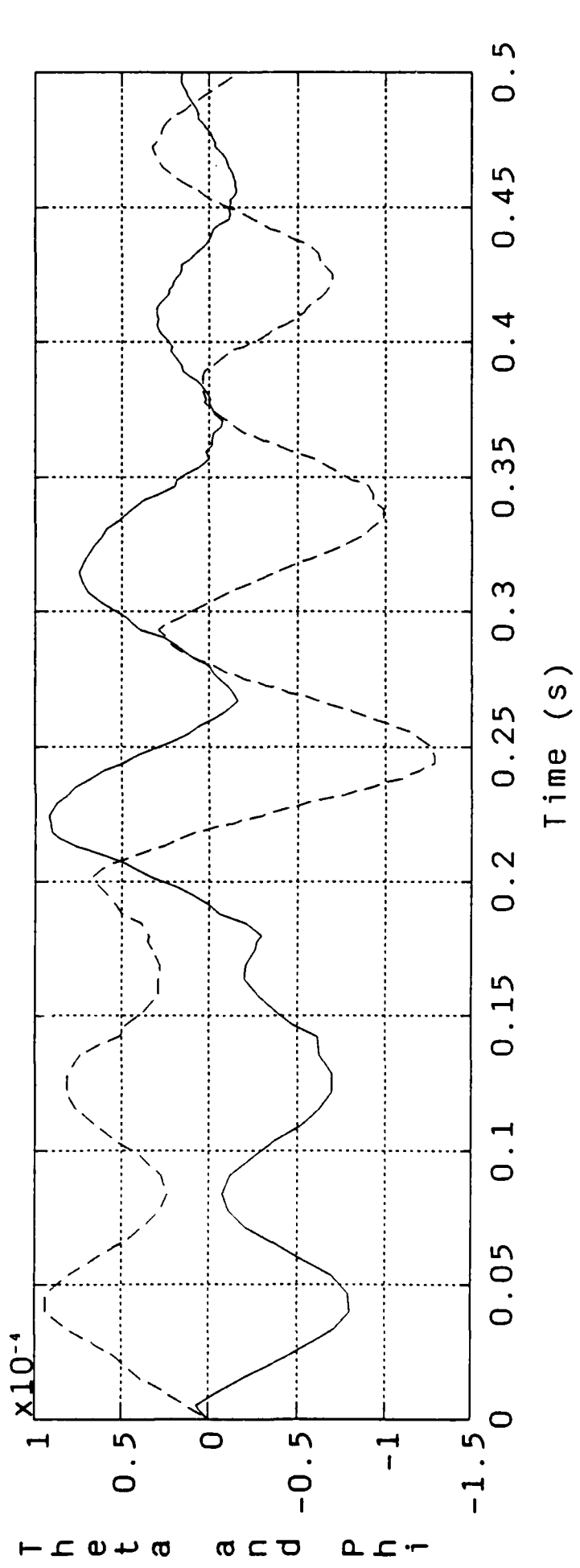
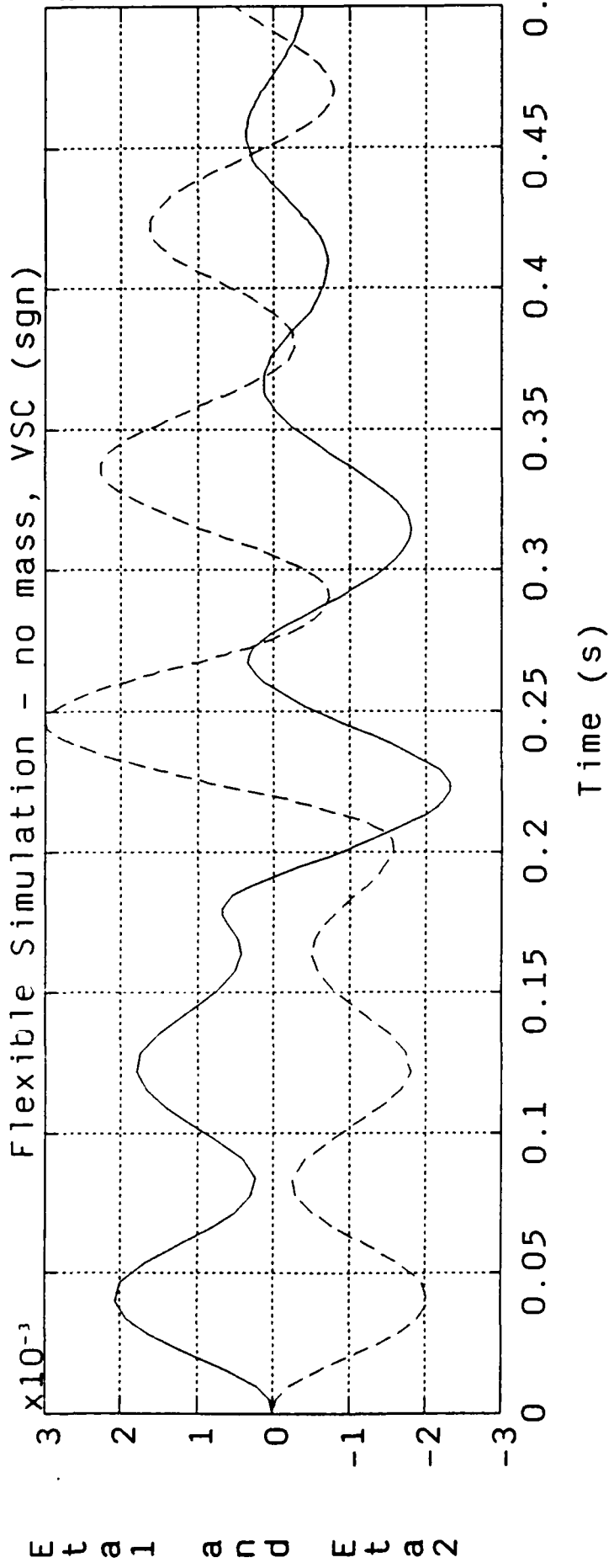
0.3

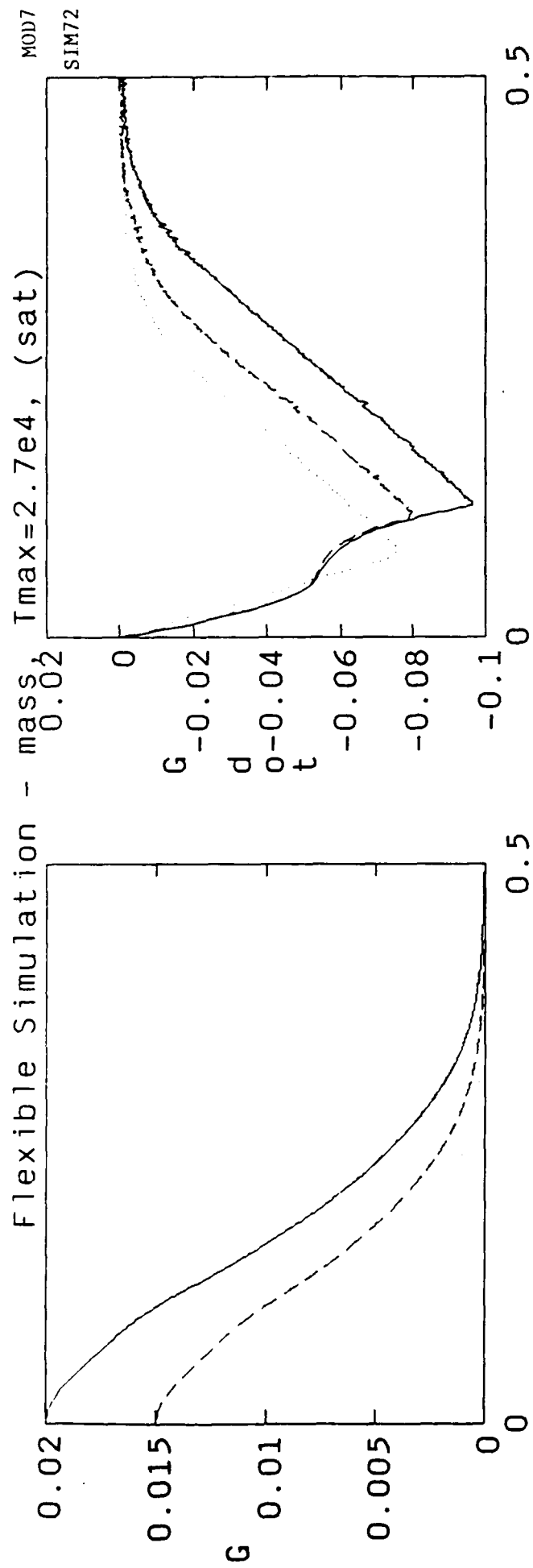
0.4

0.5

0.6

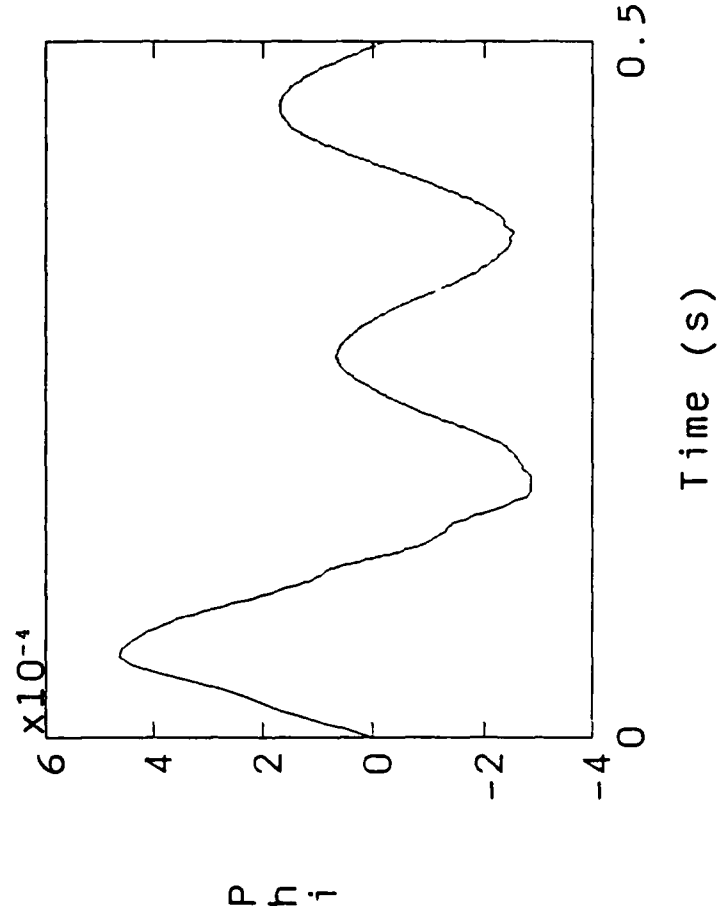
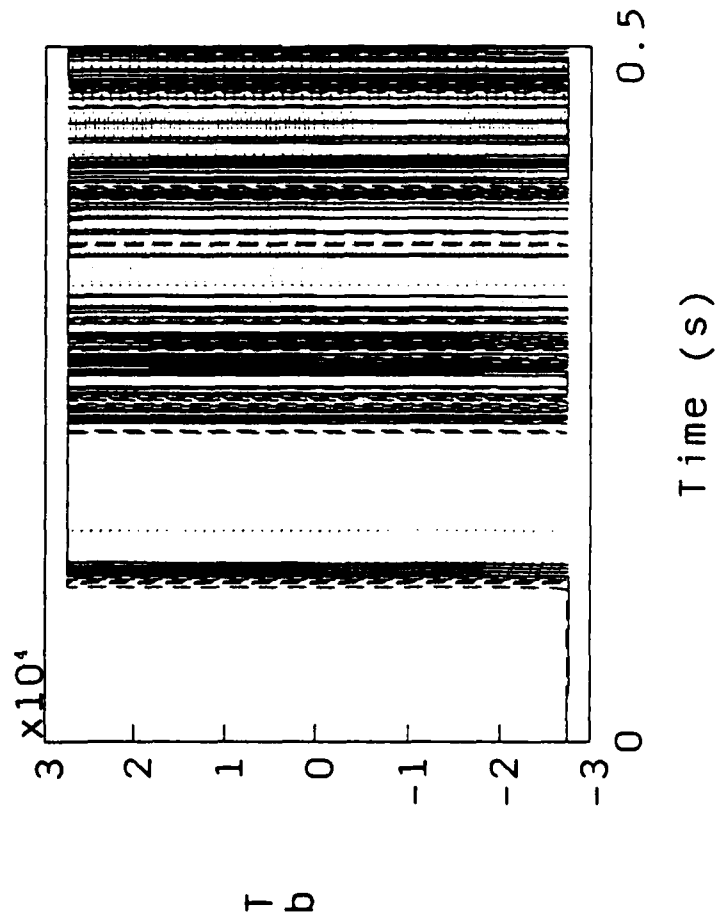
Flexible Simulation - no mass, VSC (sgn)





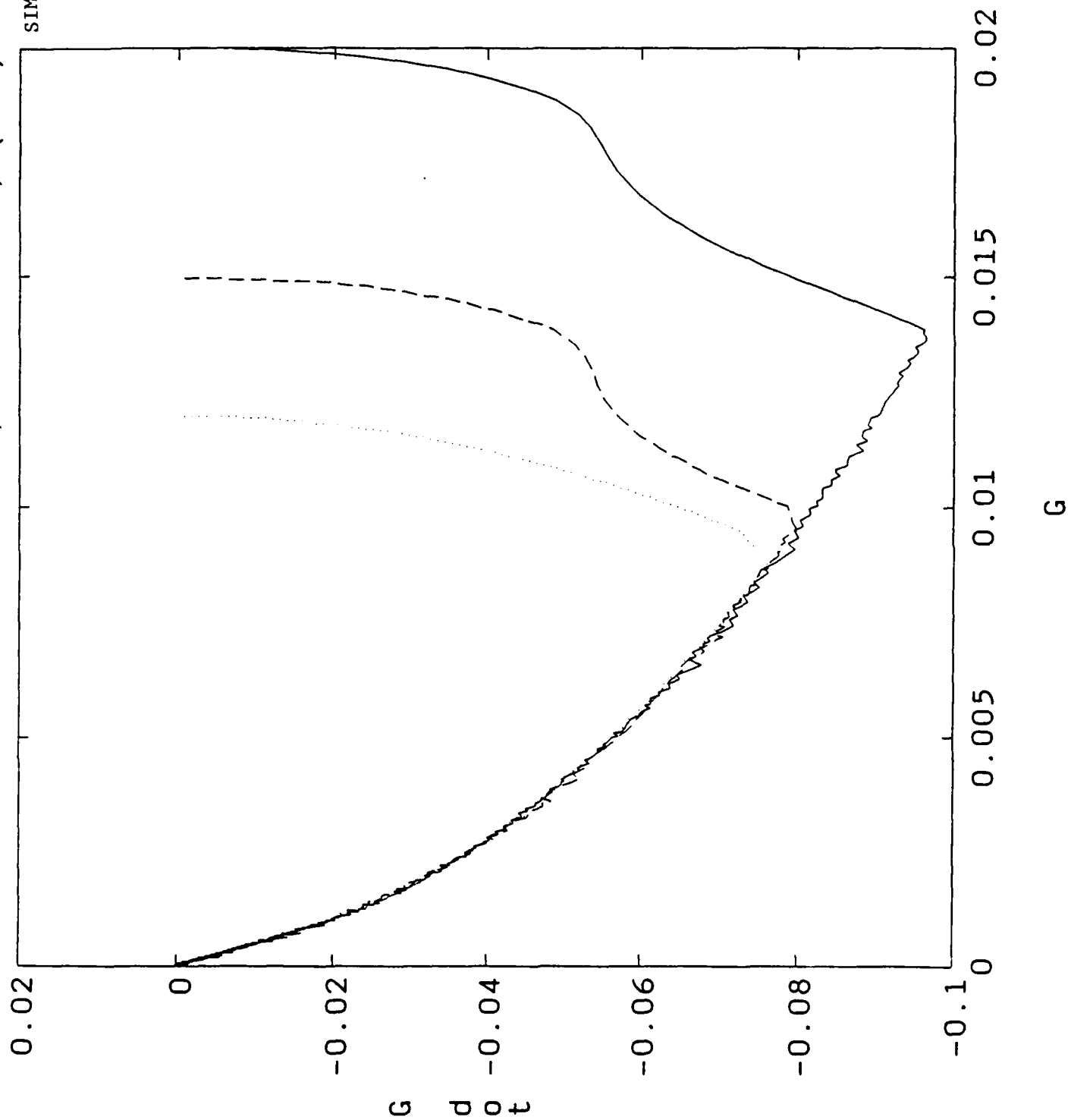
Time (s)

Time (s)



Time (s)

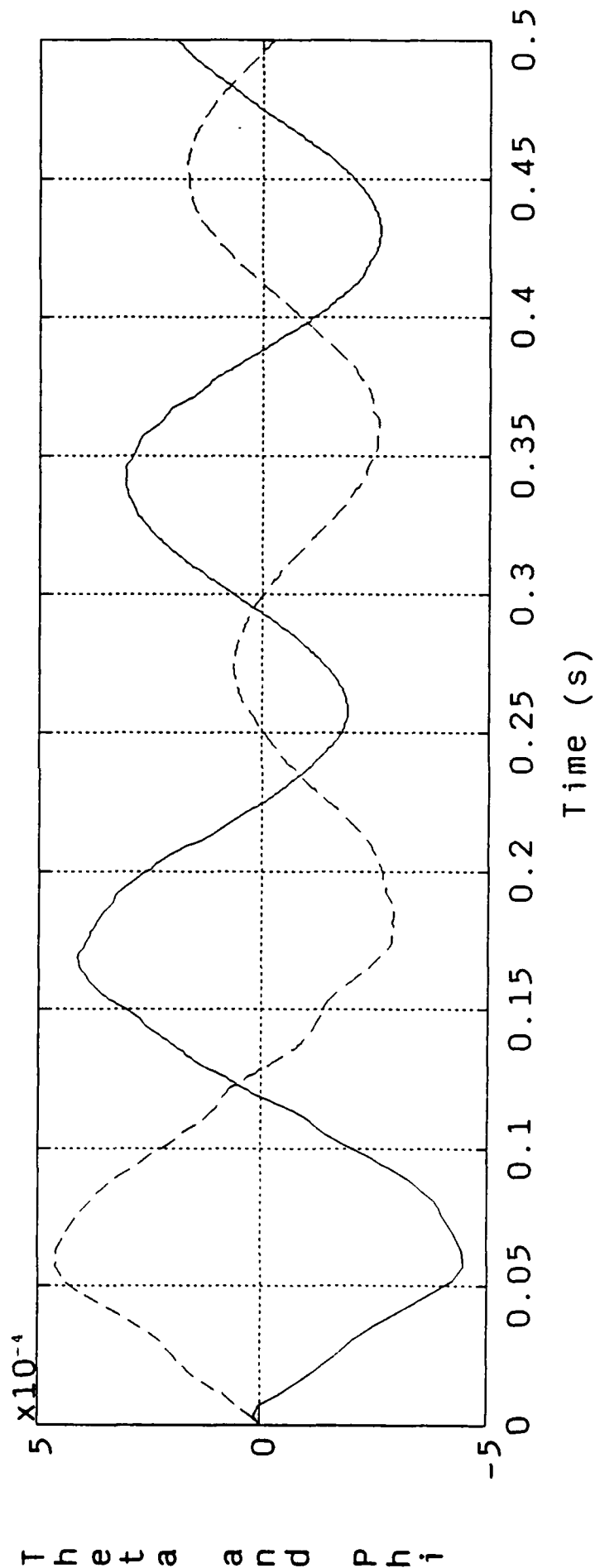
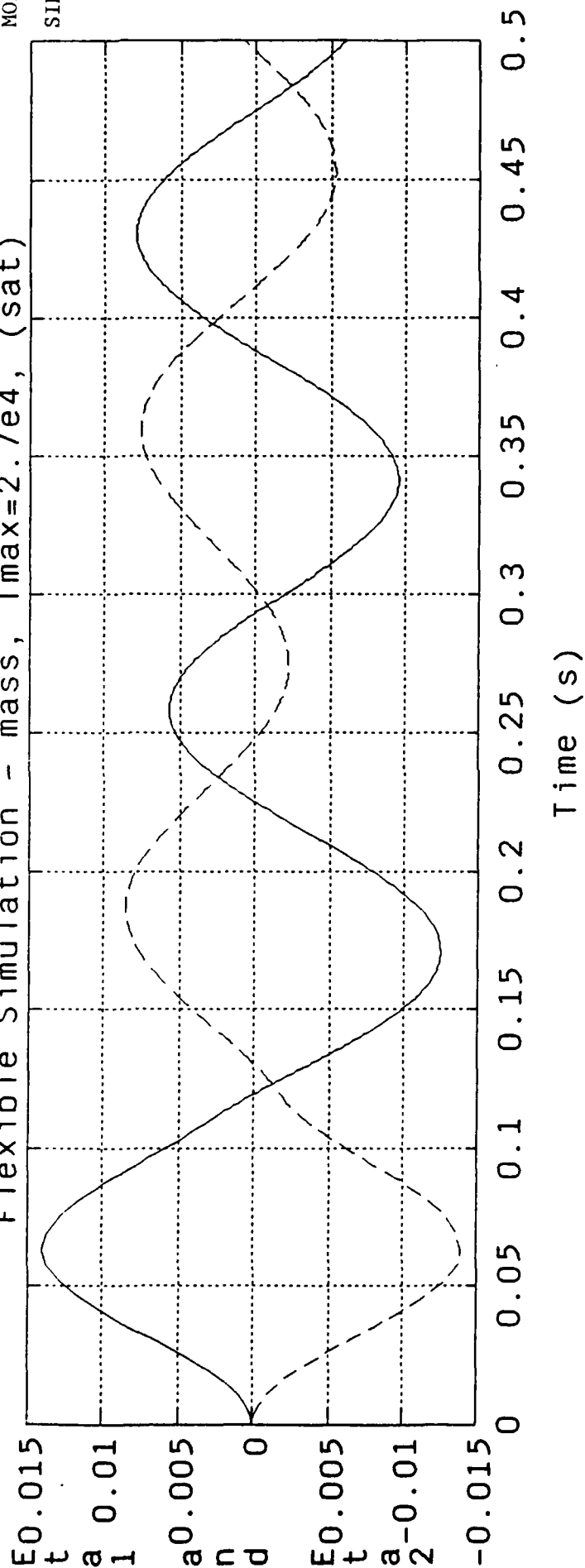
Time (s)



Flexible Simulation - mass, T_{max}=2.7e4, (sat)

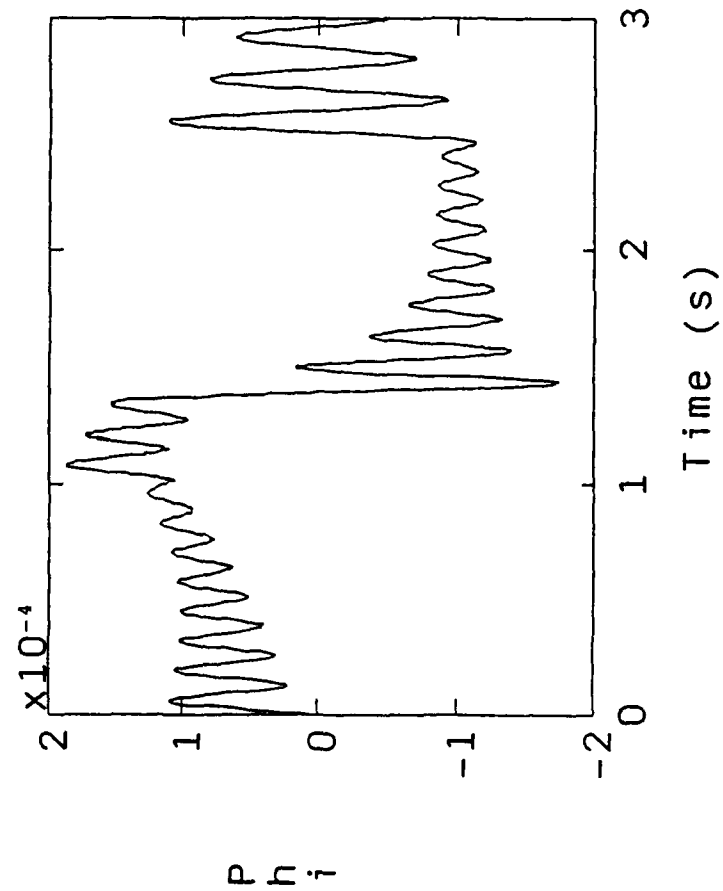
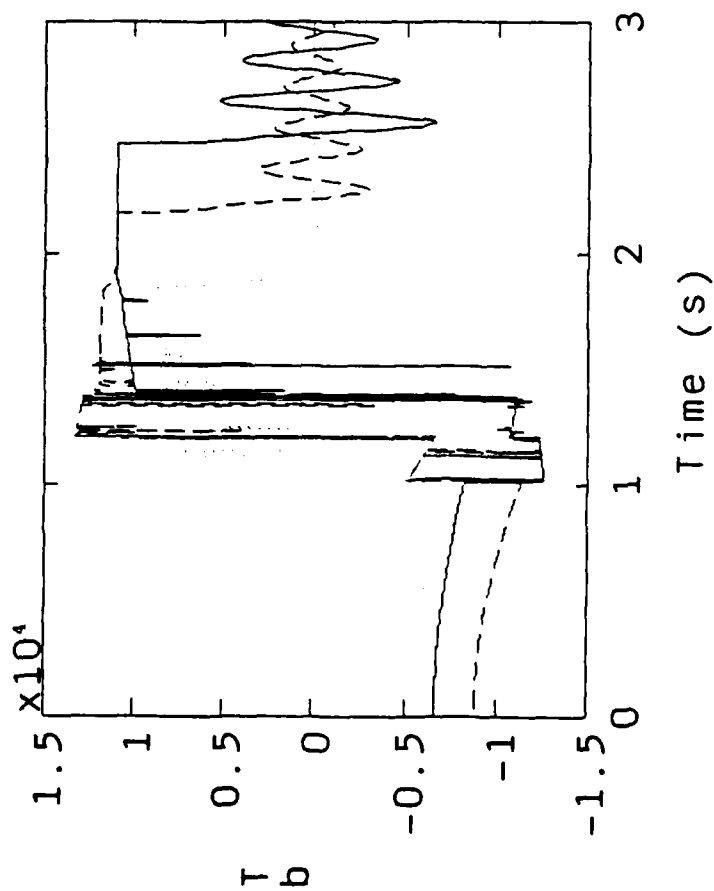
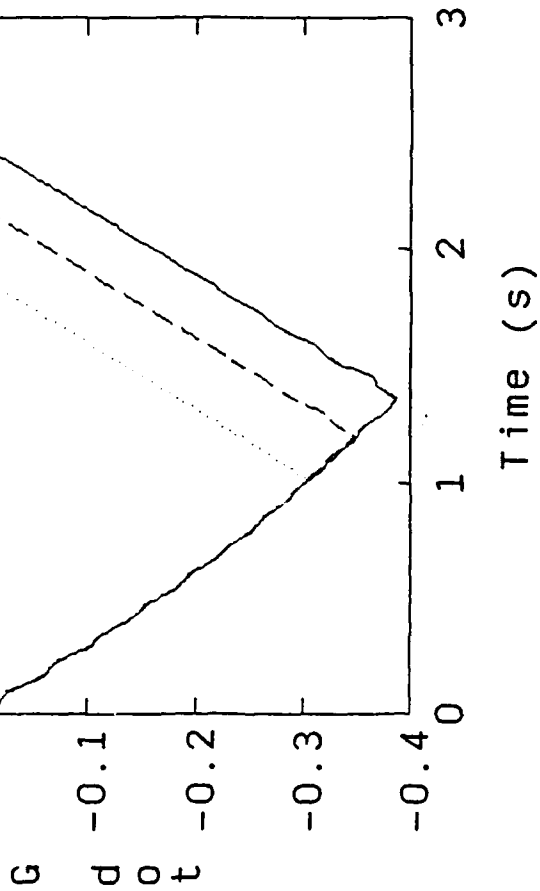
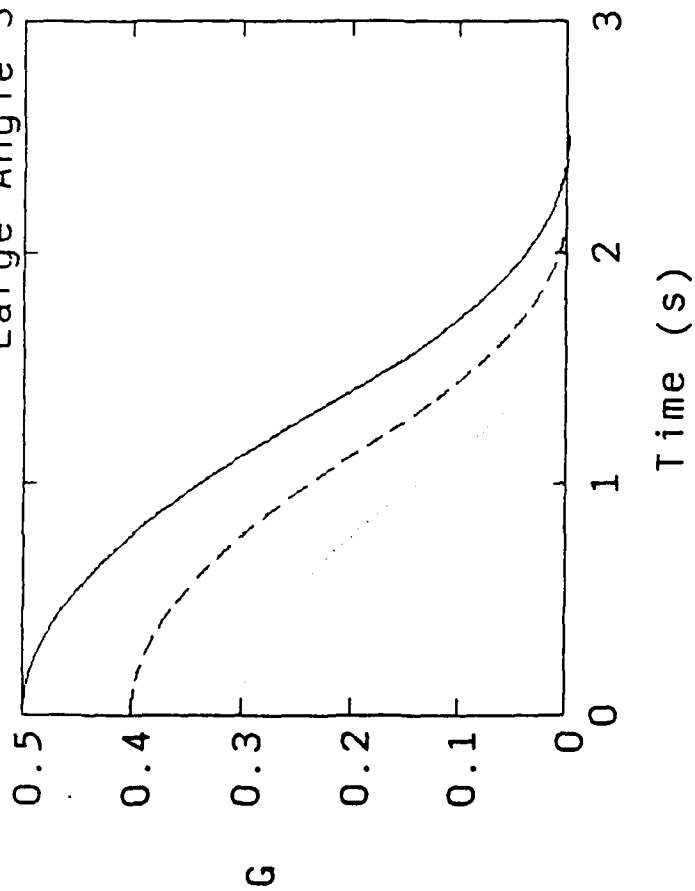
MOD7

SIM72



Large Angle Slew - mass 190 kg, r=3

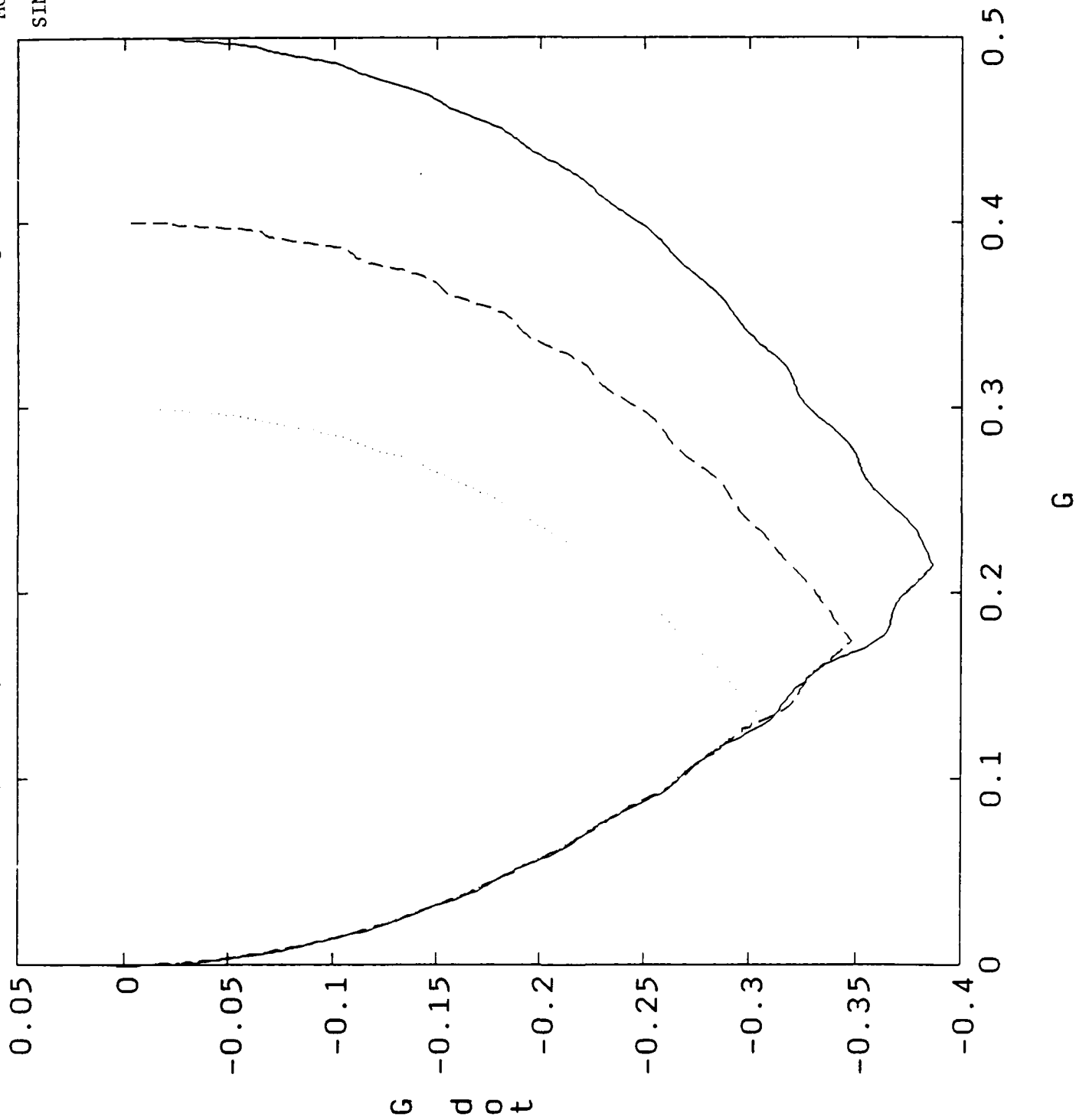
MOD1
SIM15



Large Angle Slew - mass 190 kg, $r=3$

MOD1

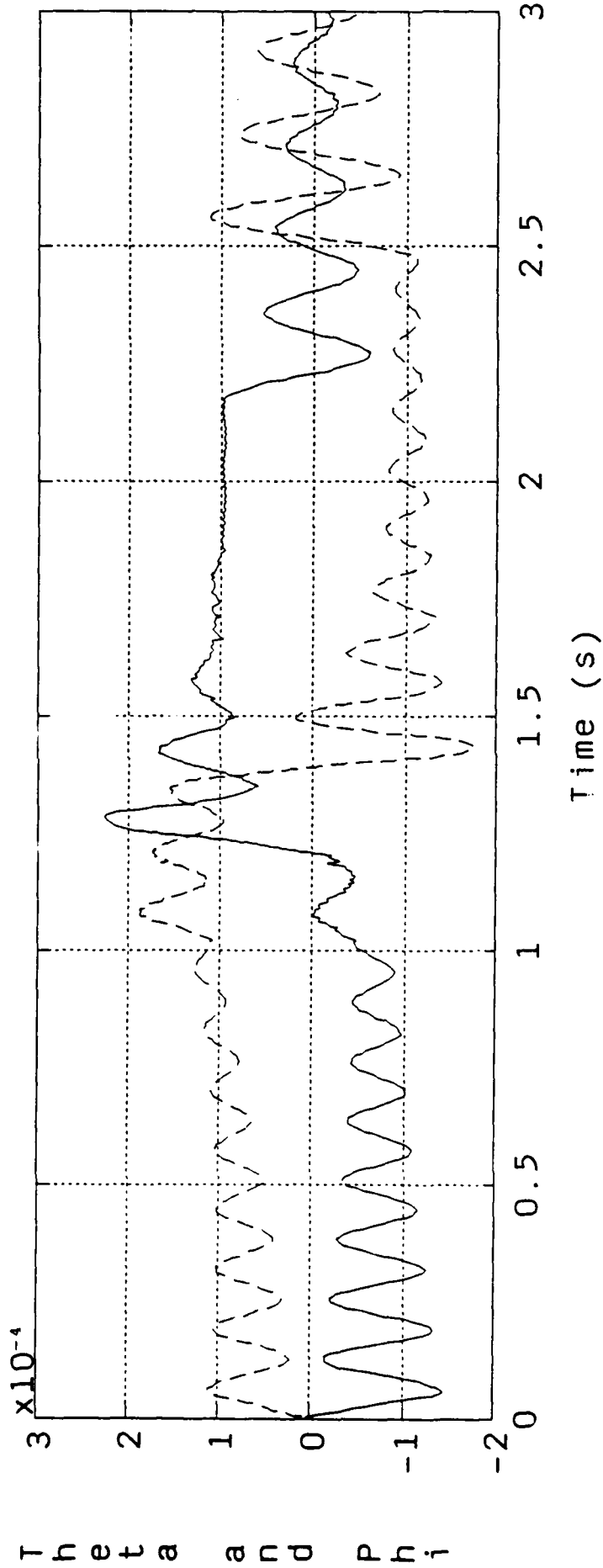
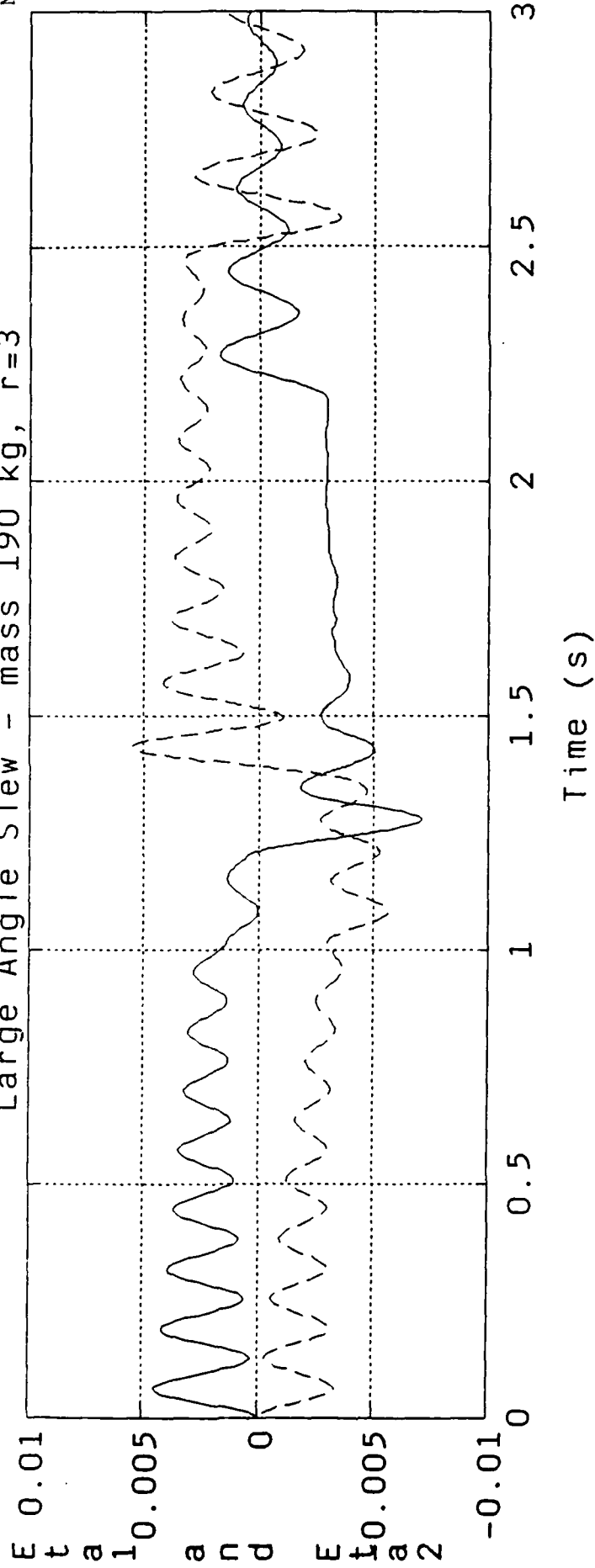
SIM15



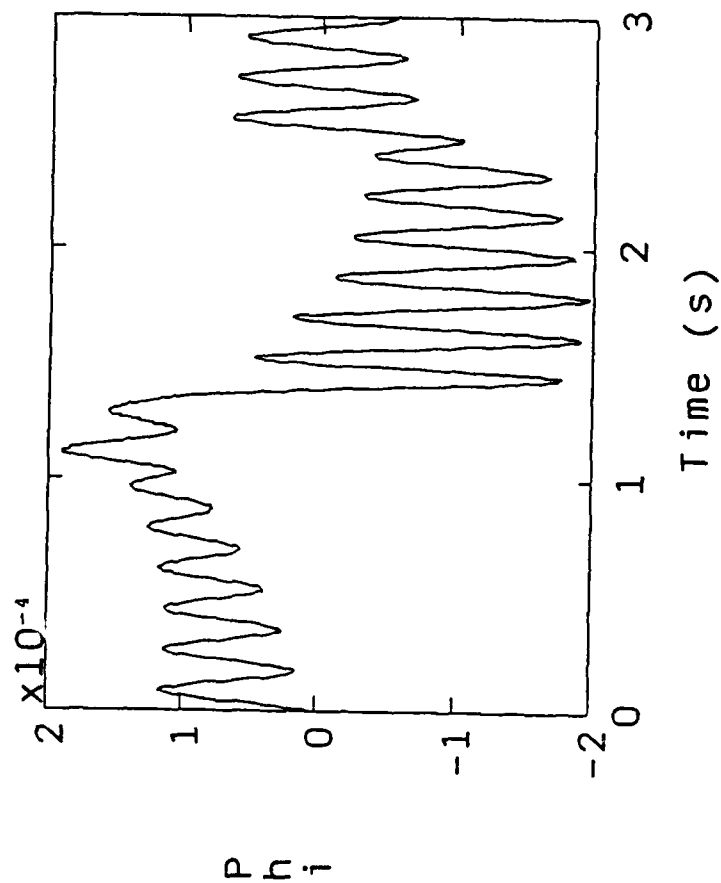
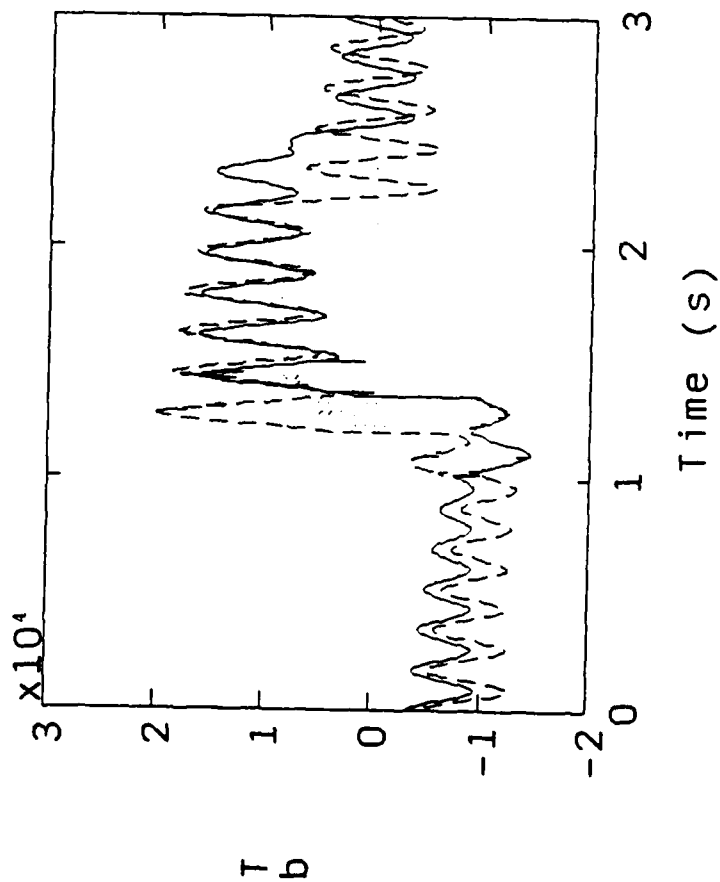
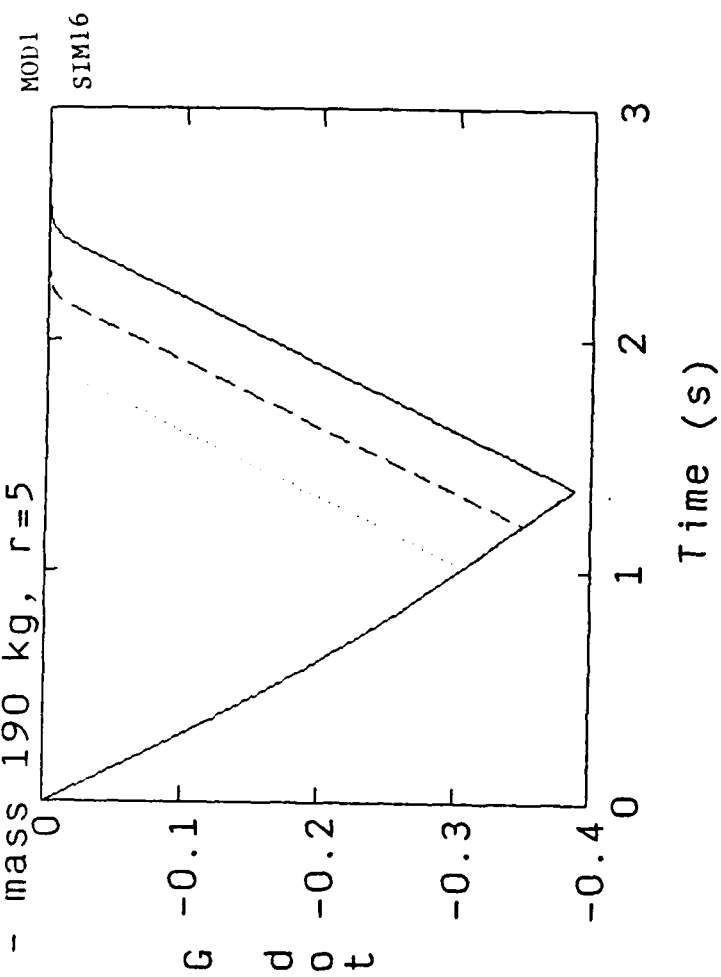
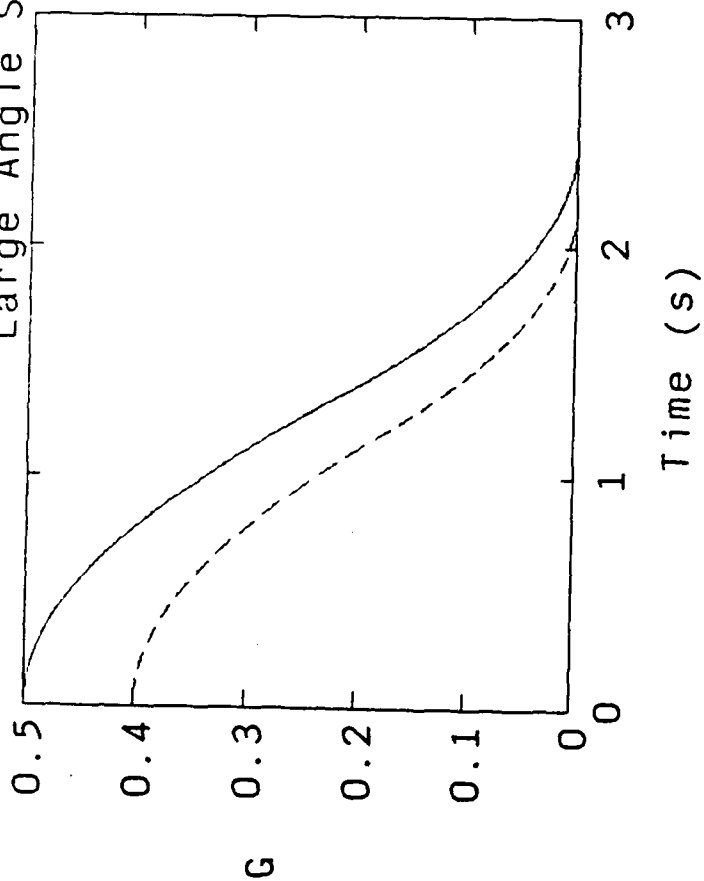
Large Angle Slew - mass 190 kg, r=3

MOD1

SIM15



Large Angle Slew - mass 190 kg, r=5

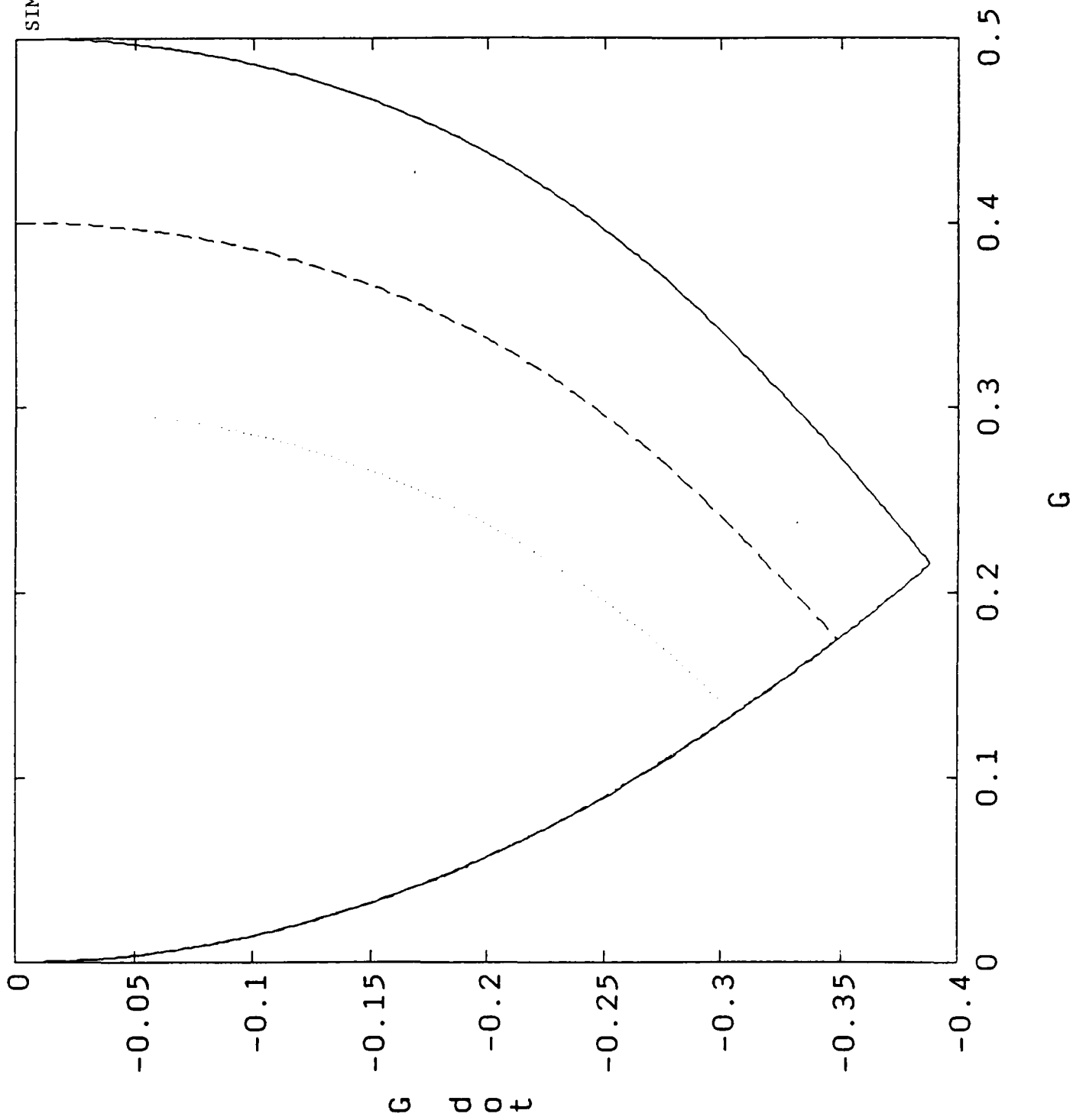


MOD1
SIM16

Large Angle Slew - mass 190 kg, $r=5$

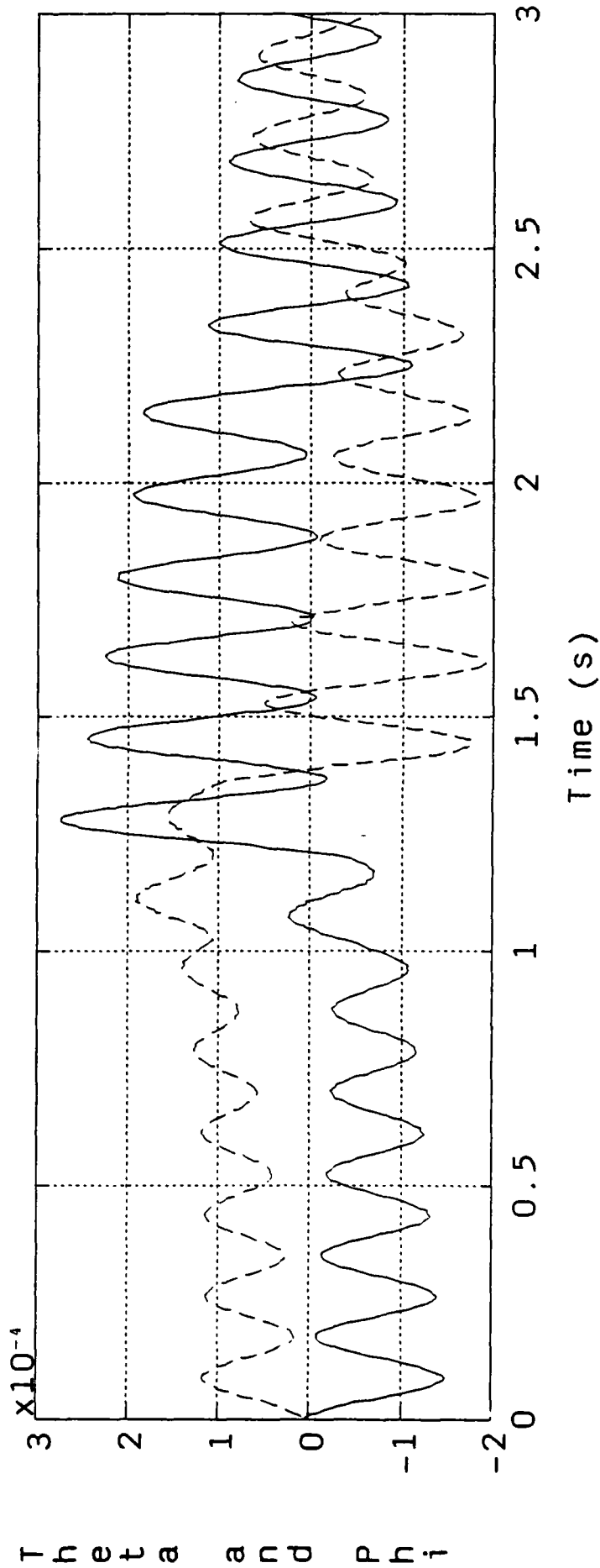
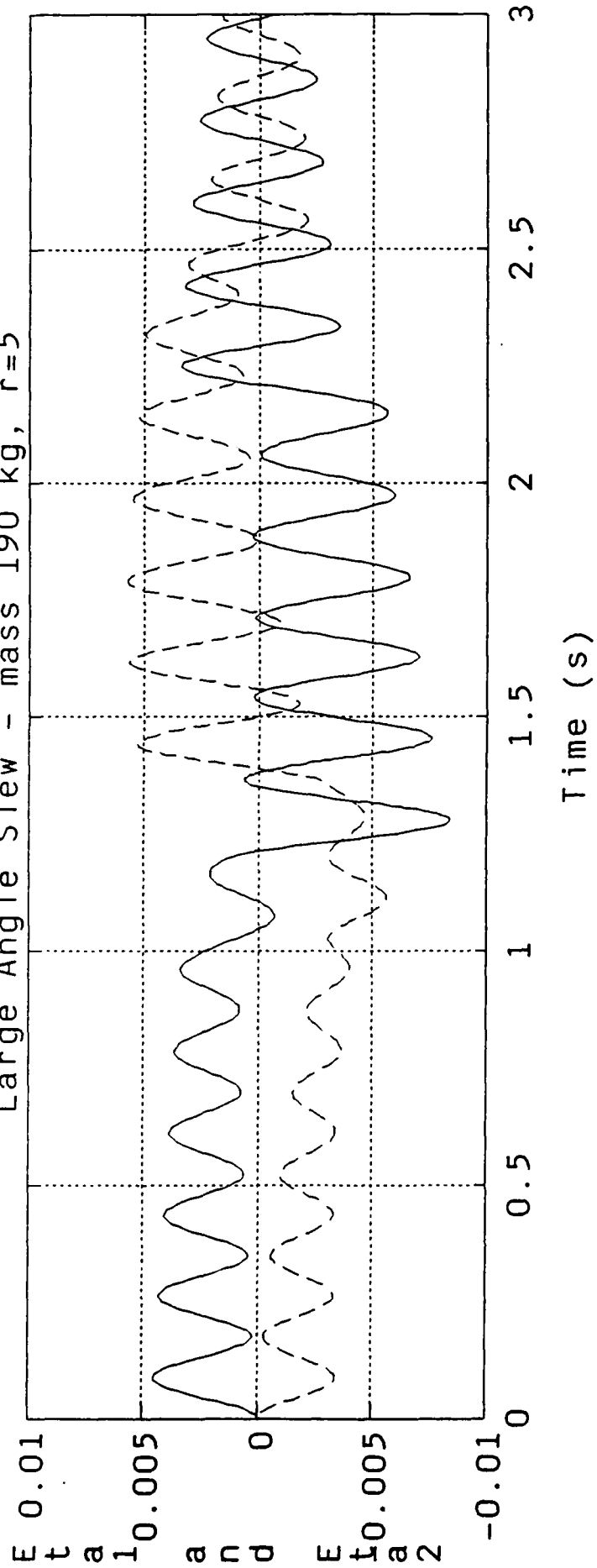
MOD1

SIM16



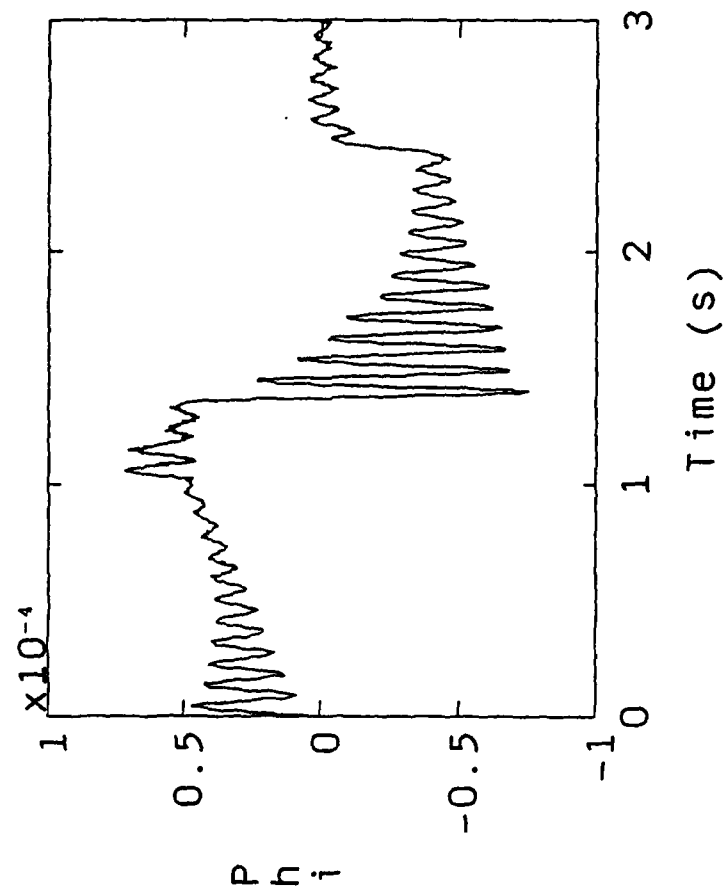
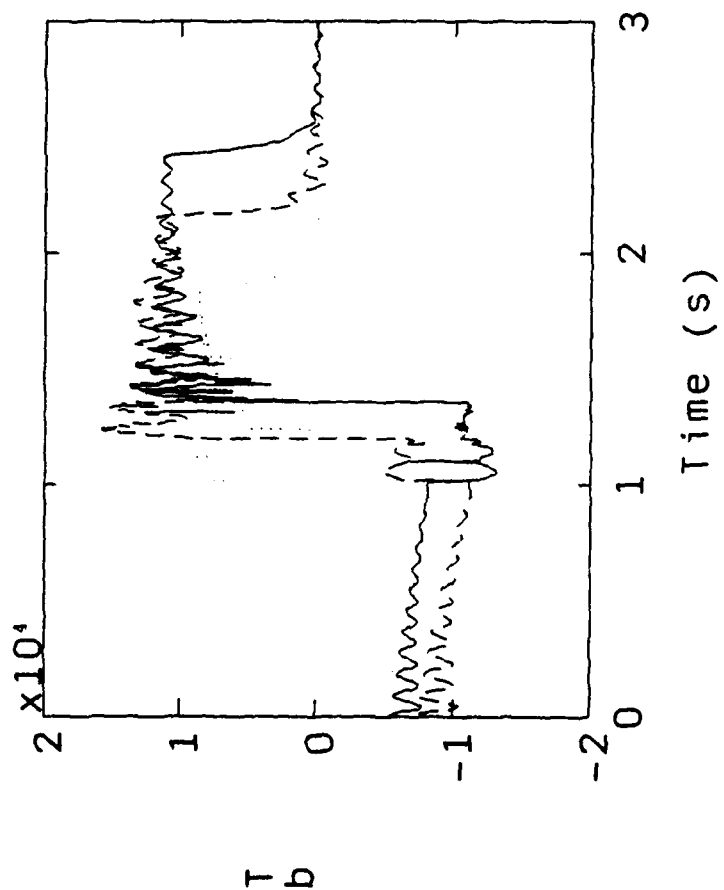
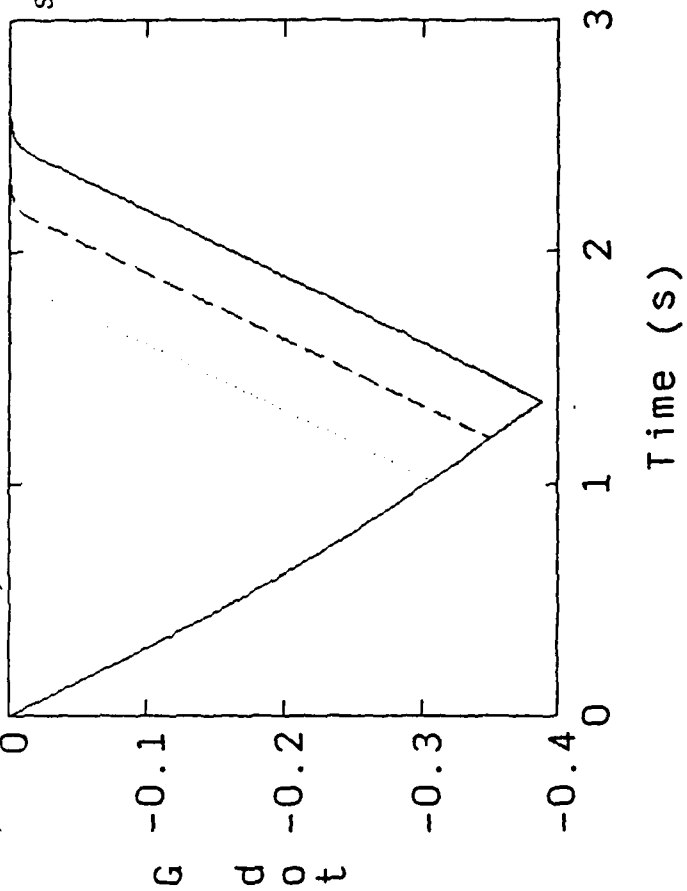
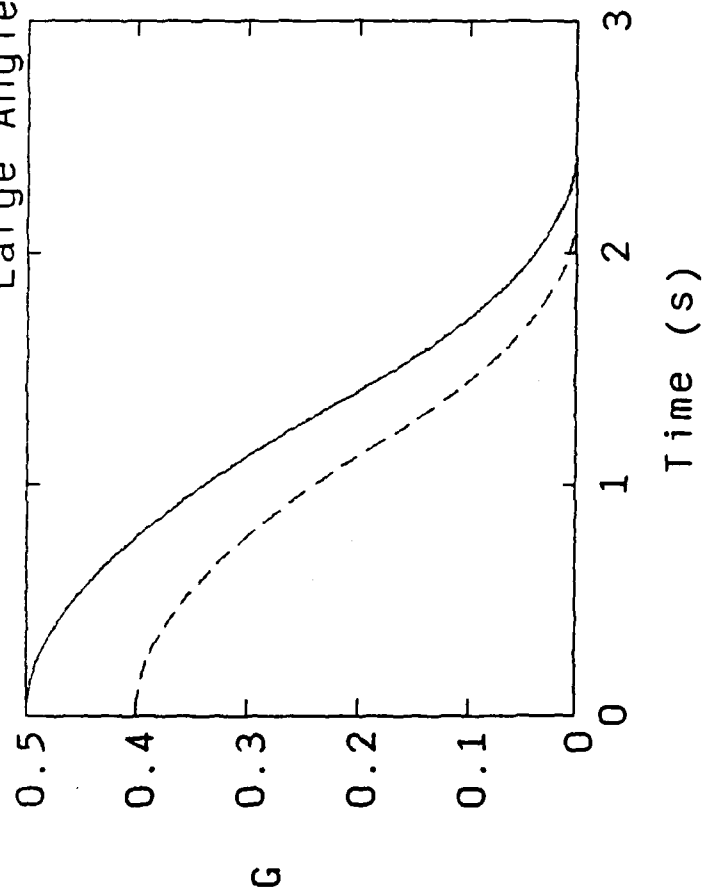
Large Angle Slew - mass 190 kg, r=5

MOD1
SIM16

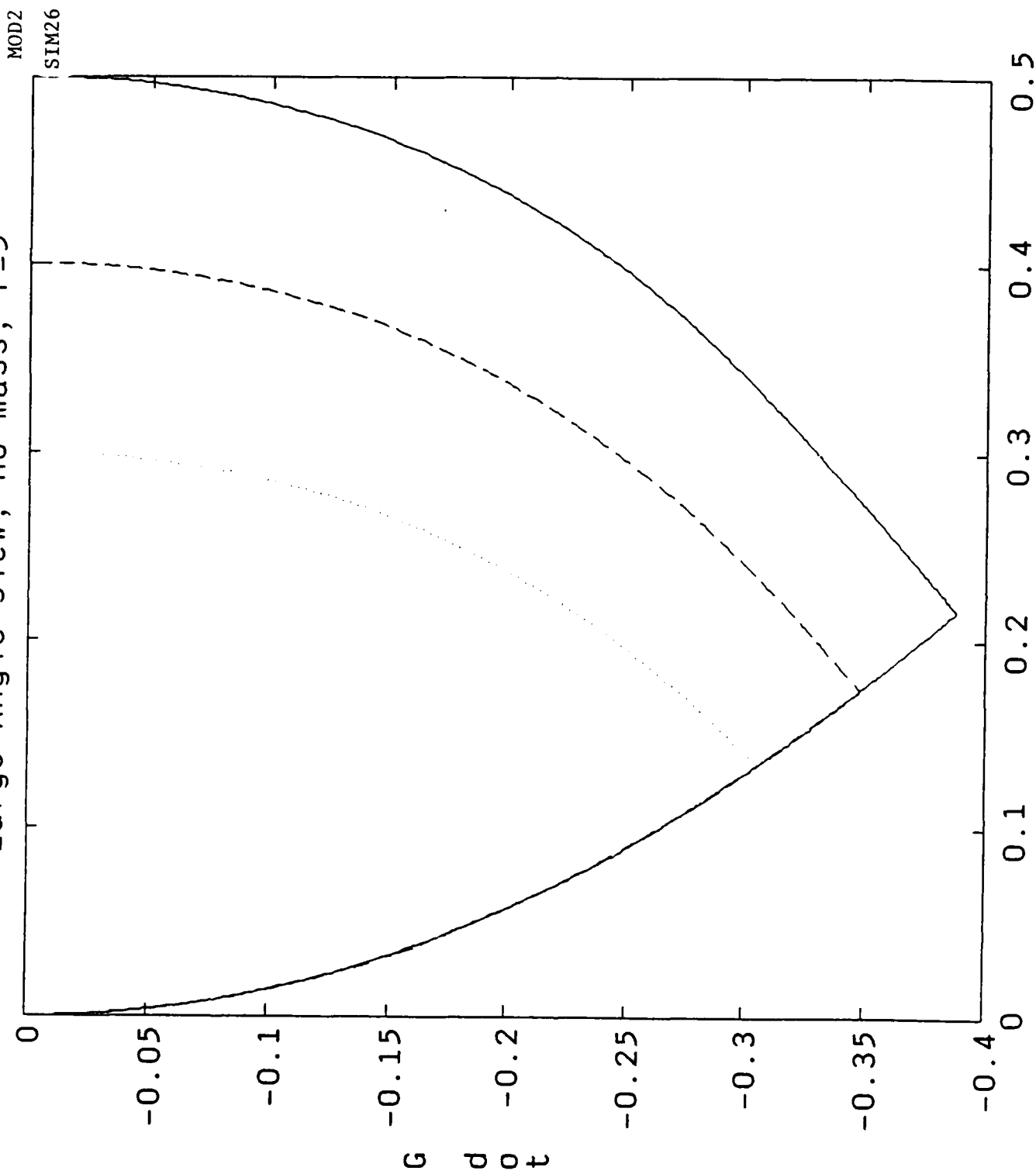


Large Angle Slew, no mass, r=5

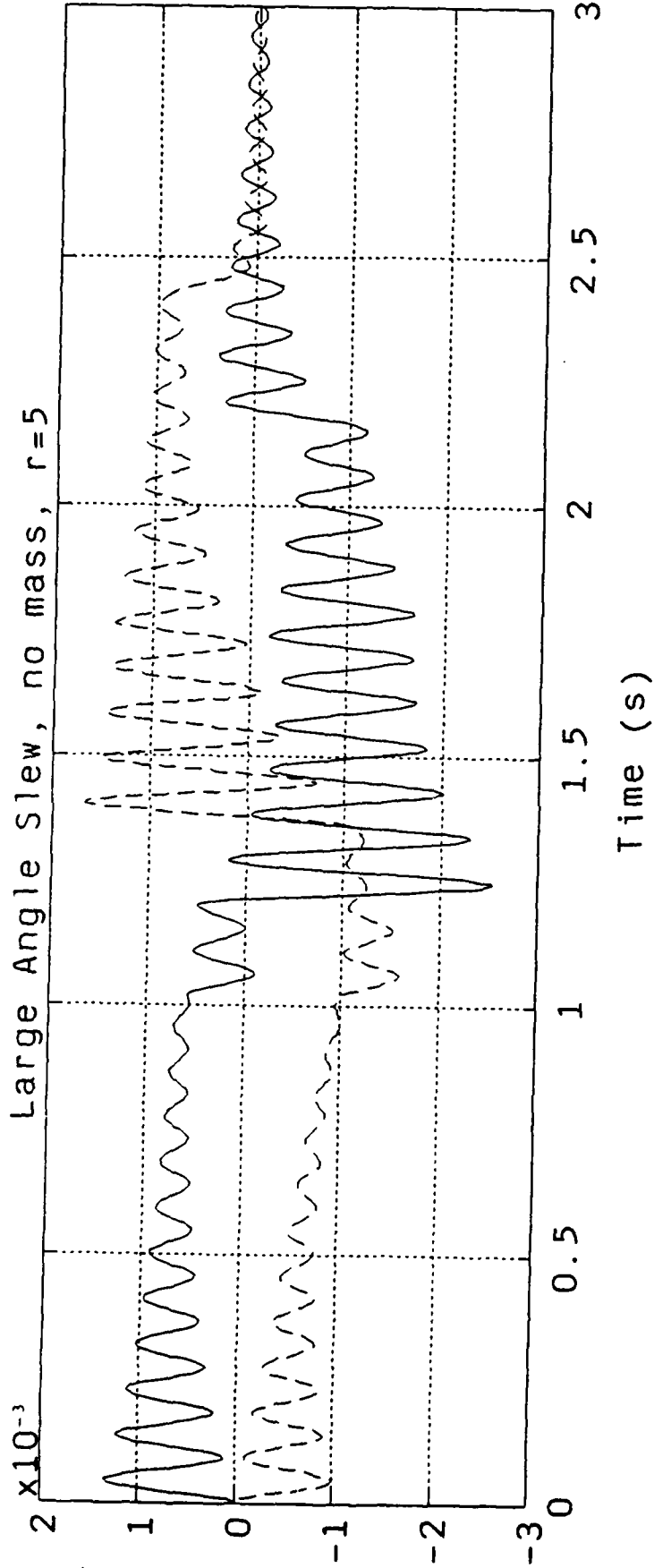
MOD2
SIM26



Large Angle Slew, no mass, $r=5$



E t a 1 a n d E t a 2



T h e t a a n d P h i

